

## Investigation of the effect of disulfiram on the chemoresistance and invasiveness in pancreatic cancer cells

|               |   |
|---------------|---|
| Item Type     | Thesis or dissertation  |
| Authors       | Nkeonye, Ogechi   |
| Citation      | Nkeonye, O. (2022) Investigation of the effect of disulfiram on the chemoresistance and invasiveness in pancreatic cancer cells. University of Wolverhampton. <a href="http://hdl.handle.net/2436/624947">http://hdl.handle.net/2436/624947</a> |
| Publisher     | University of Wolverhampton   |
| Rights        | Attribution-NonCommercial-NoDerivatives 4.0 International   |
| Download date | 2026-06-11 09:40:08   |
| License       | <a href="http://creativecommons.org/licenses/by-nc-nd/4.0/">http://creativecommons.org/licenses/by-nc-nd/4.0/</a>   |
| Link to Item  | <a href="http://hdl.handle.net/2436/624947">http://hdl.handle.net/2436/624947</a>   |



**INVESTIGATION OF THE EFFECT OF DISULFIRAM ON THE  
CHEMORESISTANCE AND INVASIVENESS IN PANCREATIC CANCER CELLS**

**By**

**Ogechi Nkeonye**

**Student Number: 1629449**

**A thesis submitted in partial fulfilment for the degree of Doctor of Philosophy in  
Molecular Oncology**

**Research Institute in Healthcare Science**

**Faculty of Science and Engineering**

**University of Wolverhampton**

**July 2022**

## **DECLARATION**

I hereby declare that this work has not been presented to any university or establishment for assessment or publication unless otherwise stated. The intellectual part of this work was done by me except for those expressed in the acknowledgement and references.

The right of Ogechi Nkeonye to be identified as an author of this work is asserted in accordance with ss.77 and 78 of the Copyright, Designs and Patents Act 1988. At this date, Copyright is owned by the author.

Signature\_\_\_\_\_

Date \_\_\_\_\_

## **DEDICATION**

This thesis is dedicated to my family because of their unending support.

## **ACKNOWLEDGEMENTS**

I would like to use this opportunity to appreciate the effort of the people who have assisted me in this doctoral research journey. First and foremost, I would thank God Almighty for leading me in this direction and giving me the strength to continue with this research. It hasn't been easy yet He remains faithful to His word.

I am greatly thankful to PCUK for funding this research and Professor Heeshcen's lab at Bart's Cancer Institute, Queen Mary University, London for their collaboration.

I am deeply grateful and indebted to my Principal Supervisor Professor Weiguang Wang for his guidance, support and unending words of encouragement. My sincere gratitude goes to Dr. Mark Morris and Dr. Vinodh Kannappan for their excellent co-supervision, assistance and advice. Special thanks to my colleagues Drs Rajagopal Kilari, Karim Azar, Kate Butcher, Yoshita Lakshmanan, Mayur Sopan Kale, Satishkumar Kurusami and Ms Garima Tyagi for their contributions to this research.

I would also like to appreciate the academic and technical staff of the Research Institute in Healthcare Science (RIHS), Faculty of Science and Engineering, University of Wolverhampton for their assistance throughout the course of my research.

Lastly, I would love to appreciate the efforts and support of my parents and siblings.

## ABSTRACT

Pancreatic ductal adenocarcinoma (PDAC) is one of the most lethal cancers worldwide with a mortality to incidence ratio of 94%. It is the 10<sup>th</sup> most common cancer in the UK with a 5-year survival less than 7%. In contrast to the improved therapeutic outcomes in many other cancers, the prognosis of PDAC remains dismal. One reason for this is because most PDAC patients are asymptomatic and end up being diagnosed after the cancer has advanced to a late stage. Another major obstacle in PDAC management is that PDAC cells are highly resistant to currently available anticancer drugs and the resistant cells metastasize to vital organs leading to a high rate of fatalities. Cancer stem cells (CSCs) are responsible for chemoresistance, relapse and metastasis. It is widely accepted that CSCs are located in the hypoxic niche which is responsible for maintaining stemness and epithelial to mesenchymal transition (EMT). The stemness of cancer cells is a reversible state mediated by the hypoxic tumour microenvironment. Hypoxia initiates stemness in cancer cells by activating genes which inhibit apoptosis, modify glucose metabolism, increase cell proliferation and enhance cell pluripotency. Therefore, development of new drugs to target hypoxia-induced CSCs will be of clinical urgency in PDAC treatment. Due to the time and costs for new drug development, repositioning of old drugs for new ailments is an emerging drug R&D strategy in recent years. Disulfiram (DS) is an anti-alcoholism drug used in clinic for over 60 years. It demonstrates excellent activity against a wide range of cancers such as glioblastoma, non-small cell lung cancer and, head and neck squamous cell carcinoma without toxicity to normal cells. Whereas, its effect on PDAC cells is still largely unknown.

In this study, the *in vitro* effect of hypoxia on the stemness, chemosensitivity and invasiveness of Panc-1, a PDAC cell line, and a panel of patient-derived PDAC primary cultures was investigated. The sphere-cultured PDAC cells contained high hypoxic population which demonstrated CSC/EMT traits and were resistant to the first line anti-PDAC drugs;

gemcitabine and paclitaxel. The study manifested that the hypoxia-cultured monolayer PDAC cell line and primary cells also expressed CSC markers, 'ALDH, CD133, ABCG2' and EMT markers, 'Vimentin, Snail1, N-cadherin, Snail2'. The hypoxia-cultured cells were highly resistant to gemcitabine and paclitaxel. Significantly higher migration and invasion activities were detected in the hypoxia-cultured PDAC cells compared to the normoxic cultures.

Our previous studies demonstrated that copper is essential for the anticancer activity of DS. In this study, the effect of cyclodextrin encapsulated DS and copper (CycDex DS/Cu) on PDAC cells was examined. In line with previous studies, CycDex DS/Cu showed strong cytotoxicity in sphere- and hypoxia-cultured PDAC cells. It blocked hypoxia-induced CSC/EMT traits and reversed hypoxia-induced chemoresistance to gemcitabine and paclitaxel in PDAC cells. DS is an FDA approved medicine. The study suggests that further studies may translate it into PDAC clinic application in a fast track.

Many hypotheses claim that hypoxia activates NFκB which in turn activates a cascade of genes that promote metastasis and chemoresistance in cancer. Our previous results indicate that NFκB plays a key role in chemoresistance and invasiveness in some types of cancer. For these reasons, the effect of NFκB on PDAC cells was investigated; NFκBp65 was genetically overexpressed and knocked out in Panc-1 PDAC cell line. The NFκBp65 overexpressed clones showed significantly higher migration rate but failed to induce chemoresistance. In contrast to our previous findings, the NFκBp65 overexpression and knockout did not influence the expression of CSC/EMT markers. These results suggest that we still need to set up further studies to elucidate the molecular anti-PDAC mechanisms of cyclodextrin encapsulated DS/Cu in PDAC cells.

## TABLE OF CONTENTS

|  |          |
|--|----------|
| Declaration                                  | ii       |
| Dedication                                   | iii      |
| Acknowledgements                             | iv       |
| Abstract                                     | v        |
| Table of Contents                            | vii      |
| List of Tables                               | xvi      |
| List of Figures                              | xvii     |
| Abbreviations                                | xx       |
| <b>CHAPTER 1 Introduction</b>                | <b>1</b> |
| 1.1 Pancreatic ductal adenocarcinoma (PDAC)  | 2        |
| 1.1.1 Cancer Overview                        | 2        |
| 1.1.2 PDAC Epidemiology                      | 2        |
| <i>1.1.2.1 Incidence</i>                     | 2        |
| <i>1.1.2.2 Mortality</i>                     | 3        |
| <i>1.1.2.3 Survival</i>                      | 4        |
| 1.1.3 PDAC Etiology                          | 4        |
| <i>1.1.3.1 Risk factors</i>                  | 4        |
| <i>1.1.3.1.1 Modifiable risk factors</i>     | 4        |
| <i>1.1.3.1.2 Non-modifiable risk factors</i> | 6        |
| <i>1.1.3.2 Screening and diagnosis</i>       | 10       |
| <i>1.1.3.3 PDAC Stages</i>                   | 11       |
| 1.1.4 Classification of PDAC                 | 12       |
| <i>1.1.4.1 Anatomy of the pancreas</i>       | 12       |

|  |    |
|--|----|
| 1.1.4.2 <i>Pancreatic Cancer Histology</i>           | 13 |
| 1.1.5 PDAC Management                                | 13 |
| 1.1.5.1 <i>Surgery</i>                               | 14 |
| 1.1.5.2 <i>Radiotherapy</i>                          | 15 |
| 1.1.5.3 <i>Chemotherapy</i>                          | 16 |
| 1.1.5.3.1 <i>Gemcitabine</i>                         | 16 |
| 1.1.5.3.2 <i>Paclitaxel</i>                          | 20 |
| 1.1.5.3.3 <i>5-Fluorouracil</i>                      | 23 |
| 1.2 Drug Resistance in PDAC                          | 26 |
| 1.2.1 PDAC tumour microenvironment                   | 26 |
| 1.2.2 Increased activity of drug efflux transporters | 27 |
| 1.2.3 Modification of Drug Targets and DNA Repair    | 28 |
| 1.2.4 Aberrant Regulation of the Cell Cycle          | 29 |
| 1.2.5 Evasion of apoptosis                           | 30 |
| 1.2.6 PDAC signalling pathways                       | 31 |
| 1.2.7 <i>MicroRNAs</i>                               | 32 |
| 1.2.8 Autophagy                                      | 33 |
| 1.3 Hypoxia  | 34 |
| 1.3.1 Hypoxia and HIFs                               | 35 |
| 1.3.2 Hypoxia and CSCs                               | 37 |
| 1.3.3 Hypoxia and metastasis                         | 37 |
| 1.3.4 Hypoxia and chemoresistance                    | 38 |
| 1.4 Cancer stem cells (CSCs)                         | 39 |
| 1.4.1. Identification of Cancer stem cells           | 41 |
| 1.4.2 Cancer stem cell markers                       | 41 |

|         |  |    |
|---------|--|----|
| 1.4.2.1 | <i>Aldehyde dehydrogenase</i>                                      | 41 |
| 1.4.2.2 | <i>Octamer-binding transcription factor (OCT4)</i>                 | 43 |
| 1.4.2.3 | <i>NANOG</i>   | 44 |
| 1.4.2.4 | <i>SOX2</i>  | 44 |
| 1.4.2.5 | <i>CD133</i>   | 45 |
| 1.4.3   | Cancer stem cells and chemoresistance                              | 45 |
| 1.5     | Epithelial to Mesenchymal transition                               | 46 |
| 1.5.1   | EMT markers  | 47 |
| 1.5.1.1 | <i>SNAIL1</i>  | 47 |
| 1.5.1.2 | <i>E-cadherin</i>  | 48 |
| 1.5.1.3 | <i>N-cadherin</i>  | 49 |
| 1.5.1.4 | <i>Vimentin</i>  | 50 |
| 1.5.1.5 | <i>Matrix metalloproteinase</i>                                    | 50 |
| 1.6     | Nuclear Factor Kappa B (NFκB)                                      | 51 |
| 1.6.1   | NFκB and Hypoxia   | 52 |
| 1.6.2   | NFκB and metastasis  | 54 |
| 1.6.3   | NFκB and chemoresistance   | 55 |
| 1.7     | Repositioning of Disulfiram into cancer treatment                  | 56 |
| 1.7.1   | Comparison of traditional drug development with drug repositioning | 56 |
| 1.7.2   | Non-oncology drugs currently repositioned for Cancer treatment     | 58 |
| 1.7.3   | The developmental history of Disulfiram                            | 59 |
| 1.7.4   | Disulfiram and Cancer  | 60 |
| 1.7.4.1 | <i>Mechanism of action of disulfiram</i>                           | 60 |
| 1.7.4.2 | <i>Limitations of disulfiram as an oncology drug</i>               | 64 |
| 1.7.4.3 | <i>Nanotechnology</i>  | 64 |

|  |           |
|--|-----------|
| 1.7.4.4 <i>Nano-drug-delivery systems transforms Disulfiram for cancer treatment</i> | 65        |
| 1.7.5 Cyclodextrins  | 67        |
| 1.8 Aim and Objectives   | 69        |
| <b>CHAPTER 2 Materials and Methods</b>   | <b>70</b> |
| 2.1 Materials  | 71        |
| 2.1.1 Cell lines   | 71        |
| 2.1.2 Reagents, enzymes and kits   | 71        |
| 2.1.3 Antibodies   | 73        |
| 2.1.4 Equipment and Labware  | 73        |
| 2.1.5 Buffers  | 74        |
| 2.2 Methodology  | 77        |
| 2.2.1 Cell Culture   | 77        |
| 2.2.2 MTT Cytotoxicity Assay   | 78        |
| 2.2.3 Hypoxyprobe Analysis by Flow Cytometry   | 79        |
| 2.2.4 Immunocytochemistry  | 80        |
| 2.2.5 Sphere Reformation Assay   | 82        |
| 2.2.6 Flow Cytometry   | 83        |
| 2.2.7 Annexin Apoptosis Assay  | 84        |
| 2.2.8 Western Blot   | 86        |
| 2.2.9 Real-time Polymerase Chain Reaction (Rt-PCR)                                   | 90        |
| 2.2.10 In vitro Migration Assay  | 94        |
| 2.2.11 In vitro Invasion Assay   | 96        |
| 2.2.12 Stable Transfection   | 97        |
| 2.2.13 CRISPR-Cas9 knockout  | 100       |
| 2.2.14 Statistical Analysis  | 101       |

|   |            |
|---|------------|
| <b>CHAPTER 3 Hypoxia induces stemness, chemoresistance and invasiveness in Panc1<br/>pancreatic ductal adenocarcinoma cell line</b> | <b>102</b> |
| 3.1 Introduction  | 103        |
| 3.2 Experimental design   | 105        |
| 3.2.1 Cell line   | 105        |
| 3.2.2 Cell culture  | 105        |
| 3.2.3 Flow cytometry analysis of CSC markers  | 105        |
| 3.2.4 Detection of embryonic stem cell markers and EMT markers using Real-time<br>PCR   | 106        |
| 3.2.5 Immunocytochemistry   | 106        |
| 3.2.6 Cell migration assay  | 106        |
| 3.2.7 Cell invasion assay   | 106        |
| 3.2.8 MTT Cell Viability assay  | 107        |
| 3.2.9 Sphere reformation assay  | 107        |
| 3.3 Results   | 107        |
| 3.3.1 Spheroids derived from panc-1 PDAC cell line are resistant to conventional<br>anticancer drugs                                | 107        |
| 3.3.2 Spheroids cultured from panc-1 PDAC cell line express CSC markers   | 109        |
| 3.3.3 Hypoxic population detected in spheroids and hypoxia cultured panc-1<br>PDAC cell line  | 111        |
| 3.3.4 Hypoxia cultured panc-1 PDAC cell line shows increased expression of CSC<br>markers   | 113        |
| 3.3.5 Hypoxia induces chemoresistance in panc-1 PDAC cell line  | 115        |

|   |            |
|---|------------|
| 3.3.6 Hypoxia and sphere cultured panc-1 PDAC cell line shows increased EMT characteristics                       | 117        |
| 3.4 Discussion  | 119        |
| 3.5 Conclusion  | 122        |
| <b>CHAPTER 4 Hypoxia induces stemness and chemoresistance in a panel of patient derived primary cell cultures</b> | <b>123</b> |
| 4.1 Introduction  | 124        |
| 4.2 Experimental Design   | 125        |
| 4.2.1 Cell line   | 125        |
| 4.2.2 Cell culture  | 126        |
| 4.2.3 Sphere reformation assay  | 126        |
| 4.2.4 Immunocytochemistry   | 126        |
| 4.2.5 Detection of FITC hypoxypopulation by flow cytometry analysis   | 127        |
| 4.2.6 Flow cytometry analysis of CSC markers  | 127        |
| 4.2.7 MTT Cell Viability assay  | 127        |
| 4.3 Results   | 127        |
| 4.3.1 Patient derived PDAC spheroid cells are resistant to conventional anticancer drugs                          | 128        |
| 4.3.2 Patient derived PDAC spheroid cells have CSC characteristics  | 131        |
| 4.3.3 Hypoxic populations detected in spheroid and hypoxic cultures of patient derived PDAC cells                 | 134        |
| 4.3.4 Hypoxic patient derived PDAC cells show increased CSC characteristics                                       | 137        |
| 4.3.5 Hypoxia induces chemoresistance in patient derived PDAC cells   | 140        |
| 4.4 Discussion  | 142        |
| 4.5 Conclusion  | 145        |

|   |            |
|---|------------|
| <b>CHAPTER 5 Cyclodextrin encapsulated disulfiram plus copper targets cancer stem cells and blocks chemoresistance and invasiveness in PDAC cells</b> | <b>146</b> |
| 5.1 Introduction  | 147        |
| 5.2 Experimental Design   | 149        |
| 5.2.1 Cell culture  | 149        |
| 5.2.2 Sphere reformation assay  | 149        |
| 5.2.3 Cell Apoptosis Assay  | 149        |
| 5.2.4 Flow Cytometry Analysis   | 150        |
| 5.2.5 MTT Cell Viability assay  | 150        |
| 5.2.6 Detection of embryonic stem cell markers using Real-time PCR  | 150        |
| 5.3 Results   | 151        |
| 5.3.1 PDAC cells are resistant to first line anti-PDAC drugs (GEM and PAC) induced apoptosis but sensitive to CycDex DS/Cu                            | 151        |
| 5.3.2 CycDex DS/Cu is cytotoxic to PDAC cells and enhances the cytotoxicity of first line anti-PDAC drugs in normoxia cultured PDAC cells.            | 153        |
| 5.3.3 CycDex DS/Cu is cytotoxic to PDAC cells and enhances the cytotoxicity of first line anti-PDAC drugs in hypoxia cultured PDAC cells.             | 158        |
| 5.3.4 Cyclodextrin Disulfiram/Cu decreased the PDAC CSC population in PDAC hypoxic cultures.  | 162        |
| 5.3.5 Cyclodextrin Disulfiram/Cu inhibits the hypoxia induced CSC markers.  | 166        |
| 5.3.6 Cyclodextrin Disulfiram/Cu decreased the CSC population in spheroid cultures of primary PDAC cells.   | 168        |
| 5.3.7 Cyclodextrin Disulfiram/Cu inhibited the sphere reformation ability of CSC population in spheroid cultures of primary PDAC cells.               | 172        |
| 5.4 Discussion  | 174        |

|  |            |
|--|------------|
| <b>CHAPTER 6 Investigation of the molecular effect of NFκB pathway on stemness and chemoresistance in PDAC cell line</b> | <b>178</b> |
| 6.1 Introduction   | 179        |
| 6.2 Methods  | 182        |
| 6.2.1 Cell culture   | 182        |
| 6.2.2 Stable Transfection  | 182        |
| 6.2.3 CRISPR p65 Knockout  | 182        |
| 6.2.4 Real-time PCR  | 183        |
| 6.2.5 Western Blot   | 183        |
| 6.2.6 MTT Cell Viability assay   | 183        |
| 6.3 Results  | 184        |
| 6.3.1 Spheroid and hypoxic cultures of PDAC cells have high expression of NFκB   | 184        |
| 6.3.2 Ectopic overexpression of NFκB in Panc-1 PDAC cells  | 186        |
| 6.3.3 CRISPR Cas9 knock out of NFκB p65 in Panc-1 PDAC cells   | 187        |
| 6.3.4 NFκB p65 plays an insignificant role in regulating stemness in Panc-1 PDAC cells                                   | 188        |
| 6.3.5 NFκB p65 does not play a role in regulating EMT markers in Panc-1 PDAC cells                                       | 190        |
| 6.3.6 Overexpression of NFκB p65 drives resistance to first line PDAC anticancer drugs in Panc1 PDAC cells               | 192        |
| 6.3.7 Knockdown of NFκB p65 sensitises PDAC cells to PAC but not significantly to Gemcitabine                            | 194        |
| 6.4 Discussion   | 196        |
| <b>CHAPTER 7 Discussion</b>  | <b>200</b> |

**Conclusion**

207

**References**

209

## LIST OF TABLES

|  |     |
|--|-----|
| <b>Table 2.1</b> Preparation of RIPA buffer  | 76  |
| <b>Table 2.2</b> Preparation of Separating gel   | 88  |
| <b>Table 2.3</b> Preparation of Stacking gel   | 88  |
| <b>Table 2.4</b> Preparation of RT-master mix  | 93  |
| <b>Table 2.5</b> Preparation of RT-PCR mix   | 93  |
| <b>Table 2.6</b> Reaction pathway for RT-PCR   | 94  |
| <b>Table 4.1</b> IC <sub>50s</sub> of gemcitabine and paclitaxel for primary PDAC cells cultures under normoxia and hypoxic conditions | 142 |
| <b>Table 5.1</b> IC <sub>50s</sub> of drugs singly used and in combination with CycDex DS/Cu in normoxia-cultured PDAC cells           | 157 |
| <b>Table 5.2</b> The combination index (CI) of anticancer drugs in combination with CycDex DS/Cu in normoxia-cultured PDAC cells       | 157 |
| <b>Table 5.3</b> IC <sub>50s</sub> of drugs singly used and in combination with CycDex DS/Cu in hypoxic PDAC cells                     | 161 |
| <b>Table 5.4</b> The combination index (CI) of anticancer drugs in combination with CycDex DS/Cu                                       | 161 |

## LIST OF FIGURES

|   |     |
|---|-----|
| <b>Figure 1.1</b> Bar chart showing the age standardized incidence rate by sex for pancreatic cancer in the world in 2020 | 3   |
| <b>Figure 1.2</b> Model showing genetic progression of pancreatic cancer  | 9   |
| <b>Figure 1.3</b> Diagram showing the morphology of pancreas and its components   | 13  |
| <b>Figure 1.4</b> Molecular structure of gemcitabine  | 16  |
| <b>Figure 1.5</b> Mechanism of chemoresistance of dFdC  | 19  |
| <b>Figure 1.6</b> Molecular structure of PTX  | 20  |
| <b>Figure 1.7</b> Mechanism of chemoresistance of PTX   | 22  |
| <b>Figure 1.8</b> Molecular structure of 5-Fluorouracil   | 23  |
| <b>Figure 1.9</b> Mechanism of chemoresistance of 5-Fluorouracil  | 25  |
| <b>Figure 1.10</b> Hypoxia and HIF Pathway Activation   | 36  |
| <b>Figure 1.11</b> Relationship between hypoxia and CSCs  | 38  |
| <b>Figure 1.12</b> Hypoxia and NFκB Pathway Activation  | 53  |
| <b>Figure 1:13</b> Illustration of the stages involved in Denovo drug development and drug repurposing                    | 57  |
| <b>Figure 1.14</b> Mechanism of anticancer activity of disulfiram   | 61  |
| <b>Figure 1.15</b> Molecular structure of β-cyclodextrins   | 67  |
| <b>Figure 3.1</b> Panc-1 PDAC cell line is resistant to first line anticancer drugs gemcitabine and paclitaxel            | 108 |
| <b>Figure 3.2</b> Panc-1 PDAC spheroid cells have high CSC characteristics  | 110 |
| <b>Figure 3.3</b> Spheroid and hypoxic panc-1 cells have high hypoxic cell population                                     | 112 |
| <b>Figure 3.4</b> Hypoxic panc-1 PDAC cells have high CSC characteristics   | 115 |
| <b>Figure 3.5</b> Hypoxia promotes chemoresistance in panc-1 PDAC cells   | 117 |

|  |     |
|--|-----|
| <b>Figure 3.6</b> Hypoxia increases EMT characteristics and cell motility in panc-1 PDAC cells   | 118 |
| <b>Figure 4.1</b> Patient derived PDAC cells are resistant to first line anticancer drugs  | 130 |
| <b>Figure 4.2</b> Patient derived PDAC spheroid cells have CSC characteristics   | 133 |
| <b>Figure 4.3</b> Spheroid and Hypoxic patient derived PDAC cells have high hypoxic cell populations                                   | 136 |
| <b>Figure 4.4</b> Hypoxic patient derived PDAC cells have high CSC characteristics   | 139 |
| <b>Figure 4.5</b> Hypoxia increases chemoresistance in patient derived PDAC cells  | 141 |
| <b>Figure 5.1</b> PDAC cells are resistant to first line anti-PDAC drugs (GEM and PAC) induced apoptosis but sensitive to CycDex DS/Cu | 153 |
| <b>Figure 5.2 A</b> PAC and CycDex DS/Cu mutually enhance the in vitro cytotoxicity in normoxia cultured PDAC cells                    | 155 |
| <b>Figure 5.2 B</b> GEM and CycDex DS/Cu mutually enhance the in vitro cytotoxicity in hypoxia cultured PDAC cells                     | 156 |
| <b>Figure 5.3 A</b> GEM and CycDex DS/Cu mutually enhance the in vitro cytotoxicity in hypoxia cultured PDAC cells                     | 159 |
| <b>Figure 5.3 B</b> PAC and CycDex DS/Cu mutually enhance the in vitro cytotoxicity in hypoxia cultured PDAC cells                     | 160 |
| <b>Figure 5.4</b> CycDex DS/Cu targets hypoxia induced ALDH +VE CSC population   | 163 |
| <b>Figure 5.5</b> CycDex DS/Cu targets hypoxia induced CD133 +VE CSC population  | 164 |
| <b>Figure 5.6</b> CycDex DS/Cu targets hypoxia induced ABCG2 +VE CSC population  | 165 |
| <b>Figure 5.7</b> CycDex DS/Cu inhibits the expression of hypoxia-induced embryonic stem cell markers                                  | 167 |
| <b>Figure 5.8.</b> CycDex DS/Cu targets ALDH +VE CSC population in spheroid cultures of PDAC cells                                     | 169 |

|   |     |
|---|-----|
| <b>Figure 5.9.</b> CycDex DS/Cu targets CD133 +VE CSC population in spheroid cultures of PDAC cells   | 170 |
| <b>Figure 5.10.</b> CycDex DS/Cu targets CD133 +VE CSC population in spheroid cultures of PDAC cells  | 171 |
| <b>Figure 5.11.</b> CycDex DS/Cu inhibited the sphere reformation ability of CSC populations in spheroid cultures of PDAC cells                   | 173 |
| <b>Figure 6.1</b> Protein expression of P65 in spheroids and hypoxia cultured PDAC cells  | 185 |
| <b>Figure 6.2</b> Expression of p65 in NFκB p65 overexpressed clones of PDAC cells  | 186 |
| <b>Figure 6.3</b> Expression of p65 in CRISPR cas9 NFκB p65 knock out clones of PDAC cells  | 187 |
| <b>Figure 6.4</b> Expression of cancer stem cell markers in NFκB p65 overexpressed clones and CRISPR cas9 NFκB p65 knock out clones of PDAC cells | 189 |
| <b>Figure 6.5</b> Expression of EMT markers in NFκB p65 overexpressed clones and CRISPR cas9 NFκB p65 knock out clones of PDAC cells              | 191 |
| <b>Figure 6.6</b> Cytotoxicity of NFκB p65 overexpressed clones to first line anti-PDAC drugs gemcitabine and paclitaxel                          | 193 |
| <b>Figure 6.7</b> Cytotoxicity of NFκB p65 knock out clones to first line anti-PDAC drugs gemcitabine and paclitaxel                              | 195 |

## ABBREVIATIONS

|                 |   |
|-----------------|---|
| <b>ABC</b>      | <i>ATP-Binding Cassette</i>                                   |
| <b>ABCB1</b>    | <i>ATP-binding cassette subfamily B member 1</i>              |
| <b>ABCG2</b>    | <i>ATP-binding cassette subfamily G member 2</i>              |
| <b>ADEX</b>     | <i>Aberrantly Differentiated Endocrine Exocrine</i>           |
| <b>AIDS</b>     | <i>Acquired Immunodeficiency Syndrome</i>                     |
| <b>AKT1</b>     | <i>v-akt murine thymoma viral oncogene homolog 1</i>          |
| <b>ALDH</b>     | <i>Aldehyde Dehydrogenase</i>                                 |
| <b>ATG9A</b>    | <i>Autophagy-related protein 9A</i>                           |
| <b>PRMT3</b>    | <i>Arginine Methyltransferase 3</i>                           |
| <b>BAX</b>      | <i>BCL-2-like Protein 4</i>                                   |
| <b>BCL2</b>     | <i>B-cell Lymphoma 2</i>                                      |
| <b>CA 19-9</b>  | <i>Cancer Antigen 19-9</i>                                    |
| <b>CA-50</b>    | <i>Cancer Antigen 50</i>                                      |
| <b>CAF</b>      | <i>Cancer Associated Fibroblasts</i>                          |
| <b>CD</b>       | <i>Cyclodextrin</i>   |
| <b>CD133</b>    | <i>Cluster of Differentiation 133</i>                         |
| <b>(CDKN)2A</b> | <i>Cyclin-Dependent Kinase Inhibitor</i>                      |
| <b>c-Met</b>    | <i>Tyrosine-protein Kinase Met</i>                            |
| <b>c-MYC</b>    | <i>Avian myelocytomatosis virus oncogene cellular homolog</i> |
| <b>COX-2</b>    | <i>Cyclooxygenase-2</i>                                       |
| <b>CSC</b>      | <i>Cancer Stem Cell</i>                                       |
| <b>CT</b>       | <i>Computerised Tomography</i>                                |
| <b>CTC</b>      | <i>Circulating Tumour Cells</i>                               |
| <b>CXCR4</b>    | <i>C-X-C Motif Chemokine Receptor 4</i>                       |
| <b>CYC DS</b>   | <i>Cyclodextrin Disulfiram</i>                                |
| <b>dCK</b>      | <i>Deoxycytidine kinase</i>                                   |
| <b>DCLK1</b>    | <i>Doublecortin Like Kinase 1</i>                             |
| <b>DDC</b>      | <i>Diethylthiocarbamate</i>                                   |
| <b>dFdC</b>     | <i>2',2'-difluoro-2'-deoxycytidine</i>                        |

|                |  |
|----------------|--|
| <b>dFdCMP</b>  | <i>2',2'-difluoro-2'-deoxycytidine monophosphate</i> |
| <b>DIMATE</b>  | <i>Dimethyl ampal thiolester</i>                     |
| <b>DKK-1</b>   | <i>Dickkopf-1</i>                                    |
| <b>DNA</b>     | <i>Deoxyribonucleic Acid</i>                         |
| <b>dNTP</b>    | <i>Deoxynucleoside Triphosphate</i>                  |
| <b>DS</b>      | <i>Disulfiram</i>                                    |
| <b>dTMP</b>    | <i>Deoxythymidine Monophosphate</i>                  |
| <b>DUPAN-2</b> | <i>Duke Pancreatic Monoclonal Antigen Type 2</i>     |
| <b>ECM</b>     | <i>Extracellular Matrix</i>                          |
| <b>EGFR</b>    | <i>Epidermal Growth Factor Receptor</i>              |
| <b>EMT</b>     | <i>Epithelial to Mesenchymal Transition</i>          |
| <b>EpCAM</b>   | <i>Epithelial Cell Adhesion Molecule</i>             |
| <b>ER</b>      | <i>Endoplasmic Reticulum</i>                         |
| <b>ERK</b>     | <i>Extracellular-Signal-Regulated-Kinase</i>         |
| <b>ESA</b>     | <i>Erythropoiesis stimulating agent</i>              |
| <b>ESL</b>     | <i>Epithelial cell adhesion molecule</i>             |
| <b>EST</b>     | <i>Erythroblast Transformation-Specific</i>          |
| <b>FDA</b>     | <i>Federal Drug Agency</i>                           |
| <b>FLK1</b>    | <i>Fetal Liver Kinase-1</i>                          |
| <b>FOXC2</b>   | <i>Forkhead Box Protein C2</i>                       |
| <b>FOXO3</b>   | <i>Forkhead Box O3</i>                               |
| <b>FZD4</b>    | <i>Frizzled 4</i>                                    |
| <b>5-FU</b>    | <i>5-fluorouracil</i>                                |
| <b>5-FdUMP</b> | <i>5-fluorodeoxyuridine monophosphate</i>            |
| <b>FGF</b>     | <i>Fibroblast Growth Factor</i>                      |
| <b>FUTP</b>    | <i>5-fluorouridine 5'triphosphate</i>                |
| <b>G2/M</b>    | <i>Gap2/Metaphase</i>                                |
| <b>GI</b>      | <i>Gastrointestinal</i>                              |
| <b>GLUT1</b>   | <i>Glucose Transporter 1</i>                         |
| <b>GPCR</b>    | <i>G protein-coupled receptor</i>                    |

|   |  |
|---|--|
| <b>GSH</b>                                      | <i>Glutathione</i>   |
| <b>GSK-3<math>\beta</math></b>                  | <i>Glycogen Synthase Kinase 3 Beta</i>   |
| <b>HDACs</b>                                    | <i>Histone Deacetylases</i>  |
| <b>hENT1</b>                                    | <i>Human equilibrative nucleoside transporter-1</i>  |
| <b>Hh</b>                                       | <i>Hedgehog</i>  |
| <b>HIF</b>                                      | <i>Hypoxia Inducible Factor</i>  |
| <b>HMTase</b>                                   | <i>Histone Methyltransferase</i>   |
| <b>HO-1</b>                                     | <i>Heme oxygenase-1</i>  |
| <b>HRAS</b>                                     | <i>Harvey rat sarcoma viral oncogene homolog</i>   |
| <b>HREs</b>                                     | <i>Hypoxia Response Elements</i>   |
| <b>HuR</b>                                      | <i>Hu antigen R</i>  |
| <b>ICD</b>                                      | <i>Immunogenic Cell Death</i>  |
| <b>Ifs</b>                                      | <i>Intermediate Filaments</i>  |
| <b>IGF</b>                                      | <i>Insulin-like growth factor receptor</i>   |
| <b>I<math>\kappa</math>B<math>\alpha</math></b> | <i>Nuclear factor of kappa light polypeptide gene enhancer in B-cells inhibitor, alpha</i> |
| <b>IKK<math>\alpha</math></b>                   | <i>Inhibitory-<math>\kappa</math>B Kinase</i>  |
| <b>IMRT</b>                                     | <i>Intensity-modulated radiotherapy</i>  |
| <b>IPAS1</b>                                    | <i>Inhibitory (Per/Arnt/Sim) domain protein</i>  |
| <b>IPMN</b>                                     | <i>Intraductal papillary mucinous neoplasms</i>  |
| <b>JAK/STAT</b>                                 | <i>Janus Kinase/Signal Transducer and Activators of Transcription</i>                      |
| <b>Keap</b>                                     | <i>Kelch-like ECH-associated protein 1</i>   |
| <b>KFL4</b>                                     | <i>Kruppel-like Factor 4</i>   |
| <b>KRAS</b>                                     | <i>Kristen Rat Sarcoma Viral Oncogene Homolog</i>  |
| <b>LAPC</b>                                     | <i>Locally Advanced Pancreatic Cancer</i>  |
| <b>LPCAT2</b>                                   | <i>LysoPC Acyltransferase 2</i>  |
| <b>LRP</b>                                      | <i>Low-Density Lipoprotein Receptor-Related Protein</i>                                    |
| <b>LSD</b>                                      | <i>d-Lysergic Acid Diethylamide</i>  |
| <b>MAPK</b>                                     | <i>Mitogen-Activated Protein Kinases</i>   |
| <b>MCN</b>                                      | <i>Mucinous Cystic Neoplasms</i>   |

|                         |   |
|-------------------------|---|
| <b>MDR</b>              | <i>Multidrug Resistance</i>   |
| <b>MerTK</b>            | <i>MER Tyrosine Kinase</i>  |
| <b>MiRNA</b>            | <i>MicroRNA</i>   |
| <b>MMP</b>              | <i>Matrix metalloproteinase</i>                                       |
| <b>MMR</b>              | <i>Mismatch Repair</i>  |
| <b>MRI</b>              | <i>Magnetic Resonance Imaging</i>                                     |
| <b>mRNA</b>             | <i>Messenger RNA</i>  |
| <b>mTOR</b>             | <i>The Mammalian Target of Rapamycin</i>                              |
| <b>MUC</b>              | <i>Cell Surface-associated Mucins</i>                                 |
| <b>NADP<sup>+</sup></b> | <i>Nicotinamide Adenine Dinucleotide Phosphate</i>                    |
| <b>NFκB</b>             | <i>Nuclear factor kappa-light-chain-enhancer of activated B-cells</i> |
| <b>NPL4</b>             | <i>Nuclear Protein Localization Protein 4 Homolog</i>                 |
| <b>NRAS</b>             | <i>Neuroblastoma Ras Viral Oncogene Homolog</i>                       |
| <b>NRF2</b>             | <i>Nuclear Factor Erythroid 2-Related Factor 2</i>                    |
| <b>NRP</b>              | <i>Neuropilin</i>   |
| <b>NSAID</b>            | <i>Non-steroidal anti-inflammatory drug</i>                           |
| <b>OCT4</b>             | <i>Octamer-Binding Transcription Factor 4</i>                         |
| <b>PanIN</b>            | <i>Pancreatic Intraepithelial Neoplasms</i>                           |
| <b>PANR</b>             | <i>Pancreatic Cancer-Associated Neural Remodelling</i>                |
| <b>PCUK</b>             | <i>Pancreatic Cancer UK</i>   |
| <b>PDAC</b>             | <i>Pancreatic Ductal Adenocarcinoma</i>                               |
| <b>PET</b>              | <i>Positron-emission tomography</i>                                   |
| <b>P-gp</b>             | <i>P-glycoprotein</i>   |
| <b>pH</b>               | <i>Potential of Hydrogen</i>  |
| <b>PHDs</b>             | <i>Prolyl Hydroxylase Domain Enzymes</i>                              |
| <b>PHD-1-4</b>          | <i>Prolyl-Hydroxylase Enzymes</i>                                     |
| <b>PHGDH</b>            | <i>Phosphoglycerate Dehydrogenase</i>                                 |
| <b>PI3K</b>             | <i>Phosphotidalinositol 3-Kinase</i>                                  |
| <b>PNI</b>              | <i>Perineural Invasion</i>  |
| <b>PPP</b>              | <i>Pentose Phosphate Pathway</i>                                      |

|              |   |
|--------------|---|
| <b>PSCs</b>  | <i>Pancreatic Stellate Cells</i>                                |
| <b>PTCH1</b> | <i>Protein Patched Homolog 1-Homo sapiens</i>                   |
| <b>pVHL</b>  | <i>von-Hippel-Lindau protein</i>                                |
| <b>RB</b>    | <i>Retinoblastoma Protein</i>                                   |
| <b>RNA</b>   | <i>Ribonucleic Acid</i>   |
| <b>RNAi</b>  | <i>Genetic Inhibition</i>                                       |
| <b>ROS</b>   | <i>Reactive Oxygen Species</i>                                  |
| <b>RRM2</b>  | <i>Ribonucleotide Reductase Subunit 2</i>                       |
| <b>RUNX1</b> | <i>Runt-Related Transcription Factor 1</i>                      |
| <b>SCD-1</b> | <i>Stearoyl-Coenzyme A Desaturase-1</i>                         |
| <b>SDF-1</b> | <i>Stromal Cell-Derived Factor 1</i>                            |
| <b>SHH</b>   | <i>Sonic Hedgehog ligands</i>                                   |
| <b>SMAD4</b> | <i>Mothers Against Decapentaplegic Homolog 4</i>                |
| <b>SMO</b>   | <i>G-protein-coupled receptor Smoothened</i>                    |
| <b>SOX2</b>  | <i>Sex Determining Region Y-Box 2</i>                           |
| <b>SPARC</b> | <i>Secreted Protein Acidic and Rich in Cysteine</i>             |
| <b>TCF</b>   | <i>T-Cell Transcription Factor</i>                              |
| <b>TCL1</b>  | <i>T-Cell Leukemia/Lymphoma 1A Oncogene</i>                     |
| <b>TFEB</b>  | <i>Transcription Factor EB</i>                                  |
| <b>TGFβ</b>  | <i>Transforming Growth Factor β</i>                             |
| <b>TICs</b>  | <i>Tumour Initiating Cells</i>                                  |
| <b>TIMPs</b> | <i>Tissue Inhibitors of MMPS</i>                                |
| <b>TNF</b>   | <i>Tumour Necrosis Factor</i>                                   |
| <b>TRAIL</b> | <i>Tumour Necrosis Factor-Related Apoptosis-Inducing Ligand</i> |
| <b>TYRO3</b> | <i>Tyrosine-Protein Kinase Receptor</i>                         |
| <b>USP22</b> | <i>Ubiquitin-Specific Protease 22</i>                           |
| <b>VEGF</b>  | <i>Vascular Endothelial Growth Factor</i>                       |
| <b>WNT</b>   | <i>Wingless/Int</i>   |
| <b>ZO-1</b>  | <i>Zonula Occludens 1</i>                                       |
| <b>ZEB1</b>  | <i>Zinc-Finger E-Box Binding Homeobox 1</i>                     |

# **CHAPTER 1**

## **INTRODUCTION**

## **1.1 Pancreatic ductal adenocarcinoma (PDAC)**

### **1.1.1 Cancer Overview**

After cardiovascular disease, cancer is the second most common life-threatening disease in the world (Hassan et al., 2018). Cancer is a disease characterised by abnormal cell growth. The incidence of cancer is still rising (Tan et al., 2018). The different risk factors that can cause cancer are age, heredity, DNA mutation, hormones, growth factors, inflammation and exogenous risk factors such as radiation, chemical carcinogen, smoking, virus, lack of exercise, etc (Wu et al., 2018). In the past decade, there has been a decline in cancer related death rates worldwide with 1.4% decline in women and 1.8% in men (Siegel et al., 2019). This decline is due to a better understanding of cancer biology, improved diagnostic tools and more efficient drug development (Banerjee et al., 2019).

### **1.1.2 PDAC Epidemiology**

#### **1.1.2.1 Incidence**

Pancreatic cancer is one of the most aggressive cancer types which is predicted to become the second most common cause of cancer related death in the next decade because of a lack of significant treatment regimen in the last few decades (Sinn et al., 2016). Figure 1.1 shows the incidences of pancreatic cancer in men and women worldwide (GLOBOCAN, 2020). The incidence of pancreatic cancer in African-Americans is 31 to 65% higher than in people of other ethnic groups in U.S.A. Contrarily, pancreatic cancer incidence is much higher in America and Europe (11.8 to 12.5 cases per 100,000 people) than most of Africa (<3.5 cases per 100,000 people) (Sellam et al., 2015). Europe has one-ninth of the world's population and a quarter of the global pancreatic cancer incidences (Carrato et al., 2015). In Europe, pancreatic cancer accounts for 2.8% of cancers occurring in men and 3.3% of cancers occurring in women (Maisonneuve, 2019). There is a 30-fold difference in the incidence rates of countries with

highest pancreatic cancer incidence rate (Hungary, 10.8) and lowest incidence rate (Guinea, 0.35). The most common type of pancreatic cancer with a 95% incidence rate is pancreatic ductal adenocarcinoma (PDAC) (Blum and Kloog, 2014).

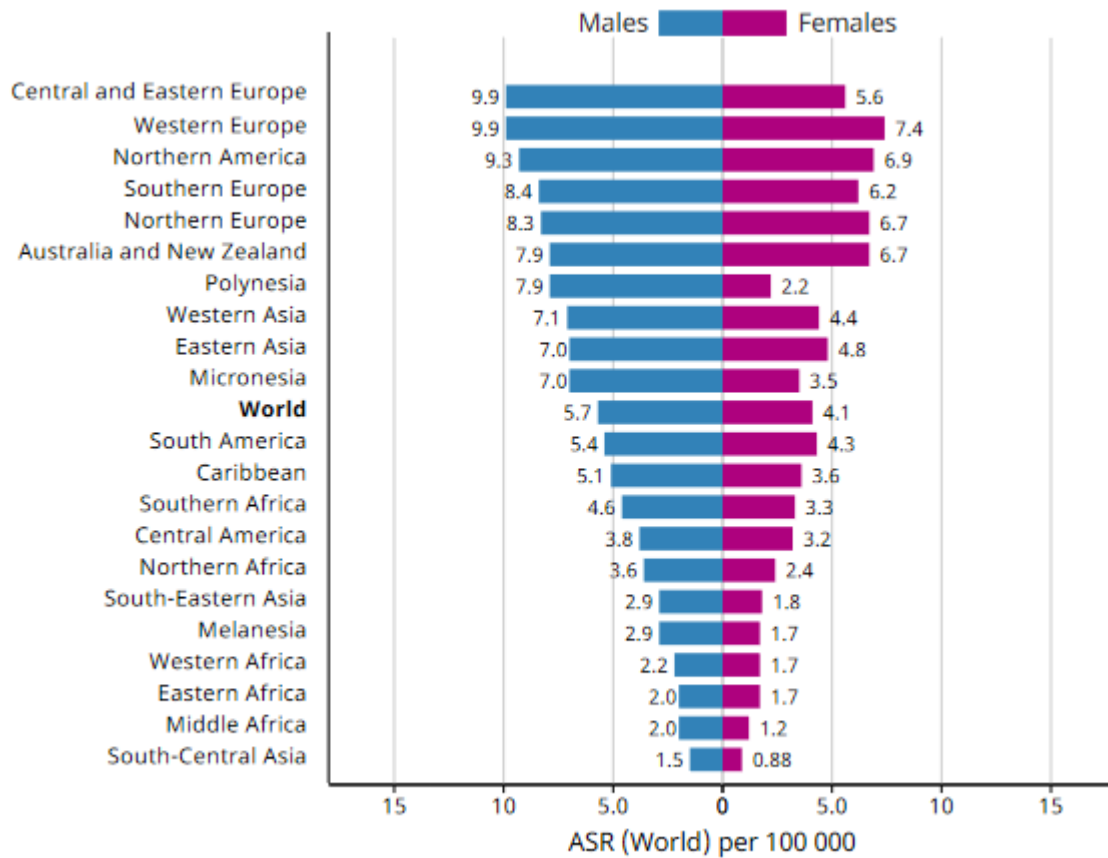


Figure 1.1: Bar chart showing the age standardized incidence rate by sex for pancreatic cancer in the world in 2020. Adapted from GLOBOCAN 2020.

### 1.1.2.2 Mortality

According to GLOBOCAN 2018, pancreatic cancer accounts for 48,312 deaths in men which is equivalent to 6% of cancer related deaths and 47,061 deaths in females which is equivalent to 7.5% of cancer related deaths in Europe. The incidence and deaths related to pancreatic cancer has been on the increase in the past 50 years and this may be attributed to improvement in pancreatic cancer diagnostics (Lowenfels and Maisonneuve, 2004; Maisonneuve, 2019). Generally, early diagnosis of pancreatic cancer is difficult because of its location in the body (Maisonneuve, 2019).

### **1.1.2.3 Survival**

Numerous factors such as age, sex, tumour size, lifestyle, serum albumin level, differences and availability of healthcare systems, treatment modalities, and the stage at diagnosis affect the response of PDAC patients to treatment (Idachaba et al., 2019; Rawla et al., 2019). PDAC patients have a median survival time of 4.6 months which is the worst survival rate of all cancers (Lucenteforte et al., 2012). Currently, pancreatic cancer is one of the most fatal cancers with a mortality to incidence ratio of 94%. As a result of the improvement in cancer treatment modalities, the 5-year survival rate of pancreatic cancer patients has increased from 6% to 9% since 2014 to 2018 (Rawla et al., 2019).

### **1.1.3 PDAC Etiology**

#### **1.1.3.1 Risk factors**

##### **1.1.3.1.1 Modifiable risk factors**

These modifiable risk factors account for 26% and 24.5% of pancreatic cancer incidences in men and women respectively (Maisonneuve, 2019).

##### *Smoking*

The risk of pancreatic cancer is 2 times higher in smokers than non-smokers (Kuzmickiene et al., 2013; Pelucchi et al., 2014; Rawla et al., 2019). The risk can be as high as 50% in passive smokers (Vrieling et al., 2010; Mizuno et al., 2014; Lynch et al., 2009; Rawla et al., 2019). In 2011, the United Kingdom was estimated to have 26.2% and 31% of male and female tobacco associated pancreatic cancer patients respectively (Parkin et al., 2011; Rawla et al., 2019). People who smoke and drink also have increased pancreatic cancer risks (Rawla et al., 2019).

### *Alcohol*

In the body, alcohol is metabolised by alcohol dehydrogenase to acetaldehyde which is toxic and can result in the release of pro-inflammatory mediators such as cytokines, COX-2 and NFκB which can cause cell damage and genetic mutation, that may lead to pancreatic cancer (Midha et al., 2016). People with alcohol addiction have a 22% increased risk of developing pancreatic cancer (Pandol et al., 2012).

### *Obesity*

People who are obese tend to live an unhealthy lifestyle, are physically inactive and eat unhealthy diet. All these predispose them to pancreatic cancer. Adipocytes have the tendency to release VEGF, adipokines, IGF or cause inflammation in cells leading to tumorigenesis (Midha et al., 2016). Different analyses of multiple studies have revealed that people with higher body mass index (BMI) and central obesity have elevated risks of pancreatic cancer (Tsai and Chang, 2019; Genkinger et al., 2015; Aune et al., 2012).

### *Dietary factors*

The risk of dietary factors on pancreatic cancer is as high as 30 to 50% (Michaud et al., 2005). Eating red meat cooked at high temperature or processed meats can increase the chances of getting pancreatic cancer because they contain carcinogens like nitrosamines (Rawla et al., 2019; Beaney et al., 2017). The pancreas plays a significant role during digestion of food. Consuming fried foods or foods with high levels of meat and cholesterol could lead to pancreatic cancer. Contrarily, foods with high antioxidant contents such as citrus fruits can reduce the risk of getting pancreatic cancer (Midha et al., 2016). In 2016, a UK study revealed that the mortality rate for pancreatic cancer was 50% less in vegans and vegetarians than in normal meat eaters (Appleby et al., 2016; Rawla et al., 2019).

### *Chronic pancreatitis*

Alcoholism and smoking are some of the common causes of chronic pancreatitis (Lowenfels et al., 1993). People who have had chronic pancreatitis for a minimum of 5 years have a 14-fold risk of developing pancreatic cancer (Lowenfels et al., 1993; Pandol et al., 2012). A small percentage of people inherit genes that predispose them to chronic pancreatitis which puts them at greater risk of 40-55% for developing pancreatic cancer during their lifetime (Pandol et al., 2012).

#### **1.1.3.1.2 Non-modifiable risk factors**

##### *Family history*

About 5 to 10% of people with a first degree relative who has had pancreatic cancer, may develop pancreatic cancer during their life time. The risk is elevated if the person has a relative with early onset (age < 50 years) of pancreatic cancer (Rawla et al., 2019).

##### *Diabetes*

Diabetes can be a risk factor or consequence of pancreatic cancer. There is a decreased risk of pancreatic cancer in diabetes patients taking only oral anti-diabetic medications especially metformin compared to those taking oral medication in combination with insulin therapy (Wang et al., 2006; Khadka et al., 2018). It has also been observed that surgical resection of the tumour improves pancreatic cancer-related diabetes (Khadka et al., 2018). A study carried out on 100 cancer patients revealed that 68% of the PDAC patients also had diabetes (Andersen et al., 2017). Diabetes patients using insulin and sulfonylureas therapy have increased risk for PDAC because of the mitogenic and anti-apoptotic activity of insulin (Sharma and Chari, 2018). There is evidence that some patients who have had type II diabetes for over 10 years have increased risk for pancreatic cancer (Midha et al., 2016; Lu et al., 2015).

### *Blood group*

Mounting evidence has shown that there is a correlation between the ABO blood type and pancreatic cancer (Pelzer et al., 2013). A study conducted on 316 pancreatic cancer patients revealed that 17% of the cases were attributed to them having a non-O blood group (blood group A, B or AB) (Wolpin et al., 2009) while people with blood type A were more susceptible to pancreatic cancer. It is suspected that the high glucosyltransferase activity of the ABO protein in blood type A could lead to carcinogenesis (El Jellas et al., 2017). According to United States Nurse Health Study and Health Professionals Follow-up Study, people with the O-blood group have less chances of getting pancreatic cancer than people with blood group A (HR: 1.32, 95%CI: 1.02-1.72), AB (HR: 1.51, 95%CI: 1.02-2.23), or B (HR: 1.72, 95%CI: 1.25-2.38) which is due to their difference in glycosyltransferase specificity and host inflammatory states (Wolpin et al., 2009; McGuigan et al., 2018).

### *Age and sex*

Pancreatic cancer occurs mostly in people aged 65 to 75 years (Nattress and Hallden, 2018). About 20% of pancreatic cancer patients are younger than age 60, with 3% being less than 45 years old (McWilliams et al., 2016). There are more male than female pancreatic cancer patients (McGuigan et al., 2018). The worldwide incidence rate for pancreatic cancer is 5.5 per 100,000 in men and 4.0 per 100,000 in women. The reason for this is suspected to be because of men's greater consumption rate of alcohol and tobacco (Rawla et al., 2019).

### *Gut microbiome*

There are more lipopolysaccharide-producing bacteria and pathogens, and less butyrate-producing bacteria in the pancreas of pancreatic cancer patients than in a healthy pancreas. Generally, there is more bacteria in the pancreas of a pancreatic cancer patient. The reason for this is not fully understood (Tsai and Chang, 2019).

### *Ethnicity*

African Americans are 30 to 70% more predisposed to pancreatic cancer than people of other racial groups. This is likely due to their variations in modifiable risk factors such as smoking, diet and alcohol or difference in their genetics which can elevate the risks of acquired mutations. The pancreas requires elevated levels of zinc to function properly and black people are suspected to have reduced zinc absorption capacity in their pancreas compared to people of other ethnicities (Silverman et al., 2003; Blackford et al., 2009a; Arnold et al., 2009; Scarton et al., 2018). African Americans also have increased rates of KRAS mutations to valine and reduced KRAS mutations to cysteine. It has also been observed that the KRAS and p53 expression of Chinese pancreatic cancer patients contrasts from that of Japanese and western patients. The pancreatic cancer survival rate of Asians is higher than that of non-Asians (Longnecker et al., 2000; Midha et al., 2016). All these suggest that ethnicity plays a role in pancreatic cancer development (Midha et al., 2016).

### *Genetics*

The pancreas has the potential to develop different types of cystic neoplasms such as pancreatic intraepithelial neoplasms (PanINs), intraductal papillary mucinous neoplasms (IPMNs), serous cystadenomas (SCAs) and mucinous cystic neoplasms (MCNs) which can in turn develop into invasive pancreatic cancer with the exception of SCAs which are benign (Allen, 2017; Distler et al., 2014; Bulle et al., 2017). Some studies discovered that more than 96% of IPMNs have a GNAS complex locus or KRAS mutation and more than 50% of IPMNs have both. MCNs with low grade dysplasia have KRAS mutation while those with high grade dysplasia and invasive tumours have p16, TP53, SMAD4/DPC4 (Distler et al., 2014; Furukawa et al., 2011; Wu et al., 2011). There have been several unsuccessful trials targeting genes involved in pancreatic cancer in order to improve clinical outcomes. The early stages of pancreatic cancer is caused

by gene alterations or epigenetics yet the progress of the disease is mediated by the tumour microenvironmental factors such as hypoxia, angiogenesis and fibrous tissue (Bulle et al., 2017). Advancement of these lesions to cancer is due to the aggregation of genetic mutations.

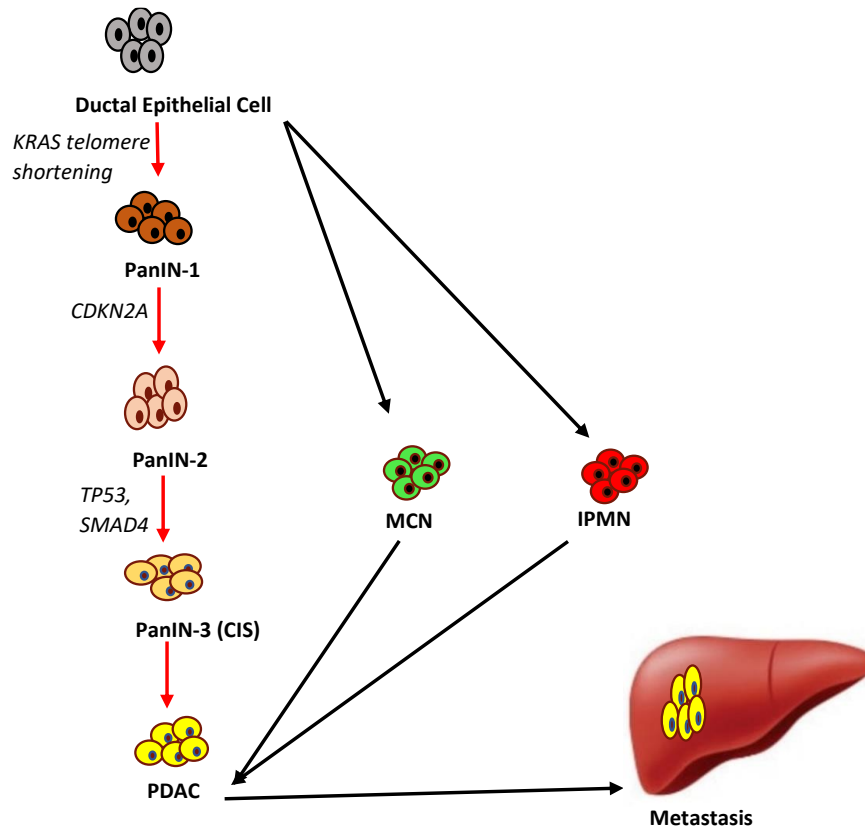


**Figure 1.2: Model showing genetic progression of pancreatic cancer.** Image shows step by step development of pancreatic cancer from epithelial cells PDAC arises from IPMNs, PanINs and MCNs (mucinous cystic neoplasm). PanIN-1 is developed by telomere shortening of an epithelial cell. Mutation of the CDKN2A converts panIN-1 to panIN-2 and the mutation of TP53 and SMAD4 converts panIN-2 to panIN-4.

Exome sequencing has proved that KRAS is the most commonly mutated gene in PDAC (95%). KRAS mutation on its own cannot cause cancer except with the presence of other gene mutations as shown in Figure 1.2 (Rozenfurt et al., 2018). Certain genes such as Von Hippel-Lindau syndrome and having family history of pancreatic cancer can predispose a person to pancreatic cancer (Maisonneuve, 2019). In most PDAC patients, the tumour suppressor gene p53 is completely inactivated while SMAD4 is mutated in 45% of PDAC patients (Nattress and Hallden, 2018). There are also epigenetic regulators which play significant roles in the

development of pancreatic cancer. Epigenetic regulation arises due to covalent modification of DNA or histones, nucleosome positioning and non-coding RNA (Sharma et al., 2010). The presence or absence of biomarkers for these epigenetic regulators can predict if a patient is predisposed to pancreatic cancer or not. This is because these genetic biomarkers expose downstream signalling pathways (Hung et al., 2019).

### **1.1.3.2 Screening and diagnosis**

Only 9% of pancreatic cancer patients are diagnosed at the initial stage while 52% are diagnosed at a late stage (Gzil et al., 2019). Patients experience a range of symptoms mostly at the later stage of the cancer depending on the size and location of the tumour. Some of these symptoms include nausea, upper abdominal pain, jaundice, digestive difficulty, fatigue, lower back pain, infection (Blum and Kloog, 2014), pruritus, dark urine and acholic stools (Razi et al., 2019). Many of these symptoms can be mistaken for those of minor ailments thereby contributing to the late diagnosis of pancreatic cancer. Most pancreatic cancer patients are diagnosed at stage III and IV while some are diagnosed during the autopsy after their death. This is because many patients remain asymptomatic till late stages of the disease (Rawla et al., 2019).

Pancreatic cancer can be diagnosed using magnetic resonance imaging (MRI), computed tomography (CT), positron-emission tomography (PET), ultrasound and nuclear scans. Some of these modalities such as CT scan and PET scan are used in combination (PET-CT) to improve the efficiency of the diagnosis (Idachaba et al., 2019). Biomarkers play a very important role in the early diagnosis and prognosis of PDAC (Rawla et al., 2019). The serum biomarker used widely for diagnosing PDAC is carbohydrate antigen 19-9 (CA19-9). Unfortunately, it is only elevated in roughly 65% of PDAC patients (Sturgeon et al., 2010). CA19-9 also increases in pancreatitis and other cancer types (Torres and Grippo, 2018).

Patients with acute pancreatitis have elevated levels of CA19-9 when there are additional health complications such as gall stones or biliary tract malignancies (Binicier et al., 2019). Other biomarkers less widely used for pre-invasive PDAC diagnosis are CA-50, SPAN-1, DUPAN-2, cell surface-associated mucins (MUC), carcinoembryonic antigen and heatshock protein (Rawla et al., 2019). Circulating tumour cells (CTCs) are cells which dislodge from the primary tumour and enter into the bloodstream. CTCs play a significant role in distant metastasis of PDAC (Pantel and Speicher, 2015). There are studies currently targeted to detect CTCs for PDAC diagnosis and prognosis (Torres and Grippo, 2018; Kulemann et al., 2017).

There is a pressing need for targets to help diagnose PDAC in its earlier stages to improve therapeutic response.

### **1.1.3.3 PDAC Stages**

The staging of PDAC is the assessment of the size and location of the tumour usually through clinical, radiographic or/and pathological means. According to the American Joint Committee on Cancer (AJCC), tumour staging is based on three factors: tumour size (T), degree of spread to lymph nodes (N) and degree of metastasis (M) (Allen et al., 2017).

PDAC can be subdivided into four main stages based on tumour size and metastatic status: stage I (2cm to < 4cm, no spread, surgically resectable followed by adjuvant chemotherapy), stage II (>4cm, locally spread, may be surgically resectable followed by adjuvant therapy), stage III (widely spread, managed with neoadjuvant chemotherapy) and stage IV (poor prognosis, managed with systemic/palliative therapy). PDAC patients can also be classified into 3 groups based on their performance status. Stage I with high performance status is treated with Abraxane and Folfirinox, Stage II with reduced performance status is treated with Abraxane and Erlotinib + gemcitabine while Stage III with poor performance status is treated with gemcitabine alone or gemcitabine + Abraxane (Razi et al., 2019; Rawla et al., 2019).

Therefore, an accurate diagnosis of the stage of a PDAC tumour determines the choice of treatment and overall survival (Adamska et al., 2017).

#### **1.1.4 Classification of PDAC**

##### **1.1.4.1 Anatomy of the pancreas**

In humans, the pancreas weighs 50 to 100g and is about 14 to 18cm long. It has 3 main parts; the head, the middle and the tail. The C-shaped head is aligned with the upper curvature of the duodenum. The body of the pancreas which has a flat shape lies horizontally beneath the stomach. It lies across the superior mesenteric artery and vein, abdominal aorta, inferior vena cava, and portal vein. The tail has contact with the hilum of the spleen (Dolensek et al, 2015). The two functional regions of the pancreas are the exocrine and the endocrine region. The exocrine region produces digestive enzymes such as lipases, proteinases and amylases that enter the small intestine through pancreatic ducts while the endocrine region (Islets of Langerhans) produces hormones like insulin. The endocrine islets comprise less than 5% of the pancreas yet are over a billion in number. Each of the five main islets secretes a different type of hormone. The  $\beta$ -cells produce insulin,  $\alpha$ -cells produce glucagon,  $\delta$ -cells produce somatostatin, F-cells produce pancreatic polypeptides and  $\epsilon$ -cells produce ghrelin as shown in Figure 1.3. The blood glucose levels are regulated by insulin and glucagon after they are released into the blood stream (Zhou and Melton., 2018; Ellis, 2013; McCarthy, 2010; Flannick and Florez, 2016). PDAC arises from both acinar and ductal cells (Xu et al., 2019).

Most pancreatic tumours (65%) occur in the head of the pancreas, 15% in the body, 10% in the tail and 10% occur in more than one location at a time. The hepatoportal venous drainage of the pancreas frequently makes the liver the first location for metastasis (Nattress and Hallden, 2018; Ghaneh et al., 2008).

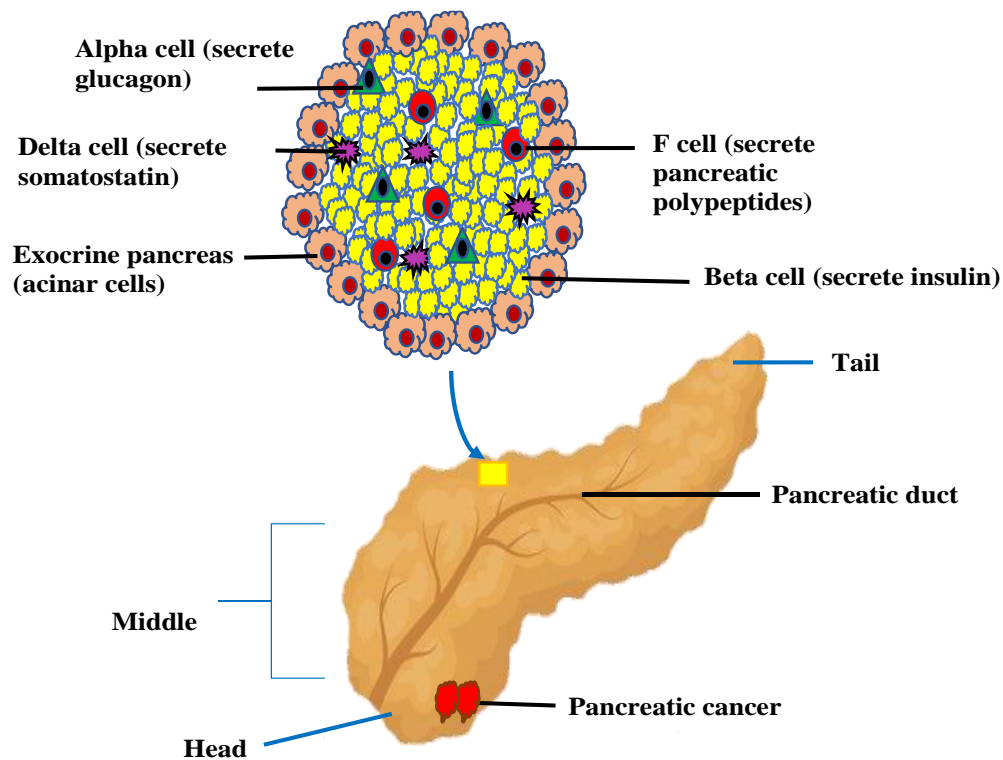


*Figure 1.3: Diagram showing the morphology of pancreas and its components. The pancreas consists of alpha cells, beta cells, delta cells, F-cells and acinar cells. The pancreas is divided into 3 sections namely; head, middle and tail. PDAC develops from acinar and ductal cells.*

#### 1.1.4.2 Pancreatic Cancer Histology

Pancreatic cancer can be divided into different histological subtypes: adenocarcinoma (85%), adenosquamous (0.38 – 10%), mucinous cyst adenocarcinoma (2%), intraductal papillary mucinous carcinoma (3%), acinar cell (<1%), spindle cell, undifferentiated (<1%) and pancreatoblastoma in young children (Borazanci et al., 2015). Ductal carcinomas mainly arise in the exocrine part of the pancreas while pancreatic neuroendocrine tumours (PNET) arise from the endocrine part of the pancreas (Zhou et al., 2018). PNETs constitute 1% to 2% of pancreatic cancers. About 60% to 90% of PNET patients are asymptomatic (Ma et al., 2020b).

#### 1.1.5 PDAC Management

The main techniques used for managing or treating pancreatic cancer are surgery, chemotherapy and radiotherapy (Tan et al., 2018).

### 1.1.5.1 Surgery

On rare occasions where PDAC is detected early, surgical resection can be used for complete removal of the tumour (Koninger et al., 2008). Patients with stages I and II PDAC are eligible for surgery. However, the 5-year survival rate for patients with tumours <2cm is 50% while those with tumours <1cm is about 100% (Ansari et al., 2014; Ansari et al., 2015).

The complete surgical removal of the tumour followed by adjuvant therapy is the most effective treatment for pancreatic cancer. The consideration for surgery depends on the venous involvement of the tumour. The different types of surgical resections are: pancreaticoduodenectomy (head/body of the pancreas and nearby organs are removed), distal pancreatectomy (tail, body and spleen), total pancreatectomy (whole pancreas and nearby organs) or palliative surgery (stent or bypass) which reduces symptoms associated with biliary and gastric outlet obstruction (American Cancer Society Surgery for Pancreatic Cancer, 2017). The most successful of these procedures is pancreaticoduodenectomy, also known as Whipple procedure which consists of: exploration, resection and reconstruction (Neoptolemos et al., 2001; Adamska et al., 2017). The late onset of symptoms in PDAC patients has resulted in only a small percentage of 15 to 20% being eligible for surgical resection after diagnosis. Unfortunately, despite the surgery, most of the patients suffer a relapse within a year (Zeng et al., 2019). Several factors affect surgical outcome such as the stage of the cancer, vascular invasion, completeness of resection, degree of differentiation and lymph node status. It is suggested however that patients with SMAD4 inactivation should avoid surgery because of the high tendency for their cancer to metastasize (Blackford et al., 2009b). After the surgery, pancreatic cancer patients must be given chemotherapy or radiotherapy to improve treatment outcomes (Hall and Goodman, 2019).

### **1.1.5.2 Radiotherapy**

Radiation has been shown to improve pancreatic cancer symptoms, boost probability for secondary resectability, extend survival time and suppress disease progression (Goldsmith et al., 2018). In response to ionizing radiation, normal and tumour tissues undergo inflammation or apoptosis depending on the dose and fractionation of the radiation (Formenti and Demaria, 2013). In tumour microenvironment, radiotherapy leads to cycling hypoxia, immune modulation, vascular regeneration, inflammation and fibrosis (Wang et al., 2019d). Radiation is an option for patients with inoperable tumours such as lung cancer (Ghita et al., 2019). There has been no significant improvement after patients with locally advanced unresectable pancreatic cancer (LAPC) are treated with standard doses of radiation (Reyngold et al., 2019). Unresectable LAPC has been observed in 35% of pancreatic cancer cases which is managed with surgery and the option of radiation. About a third of pancreatic cancer patients die before the cancer metastasizes proving that local control of the tumour can improve the quality of life of pancreatic cancer patients. One major challenge associated with administering radiotherapy to pancreatic tumours is that the pancreas is surrounded by radio sensitive gastrointestinal (GI) organs such as the stomach and duodenum which can develop GI toxicity if over irradiated. New radiation techniques like intensity-modulated radiotherapy (IMRT) helps to send high doses of radiation to a target organ while protecting the neighbouring organs (Goto et al., 2018; Nakamura et al., 2012; Yovino et al., 2011). Another radiation technique known as gamma knife stereotactic radiosurgery (GKSRS) which also focuses the radiation on the tumour while protecting surrounding tissues. GKSRS has been used to successfully treat brain metastasis (Wei et al., 2017).

### 1.1.5.3 Chemotherapy

Pancreatic cancer occurs at a rate which is almost equivalent to its mortality rate. The overall survival and clinical response of pancreatic cancer patients is increased by chemotherapy, with some drugs being more effective than others. Many of the molecular drugs designed for targeting pancreatic cancer have been unsuccessful at improving patients' lifespan (Tada et al., 2011). The drugs commonly used for managing pancreatic cancer are gemcitabine, 5-fluorouracil (5-FU), irinotecan, oxaliplatin, albumin-bound paclitaxel (Abraxane, nab-paclitaxel), cisplatin, paclitaxel (Taxol), docetaxel (Aslan et al., 2018) and folfirinox. These drugs are either used singly or in combination with other anticancer drugs (Zeng et al., 2019). Some drugs have a synergistic effect when combined leading to a decrease in the required drug concentrations (Sun et al., 2016). Folfirinox is a drug combination comprising of oxaliplatin, leucovorin, 5-fluorouracil and irinotecan. It is one of the first line treatments for PDAC (Adamska et al., 2018).

#### 1.1.5.3.1 Gemcitabine

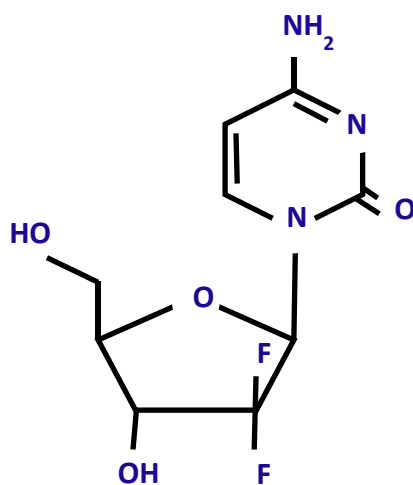


Figure 1.4: *Molecular structure of gemcitabine*

Gemcitabine (2',2'-difluoro-2'-deoxycytidine; dFdC), a prodrug is a nucleoside analog with multiple mechanisms of action. In addition to pancreatic cancer, dFdC is also used for treating breast, bladder and non-small cell lung cancer (de Sousa Cavalcante and Monteiro, 2014).

Patients are usually given high doses of dFdC after short intervals because of dFdC's short half-life in the body leading to a number of side effects (Aslan et al., 2018). In addition, dFdC is either used independently or in combination with other anticancer drugs such as 5-fluorouracil (Kurata et al., 2011). The structure of dFdC is shown in Figure 1.4 (Vande Voorde et al., 2015).

#### *Mode of dFdC action*

DFdC has different modes of action which include inhibiting DNA synthesis, inducing apoptosis and inhibiting enzymes involved in deoxynucleotide metabolism. In the cytoplasm, dFdC is phosphorylated by deoxycytidine kinase (dCK) to give the monophosphate (dFdCMP) which is then phosphorylated by pyrimidine nucleoside monophosphate kinase (de Sousa Cavalcante and Monteiro, 2014) to give gemcitabine diphosphate and gemcitabine triphosphate which are cytotoxic and competitive inhibitors of DNA polymerase. Gemcitabine triphosphate binds to DNA causing early termination of the DNA strand and failure of the DNA repair mechanism while gemcitabine diphosphate inhibits ribonucleotide reductase leading to decreased DNA synthesis (Zeng et al., 2019).

#### *Mechanism of dFdC resistance*

One of the mechanisms of gemcitabine resistance in pancreatic cancer is impaired control of proteins involved in gemcitabine metabolic pathways such as low expression of hENT1, low expression of HuR (Hu antigen R), decreased expression of dCK and overexpression of RRM1/RRM2 can lead to chemoresistance (Jia and Xie, 2015). Decreased expression of the nucleoside transporter, hENT1 can reduce dFdC uptake and lead to drug resistance as shown in Figure 1.5. Research has proved that the prognosis of patients with low hENT1 expression is poor. In some patients, the rate limiting enzyme for dFdC metabolism, dCK is either limited or poorly expressed leading to poor prognosis when treated with dFdC. The Hu antigen R

(HuR) is a protein which controls dCK levels after transcription. Cancer cells which overexpress HuR are 30 times more sensitive to dFdC and vice versa. Ribonucleotide reductase, the rate limiting enzyme during DNA synthesis, converts ribonucleotides to dNTPs which are paramount for DNA assembly and repair. Increased expression of ribonucleotide reductase can competitively inhibit gemcitabine triphosphate leading to chemoresistance. Epithelial to mesenchymal transition (EMT) has also been shown to enhance chemoresistance by activating genes like ZEB1 which enhance the activity of the more aggressive phenotype leading to decreased expression of nucleoside transporters to transport dFdC into cells (Mackey et al., 1998; Nakahira et al., 2007; Zeng et al., 2019). MiRNA are small non-coding RNA molecules of about 19 to 25 nucleotides in length that play a big role in the post transcriptional regulation of gene expression by reducing or blocking mRNA translation (Zhu et al., 2015). These MiRNA bind to target mRNA strands to form a defective complimentary strand. This causes the mRNA to be silenced or broken down leading to decreased level of the protein encoded by that mRNA in the body (Zeng et al., 2019). Studies have shown that MiRNAs can act as either an oncogene or tumour suppressor. Various studies have suggested that some miRNA such as miR-21, miR-15a, miR-23a and miR-27a act as tumour suppressors (Zhang et al., 2007; Li et al., 2016a). Increased expression of miR-210 has been shown to enhance chemosensitivity of dFdC (Zeng et al., 2019). Genetic aberrations can cause the NF $\kappa$ B, AKT, MAPK, HIF1 $\alpha$ , hedgehog, notch and Wnt pathways to create gemcitabine resistance (Jia and Xie, 2015). Ribonucleotide reductase (RR) is a rate limiting enzyme which plays an important role in DNA synthesis and repair. RR has the subunits M1 and M2. Some studies have shown that elevated expressions of RRM1 and RRM2 in pancreatic cancer led to gemcitabine resistance (Wang et al., 2015a; Nakahira et al., 2007; Zeng et al., 2019). High levels of RR increase dNTP synthesis and competitively inhibits dFdCTP incorporation to DNA. The elevated levels of dNTP cause negative feedback regulation by decreasing gemcitabine phosphorylation (Zeng et

al., 2019; Nakahira et al., 2007; Goan et al., 1999). High expression of drug efflux pumps like ABC transporters which have an elevated expression rate in CSCs can also lead to dFdC resistance (Jia and Xie, 2015). In tumour micro environment, the dense desmoplastic stroma of pancreatic cancer leads to rigidity and prevents dFdC circulation within the tumour (Du et al., 2020). Cancer associated fibroblasts (CAFs) metabolize dFdC to dFdCTP thereby contributing to chemoresistance. The inability of dFdCTP to pass through the cell membrane causes it to scavenge dFdC leading to decreased tumoral drug concentration (Orth et al., 2019; Hessmann et al., 2018).

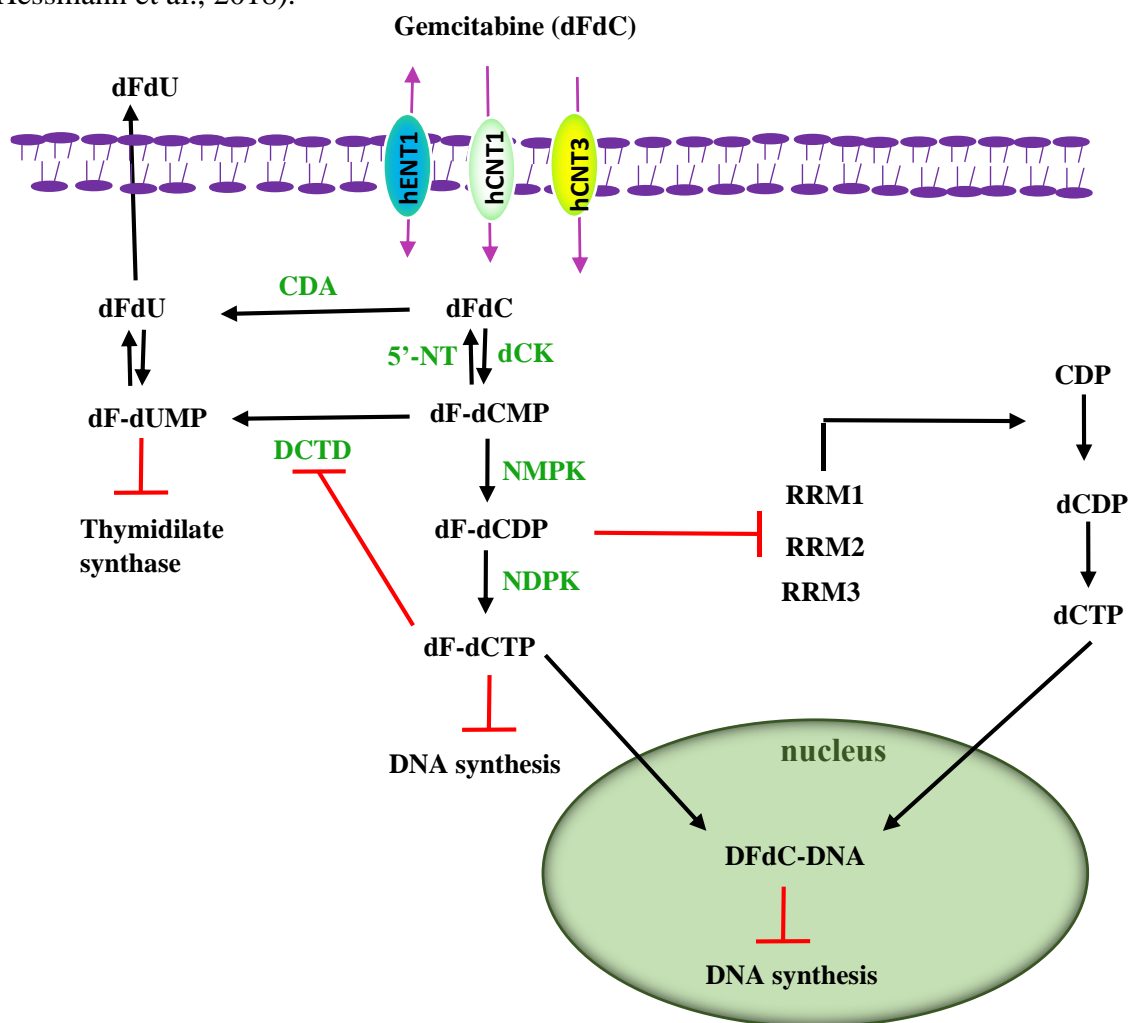


**Figure 1.5: Mechanism of chemoresistance of dFdC.** Gemcitabine is transported into the cell by hENT1 where intermediates of dFdC inhibit mRNA translation. dCK= deoxycytidine kinase, hENT & hCNT= nucleoside transporters, CDA= cytidine deaminase, NDPK= nucleoside diphosphate kinase, DCTD= deoxycytidylate deaminase, NMPK= nucleoside monophosphate kinase, RRM= ribonucleotide reductase, 5'NT= 5'-nucleotidase.

### 1.1.5.3.2 Paclitaxel

Paclitaxel (PTX) is a hydrophobic anticancer drug with a high molecular weight of 853.9 and low solubility in water (Stage et al., 2018). PTX was first isolated from the Pacific yew tree in the 1960s. PTX whose molecular structure is shown in Figure 1.6, is a member of the taxane family of microtubule inhibitors which suppresses mitosis and initiates apoptosis in tumour cells. PTX has been used in the treatment of a wide range of cancers such as non-small cell lung cancer, cervical cancer, breast cancer, endometrial cancer, bladder cancer, etc. Excretion of PTX is mainly through faeces. Numerous studies have shown that the anticancer effect of PTX is enhanced when administered in combination with some other anticancer drugs. After PTX administration, patients tend to experience nausea, vomiting, loss of appetite, neutropenia and thrombocytopenia (Khanna et al., 2015; Ozols, 2000).

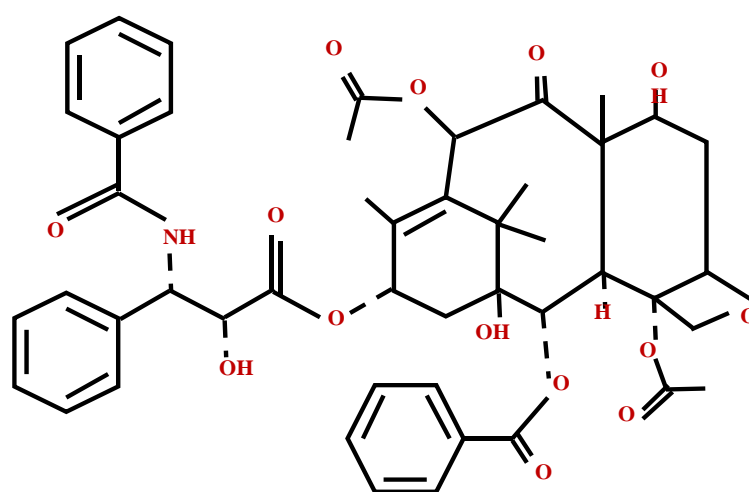


Figure 1.6: Molecular structure of PTX

### Mode of PTX action

Tubulin has  $\alpha$  and  $\beta$  heterodimers which play important roles in many cellular processes. The  $\beta$ -tubulin isotypes ( $\beta$ III and  $\beta$ IV) have elevated expression in pancreatic cancer but is not expressed in a healthy pancreas (Lee et al., 2007; McCarroll et al., 2015; Kashyap et al., 2019).

The assembly of microtubules requires GTP-charged  $\beta$ -tubulin. This complex is hydrolyzed when tubulin dimer is added to elongating microtubule making the GTP non-exchangeable. Microtubules comprise of GDP- $\beta$  tubulin or GTP- $\alpha$  tubulin with the growing end capped with GTP (or GDP·P<sub>i</sub>); $\beta$ -tubulin which stabilizes the microtubules. The loss of the GTP cap causes rapid depolymerization of the microtubule (Nogales, 2000; Orr et al., 2003). In the body, PTX is degraded into 6-hydroxypaclitaxel and 3-phenyl hydroxyl paclitaxel (Stage et al., 2018). PTX affects microtubules which are required for mitotic spindle formation during cell division. These microtubules play important roles in the maintenance of cell structure, motility and cytoplasmic movement (Kampan et al., 2015). PTX decreases the critical concentration of tubulin subunits required for microtubule polymerisation leading to cell death (Weaver, 2014). PTX attaches itself to polymeric tubulin causing the stabilization of microtubules and hinders tubulin disassembly. This prevents metaphase-anaphase transitions which stops mitosis and apoptosis (Amos and Lowe, 1999; Khanna et al., 2015). PTX promotes the assembly of stable microtubules and suppresses their depolymerisation which hinders cell division leading to apoptosis as shown in Figure 1.7. Paclitaxel initiates many signal transduction pathways linked to proapoptotic signalling. Paclitaxel has been linked to TLR-4 dependent pathway, c-Jun N-terminal kinase, P38 MAP kinase, NF $\kappa$ B, JAK signal transducer and STAT pathway. Paclitaxel uses the MAPK pathway to dephosphorylate Bad and Bax, and phosphorylate Bcl2 leading to apoptosis. Weekly PTX has also been shown to inhibit VEGF expression (Kampan et al., 2015; Wang et al., 2006; Yakirevich et al., 2006; Szakacs et al., 2006; Pfannenstiel et al., 2010). However, PTX is only effective on cells which have undergone mitosis. There are many hypotheses concerning its mode of action (Weaver, 2014).

## Mechanisms of PTX resistance

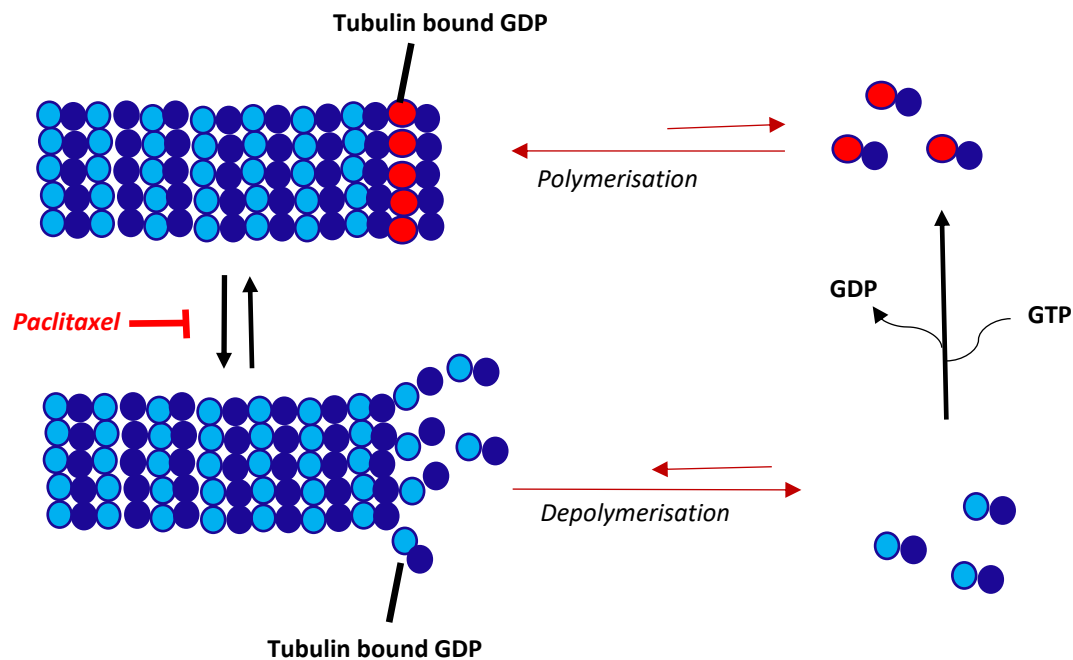


**Figure 1.7: Mechanism of chemoresistance of PTX.** PTX binds to the inner surface of  $\beta$ -tubulin microtubules, causing depolymerisation which leads to apoptosis.

The efficacy of PTX is affected by an overexpression of ATP-Binding Cassette (ABC) transporters which actively pumps drugs out of the cell leading to acquired resistance to the drug (Eom et al., 2019). Cancer cells resist PTX by modifying the tubulin through mutations, isotype selection and post-translational alterations of tubulin and associated regulatory proteins (Khanna et al., 2015). PTX has poor solubility issues (Adamska et al., 2018). Nab-paclitaxel is a form of PTX coated with albumin to boost transport of PTX into the tumour compared to uncoated PTX. It is hypothesized that the accumulation of nab-paclitaxel in PDAC is due to the stromal fibroblasts around the PDAC tumour which excessively express secreted protein acidic and rich in cysteine (SPARC) that binds strongly to albumin. Nab-paclitaxel enhances gemcitabine transport into PDAC tumours by deactivating cytidine deaminase (Zhang et al., 2015). KRAS mutations are strongly suspected to be involved in dFdC and nab-paclitaxel

resistance (Grasso et al., 2017; Yardley et al., 2013). A study showed that after administration of dFdC and nab-paclitaxel, the growth of the cancer cell population was suppressed by 67% and 72% respectively (Giordano et al., 2017).

#### *1.1.5.3.3 5-Fluorouracil*

The realization that rat hepatomas utilised uracil rapidly than normal tissues led to the development of fluoropyrimidine-based drugs such as 5-fluorouracil (5-FU) in the 1950s. The molecular structure of 5-FU is shown in Figure 1.8 (Longley et al., 2003). 5-FU is an analogue of S-phase specific uracil and large quantities of intracellular 5-FU in tumour cells initiates apoptosis (Adamska et al., 2018).

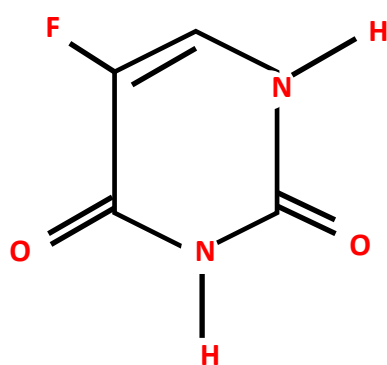


*Figure 1.8: Molecular structure of 5-Fluorouracil*

#### *Mode of 5-FU action*

5-FU is a pyrimidine analog which carries out its anticancer therapeutic effect by inhibiting thymidilate synthase and the binding of its intermediate to DNA and RNA. A metabolite of 5-FU, 5-fluorodeoxyuridine monophosphate (5-FdUMP) binds to thymidylate synthase and suppresses its activity leading to the production of deoxythymidine monophosphate (dTMP) (Wang et al., 2014). In the body, 5-FU dissociates into fluorodeoxyuridine monophosphate (FdUMP), fluorouridine triphosphate (FUTP) and fluorodeoxyuridine triphosphate (FdUTP) which interfere with RNA synthesis and TS activity. During 5FU catabolism, the rate limiting

enzyme dihydropyrimidine dehydrogenase (DPD) catalyses the conversion of 5FU to dihydrofluorouracil (DHFU) (Diasio et al., 1989; Longley et al., 2003). TS catalyses the conversion of dUMP to dTMP which produces thymidylate required for DNA repair and replication (Longley et al., 2003). 5-FU suppresses RNA synthesis by converting to 5-fluorouridine 5'triphosphate (FUTP) which binds to RNA. 5-FU also eliminates tumour cells by ROS production, overexpression of phospho-Bcl2 and caspase-6 activation. Phase 3 studies revealed that the one-year survival rate of patients treated with gemcitabine was 9-fold greater than those treated with 5-FU (Adamska et al., 2018). There is an oral version of 5-FU known as S-1 with increased anticancer activity. S-1 consists of tegafur (prodrug of 5-FU), gimeracil and oteracil in the ratio of 1:0.4:1. After oral administration, the liver converts tegafur to 5-FU, then gimeracil prevents 5-FU degradation and oteracil suppresses the phosphorylation of 5-FU in the gastrointestinal tract. Pancreatic cancer patients treated with a combination chemotherapy of gemcitabine and S-1 have increased median survival of 7.89 to 12.5 months (Sudo et al., 2014).

#### *Mechanism of 5-FU resistance*

Multidrug resistance proteins (MRP) can cause ATP-dependent drug efflux intracellularly leading to chemoresistance. 5-FU initiates the overexpression of FOXM1 which in turn increases the expression of ABC10, a member of the MRP superfamily causing 5-FU resistance. Many cancer cells express ABCB1 which plays a big role in multidrug resistance (Blondy et al., 2020). Patients with thymidylate synthase overexpression are resistant to 5-fluorouracil therapy because elevated TS levels displaces FdUMP. In response to DNA damage, tumour suppressor gene, p53 activates the pro-apoptotic genes BAX and FAS. However, some clinical studies show that 5-FU reduces the stability of p53 through an unknown mechanism leading to drug resistance. Microsatellite instability (MSI) is an inherited mutation which results in the inability of MMR to correct errors in DNA. Patients with MSI-

negative tumours respond poorly to 5FU treatment. Research has shown that patients who are deficient in dihydropyrimidine dehydrogenase have reduced ability to catabolise 5FU leading to acute toxicity. The enzyme thymidine phosphorylase reversibly catalyses the conversion of 5-FU to 5-fluorodeoxyuridine which is further converted to FdUMP as shown in Figure 1.9. The level of thymidine phosphorylase in a tumour is said to play a role in its sensitivity to 5-FU. However, there are contradictions as to whether high levels of thymidine phosphorylase increase or decrease 5-FU sensitivity in tumours (Longley et al., 2003).

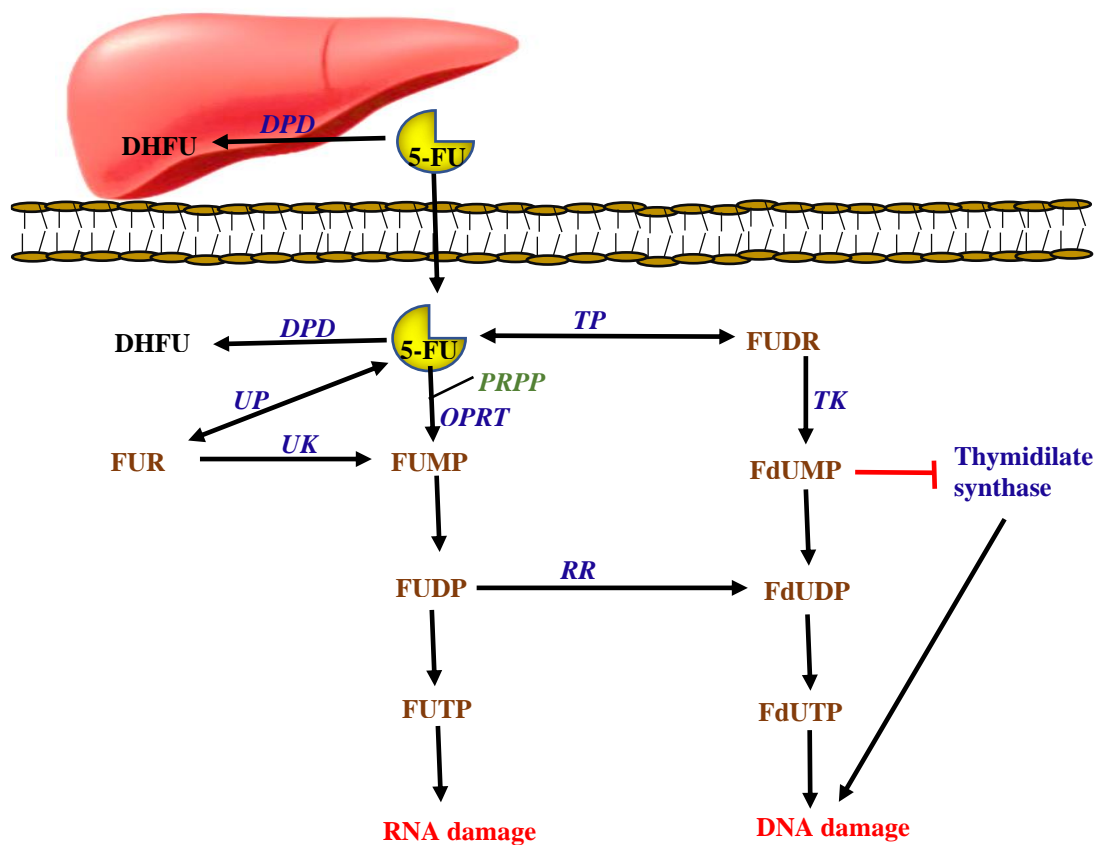


**Figure 1.9: Mechanism of chemoresistance of 5-Fluorouracil.** After administration, most of the 5-FU is converted into dihydrofluorouracil (DHFU) by dihydropyrimidine dehydrogenase (DPD). The remaining 5-FU is transported across the cell membrane and converted into FdUMP by either orotate phosphoribosyltransferase (OPRT) using phosphoribosyl pyrophosphate as a cofactor or fluorouridine (FUR) using uridine phosphorylase (UP) and uridine kinase (UK). FUMP is phosphorylated to FUDP which is further converted to FUTP. FUDP can also be converted into fluorodeoxyuridine diphosphate (FdUDP) by ribonucleotide reductase (RR) (Longley et al., 2003).

## **1.2 Drug Resistance in PDAC**

### ***1.2.1 PDAC tumour microenvironment***

The stroma-rich microenvironment in PDAC makes up 90% of the tumour mass. This microenvironment nourishes the PDAC cells and protects them from the body's immune system and chemotherapy by forming a thick, protective and fibrous tissue layer around the tumour cells (Neesse et al., 2011; Bulle et al., 2017; Feig et al., 2012). The microenvironment also gives the PDAC cells the ability to metastasize to other organs and tissues. The stroma contains many components which aid tumour growth such as growth factors, fibroblasts, blood vessels, immune cells, myofibroblasts, extracellular matrix and cytokines. The microenvironment is also hypoxic and of low pH (Bulle et al., 2017; Kleef et al., 2007). The low oxygen resulting from reduced blood supply leads to increased levels of growth factors such as VEGF and angiopoietin which initiates angiogenesis. However, the new blood vessels formed have defects and leak leading to an increase in interstitial fluid pressure in the tumour (Bulle et al., 2017; Chauhan et al., 2014). The thick fibrotic stroma of PDAC is called desmoplasia with a cellular portion that originates from pancreatic stellate cells that are stimulated by alcohol, growth factors and cytokines (Nielson et al., 2016; Erkan et al., 2012). Prior research on animal models has shown that removing the desmoplasia results in the tumour becoming more aggressive (Chen et al., 2018). The most common cell type in the stroma of pancreatic cancer is cancer associated fibroblasts (CAF) (Ostman and Augsten, 2009; Kalluri and Zeisberg, 2006; Pietras and Ostman, 2010). CAFs provide growth factors, cytokines and hormones which initiate tumour cell growth (Bhowmick et al., 2004; Pietras and Ostman, 2010). CAFs produce different types of collagen, insulin-like growth factor 1 and insulin like growth factor 2 in the extracellular matrix (ECM). With the exception of VEGF-A, stromal cells produce more quantities of angiogenic inducers than cancer cells. CAFs produce TGF $\beta$  and HGF which triggers the process of epithelial to mesenchymal transition (Pietras and

Ostman, 2010). Preclinical studies have shown that using hedgehog signalling inhibitors or enzymatic digestion of the ECM (hyaluronidase) to disrupt pancreatic stroma leads to tumour growth inhibition and enhanced drug delivery (Ogier et al., 2018). PDAC microenvironment causes a dysfunctional vasculature that increases stromal interstitial pressure thereby reducing drug distribution within the tumour. Furthermore, stromal cells promote EMT and affect gene expression (Nattress and Hallden, 2018).

Pancreatic tumours also contain numerous pancreatic stellate cells (PSCs). Activated PSCs are precursors of CAFs which boosts the formation of the fibrotic stroma that aids metastasis. A certain study showed that targeting PSCs improved the effectiveness of chemotherapy (Han et al., 2018). In addition to CAFs, the desmoplastic stroma of PDAC also contains many nerve fibres. This is linked to pancreatic cancer-associated neural remodelling (PANR) which is suspected to be the reason for the chronic pain felt by PDAC patients (Roger et al., 2019; Bapat et al., 2011). However, there is a phenomenon known as perineural invasion (PNI) where cancer cells infiltrate nerve fibers causing pain and metastasis in pancreatic cancer patients (Roger et al., 2019; Bapat et al., 2011).

### **1.2.2 Increased activity of drug efflux transporters**

One major challenge of chemotherapy in cancer treatment is that drug efflux transporters pump the drug out leading to reduction of the effective drug concentration in the cell (Gottesman et al., 2002; Garofalo et al., 2013). ABC transporters are the main transmembrane transporters involved in drug efflux. Humans have 48 ABC genes and 7 subfamilies. ABCB1 (P-gp or MDR1), ABCC1 and ABCG2 are greatly involved in the development of multidrug resistance (MDR) to chemotherapy (Wang et al., 2019c). ATP-binding cassette (ABC) membrane transporters transport drugs from the cytosol to the extracellular space (Garajova et al., 2014) through the cell membrane against a concentration gradient using ATP as an energy source.

The primary role of ABC transporters is detoxification and to protect cells from oxidative stress and xenobiotics (Begicevic et al., 2017; Quinonero et al., 2019). However, during ABC transporter-mediated detoxification, drugs escape from the cell with the aid of the receptors: MDR1, BCRP and MRP1 leading to chemoresistance (Fletcher et al., 2016; Quinonero et al., 2019). In PDAC, there is an overexpression of MRP4 which promotes tumour growth and colony formation of cancer cells (Zhang et al., 2012; Quinonero et al., 2019). P-glycoprotein (P-gp) is a multidrug efflux pump whose overexpression is as a result of the activation of the MDR1 gene (Garajova et al., 2014). Arginine methyltransferase 3 (PRMT3) increases ABCG2 by binding to ABCG2 mRNA, thereby promoting PDAC chemoresistance to gemcitabine (Luo et al., 2019).

### **1.2.3 Modification of Drug Targets and DNA Repair**

Creating DNA damage is the main mode of action of many anticancer drugs. However, these damaged cells have a DNA damage response (DDR) mechanism which protects them leading to chemoresistance (Wang et al., 2019c). DNA repair usually happens immediately after DNA damage to prevent transfer of inaccurate genetic information during cell division. The malfunction of the DDR mechanism leads to accumulation of genetic defects, cancer development and progression, and more damage to the DDR mechanism (Li et al., 2016b). About 10% of pancreatic cancers occur in patients who have had at least 2 first degree relatives affected by the disease (Klein et al., 2004; Perkhofer et al., 2021). The genes associated with inherited DDR mutations are BRCA1, BRCA2, ATM, PMS2, MLH1, MSH2 and STK11 while those generally associated with tumour formation are CDKN2A and TP53 (Perkhofer et al., 2021). Ribonucleotide reductase subunit 2 (RRM2), an important target of dFdC, is regulated by miR-211 which has elevated levels in PDAC patients with longer overall survival (Giovannetti et al., 2012). Let-7 reduces the expression of RRM2 in dFdC-resistant PDAC cells. The level of deoxyadenosine triphosphate is depleted when ribonucleotide reductase is

suppressed by dFdC, leading to errors in DNA replication (Matthaios et al., 2011). Changes in MMR reduces the therapeutic ability of 5-FU by affecting the binding of 5-FU metabolites into DNA which arrests G2/M and initiates apoptosis (Garajova et al., 2014).

Chemoresistance is also caused by mutation or change in expression levels of drug targets (Garofalo et al., 2013). Some chemotherapy eliminates cancer cells by suppressing the activity of target proteins involved in cancer progression making them less harmful to non-cancerous cells. Unfortunately, this targeted drug therapy can cause target proteins to undergo epigenetic alterations or secondary mutations which modify the target protein leading to chemoresistance (Wang et al., 2019c).

#### **1.2.4 Aberrant Regulation of the Cell Cycle**

Cell cycle is a well-organized pathway through which cells duplicate and multiply. Interphase and mitosis are the two main phases of cell cycle in eukaryotic cells. The interphase consists of 3 subphases: G1, S and G2. The S phase involves the start and end of DNA replication, making it the critical point targeted by a lot of chemotherapy drugs (Sun et al., 2021). The regulation of cell cycle is tightly controlled by numerous cyclin dependent kinases (CDKs) which function together with their cyclin partners. The activity of these CDKs can be suppressed by the activation of cell cycle checkpoints after DNA damage (Otto and Sicinski, 2017). In cancer cells, the cell cycle is modified leading to rapid cell proliferation as a result of the mutation of regulator genes such as p16 and cyclin D1 which control the phosphorylation of retinoblastoma protein (RB) and control exit from the G1 phase of the cell cycle or the tumour suppressor (Sherr et al., 2000; Garajova et al., 2014). A study using IHC showed that 68% of pancreatic cancer specimens had an elevated expression of cyclin D1, proving that cell cycle mutations play a big role in pancreatic cancer occurrence. In addition, overexpression of cyclin D1 is associated with poor prognosis in pancreatic cancer. The overexpression of p21<sup>Cip1</sup>

is a common occurrence in the early stages of pancreatic neoplasia (Mikhail et al., 2015). Cyclin-dependent kinase inhibitor 1B (CDKN1B) is a cell cycle inhibitor and tumour suppressor which is a direct target of miR-221 whose expression is elevated in PDAC cells (Garajova et al., 2014).

### **1.2.5 Evasion of apoptosis**

One of the major ways aggressive tumours become chemoresistant is by evading apoptosis (Garajova et al., 2014). Apoptosis is a well-controlled process used to maintain tissue homeostasis (Westphal and Kalthoff, 2003). Apoptotic cells undergo cell shrinkage, chromatin condensation and ruffling of the plasma membrane (Samm et al., 2010). There are two main apoptosis pathways. The extrinsic pathway is regulated by death receptors of the tumour necrosis factor (TNF)-receptor family. The intrinsic pathway is regulated by Bcl-2 proteins (Garajova et al., 2014). Dysregulation of the apoptotic pathway could cause tumorigenesis. Most chemotherapy and radiotherapy drugs induce apoptosis in cancerous cells so defects in the apoptotic pathway can lead to chemoresistance (Westphal and Kalthoff, 2003). Some cancer cells have elevated expression of anti-apoptotic proteins which enables them to evade apoptosis (Garajova et al., 2014). Bcl2, Bcl-xL, Bcl-w and Mcl-1 are anti-apoptotic proteins which inhibit apoptosis in cancerous cells by sequestering and preventing the oligomerization of the pro-apoptotic proteins Bax and Bak. It has been observed that many cancers have an upregulation of Bcl2 and Bcl-xL (Hari et al., 2015). Even though the intrinsic and extrinsic apoptotic pathways are initiated by different factors, both can be controlled by specific MiRNAs (Garajova et al., 2014). MiR21 activates the overexpression of Bcl2 thus inhibiting apoptosis, creating chemoresistance to gemcitabine and proliferation of MIA PaCa-2 cells (Dong et al., 2011; Garajova et al., 2014). In a certain study, verticillin A, a selective histone methyltransferase (HMTase) inhibitor caused gemcitabine treatment to enhance apoptosis in PDAC cells (Luo et al., 2019).

### 1.2.6 PDAC signalling pathways

There are many signalling pathways in PDAC which play significant roles in chemoresistance such as Notch, TGF- $\beta$ , SMAD, epidermal growth factor receptor (EGFR), mitogen-activated protein kinases (MAPK), SDF-1/CXCR4 pathway, JAK/STAT, Hedgehog, PI3K, RAS, NF $\kappa$ B, c-Met and WNT- $\beta$ -catenin (Luo et al., 2019). The gene for activating KRAS mutation is present in more than 90% of PDAC patients. RAS GTPases promote GTP hydrolysis and reversal of the RAS activation step under normal conditions. However, in cancerous cells, GAP proteins cannot stop the activating mutated RAS. KRAS controls the expression of miR-21, an MiRNA whose expression levels correlates with the degree of aggressiveness of the tumour. Elevated levels of miR-96 decrease KRAS expression leading to reduced tumour growth (Garajova et al., 2014).

RAS/MAPK and PI3K/AKT signalling pathways, and VEGFR are activated by growth factors such as EGFR and elevated in PDAC. The signals from these receptors have been shown to elevate receptor tyrosine kinase and activate RAS proteins. Porphyrins stop EMT and inhibit tumour growth thereby strongly suppressing metastasis. Notch signalling in PDAC stimulates KRAS leading to cell proliferation, metastasis and tumour progression (Luo et al., 2019). The inhibition of Akt increases the apoptotic effect of anticancer drugs on pancreatic cancer cells (Muilenburg et al., 2014). In PDAC, the activation of the phosphatidylinositol-3 kinase (PI3K)/AKT pathway controls the antiapoptotic proteins: BAD, Caspase-9 and Bcl-xL. In addition, the activity of NF $\kappa$ B, FOXO and c-myc is regulated by Akt in PDAC (Hamacher et al., 2008). Anticancer drugs which target PI3K/AKT/mTOR pathways are combined with gemcitabine, they decrease pAKT expression leading to apoptosis (Garajova et al., 2014; Li et al., 2009).

### 1.2.7 MicroRNAs

MicroRNAs (miRNA) comprises of a family of small non-coding RNA that control gene expression through MiRNA degradation or translatory inhibition in many biological processes, leading to gene silencing. In pancreatic cancer, miRNA can either act as tumour promoters or tumour suppressors (Daoud et al., 2019; Pu et al., 2020). In cancer, miRNAs control the expression of numerous genes and signalling pathways involved in tumour progression by interacting with the 3'untranslated region of mRNAs (Zhao et al., 2018). MiRNAs initiate tumour progression through many mechanisms such as cancer stemness, EMT, matrix metalloproteases (MMP) and a vast number of signalling pathways (Hu et al., 2018). MiRNAs can cause protein degradation or halt protein synthesis by interacting with a complementary mRNA sequence (Yan et al., 2018). Several recent studies have shown that microRNAs which play a significant role in tumorigenesis, break off from the original tumour and circulate in the serum of the patient. Surprisingly, these miRNAs are not degraded by endogenous RNase in the blood stream and can be used for detecting and monitoring PDAC (Morimura et al., 2011). MiRNA targets multiple mRNAs. MiRNA can regulate self-renewal and differentiation of stem cells, and play a significant role in CSC maintenance. The MiR-34 family is a tumour suppressor which plays significant roles in apoptosis, invasion, EMT, stemness, differentiation and cell cycle (Bonetti et al., 2019). MiR-34a is a strong suppressor of cell growth, invasion, self-renewal and EMT in human PDAC and pancreatic CSCs (Garajova et al., 2014). Increasing evidence have shown that miR-21 is upregulated in PDAC and plays a big role in dFdc resistance. In addition, inhibition of miR-21 led to a decrease in tumour progression of PDAC, breast and hepatocellular cancers (Giovanetti et al., 2010; Dillhoff et al., 2008; Zhang et al., 2020a). One miRNA that leads to invasion and metastasis of pancreatic cancer is miR-367 (Zhu et al., 2015). Another MiRNA which plays a significant role in cancer is MiRNA629. Its levels are said to be upregulated in pancreatic cancer cells and downregulating miRNA629

reduced cell proliferation and metastasis in pancreatic cancer cells. MiR-629 achieves this by negatively regulating FOXO3 (Yan et al., 2017), a protein which initiates apoptosis. An MiRNA of interest is mir-506 with a highly methylated promoter unlike in non-cancerous tissues. MiR-506 hinders rapid cell growth so a decrease in its expression levels correlates with poor prognosis and advanced tumour stage in pancreatic cancer patients. MiR-506 is thought to inhibit tumour formation by suppressing the expression of sphingosine kinase 1 thereby blocking NFκB and Akt pathway (Li et al., 2016a).

### **1.2.8 Autophagy**

Autophagy is a tightly controlled catabolic process that tucks away mutated proteins, damaged and old organelles from the cytoplasm into vesicles known as autophagosomes which bind to lysosomes, leading to the digestion of the tucked away proteins (Onorati et al., 2018). There are limited oxygen and nutrients in a tumour microenvironment leading to accumulation of lactic acid which causes the tumour microenvironment to be hypoxic and acidic. Tumour cells adapt to the acidic and hypoxic microenvironment by intracellular degradation and autophagy (Ma et al., 2020a). In the presence of stress, autophagy maintains tissue and organ homeostasis (Fiorini et al., 2015). In pancreatic cancer, autophagy has a dual role of either promoting cell death or aiding cell survival (Fiorini et al., 2015). Onconase activates Beclin1-mediated autophagic cell death thus making PDAC cells sensitive to gemcitabine (Fiorini et al., 2015; Luo et al., 2019). Hypoxia initiates the expression of autophagy-related genes such as Beclin-1, ATG5, ATG7 and ATG12 resulting in the amassing of several autophagosomes (Ma et al., 2020a). MiR-29a blocks autophagy by suppressing autophagy flux and decreasing the expression of autophagy proteins such as TFEB and ATG9A which in turn reduces pancreatic cancer cell invasion and sensitises tumour cells to gemcitabine. Two autophagy inhibitors are genetic inhibition (RNAi) and pharmacologic inhibition (chloroquine). Chloroquine is originally used for malaria treatment but in cancer treatment, it is used to elevate intralysosomal

pH and disrupt lysosomal autophagosome degradation. Recent studies have revealed that chloroquine is more effective as an anti-autophagic drug when administered in combination with other anticancer drugs (Luo et al., 2019; Kwon et al., 2016).

### **1.3 Hypoxia**

Hypoxia refers to oxygen levels which are below 1.5% while normoxia correlates with atmospheric oxygen pressure or 20% oxygenation of cell culture (Shah et al., 2020). Hypoxia is the main force behind cancer metastasis. Hypoxia stabilizes and activates HIFs which in turn activates the genes responsible for tumour proliferation, EMT and metastasis (Wang et al., 2018). The hypoxic microenvironment and the hypoxia driven EMT are suspected to be the key players for tumour progression and metastasis in pancreatic cancer (Li et al., 2017). Activated HIFs in turn lead to activation of a large number of downstream transactivating genes that encode for glucose transporters and glycolytic enzymes (Tan et al., 2020). Cancerous tumours continuously increase in size till the blood vessels are unable to supply enough blood with oxygen around the tumour. This leads to development of regions which are deficient in oxygen and results in the cancer cells stimulating some responses to enable them adapt to their new environment. The first response is usually the activation of hypoxia inducible factor- $\alpha$  (HIF- $\alpha$ ). These responses include initiating angiogenesis, modification of glucose metabolism, adjusting to acidic pH, inhibition of genes involved in apoptosis via BCL2 and increased activity of genes involved in metastasis (Strese et al. 2013). Most solid tumours are hypoxic in nature leading to increased tendency for cell proliferation, metastasis and chemoresistance (Sun et al., 2020). There are two types of tumoural hypoxia: acute and chronic. In acute hypoxia, there is poor blood circulation between tumour tissues and nearby blood vessels while chronic hypoxia occurs in cells which are farthest from blood vessels and lacking blood supply within a tumour. Cells with acute hypoxia have high levels of HIF1 $\alpha$  while those with chronic hypoxia have higher levels of HIF2 $\alpha$  (Najafi et al., 2020). PDAC has a dense stroma leading to elevated

intratumoral interstitial fluid pressure which in turn causes decreased tissue perfusion, vascular compression and hypoxia (Jiang et al., 2020).

### ***1.3.1 Hypoxia and HIFs***

The transcription factors which play critical roles in intracellular oxygen signalling pathways are called hypoxia inducible factors (HIFs). In the presence of oxygen, HIFs are hydroxylated then degraded by ubiquitination (Sun et al., 2020; Najafi et al., 2020) while in the absence of oxygen, HIFs translocate into the nucleus where they bind with hypoxic response elements to transcribe target genes as shown in Figure 1.11 (Sun et al., 2020). HIFs have 3 alpha subunits known as HIF1 $\alpha$ , HIF2 $\alpha$  and HIF3 $\alpha$ . The role of HIF3 $\alpha$  is unknown however, HIF2 $\alpha$  plays a more important role in disease progression than HIF1 $\alpha$  (Heddleston et al., 2010).

Semenza discovered HIF1 in 1992 which has an  $\alpha$ -subunit that is sensitive to oxygen and a stable  $\beta$ -subunit. These subunits break down in the presence of oxygen (Tirpe et al., 2019). Cancer cells have deregulated HIF activity which cause changes in energy metabolism and protects cells from hypoxia-induced cell death. In the presence of oxygen, HIF1 $\alpha$  and HIF2 $\alpha$  are steadily hydroxylated by prolyl-hydroxylase enzymes (PHD-1-4). The hydroxylated HIF $\alpha$  binds to von Hippel-Lindau (VHL) protein leading to ubiquitination and degradation by 26S proteasome<sup>1</sup>. However, in hypoxic conditions, PHDs are inhibited leading to the stabilization of HIF1 $\alpha$  and HIF2 $\alpha$  and their subsequent translocation to the nucleus where they form complexes with HIF $\beta$  and activate many hypoxia responsive genes.

In hypoxic condition, there is reduced cellular energy production causing a decrease in protein translation (Ivanova et al., 2019). The PHD enzymes require oxygen as a substrate. After hydroxylation, HIF- $\alpha$  is recognized by the von Hippel-Lindau (VHL) tumour suppressor protein, an E3 ubiquitin ligase complex member, resulting in HIF-1 $\alpha$  ubiquitination, targeting to the proteasome and degradation (Mylonis et al., 2019). HIF1 and HIF2 regulate oxygen

homeostasis and their alpha subunit is responsible for their stability and activation. A HIF3 isoform known as IPAS1 is suspected to suppress hypoxia induced gene expression. In the hereditary genetic condition known as von Hippel–Lindau’s disease/syndrome, there are elevated levels of HIF1 and HIF2 proteins in the body of the patient (Martin et al., 2011).

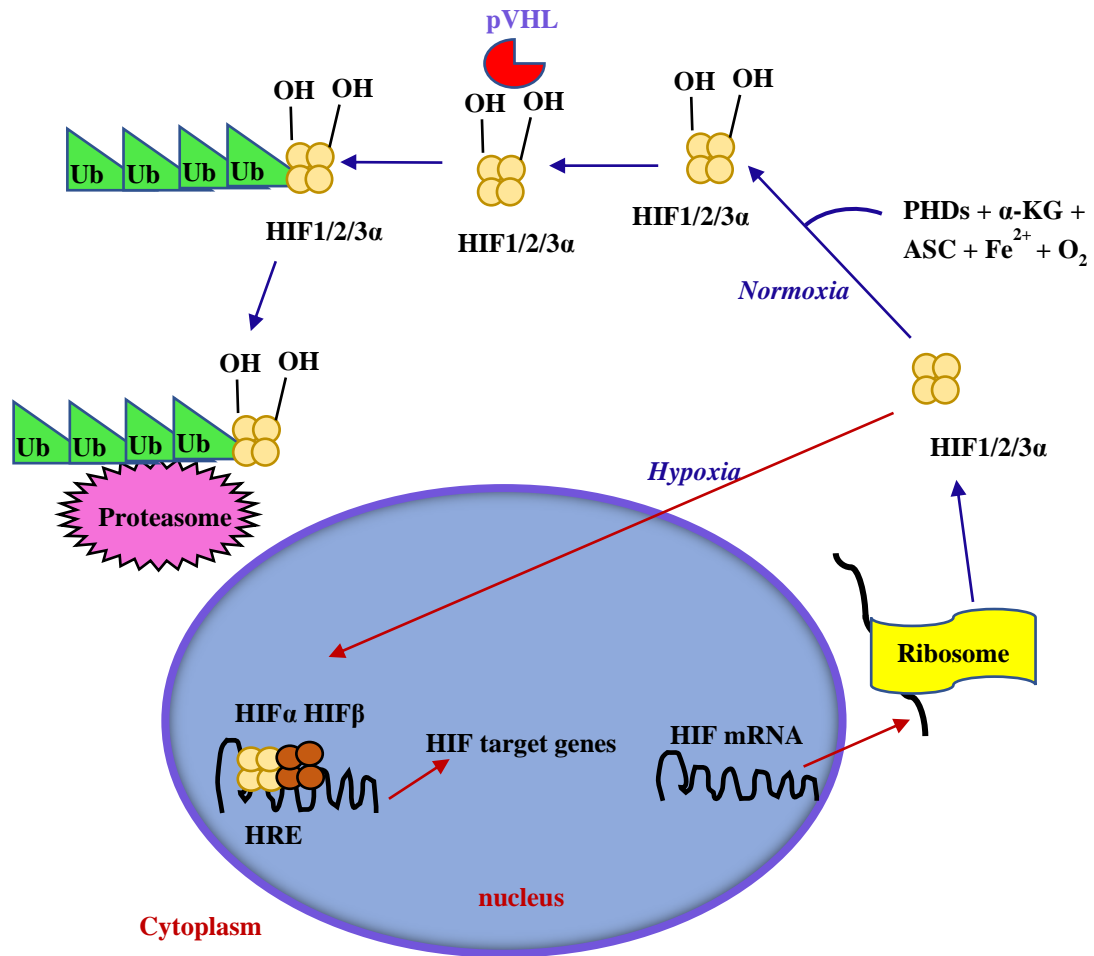


**Figure 1.10: Hypoxia and HIF Pathway Activation.** In normoxic conditions, HIF1/2/3 $\alpha$  bind to prolyl hydroxylases (PHDs) in the presence of iron ( $Fe^{2+}$ ),  $\alpha$ -ketoglutarate ( $\alpha$ -KG) and ascorbic acid (ASC) leading to hydroxylation of HIF1/2/3 $\alpha$ , polyubiquitination and degradation by 26S proteasome. However, under hypoxic conditions, HIF1/2/3 $\alpha$  translocates to the nucleus and binds to HRE to transcribe target genes.

### ***1.3.2 Hypoxia and CSCs***

A normal stem cell niche controls cell growth, apoptosis resistance and maintains cell stemness. Sometimes, a normal stem cell can defy the normal control mechanism and transform into a cancer stem cell leading to tumour initiation (Melzer et al., 2017). Hypoxia controls the activity of CSCs. HIF1 $\alpha$  and HIF2 $\alpha$  use the activation of the notch pathway to retain stemness characteristics of CSCs (Sun et al., 2020). Tumour microenvironment has little (hypoxia) or no oxygen (anoxia) as a result of insufficient blood supply (Visvader and Lindeman, 2008). In solid tumours, 50-60% consists of hypoxic regions (Vaupel et al., 2004). The hypoxic condition of the tumour initiates pathways which enable some of the cells to develop CSC characteristics (Hicklin and Ellis, 2005). Attention is being devoted to studies showing that cancer cells are vulnerable to high levels of reactive oxygen species (Tafani et al., 2012). HIF1 $\alpha$  activates the Wnt pathway which controls stem cell renewal (Sun et al., 2020). Hypoxia maintains CSC stemness by activating stemness-related pathways (TGF- $\beta$ , Wnt, Notch, etc), inhibiting differentiation-related genes, activation of EMT, using ROS activated response to stressors and induction of genes related to stemness (SOX2, OCT4, NANOG, KLF4, Myc and BMI1) as shown in Figure 1.12 (Najafi et al., 2020).

### ***1.3.3 Hypoxia and metastasis***

HIF-1 $\alpha$  levels are increased during periods of extreme oxygen deficiency to temporarily help cells overcome stress unlike HIF-2 $\alpha$  whose levels increase during periods of moderate hypoxia. HIF-2 $\alpha$  has been shown to promote tumour growth and induce EMT in mouse models. Increased expression levels of HIF-2 $\alpha$  correlates with poor prognosis in cancer patients (Zhang et al., 2017). Once a tumour grows beyond 3mm<sup>3</sup>, new blood vessels are required to provide nutrients to the tumour. In low oxygen conditions, the VEGF pathway is activated by HIF1 (Tirpe et al., 2019). In hypoxia, both endothelial cells and cancer stem cells express VEGF

which plays a critical role in angiogenesis (Najafi et al., 2020). In the absence of oxygen, SNAIL, TWIST, miRNA and HIFs can initiate EMT (Sun et al., 2020).

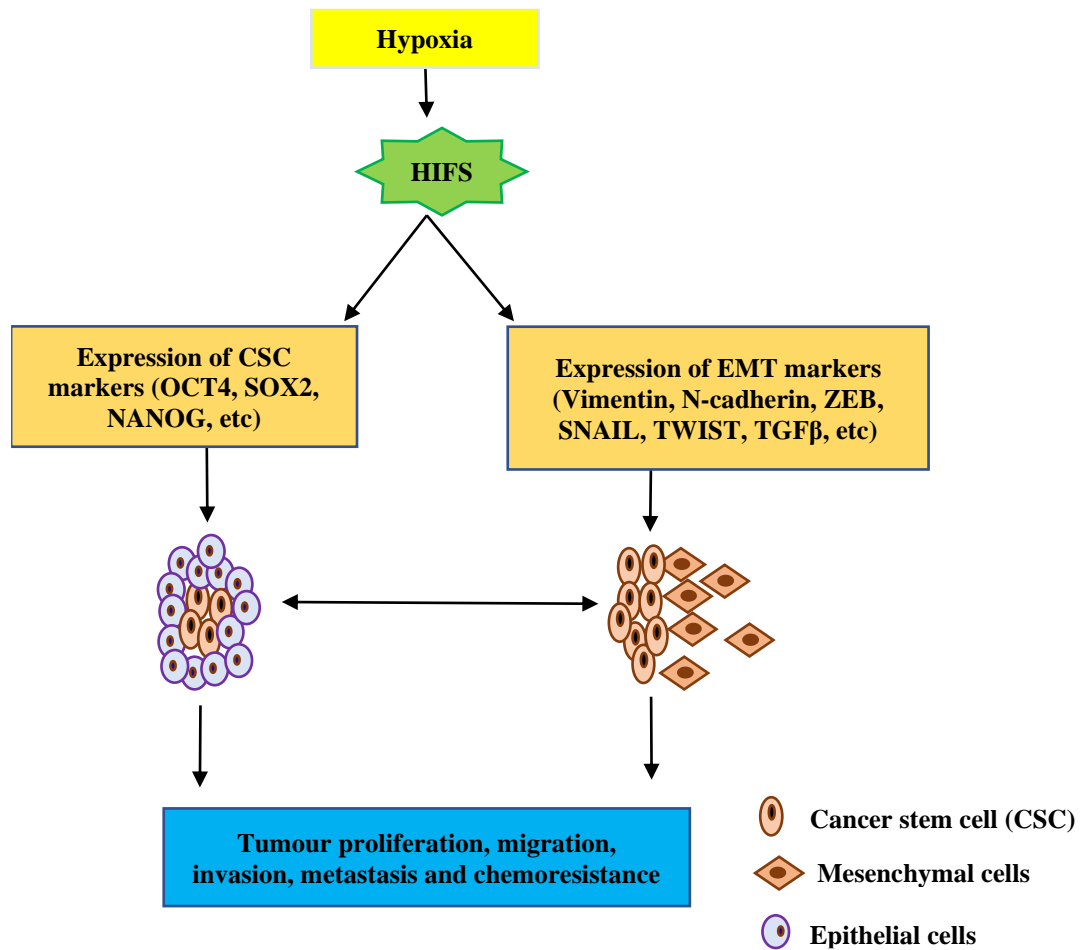


**Figure 1.11: Relationship between hypoxia and CSCs.** Hypoxia activates HIFs which leads to the expression of CSC and EMT markers that gives cancer cells stemness and invasive characteristics leading to tumour growth, cell migration and invasion, metastasis and chemoresistance.

### 1.3.4 Hypoxia and chemoresistance

The major challenge with cancer treatment is resistance to medication (He et al., 2016). Within pancreatic cancers, there is high interstitial fluid pressure and insufficient blood supply which creates hypoxic niches and reduces drug circulation (Tan et al., 2020). Hypoxia promotes the conversion of glucose to lactate which in turns aids the maintenance of CSC traits that promote chemoresistance. Hypoxia increases chemoresistance by maintaining cancer cells in a

quiescent state thus helping them evade drugs which target rapidly proliferating cells (Da Ros et al., 2018). The cytotoxic effect of a drug is more on cells that are rapidly proliferating while cells which are far away from the blood vessel are slow dividing and in less contact with the drug in the blood (Strese et al. 2013). The acidic pH of the tumour microenvironment remodels the ECM, reduces radiotherapy-induced ROS formation, increases pump activity of P-gp and reduces the uptake and efficiency of drugs such as anthracyclines, anthraquinones and vinca alkaloids (Da Ros et al., 2018). ABCG2 is a drug efflux pump in pancreatic cancer whose expression is controlled at the promoter level by sex hormones, hypoxia and methylation status (He et al., 2016). In hypoxic tumours, ABCG2 is overexpressed when HIF1 $\alpha$  complexes with HRE on the promoter region of ABCG2 resulting in drug resistance (Krishnamurthy et al., 2006; He et al., 2016). The effect of hypoxia is seen in cancer cells with reduced p53 expression so as to limit p53-related apoptosis. There is also an increased expression of p-glycoprotein (p-gp) which plays an important role in chemoresistance (Strese et al. 2013). Hypoxia activates the notch pathway which in turn elevates the activity of the SOX2 promoter that enhances chemoresistance (Sun et al., 2020). The involvement of cancer stem cells in metastasis and therapeutic response/chemoresistance affects the efficiency of chemotherapy (Klutznny et al., 2018).

#### **1.4 Cancer stem cells (CSCs)**

There are many hypotheses concerning the origin of cancer stem cells. They postulate that CSCs develop from misplaced somatic stem cells, genetic instability, chromosomal rearrangement or DNA mutation. Tumourigenic cells are usually identified by *in vitro* spheroid colony formation and *in vivo* tumourigenic cell transplant in immunodeficient mice. CSCs evade chemotherapy through overexpression of ABC transporters, overexpression of antiapoptotic factors and its ability to remain in a quiescent state to avoid apoptosis (Tong et al., 2018). Cancer stem cells (CSCs) were first discovered in the 1970s as a small population

of cells with increased ability to grow, differentiate and self-renewal abilities. These CSCs promote tumour growth and metastasis (Sun et al., 2020). CSCs are a small population of cells which possess stem-like characteristics that can lead to tumour formation in the pancreas (Gzil et al., 2019). CSCs are also known as tumour initiating cells (TICs) and their growth is mediated by the hypoxic microenvironment in a tumour. CSCs are responsible for tumourigenesis, chemotherapy, cancer relapse and metastasis (Phi et al., 2018). CSCs have the ability to divide asymmetrically to form cancer cells which in turn can undergo reversible reprogramming to generate cancer stem cells (Liu et al., 2018). In pancreatic cancer, CSCs express many markers such as CD44, CD133, CD24, OCT4, ABCB1, ESA, ALDH-1, nestin, EpCAM, c-Met, DCLK1 and CXCR4 (Gzil et al., 2019). The best three CSC markers for pancreatic cancer are CD24+, CD44+ and ESA+. However, CD133+ cells are more metastatic than CD24+ and CD44+ cells (Razi et al., 2019). CD133 is a transmembrane protein which is regulated by the promoter P5 in pancreatic cancer CSCs. P5 is suspected to be targeted by HIF-1 $\alpha$  and HIF-2 $\alpha$  because of its increased expression under hypoxic conditions and subsequent increase in CD133 expression levels. The increased expression of CD133 leads to increased NF $\kappa$ B signalling (Gzil et al., 2019). CSCs can take over the niche of non-CSCs by converting fibroblasts to CAFs which cause stemness (Carnero and Leonart, 2016). Circulating tumour cells (CTCs) are cells which break off from the primary tumour and enter into systemic circulation. It has been postulated that CSCs are responsible for metastasis. However, metastasis is caused by circulating tumour cells (CTCs) suggesting that CTCs possibly arise from CSCs (Rodrigues-Aznar et al., 2019). Pancreatic CSC niche comprises of PSCs, CAFs, immune cells, blood, lymphatic vessels, stem cells, cytokines, chemokines, growth factors and ECM (Zhao et al., 2017). PDAC cells that have undergone EMT express Zeb1 which is mainly responsible for their CSC traits (Rhim et al., 2012; Krebs et al., 2017; Rodrigues-Aznar et al.,

2019). Evidence shows that the number of CTCs in the blood of pancreatic cancer patients can be used as a biomarker for diagnosis and staging (Ankeny et al., 2016).

#### ***1.4.1. Identification of Cancer stem cells***

The difficulty in isolating pure CSC cultures, lack of CSC cell lines and reliable characterization methods have made it hard to have a complete CSC profile. The methods currently used for CSC analysis are flow cytometry, tumoursphere assay and colony formation assay. The CSC population detected usually depends on the type of cancer or biomarker used (Jariyal et al., 2019). Pancreatic cancer CSCs can be identified by flow cytometry analysis of their surface markers such as CD44, c-Met, CD133, CD24, ABCB<sub>1</sub>, ABCG<sub>2</sub>, ALDH-1, EpCAM, ESA, DCLK<sub>1</sub>, nestin and CXCR<sub>4</sub> or with transcription factors such as SOX2 and OCT4 (Domenichini et al., 2019; Gzil et al., 2019). The genes that cause pluripotency in CSCs are SOX2, OCT4 and NANOG, the ones which give the CSC traits are CD44, CD34, CD133 and CD24; the one responsible for drug resistance *in vivo* are ABC transporters and aldehyde dehydrogenase; and the ones involved in metastasis are Vimentin, N-cadherin, Snail, Twist and Zeb (Yeo et al., 2016). Pancreatic cancer CSCs can be detected using MRI, PET and CT scans while exogenous PCSCs can be detected using specific probes implanted in mouse models (Jariyal et al., 2019). It is however uncertain if the different PDAC CSC markers identify the same or specific CSC populations (Nimmakayala et al., 2019).

#### ***1.4.2 Cancer stem cell markers***

##### ***1.4.2.1 Aldehyde dehydrogenase***

A marker commonly used for characterising cancer stem cells is aldehyde dehydrogenase (ALDH) (Klutznny et al., 2018). The metabolic process in normal cells produce minimum amount of reactive oxygen species and oxidative damage. However, in cancerous cells, there is increased oxidative damage causing increased ROS production, lipid peroxidation and

accumulation of toxic aldehydes. The intracellular accumulation of ROS causes immunogenic cell death and the accumulation of toxic aldehydes initiates apoptosis in cells with reduced ALDH expression levels. ALDH is an NADP<sup>+</sup> dependent enzyme which converts aldehydes to carboxylic acids. The highest levels of ALDH activity have been detected in the liver, kidney, uterus and brain of mammalian tissues. There are 19 ALDH isoforms identified in humans. Some isoforms such as ALDH1A1, ALDH3A1, ALDH18A1, ALDH7A1 and ALDH5A1 play significant roles in tumour growth. The ALDH18A1 isoform plays a significant role in Warburg Effect by aiding proline and ornithine synthesis. Elevated ALDH expression increases the expression of Nr2f which is a transcription factor for many antioxidants; production of compounds such as retinoic acid which aid cell differentiation, survival and growth (Dinavahi et al., 2019). Three isoforms of ALDH (ALDH1, ALDH2, ALDH3) control 3 apoptogenic aldehydes. Cancer cells protect themselves from the apoptogenic effect of these aldehydes by the ALDHs that oxidize them to their non-apoptogenic carboxylic acids (Fournet et al., 2013; Venton et al., 2016). Dimethyl ampal thiolester (DIMATE), an  $\alpha,\beta$ , acetylenic N-substituted aminothioliol ester is an irreversible inhibitor of ALDH 1 and 3 which can be used for cancer treatment. Studies have shown that Dimate has an apoptotic effect on some cancer cell types (Venton et al., 2016). Aldehydes, though useful in the body, could become harmful if the mechanism for their degradation is hampered. This could generate large volumes of reactive oxygen species, oxidative damage and lipid peroxidation (Dinavahi et al., 2019). ALDH levels can be measured by using Aldefluor reagent in a technique known as flow cytometry (Klutznny et al., 2018). Flow cytometric assay (Aldefluor) is the first method that was ever used to detect cell populations based on their ALDH activity. The ALDH isoforms ALDH1A1 and 3A1 are responsible for the Aldefluor activity detected in stem cells of normal or cancer origin. Several studies have shown that chemotherapy can cause elevated population of cells with high ALDH expression leading to chemoresistance. For some drugs like paclitaxel, doxorubicin, oxaliplatin

which act by generating ROS, high ALDH levels can breakdown toxic aldehydes hence preventing their accumulation which was to cause cancer cell death (Yip et al., 2011; Dinavahi et al., 2019). As a result of the significant role played by ALDH in cancer cells, scientists have tried to use ALDH inhibitors to improve cancer prognosis (Koppaka et al., 2012). Some ALDH inhibitors inhibit just one ALDH isoform while some inhibit multiple isoforms. ALDH enzymes have a catalytic unit, NAD(P)<sup>+</sup> binding domain and an oligomerization domain. The NAD(P)<sup>+</sup> binding domain is exclusive to ALDH and the oligomerisation domain is responsible for the various ALDH isoforms hence the basis for design of ALDH inhibitors (Dinavahi et al., 2019). Overexpression of ALDH1A1 and ABC-transporters such as ABCG2 and p-glycoprotein confers chemoresistant abilities to CSCs (Domenichini et al., 2019).

#### ***1.4.2.2 Octamer-binding transcription factor (OCT4)***

OCT4 is a 38.6kDa protein that is also referred to as POU5F1 (Kaufhold et al., 2016). OCT4 is encoded by the POU5F1 gene which is expressed by pluripotent cells, CSCs, early embryo, embryonic stem cells, embryonic germ cells and embryonal carcinoma cells. Distinct characteristics of normal stem cells are self-renewal, pluripotency and cell proliferation. However, the differentiated cells produced from CSCs have unique characteristics that are not peculiar to those produced by normal stem cells (Mohiuddin et al., 2020). Previous studies showed that OCT4 together with c-MYC, KLF4 and SOX2 induce pluripotency in somatic cells (Takahashi et al., 2013; Mohiuddin et al., 2020). However, recent studies have shown that OCT4 controls pluripotency. Like normal stem cells, CSCs are mostly in the G<sub>0</sub>-phase. In studies done with glioblastoma cells, more cells became CD133<sup>+</sup> after exposure to gamma radiation and temozolomide. Many tumour cells with increased OCT4 population were resistant to conventional chemotherapy (Mohiuddin et al., 2020). Another study showed that the knockdown of OCT4 increased the sensitivity of lung tumour cells to irradiation and cisplatin (Chen et al., 2008; Cortes-Dericks et al., 2013; Mohiuddin et al., 2020). OCT4 is

activated by the Wnt pathway. Increased expression of OCT4 activates the Notch pathway. Beta catenin from the Wnt pathway increases OCT4 expression by binding to the promoter region of POU5F1. A combination of the Wnt inhibitor Dickkopf-1(DKK-1) and notch inhibitor (L68545) resulted in decreased stemness in breast cancer cells *in vivo* and *in vitro* (Mohiuddin et al., 2020).

#### **1.4.2.3 NANOG**

NANOG is a 34.6 kDa protein which has the ability to singly control pluripotency unlike OCT4 which can only function in collaboration with another gene such as SOX2. NANOG is controlled by GL1 and GL2 (Kaufhold et al., 2016). NANOG is a homeobox domain transcriptional activator which controls cell reprogramming and embryonic development. It is overexpressed in many cancers (Huang et al., 2019). NANOG, derived from the NK-2 gene, has three protein variants namely: NANOG1, NANOG2 and NANOGP8. NANOG is said to control pluripotency and self-renewal of CSCs. Increased expression of NANOG suppresses apoptosis. Studies have shown that in cells with low levels of NANOG, there is an increased expression of genes which hinder cell cycle and extra cellular matrix (ECM) formation. NANOG helps the Akt signalling pathway to impart drug resistance to cancer cells using transcriptional regulators like TCL1. In some studies, NANOG expression levels in cancer cells are more than its expression in somatic cells (Mahalaxmi et al., 2019).

#### **1.4.2.4 SOX2**

SRY-related high mobility group (HMG)-box gene 2 (SOX2) is a 34.3 kDa protein and a member of the SOXB1 family. SOX2 is expressed in stem cells and neural progenitor cells. SOX2 maintains self-renewal of embryonic cells and CSCs. The increased expression of SOX2 in pancreatic cancer cells leads to cell proliferation through cyclin D3 induction. SOX2 is a substrate of epidermal growth factor receptor (EGFR). EGFR plays a huge role in suppressing

apoptosis and initiating angiogenesis, and its suppression reduces SOX2 expression levels. SOX2 expression can be controlled by EGFR and ubiquitin-specific protease 22 (USP22) (Kaufhold et al., 2016; Lv et al., 2019). Thus, overexpression of SOX2 causes cancer cells to be resistant to different forms of therapy leading to poor prognosis. Knocking down of SOX2 has been shown to hinder cancer cell proliferation and invasion in *in vivo* and *in vitro* studies. Many studies focused on suppressing SOX2 to treat cancer have not observed any significant therapeutic effect (Zhang and Sun, 2019).

#### ***1.4.2.5 CD133***

CD133 also known as prominin-1 is one of the cancer stem cell markers used for analysing pancreatic cancer cells (Nomura et al., 2015a). CD133 is a transmembrane protein with the ability to phosphorylate tyrosine. The transcription of CD133 is controlled by five promoters, with the fifth one playing a significant role in CD133 expression in pancreatic CSCs. Hypoxia increases the expression of HIF1 $\alpha$  and Hif2 $\alpha$  in pancreatic cancer which in turn elevates the expression of CD133. In pancreatic cancer, CD133 initiates NF $\kappa$ B signalling which controls EMT. Research has shown that in pancreatic cancer, CD133 plays a significant role in lymph node metastasis, tumour differentiation and clinical TNM stage (Gzil et al., 2019). CD133 has been associated with increased expression of drug transporters and elevated metastasis (Nomura et al., 2015b).

#### ***1.4.3 Cancer stem cells and chemoresistance***

CSCs are similar to normal stem cells however they have self-renewal abilities and protective mechanisms from hypoxic microenvironment, DNA damage repair and efflux mechanism of drug transporters. The Wnt, Hedgehog and Notch pathways are involved in chemoresistance of CSCs which express high levels of drug efflux transporters that reduce intracellular drug concentration leading to chemoresistance (Sun et al., 2020). An important promoter of

resistance in CSCs is PI3K/AKT. Hypoxia activates AKT which in turn induces the Notch signalling pathway. The presence of HIF1 $\alpha$  in hypoxic cells leads to the activation and overexpression of cyclooxygenase-2 (COX-2) which activates HIF2 $\alpha$  leading to chemoresistance. Elevated levels of HIF1 $\alpha$  also cause HER2 to activate STAT3 which aids CSC self-renewal (Najafi et al., 2020). PCSCs either inhibit or activate pathways and /or factors which lead to chemoresistance. In PCSCs, there is an upregulation of JNK signalling whose overactivation is suspected to prevent intracellular accumulation of ROS leading to suppression of apoptosis and chemoresistance. PCSCs also influence chemoresistance by DNA methylation, MiRNA expression and histone acetylation (Valle et al., 2018).

### **1.5 Epithelial to Mesenchymal transition**

Epithelial to mesenchymal transition (EMT) is an important biological process whereby cells alter their shape and motility then switch from their epithelial phenotype to a mesenchymal phenotype. Epithelial cells undergoing EMT lose their polarity and adhesion to the basement membrane. They also change their shape to an elongated and flattened mesenchymal morphology. EMT takes place during embryogenesis and metastasis. Epithelial cells usually express keratin intermediate filaments (IFs) but when changing to the mesenchymal phenotype, they begin to express vimentin IFs. IFs determine and maintain cell shape. Mesenchymal to epithelial transition (MET) plays a vital role in the development of secondary metastatic tumours (Herrmann et al., 1996). During EMT, there is a reduced expression of E-cadherin and increased expression of vimentin, SNAIL, (Domenichini et al., 2019) and N-cadherin. Many pathways such as SNAIL1, SNAIL2, Zeb1, Zeb2, Twist1 and Twist2 play important role in EMT but the pathway which plays the most significant role is the transforming growth factor- $\beta$  (TGF- $\beta$ ) signalling pathway (Hu et al., 2018). The initial activation of the EMT pathway is by reactive oxygen species generation by inhibition of GSK-3 $\beta$ , followed by early SNAIL1 nuclear translocation and decreased levels of E-cadherin (Bulle et al., 2017). The expression of

signalling molecules such as SNAIL, ZEB1, TWIST1, TWIST2 is initiated by the acidic extracellular pH of cancer cells and this leads to EMT (Zhu et al., 2017). In cells undergoing EMT, there is a gradual loss in the expression of epithelial-cadherin and zonula occludens 1(ZO-1) and increase in the expression of vimentin, fibronectin and neural-cadherin. E-cadherin increases cell-to-cell adhesion and maintains the cytoskeleton. The expression of E-cadherin during EMT is reduced by zinc-finger E-box binding homeobox (ZEB), SNAIL, TWIST, KLF8, and FOXC2. Signalling pathways such as Wnt, Sonic hedgehog and TGF- $\beta$  control EMT. HIF1 activates the TGF- $\beta$  pathway which binds to TGF- $\beta$  receptor to activate SMAD3 and SMAD2. These SMAD bind with SMAD4 to form a complex which interacts with SNAIL to decrease the expression of E-cadherin and zonula occludens 1. The SMAD3-SMAD4 complex also increases the expression of TWIST (Tirpe et al., 2019). The speed of acquisition of EMT traits by tumour cells determines the occurrence of metastasis. In *in vivo* highly metastatic pancreatic cancer, EMT activates the overexpression of SNAIL and loss of E-cadherin (Sarkar et al., 2009). The upregulation of Zeb1 in PDAC inhibits E-cadherin expression and promotes chemoresistance. Silencing Zeb1 restores chemosensitivity of PDAC to anticancer drugs (Zeng et al., 2019).

### **1.5.1 EMT markers**

#### ***1.5.1.1 SNAIL1***

In the SNAIL superfamily, there are the transcription factors SNAIL1, SLUG and scratch proteins which have SMAG domains and a minimum of 4 functional zinc fingers. This SNAIL super family has been shown to play a big role in cell proliferation and survival. SNAIL1 consists of 264 amino acids and has a molecular mass of 29.1kDa. SNAIL1 initiates EMT by decreasing the expression levels of E-cadherin and claudins hence decreasing cell-to-cell adhesion and increasing cell migration. SNAIL1 can be regulated through transcription or

translation. In the transcriptional regulation, hypoxia induces HIFs to produce a transcriptional response. HIF1 $\alpha$  binds to the HRE2 of the SNAIL1 promoter to increase the transcription of SNAIL1. SMAD2, IKKA and NF $\kappa$ B also bind to the SNAIL1 promoter to increase SNAIL1 transcription. HMGA2 binds to the SNAIL1 promoter to enhance SMAD binding. SNAIL1 elevates the expression of vimentin and fibronectin. Notch1 prevents the breakdown of SNAIL1 by inhibiting GSK-3 $\beta$ -mediated phosphorylation via LOXL2 oxidation. The knockdown of SNAIL1 has been shown to suppress tumour metastasis and immunosuppression. LSD and HDAC inhibitors have been shown to stop SNAIL1 induced-EMT (Kaufhold and Bonavida., 2014; Nieto, 2002). Three common members of the SNAIL family are SNAIL (SNAI1), SLUG (SNAI2) and SMUG (SNAI3). SNAIL can also be regulated by post translational modifications such as phosphorylation, ubiquitination and lysine oxidation. SNAIL is phosphorylated by Glycogen synthase kinase 3 beta (GSK-3 $\beta$ ) to control ubiquitination (and subsequent degradation) or subcellular localization. MicroRNAs have also been shown to bind to the 3'UTR of SNAIL mRNA to control SNAIL expression levels thereby suppressing EMT (Skrzypek and Majka., 2020).

#### ***1.5.1.2 E-cadherin***

The molecules which adhere single cells together, help to maintain the integrity of cells and tissues. Therefore, any modifications to the cell-cell adhesion can cause pathological conditions such as metastasis. Cadherins are transmembrane receptor glycoproteins (D'Occhio et al., 2020). Epithelial-cadherin popularly called E-cadherin is a 120kDa calcium dependent adherin and tumour suppressor which creates tissues by forming tight bonds with catenin that hinder cell movement. E-cadherin has 3 structural domains namely, the cytosolic domain, single transmembrane domain and calcium dependent domain. In cell-cell adhesion,  $\beta$ -catenin attaches E-cadherin to the actin cytoskeleton. When there is a lack of E-cadherin such as during EMT,  $\beta$ -catenin detaches from the cell's actin cytoskeleton causing elevated levels of

cytoplasmic  $\beta$ -catenin which translocate to the nucleus and activate the Wnt pathway. E-cadherin has also been shown to inhibit the action of the transcription factors: TWIST, SNAIL, SLUG and ZEB1 thereby stopping EMT transition. When E-cadherin is lost, there will be cell movement, loss of cell polarity and increased expression of SNAIL, TWIST, VIMENTIN, N-cadherin and ZEB1 (Shenoy, 2019; Stemmler, 2008). E-cadherin regulates cell polarity (Biwas 2020). E-cadherin aids epithelial cells to resist invasion and migration. Research has shown the expression of E-cadherin is suppressed by ZEB1, ZEB2, SNAIL1, slug and TWIST (Kaufhold and Bonavida., 2014).

### ***1.5.1.3 N-cadherin***

The four groups of proteins involved in cell adhesion and cell signalling are cadherins, integrins, selectins and immunoglobulins. These molecules aid cell-to-cell or cell-to-extracellular matrix adhesion. The loss of adherens junctions causes cadherin switching which is a decreased expression of E-cadherin and an elevated expression of N-cadherin (Janiszewska et al., 2020). Neuronal cadherin also known as N-cadherin is a calcium dependent single chain transmembrane glycoprotein. In contrast to other cells in the body under normal conditions, there is an overexpression of N-cadherin by neuronal cells of the nervous system which helps them adhere to each other. Research indicates that many cancer patients contain higher levels of soluble N-cadherin in their blood than healthy people making N-cadherin a suitable biomarker for detecting metastasis in cancer patients. N-cadherin is a mesenchymal marker for EMT. Tumour cells which detach and migrate after EMT are able to avoid anoikis. N-cadherin is also implicated in tumour-related angiogenesis and normal vessel stabilization (Cao et al., 2019). The molecular weight of a mature N-cadherin is 130kDa. Vinculin is present in N-cadherin extension. The movement and stability of tissues is maintained by the interrelationship between catenin and cadherins which is important in adherens junctions. Unlike E-cadherin, N-cadherin is expressed by neural cells, endothelial cells, stromal cells and osteoblasts of non-

epithelial tissues. Some research has shown that N-cadherin plays a possible role as a tumour suppressor and plays a big role in angiogenesis. Adherens junctions connected to N-cadherin initiate the MAPK/ERK and PI3K pathway. During EMT, the expression of E-cadherin drops while that of N-cadherin increases (Loh et al., 2019). The interaction of N-cadherin and EGFR increases cell movement. Normal epithelial cells have low levels of N-cadherin which is over expressed in cancer cells undergoing EMT (Yu et al., 2019).

#### ***1.5.1.4 Vimentin***

The three main components of cellular skeleton are actin, microtubules and intermediary filaments. Intermediate filaments are made from single to multiple IF proteins. During the initial phases of embryonic development, there is vimentin expression. When cells undergo EMT, they start to lose their epithelial polarity and the adhesion at their cell-cell junctions (desmosomes) (Strouhalova et al., 2020). In mesenchymal cells, there is a 57kDa filament called vimentin. In humans, vimentin has a binding site for NF $\kappa$ B promoter and TGF $\beta$ 1 response element (Kaufhold and Bonavida., 2014). High levels of vimentin correlate with poor prognosis in cancer patients. Excessive expression of vimentin in epithelial cells causes cells to modify their structure into the elongated shape associated with mesenchymal cells, subsequently readjusting the structure of their actin and microtubules, desmosomes internalization and restructuring of keratin IFs. Studies have shown that reduction in vimentin expression levels can lead to the restoration of the epithelial phenotype. Proteins which connect actin and microtubules with IFs are called cytolinkers (Strouhalova et al., 2020).

#### ***1.5.1.5 Matrix metalloproteinase***

In 1962, Gross and Lapiere discovered MMPs act as ECM degrader, cell-cell adhesion molecules, cytokines, chemokines, clotting factors, cell receptors and proteinase (Li et al., 2020b). Matrix metalloproteinase (MMP) plays a significant role in angiogenesis. It is a

diffusible substance which initiates angiogenesis. MMPs are zinc-binding metalloproteinases that play a huge role in ECM component degradation hence enhancing metastasis and neovascularization. MMPs are also known as matrixins which have proteolytic action on many ECM components (Quintero-Fabian et al., 2019). So far, only 28 members of the MMP family have been identified (Wang and Khalil, 2018; Quintero-Fabian et al., 2019). These MMPs have been classified based on their substrate specificity. The 6 sub-families of MMPs are collagenases, gelatinases, matrilysins, stromelysins, MMP membrane-type (MT)-MMPs and other MMPs. MMPs exist as proenzymes and need proteolytic cleavage for zymogen activation. As a tumour increases in size, there is increased need for oxygen and nutrients. Through sprouting of endothelial cells, new blood vessels are formed. The angiogenic promoter, VEGF-A initiates angiogenesis by FLK1 signalling. The cofactors NRP1 and NRP2 improve the activity of VEGF. MMPs have a particular proteolytic action on multiple ECM substrates. Many studies have shown that MMP2 and MMP9 are overexpressed in cancers and have the ability to break down collagen (Quintero-Fabian et al., 2019). MMPs are classified according to their substrate or domain organisation. The sub-classes under domain organisation are archetypal MMPs, matrilysins, gelatinases and furin-activable MMPs. In physiological conditions, the homeostasis of the ECM is controlled by MMPs and endogenous tissue inhibitors of MMPs (TIMPs). In some disease conditions like rheumatoid arthritis, Alzheimer's disease and tumours, this homeostasis is disrupted by elevated MMP levels or inefficiency of TIMPs (Li et al., 2020b).

## **1.6 Nuclear Factor Kappa B (NFκB)**

In 1986, NFκB was discovered as a transcription factor which has a nuclear factor bound to the kappa light-chain of activated B cells (Hoesel and Schmid, 2013). NFκB is a transcription factor usually activated by cellular stress (Xu et al., 2017). NFκB is composed of a family of transcription factors involved in multiple biological processes and tumour progression (Huang

et al., 2014). NF $\kappa$ B is present in all mammalian cells and plays a critical role in controlling immune response. It also plays major roles in cell cycle progression, differentiation, migration and survival (Herrington et al., 2016). The 5 known members of this family are RelA, RelB, c-Rel, NF $\kappa$ B1 and NF $\kappa$ B2 (Hoesel and Schmid, 2013) which share an N-terminal Rel homology domain (RHD) used for DNA binding, I $\kappa$ B binding, homo-dimerisation and hetero-dimerisation (Hayden and Ghosh, 2004; Hayden and Ghosh, 2008). Some hypotheses state that in the early stages of cancer, there is a high expression of NF $\kappa$ B which acts as a tumour suppressor because of the elevated activity of cytotoxic immune cells (Tilbourgs et al., 2017). In Hodgkins Lymphoma, some mutations in I $\kappa$ B proteins lead to NF $\kappa$ B activation (Perkins, 2004). RelA, RelB and cRel have c-terminal transactivation domains required for transcription. NF $\kappa$ B activation is tightly regulated because it can be activated by multiple stimuli, some of which are harmful to healthy host tissue. I $\kappa$ B $\alpha$  maintains NF $\kappa$ B in an inactive state in the cytoplasm by shielding it from nuclear localization signals (Huang et al., 2014). Sometimes, some NF $\kappa$ B subunits suppress tumour development (Zhu et al., 2017).

### ***1.6.1 NF $\kappa$ B and Hypoxia***

In hypoxic condition, the I $\kappa$ B $\alpha$  is phosphorylated and degraded. Then the detached NF $\kappa$ B translocates to the nucleus where it binds to HIF-1 $\alpha$  thereby activating it and initiating the transcription of hundreds of genes which are responsible for cell proliferation, angiogenesis and suppressing apoptosis (Laurent et al., 2005; Najafi et al., 2020). In hypoxia, HIFs are stabilized by prolyl hydroxylases (PHDs) using von Hippel Lindau protein; and HIFs activate NF $\kappa$ B. Hypoxia activated NF $\kappa$ B controls the expression of apoptotic proteins leading to decreased apoptosis and enhanced angiogenesis as shown in Figure 1.13 (D'Ignazio and Rocha, 2016). NF $\kappa$ B activity is controlled by hypoxia, cytokines and chemotherapeutic drugs. Hypoxia leads to elevated expression of HIF1 $\alpha$ , initiates the NF $\kappa$ B pathway and promotes EMT in pancreatic cancer (Cheng et al., 2011). NF $\kappa$ B and HIF1 $\alpha$  regulate growth factors and their

regulators which promote tumour proliferation. Activated NF $\kappa$ B and HIF1 $\alpha$  can cause cancer cells or activated leucocytes and mesenchymal cells in the TME to secrete VEGF which promote neoangiogenesis (Tafari et al., 2013).

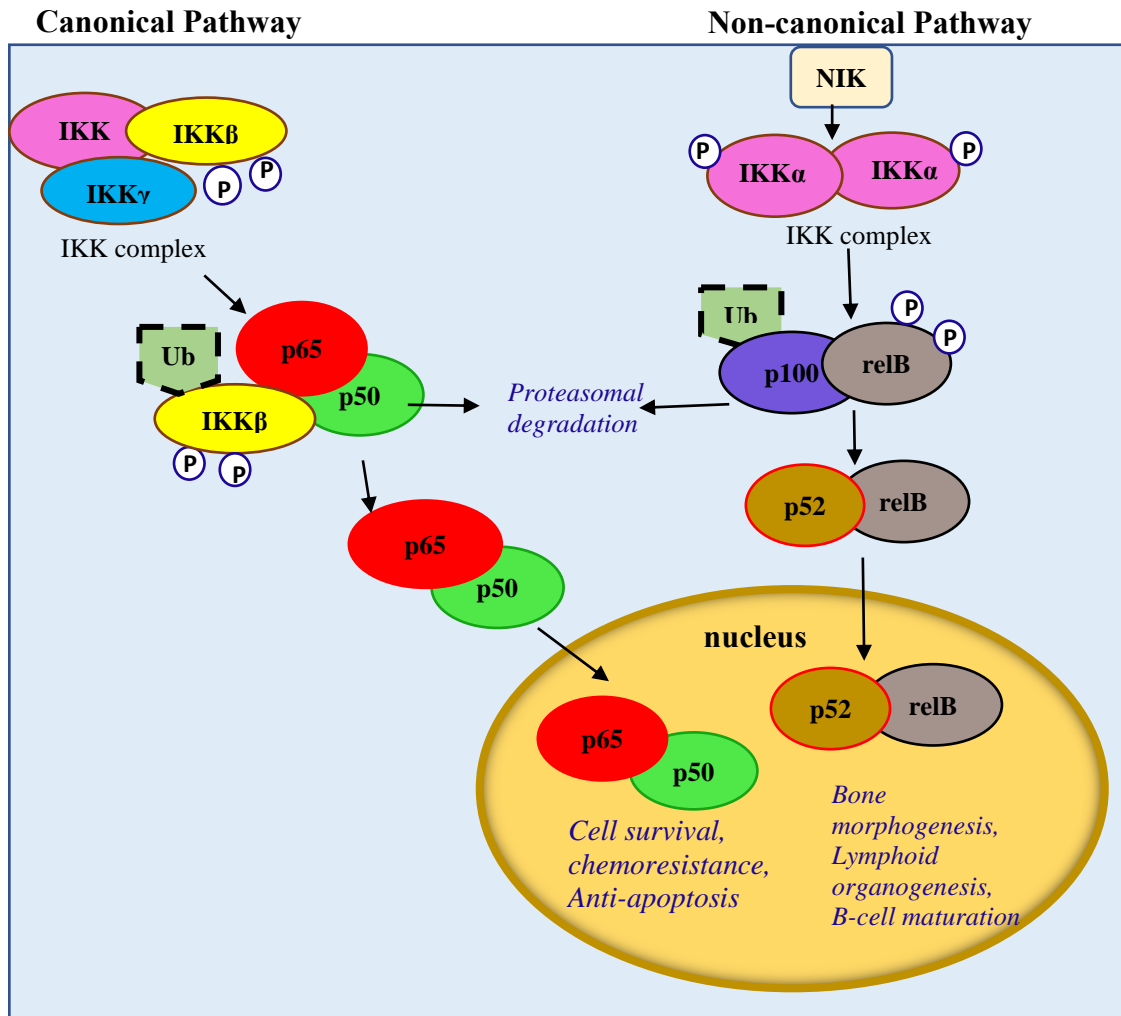


**Figure 1.12: Hypoxia and NF $\kappa$ B Pathway Activation.** Hypoxia activates NF $\kappa$ B either through the canonical pathway or the non-canonical pathway. In both pathways, hypoxia leads to the translocation of NF $\kappa$ B into the nucleus where it initiates the transcription of target genes that confer enhanced cell survival characteristics to the cell.

During tumour progression, many of the genes activated by HIFs are targeted by NF $\kappa$ B such as IL6, MMP9, COX2 and Bcl2 (D'Ignazio et al., 2017). The two main pathways involved in NF $\kappa$ B activation are the canonical and non-canonical pathway (Herrington et al., 2016). In the

canonical NF $\kappa$ B pathway, I $\kappa$ B kinases are activated by phosphorylation, then ubiquitinated for degradation by the proteasome with the release of NF $\kappa$ B which translocates to the nucleus to activate target genes while the non-canonical pathway is activated by the degradation of some TNF receptors, leading to NF $\kappa$ B inducing kinase (NIK) accumulation. NIK and IKK $\alpha$  then phosphorylate p100 leading to the release of RelB/p52 that translocates to the nucleus to activate target genes (Yu et al., 2020). Multiple layers of immune cells are formed by the NF $\kappa$ B non-canonical pathway (Yu et al., 2020). When the canonical pathway is activated, RelA and p50 heterodimers are used for gene transcription while in the non-canonical pathway, the heterodimers involved are RelB and p52 (Vallabhapurapu and Karin, 2009; Yu et al., 2020; Sun, 2017).

### ***1.6.2 NF $\kappa$ B and metastasis***

NF $\kappa$ B controls the expression of many anti-apoptotic genes and also regulates the expression of many genes involved in metastasis such as VEGF, MMPs, IL-8 and CXCR4. According to studies by Huber et al., suppressing the NF $\kappa$ B pathway inhibited EMT and metastasis in breast cancer cells proving that NF $\kappa$ B is required for metastasis (Huber et al., 2004). Several reports have shown that the activation of NF $\kappa$ B leads to an increased expression of EMT-related genes such as vimentin and N-cadherin while blocking NF $\kappa$ B reverses the process (Cao et al., 2019). NF $\kappa$ B activates anti-apoptotic genes (Bcl2-X<sub>L</sub>, X-IAP and IEX-1), COX-2, c-Myc and cyclin D1 leading to tumour progression (Perkins, 2004). The activation of I $\kappa$ B kinase (IKK) leads to the phosphorylation of I $\kappa$ B $\alpha$  by IKK $\alpha$  and IKK $\beta$ . The IKK complex comprises of the IKK $\alpha$ , IKK $\beta$  and IKK $\gamma$ . NF $\kappa$ B controls the expression of cyclooxygenase-2 (COX-2), interleukin-8 (IL-8) and I $\kappa$ B $\alpha$  which control tumor growth and metastasis (Li et al., 2004). NF $\kappa$ B activation promotes the initiation of EMT and metastasis in pancreatic cancer. According to a study done by Nomura et al, the suppression of NF $\kappa$ B reduced tumour size, decreased the expression of EMT-related genes, restored cell-cell junctions and decreased metastasis (Nomura et al., 2016).

### ***1.6.3 NFκB and chemoresistance***

NFκB induces transcription of cyclin D1, Bcl-2, survivin and VEGF which promote chemoresistance in cancer cells. Therefore, drugs which block or reverse the NFκB pathway can overcome chemoresistance (Fu et al., 2019). Ionizing radiation and drugs which damage DNA such as cisplatin and temozolomide also activate NFκB leading to chemoresistance. The response of cancer cells to DNA damage increases the expression of pro-inflammatory cytokines, increases tumourigenesis, angiogenesis and cell invasion. However, generally targeting NFκB could cause health problems such as immunodeficiency because of its physiological roles in the body. As a result, it is best to target NFκB signalling which originates from DNA damage (Wang et al., 2017b). For specific NFκB inhibition, there are ongoing studies involving targeting IκB proteins, ubiquitin-proteasome system, NFκB DNA binding, post translational modification of NFκB and post transcription gene silencing. Some of which have been effective for treating a range of tumours and autoimmune diseases, though they have unfavourable side effects (Herrington et al., 2016). Tumour necrosis factor receptor-associated factor 6 (TRAF6) is an important activator of NFκB signalling by complexing with signalling molecules such as NFκB kinase. NFκB promotes chemoresistance to gemcitabine by binding to the promoter region of P-gp. TRAF6 blocks apoptosis leading to tumour progression in PDAC (Meng et al., 2020). NFκB controls the expression of the anti-apoptotic proteins such as cIAP1 and cIAP2 which suppress etoposide-induced apoptosis. The NFκB inhibitor PS341 increases drug sensitivity of AsPc-1 pancreatic cancer cells to taxols. Inhibiting the NFκB pathway could increase the sensitivity of pancreatic cancer cells to gemcitabine (Holcomb et al., 2008). NFκB in association with HIF1 inhibits the activity of hENT1 and hENT2 leading to chemoresistance. Sulfasalazine, an IκB inhibitor inhibits the phosphorylation of IκB to stop NFκB activation and decrease chemoresistance to gemcitabine in gemcitabine-resistant cell lines (Li et al., 2018).

## **1.7 Repositioning of Disulfiram into cancer treatment**

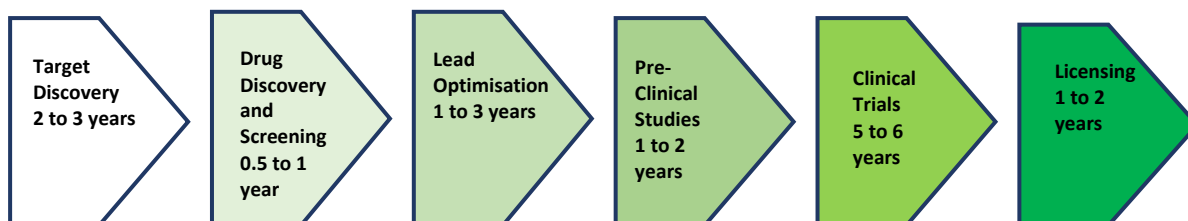
### ***1.7.1 Comparison of traditional drug development with drug repositioning.***

In the 1940s, pharmacologically active agents like mustard seeds and folic acid antagonists were the first used for cancer management. The mustard seed was suspected to inhibit the growth of some somatic cells, however the effect as an anticancer agent was temporal and had adverse effects. Folic acid on the other hand was thought to reverse megaloblastosis. Unfortunately, folate worsened leukemia in children leading to further research on folate antagonists. With several studies seeking more potent anticancer agents, by the late 1950s, there were 25,000 to 30,000 potential candidates annually and just 10 to 20 chosen for clinical trials. New statistical techniques had to be developed for analysing the survival data of the increasing number of anticancer agents (Mould and Hutson, 2017).

Currently, novel anticancer drugs cost more than 100,000 USD for an annual treatment. Twenty years ago, paclitaxel became the first anticancer drug to make a sale of 1 billion USD annually. However, in 2013, 10 anticancer drugs made sales of 1.8 to 7.8 billion USD annually. Anticancer drugs are relatively more expensive in United States than in other countries in the world. The high cost of anticancer drugs is as a result of the high cost of research required for their development. Some patients have abandoned cancer treatments which can improve their overall survival such as trastuzumab for HER2-positive breast cancer patients, as a result of insufficient funds for payment. Despite the high cost of these anticancer drugs, a study involving patients with solid tumours from 2002 to 2012 revealed that the median overall improvement in overall survival and progression-free survival was 2.1 and 2.3 months respectively (Prasad et al., 2017).

### De novo Drug Discovery and Development

10 to 17 years



### Drug Repurposing

3 to 12 years



**Figure 1:13: Illustration of the stages involved in Denovo drug development and drug repurposing.**

Most first line anticancer drugs do not eliminate CSCs leading to high number of cancer-related deaths. Therefore, development of new cancer related drugs targeting CSCs is a crucial step for treating cancer (Phi et al., 2018). The process involved in producing a new drug from scratch is time consuming, expensive and risky because only about 10% of new drugs end up being accepted by the FDA and they have a success rate of 2.01%. As a result of this, investors have developed a better strategy to develop new drugs which is gaining popularity known as drug repositioning (Xue et al., 2018). Drug repositioning, also referred to as drug repurposing, drug re-profiling, drug re-tasking or therapeutic switching. It is a process that is used to get a new use for an old drug. The theory behind this is that some drugs have multiple targets and activate multiple signalling pathways (Mohammed et al., 2018). Drug repositioning was mistakenly discovered in the 1920s (Xue et al., 2018) and has several advantages such as

reducing the cost, duration and adverse effects associated with producing a new drug from scratch which has made the strategy to be preferred by academics and pharmaceutical companies (Brown and Patel, 2016). The steps involved in *denovo* drug development and drug repurposing are shown in Figure 1.14. Many new drugs, especially anticancer drugs fail during clinical trials despite the millions spent during research of the drug. This has led to researchers screening many non-oncology drugs against cancer cell lines to determine the non-oncology drugs with anticancer activity in a strategy referred to as drug repurposing. This led to the discovery of many potential anticancer drugs among which is disulfiram (Beijersbergen, 2020).

### ***1.7.2 Non-oncology drugs currently repositioned for Cancer treatment***

A number of non-oncology drugs have been discovered to hinder tumour growth and initiate apoptosis. Some of the recently identified non-oncology drugs which have been repurposed for cancer treatment are explained below:

#### ***a. Rapamycin***

Rapamycin was originally used as an immune suppressant after organ transplant because it hinders IL-2-mediated T cell proliferation. Rapamycin is also known to inhibit mTORC1 and suppress vascular smooth muscle growth. A deeper understanding of the link between mTOR and cancer-associated signalling pathways led to drug trials which showed that rapamycin decreased leukemic progenitor cells in acute myeloid leukemia patients. Recent studies have shown that rapamycin can't be administered singly because mTOR1 suppression leads to negative feedback regulation which initiates tumour growth by activating PI3K-AKT signalling. Secondly, rapamycin barely affects mTORC2 which plays a significant role in tumour proliferation. Encouraging results have been obtained from some combination strategies involving rapamycin (Zhang et al., 2020b).

### *b. Metformin*

Metformin is a popularly known anti-diabetic drug which reduces blood glucose by increasing cell sensitivity to insulin. Many preclinical studies have shown that metformin has anticancer activity. However, its anticancer mechanism of action is not fully understood. A certain study revealed that metformin suppresses PDAC growth by interfering with the crosstalk between G protein-coupled receptor (GPCR) and insulin/insulin-like growth factor receptor (IGF) signalling pathways (Chang et al., 2018). Diabetic patients administered with metformin have a 37% reduction in the probability of them getting cancer (Hart et al., 2016). Metformin also has the ability to inhibit the activity of CD133 in cancer cells thereby decreasing tumour weight (Gzil et al., 2019).

### *c. Aspirin*

Aspirin is originally used as an anti-platelet and non-steroidal anti-inflammatory drug (NSAID). Cancer patients have increased platelet count which promotes cancer cell proliferation leading to poor prognosis. This is because activated platelets have high levels of pro-angiogenic factors such as VEGF-A, fibroblast growth factor 2 and platelet-derived growth factor. Aspirin inhibits thrombin platelet activation hence decreasing angiogenesis. Growing research shows that aspirin interferes with NFκB, RUNX1 and programmed cell death (Martini et al., 2020).

### ***1.7.3 The developmental history of Disulfiram***

The chemical name for disulfiram is Bis(diethylthiocarbamoyl) disulphide. Years after its established use as an industrial catalyst during rubber production, an American physician E.E. Williams in 1937 realised that people working with disulfiram experienced a myriad of symptoms such as headaches, sweating, heart palpitations, etc which worsened after consumption of alcohol. It was later revealed that disulfiram suppressed the activity of

acetaldehyde dehydrogenase causing the accrue ment of the acetaldehydes that caused the observed symptoms after drinking alcohol. In 1977, a female cancer patient undergoing chemotherapy and alcoholism treatment with disulfiram remained asymptomatic for a decade without further medication creating the hypothesis that disulfiram has an anticancer effect (Jiao et al., 2016). Disulfiram commercially known as antabuse has been used as an anti-alcoholism drug (Spillier et al., 2019) for over 60 years. Research has shown that DS in the presence of copper has anti-tumoural activity (Dastjerdi et al., 2014). After oral administration, the enzyme glutathione reductase and albumin quickly converts disulfiram to DDC. Once in the liver, cytochrome p450 converts DDC to S-Me-DDC then to the intermediates Me-DETC and MESO-DETC which are the forms of disulfiram involved in its anti-alcoholism activity. S-methylation and glucoronidation of disulfiram in the liver nullifies its anti-cancer activity and could be the reason for the difference in efficacies of laboratory and clinic results (Butcher et al., 2018; Najlah et al., 2019).

#### ***1.7.4 Disulfiram and Cancer***

##### ***1.7.4.1 Mechanism of disulfiram action***

###### *i. Inhibition of the NFκB pathway*

In 2003, Wang et al. showed that disulfiram inhibits the NFκB pathway. DNA damage caused by drugs stimulates/initiates the release of anti-apoptotic proteins which can cause drug resistance. Clinical trials involving the use of NFκB inhibitors on cancer cells have been unsuccessful suggesting that chemotherapy cannot just comprise of inhibitors of NFκB. High reactive oxygen species can cause apoptosis by damaging DNA and membrane structure. Cancer cells can tolerate higher levels of ROS than normal cells. However, cancer cells have a limit which when exceeded, exhausts cellular antioxidant capacity and leads to apoptosis. ROS-induced apoptosis depends on the activation of the MAPK pathway. Unfortunately,

chemotherapy induced ROS activation also activates pathways such as NFκB which affect the drug's cytotoxicity negatively (Yip et al., 2011; Wang et al., 2003).

ii. *Proteasome inhibition*

Disulfiram inhibits proteasome activity by destabilizing the homeostasis of proteins that regulate cell cycle and apoptosis leading to an accumulation of poly-ubiquitinated proteins and cytotoxic protein aggregates which lead to cancer cell death (Jiao et al., 2016). The sulfurhydryl groups on DSF have high affinity for thiol groups and chelate biological metals thus aiding its suppression of the 26S proteasome (Li et al., 2020a).

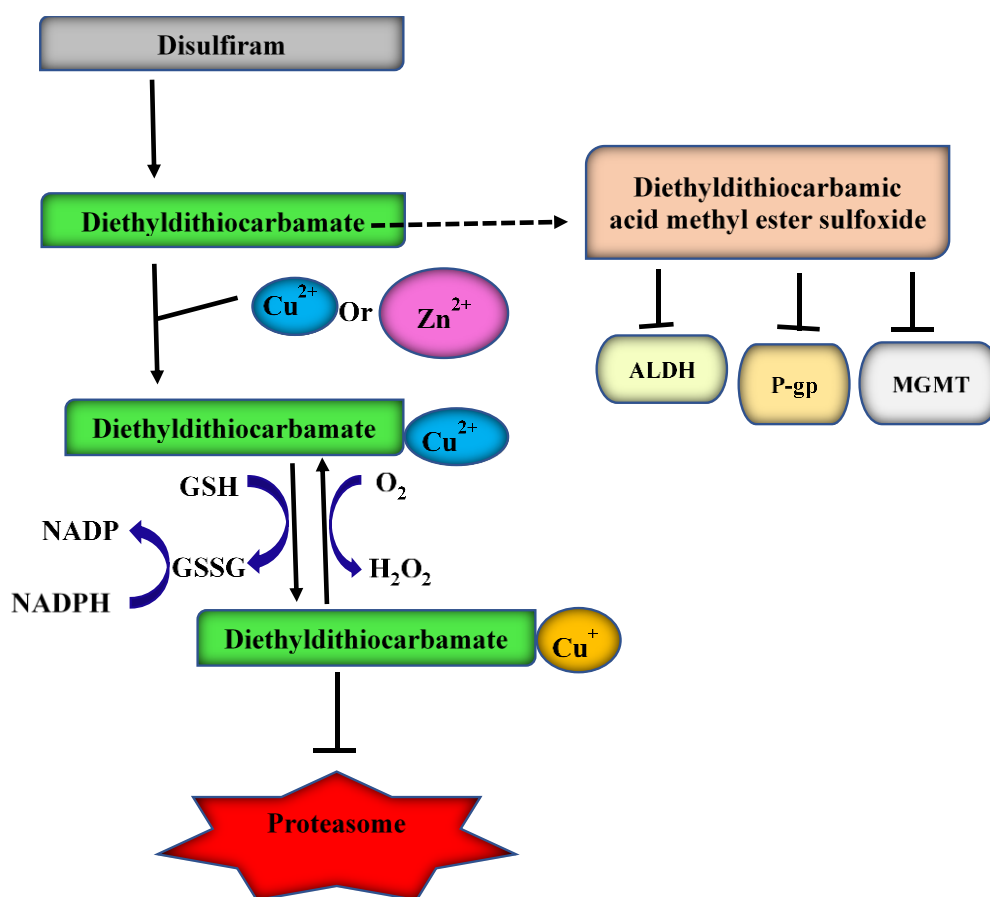


*Figure 1.14: Mechanism of anticancer activity of disulfiram.*

iii. *Inhibition of aldehyde dehydrogenase (ALDH)*

ALDH is required for the production of molecules required for cell proliferation and differentiation (Jiao et al., 2016). Normal cell microenvironment has a neutral pH while tumour cell microenvironment has a slightly acidic pH. Studies have been carried out using Diethylthiocarbamate (DDC) coated in pH dependent charge switchable nanoparticles to target cancer cells while limiting toxicity to normal cells. DDC is an irreversible inhibitor of ALDH1A1 which protects cells from aldehyde-induced oxidative stress. DDC has a wide range of applications such as for agricultural pesticides and as a pharmacological agent against tuberculosis, AIDS and cutaneous leishmaniasis (Abu-Serie, 2018).

iv. *Formation of reactive oxygen species (ROS)*

Copper is the second most important trace element in the body and plays a vital role in enzyme catalysis, in iron homeostasis, immunity, cell signalling, angiogenesis and nerve induction. It also acts as a pro-oxidant or antioxidant by scavenging ROS. Its increased level in cancer cells suggests that high levels of copper hasten angiogenesis. Many scientists suggest that the high copper level in cancer cells play a role in imparting chemoresistant abilities to cancer cells. Two drugs used clinically for chelating copper are disulfiram and tetrathiomolybdate (Hassan et al., 2018; Hassan et al., 2019). Disulfiram strongly complexes with metal ions thereby suppressing the activity of Zn and Cu-dependent enzymatic pathways thereby, creating oxidative stress (Jiao et al., 2016). ROS is a product of mitochondrial oxidative phosphorylation (Xu et al., 2017).

v. *Inhibition of NPL4*

In 2017, Skrott et al., proved that disulfiram targets cancer cells by inhibiting NPL4, a p97 segregase adaptor which plays a vital role in the turnover of proteins involved in many regulatory and stress-response pathways. Disulfiram is also a phosphoglycerate dehydrogenase

(PHGDH) inhibitor. PHGDH catalyses an initial step in the pathway for serine synthesis which is highly expressed in cancer cells (Spillier et al., 2019).

*vi. Inhibition of DNA methylation*

Disulfiram has also been shown to increase the cytotoxicity of anticancer drugs, hinder angiogenesis, promote apoptosis of cancer cells, stop cell proliferation, invasion and metastasis, interfering with DNA methyl transferase, hindering p-gp-efflux, stopping DNA replication, hindering the proteolytic action of matrix metalloprotease (MMP) (Banerjee et al., 2019).

*vii. Inhibition of pyroptosis*

In addition to its potent anticancer activity, current research shows that disulfiram also inhibits pyroptosis (Hu et al., 2020), modulates secretase (Reinhardt et al., 2018) and inhibits inflammation (Schmidt and Latz, 2020).

*viii. Inhibition of p-glycoprotein maturation*

Studies have shown that disulfiram increases the cytotoxicity of first line anticancer drugs such as cisplatin, gemcitabine, paclitaxel and 5-fluorouracil through an unknown mechanism. Some studies have shown that disulfiram has the ability to reverse multidrug resistance (MDR) through a number of mechanisms including inhibition of p-glycoprotein maturation and activity (Jiao et al., 2016; Mohammad et al., 2019). DDC has a high affinity for proteins containing sulfurhydryl groups (Abu-serie, 2018). ABC transporters require ATP-hydrolysis as a source of energy for transporting molecules across the cell membrane. DSF can irreversibly block ATP hydrolysis by modifying the cysteine at the ATP-binding site and interacting with the drug-substrate binding site leading to the reversal of P-gp mediated drug efflux (Li et al., 2020a).

#### ***1.7.4.2 Limitations of disulfiram as an oncology drug***

Despite the numerous studies proving that disulfiram is highly cytotoxic to cancer cells *in vitro*, disulfiram is rapidly degraded in a biological system (Butcher et al., 2018) leading to reduced bioavailability. The efficacy of disulfiram *in vivo* is also said to be reduced by the acidic pH. Therefore, there is a need to develop a carrier which can improve the efficiency of disulfiram *in vivo*. Many nanoparticles have been designed to carry drugs to target sites in the body while evading the body's immune system so the drug can effectively carry out their therapeutic action (Banerjee et al., 2019). As a result of the multitude of researches proving that disulfiram effectively targets cancer cells and the setback of disulfiram having limited lifespan in the blood stream, a lot of studies are being targeted at producing novel formulations of disulfiram with increased half-life in the bloodstream.

#### ***1.7.4.3 Nanotechnology***

The Greek word '*nano*' means '*dwarf*'. In medicine, nanotechnology is the combination of science and engineering to produce structures of size 1 to 100nm which are used to boost drug delivery, screen diseases and for tissue engineering. Nanoparticles are synthesized from a host of materials such as lipids, metals, protein and polymers. A wide range of polymers are used as nanoparticles depending on their properties and the requirements. These nanoparticles are used for the delivery of vaccines, recombinant proteins and drugs. Based on the material from which it originates, nanoparticles are classed into micelles, inorganic nanoparticles, liposomes, dendrimers and polymeric nanoparticles. The target drug is usually immobilized or encapsulated to the polymer then sent to the target site by diffusion or desorption. The 3 types of polymers used for drug encapsulation are polymeric micelles, linear polymers and hydrogels. There are synthetic polymers like poly (lactic-co-glycolic acid) (PLGA), polylactide–polyglycolide copolymers and polylactic acid (PLA) which are more effective than

natural polymers because their structure has been modified to improve their efficiency and they lack biological contamination. Generally, nanoparticles deliver drugs to their target site either passively or actively. In passive drug targeting, drug administered to the body preferentially accumulates in the site of interest. For example, blood vessels in tumours have increased vascular permeability therefore molecules bigger than 40kDa will seep through the tumour blood vessel and settle in the tumour making it a strategy for anticancer drug design. Active drug targeting takes advantage of the molecular structure of the drug/drug carrier and the bond it forms with molecules in the site/molecule of interest such as ligand to receptor and antibody to antigen. For example, many epithelial cancers highly express folate receptors making the folate receptors a target for many drug designs (Chenthamara et al., 2019).

#### ***1.7.4.4 Nano-drug-delivery systems transforms Disulfiram for cancer treatment***

##### *1. Poly(lactic-co-glycolic acid) encapsulated DS*

The most widely used synthetic polymer is PLGA because it is easily degraded into lactic acid and glycolic acid which are common metabolic by-products in the body. PLGA is also used in medical diagnostic devices because of the ability to control its degradation rate by altering its molecular weight or copolymer ratio there. PLGA is acidic in nature making it a poor choice for the delivery of acid-labile drugs unless it is modified (Chenthamara et al., 2019). There are formulations in which disulfiram is encapsulated with poly(lactic-co-glycolic acid) (PLGA) nanoparticles. PLGA is a synthetic polymer used for producing nanoparticles for drug delivery. These nanoparticles prevent rapid breakdown of disulfiram (Fasehee et al., 2016) and allows controlled drug release *in vitro*. The half-life of PLGA-DS was extended to 7 hours from 2 minutes and PLGA-DS/Cu suppresses the expression of Liver CSCs (Wang et al., 2017c).

## *2. PLGA-Polyethylene glycol (PEG)-folate encapsulated DS*

Folate-receptor-targeted-PLGA-PEG encapsulated DS was developed for MCF7 breast cancer cells by Fasehee et al. This formulation has a greater drug loading and entrapment efficiency of  $5.42 \pm 0.06\%$  and  $59.62 \pm 0.66\%$  compared to PLGA which has  $5.35 \pm 0.03\%$  and  $58.85 \pm 1.01\%$  respectively. PLGA-PEG-folate and PLGA released disulfiram in two phases, an initial burst phase within the first 24 hours (22.6% and 21.4% respectively) and the latter cumulative release phase which lasts for 120 hours (37.3% and 34.8% respectively). However, the difference in cytotoxicity of PLGA and PLGA-PEG-folate coated DS was not significant (Fasehee et al., 2016).

## *3. Liposome encapsulated DS*

Nanoparticles made from lipids are easily absorbed by cells through their outer lipid bilayer. The 2 main types of lipid nanoparticles are liposomes (spherical lipid bilayer vesicle confining a liquid core) and solid lipid nanoparticles (lipid monolayer and a solid lipid core) (Chenthamara et al., 2019). Different studies have shown that liposome encapsulation of DS (Lipo-DS) boosts its anticancer activity. Lipo-DS suppressed the expression of ALDH<sup>+</sup> CSC population of xenografts in the presence of copper. Liposomes extended the half-life of DS in the blood to 20 minutes (Liu et al., 2014; Najlah et al., 2019).

## *4. Injectable DS-loaded PEGylated liposomes*

A certain study used PEGylated liposomes for disulfiram encapsulation because conventional liposomes have not been efficient for DS delivery. PEGylated liposomes are smaller in size (80-90nm) and possess less polydispersity index. These injectable DS-loaded PEGylated liposomes were shown to increase the stability of DS in horse serum (Najlah et al., 2019).

## 5. TPGS-DS-NLC

A prior study by Banerjee et al. encapsulated DS with nanostructured lipid carriers (NLC) modified with D- $\alpha$ -tocopheryl polyethylene glycol 1000 succinate (vitamin E-TPGS). This nanoparticle has a drug encapsulation of 80.7%, higher cytotoxicity, lower IC<sub>50</sub> and increased cellular uptake in MCF7 and 4T1 cell lines. *In vivo* xenograft mice models of 4T1 revealed that TPGS-DS-NLC has higher tumour growth inhibition rate of 48.24% while free DS and DS-NLC were 8.49% and 29.2% respectively (Banerjee et al., 2019).

### 1.7.5 Cyclodextrins

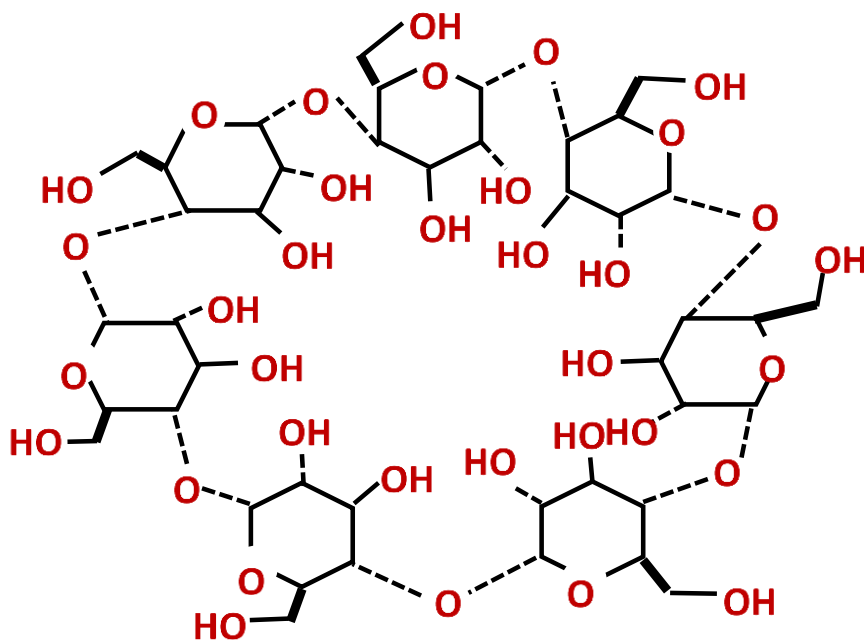


Figure 1.15: Molecular structure of  $\beta$ -cyclodextrins

A major challenge in drug production is that a vast number of cytotoxic chemotherapeutic agents are either poorly soluble in aqueous solution or have a high dissolution rate (Gidwani and Vyas, 2015). Nanotechnology improves the drug concentration at the site of interest. Nanodrug formulations are able to improve the bioavailability and metabolic stability of its

payload till they get to their target site (Brachi et al., 2019). Among the many drug delivery systems currently used are cyclodextrins (CDs).

Cyclodextrins are large cyclic oligosaccharides which have a lipophilic core and hydrophilic outer layer as shown in Figure 1.16 (Tiwari et al., 2010). Cyclodextrins are composed of six ( $\alpha$ -CD), seven ( $\beta$ -CD) and eight ( $\gamma$ -CD) dextrose sub units which can be manipulated to improve the drug delivering efficiency of cyclodextrins. Research has shown that 2HP-  $\beta$ -CD, a derivative of  $\beta$ -cyclodextrin has improved water solubility (Scantlebery et al., 2019; Saha et al., 2016). The molecules in cyclodextrins are bound by alpha-1-4-glycosidic linkages, however it complexes with guest molecules using hydrogen bond, Vander Waals and hydrophobic interaction (Singhal et al., 2018; Gidwani and Vyas, 2015). Cyclodextrins possess the unique ability to complex with and trap a foreign molecule in its core without the formation of any covalent bonds (Tiwari et al., 2010). Cyclodextrins have a conical structure with an outer hydrophilic exterior and inner hydrophobic cavity. The inner cavity has the ability to bind to different kinds of guest molecules such as polar compounds like alcohols and non-polar compounds like aromatic hydrocarbons. The outer hydrophilic exterior enables cyclodextrins to interact well with water (Lopez et al., 2011). Modern science has improved the previous limitations associated with their safety and cost of production, making them a good choice as a drug delivery system. These cyclodextrins have many advantages such as increasing drug solubility, increasing drug bioavailability, enhancing drug stability, reduction of irritation, avoiding drug incompatibility, improving substance handling and hiding bad odour or taste. In pharmaceutical companies, cyclodextrins are popularly used as drug delivery systems in eye drops, nasal sprays, oral tablets, rectal drugs, controlled drug delivery and transdermal drugs. Currently, cyclodextrins are being packaged in carrier molecules such as liposomes, microcapsules, microspheres and nanoparticles to boost its drug delivery capacity (Tiwari et al., 2010). The route through which cyclodextrins are administered determines its safety and

toxicity. Cyclodextrins taken orally may be absorbed by passive diffusion while cyclodextrins taken intravenously are completely excreted by the kidney (Gidwani and Vyas, 2015). A study by Qu et al showed that administering a DSF inclusion complex comprising of DSF, Cu and hydroxypropyl- $\beta$ -cyclodextrin (DSF/HP- $\beta$ -CD/Cu) through the intranasal route to intracranial GBM bearing male rats suppressed tumour progression and cell motility, promoted apoptosis and increased median survival time by 36.8% and 18.2% compared to model rats when administered via oral and intravenous route respectively (Qu et al., 2021).

## **1.8 AIM AND OBJECTIVES**

The aim of this project is to study the molecular mechanisms of hypoxia-induced chemoresistance and aggressiveness in PDAC cell line and investigate the eliminating effect of cyclodextrin-encapsulated disulfiram on hypoxia-induced resistance and PDAC cancer stem cells.

### ***Objectives***

- To determine the effect of hypoxia on chemosensitivity, aggressiveness and stemness in PANC-1 cell line.
- To examine the effect of hypoxia on chemoresistance and stemness in patient derived PDAC cells.
- To investigate the effect of NF $\kappa$ B pathway activation on chemosensitivity and aggressiveness in PANC-1 cell line.
- To study the effect of cyclodextrin-encapsulated disulfiram on hypoxia-induced stemness and chemoresistance in patient derived PDAC cells.

## **CHAPTER 2**

### **MATERIALS AND METHODS**

## **2.1 Materials**

### **2.1.1 Cell lines**

Six primary PDAC cell cultures: liver metastasis (A6L), primary PDAC (12560, 12556), and circulating PDAC (CX102, CX135, C76) cells characterised and very kindly provided by Professor Christopher Heeschen at Bart's Cancer Institute, Queen Mary University of London, U.K.

Panc-1 PDAC cell line was supplied by ATCC (Baltimore, MD, USA).

### **2.1.2 Reagents, enzymes and kits**

ALDEFLUOR kit (Stem Cell Technologies, Cambridge, UK).

The following reagents were purchased from Sigma (Dorset, UK): D-glucose, Insulin, 3-(4,5-dimethylthiazol-2-yl)-2,5-diphenyltetrazolium bromide (MTT), Propidium iodide, Hygromycin B, Tetraethylthiuram disulphide, Phosphate buffer saline tablets, Glycine, Ammonium persulfate, Sodium hydroxide, Methanol, 100% Ethanol, Crystal violet, Copper II chloride hydrate, N,N,N',N'-tetramethyl-ethylenediamine (TEMED), DL-Dithiothreitol solution (DTT), RNaseZAP, Trizma phosphate, Poly(2-hydroxyethylmetacrylate).

Ambion™ DNAZap™ (Invitrogen, ThermoFisher Scientific Inc, USA).

EZ-ECL chemiluminescence detection kit for horse radish peroxidase (Biological Industries, Cromwell, USA).

Fetal bovine serum (FBS), Phosphate buffered saline (PBS), Antibiotic-antimycotic, B-27 Supplement (Gibco Life Technologies, Paisley, UK).

FITC Annexin V apoptosis detection kit II (BD Biosciences, New Jersey, USA).

Giemsa stain (Riedel-de Haen, Seelze-Hannover, Germany).

Hypoxyprobe™-1 Plus Kit supplied by Hypoxyprobe Inc (Burlington, MA, USA).

Image-iT Fix-Perm kit (Molecular probes by Life technologies, Massachusetts, USA).

Lipofectamine™ 2000 reagent (Invitrogen, Thermofisher Scientific Inc, UK).

Molecular probes, MycoFluor Mycoplasma Detection Kit (Thermofisher Scientific, U.S.A.).

Mycoplasma removal agent (Bio-rad Laboratories, CA, U.S.A.).

Penicillin-streptomycin (BioWhittaker® Lonza, Walkersville, USA - Lonza, Slough, UK).

Protein estimation kit: Protein assay reagent A, Protein assay reagent B, Protein assay reagent S (Bio-rad Laboratories, Hertfordshire, UK).

Protogel stacking buffer, Accugel 19:1 bisacrylamide, 4× Protogel resolving buffer, 10× Tbe, 10× Tris/glycine (Gene Flow Limited, Lichfield, U.K.).

Reverse transcription kit: Taqman universal master mix II with UNG, 10× RT Buffer, 25× dNTP mix, 10× RT Random Primers, Reverse transcriptase. Primers 20× mix: 02387400 NANOG, 00153153 HIF1A, 01053049 SOX2, 00999632 POU5F1 (OCT4), 02786624 GAPDH, 01042014 RELA (p65), 99999909 HPRT1, 01026149 EPAS1 (HIF2α) (Applied Biosystems, CA, U.S.A.).

Rosewell Park Memorial Institute (RPMI) media, L-glutamine, 10× Trypsin (Lonza, Basel, Switzerland).

RhFGF-Basic (R&D Systems, Abingdon, UK).

Total RNA purification plus kit: Elution solution A, Buffer RL, Collection tubes, Elution tubes, Spin columns and Wash solution A (Norgen Biotek Corp, Ontario, Canada).

Vectorshield (Vector Laboratory Inc, Burlingame, CA).

### **2.1.3 Antibodies**

Anti-beta actin monoclonal antibody (Sigma Aldrich Company Ltd., Dorset, UK).

CD133/2-VioBright™ FITC, Human (Macs Milteyi Biotech, Germany).

BAX, p65, Sox2, BCL-2, E-Cadherin, Vimentin, Oct4, Nanog, N-Cadherin (Abcam, Cambridge, UK).

Enhanced ChemiLuminescence (ECL)™ anti-mouse antibody (Ab), ECL™ anti-rabbit antibody (GE Healthcare, Buckinghamshire, UK).

HIF2 $\alpha$  antibody (Novus Biologicals, CO, USA).

Horse radish peroxidase conjugated secondary anti-mouse and anti-goat antibodies (GE Healthcare UK Ltd).

### **2.1.4 Equipment and Labware**

Amersham Hybond™ -P polyvinylidene difluoride (PVDF), blotting paper (GE Healthcare Life Sciences, Buckinghamshire, UK).

BD Accuri C6 Flow cytometer (BD, New Jersey, USA).

Cell scraper, 6-well, 12-well, 24-well and 96-well flat bottom tissue culture plates, tissue culture flasks with vented caps (T25, T75 and T150), Eppendorf tubes (0.5ml and 1.5ml), vacuum filter, serological pipette (Sarstedt Ltd., Leicester, UK).

CO<sub>2</sub> incubator, O<sub>2</sub>/CO<sub>2</sub> incubator (Panasonic, Leicestershire, UK).

Evos FL Cell Imaging System (Invitrogen, California, USA).

Matrigel (BD Biosciences, Oxford, UK).

Micropipette (0.1-2 $\mu$ l, 0.5-10 $\mu$ l, 2-20 $\mu$ l, 20-200 $\mu$ l, 10-100 $\mu$ l and 100-1000 $\mu$ l), Spectrafuge mini centrifuge (Labnet, New Jersey, USA).

Microscope slide (ERIE Scientific Company, Portsmouth, NH, USA).

Mini protein electrophoresis chamber kit, tank with lid, buffer dam, gel cutter, gel plate adapters, power pack, 1.5mm glass plate, 1.5mm gel combs (BIO-RAD, Hertfordshire, UK).

MP220 pH meter (Mettler Toledo, Ohio, USA).

NanoDrop 2000, Multiskan Ascent, Multidrop 384, Fluoroskan Ascent FL, Shandon Cytospin 4, Chamber slide (Thermo Scientific, Massachusetts, USA).

PIPETBOY (Integra, Hudson, USA).

QuantStudio 6 Flex Real-time qPCR system (Applied Biosystems, CA, USA).

Sterile pipette tips ZAP filter tips (Alpha laboratories, Eastleigh, UK).

Stuart® 3-block heater (Bibby Scientific Ltd., Straffordshire, UK).

TE70 ECL Semi-Dry Transfer Unit, Hypercassette (Amersham, Biosciences, UK).

## **2.1.5 Buffers**

### ***i. Blocking buffer for western blot***

Blocking buffer is used for blocking the non-specific binding of proteins to the nitrocellulose membrane and was prepared by dissolving 5g of non-fat milk in 100ml of 1 $\times$  TBS-T.

### ***ii. Flow buffer for flow cytometry***

Flow buffer is used for stain preparation and sample incubation during flow cytometry analysis for CSC markers. Flow buffer was prepared by adding 4% FBS to PBS.

### ***iii. Running buffer***

Running buffer is used for SDS-PAGE during western blot analysis. 1× running buffer was prepared by mixing 100ml of 10× stock solution and 900ml of distilled water then storing it at room temperature.

### ***iv. Sorenson's Glycine Buffer***

Sorenson's glycine buffer is used during MTT analysis. It was prepared by dissolving 3.75g of glycine and 2.92g of NaCl in 500ml of distilled water then raising the pH to 10.5 with 5M NaOH. This buffer was stored at room temperature.

### ***v. Transfer Buffer***

Transfer buffer is used when carrying out western blot analysis. This was prepared by mixing 200ml of methanol, 700ml of distilled water and 100ml of 10× stock solution and stored at room temperature.

### ***vi. 10× Tris-Buffered Saline Buffer (TBS)***

The 10× TBS-T buffer was prepared by dissolving 12.11g Tris base and 81.8g NaCl in 1 Litre of distilled water and bringing the final pH to 7.4 and stored at room temperature.

### ***vii. 1× Tris-Buffered Saline Tween-20 (TBS-T)***

A stock of 1× TBS-T was prepared by mixing 100ml of (10×) TBS-T, 900ml of distilled water and 500µl of Tween-20.

### ***viii. Freezing Buffer***

Freezing buffer is used to suspend cells to be preserved in liquid nitrogen. It is prepared by adding 10% of DMSO to FBS.

**ix. RIPA Buffer**

RIPA buffer is used in western blot analysis for cell lysis. A 100ml stock of 10× RIPA buffer with a pH of 7.4 was prepared using the reagents in the quantities shown in the table below.

The stock was then stored in a fridge at 4<sup>0</sup>C.

**Table 2.1: Preparation of RIPA buffer**

| <b>Reagents</b>      | <b>Concentration</b> | <b>Weight/100mL</b> |
|----------------------|----------------------|---------------------|
| Tris HCl             | 25mM                 | 395mg               |
| Aprotonin            | 1mM (1-10µg/mL)      | 1mg                 |
| Triton X-100         | 1%                   | 1mL                 |
| Sodium Deoxycholate  | 0.5%                 | 0.5g                |
| NaCl                 | 0.15M                | 0.88mg              |
| EDTA                 | 1mM                  | 37.2mg              |
| Sodium Orthovanadate | 1mM                  | 18.4mg              |
| SDS                  | 0.1%                 | 0.1g                |
| Leupeptin            | 1Mm (1-10µg/mL)      | 1mg                 |
| PMSF                 | 1mM                  | 17.4mg              |

## **2.2 Methodologies**

### **2.2.1 Cell Culture**

#### ***i. Adherent cell culture***

RPMI media was prepared by adding 5ml of L-Glutamine, 5ml of penicillin-streptomycin and 50ml of fetal bovine serum (FBS) into 500ml of RPMI media. 1× trypsin was prepared by dilution of 10× trypsin in PBS. Both were stored at 4<sup>0</sup>C. All PDAC patient derived cells and cell line were maintained using RPMI media.

T75 flasks containing previously subcultured cells were removed from the incubator to a hood with laminar flow of air. The old media in the T75 flasks was aspirated using a Pasteur pipette. Immediately after, 5ml of PBS was put into each T75 flask to rinse off any trace of media in the flask. This PBS was aspirated then 3ml of 1× trypsin was added into each flask then these flasks were kept in the incubator till the cells trypsinised. After the cells trypsinised, the enzyme in each flask was neutralised with 3ml of RPMI media then collected into tubes and centrifuged at 1200rpm for 5 minutes. The supernatant was aspirated then the cells at the bottom were resuspended in 5ml of RPMI media and thoroughly mixed to break cell clumps. The resuspended cells were counted using a haemocytometer then 2 to 3 million cells were introduced into a labelled new T-75 vented flask, containing 19ml of RPMI. These new flasks were returned to the incubator at 37<sup>0</sup>C, 5% CO<sub>2</sub>.

#### ***ii. Hypoxia cell culture***

The process of hypoxic cell culture is the same as that of adherent cell culture except for the fact that 5 x10<sup>5</sup> cells were seeded in 8ml of RPMI media in T25 flasks and the cells were incubated in a hypoxic incubator with 1% O<sub>2</sub>, 37<sup>0</sup>C and 5% CO<sub>2</sub>. The cells were incubated for about 5 days and the media was changed on the 3<sup>rd</sup> day. Drug treatment was done on the 5<sup>th</sup> day and cells collected on the 6<sup>th</sup> day.

### *iii. Spheroid cell culture*

Spheroid culture is gaining fame because of its ability to better reproduce cell-cell, cell-matrix and physico-biochemical barriers in cancer tumours than monolayered cultures (Lee et al., 2020). To prepare stem cell media, approximately 500µl of heparin, 1ml of insulin, 100µl of Fibroblast growth factor (FGF), 10ml of B-27, 100µl of Epidermal growth factor (EGF), 3.1 ml of D-glucose, 5ml of L-glutamine and 5ml of penicillin-streptomycin into a 500ml bottle of DMEM-F12. The mixture was then filtered and stored in a fridge at 4<sup>0</sup>C.

PolyHema was prepared by dissolving 10mg/ml of poly(2-hydroxyethylmethacrylate) in 95% ethanol and kept on a stirrer overnight. The next day, the solution was filtered and preserved in a fridge at 4<sup>0</sup>C. Small volumes of polyHema (4ml for T75, 2ml for T25, 0.4ml for 6-well plate, 0.3ml for 24-well plate, 30µl for 96-well plate) were used to coat the bottom of flasks and plates (to prevent cells from attaching to the flasks or plates) then left overnight in an oven to dry. The next day the coated flasks and plates were rinsed twice with PBS.

About 500,000 normoxic cells were seeded in 8ml of stem cell media and these flasks were kept in an incubator for 6 days at 37<sup>0</sup>C and 5% CO<sub>2</sub>. Drug treatment was done on the 5<sup>th</sup> day and spheres collected on the 6<sup>th</sup> day.

### **2.2.2 MTT Cytotoxicity Assay**

Cytotoxicity is a cell-based assay used to analyse the effect of a test molecule such as a drug on cell death or cell proliferation. This experiment makes use of tetrazolium dye which is enzymatically reduced to a coloured crystal by viable cells. At the end of the experiment, the crystals are dissolved with dimethyl sulfoxide, then the proportion of viable cells is estimated and recorded (Riss et al., 2013). MTT reagent was prepared by dissolving 5g of 3-(4,5-dimethylthiazol-2-yl)-2,5-diphenyltetrazolium bromide in 500ml of PBS in a bottle covered with an aluminium foil, filtered and stored at 4<sup>0</sup>C.

In this experiment, for each patient derived cell, three 96 well plates were seeded with each well containing 7500 cells per 200 $\mu$ l of RPMI media. These plates were incubated overnight. The next day, the plates were aspirated then the cells were dosed with serial dilutions of different drugs both singly and in combination with other anticancer drugs. The plates were then incubated for 72 hours at 37<sup>0</sup>C and 5% CO<sub>2</sub>. After 72 hours, the plates were removed from the incubator and 20 $\mu$ l of MTT reagent was added to each well. The plates were wrapped in foil paper and returned to the incubator for 3 hours during which the MTT bound to the live cells in the wells to form purple formazan crystals. After the incubation time elapsed, the MTT-media mixture was aspirated from all the wells. The penultimate step was the addition of 80 $\mu$ l of dimethyl sulfoxide and 20 $\mu$ l of Sorensen's reagent to each well. The optical densities of the contents of the wells were read at 540nm then the result was analysed and recorded. Cell viability was calculated and used to estimate the IC<sub>50</sub> of the various drugs used.

### **2.2.3 Hypoxyprobe Analysis by Flow Cytometry**

Hypoxyprobe analysis is used for evaluating hypoxic regions in cells and tissues. Hypoxyprobe<sup>TM</sup> contains pimonidazole which is reductively activated by hypoxia to form complexes with sulfhydryl groups in amino acids, peptides and proteins (Aguilera and Brekken, 2014). These complexes can be detected by specific monoclonal antibodies using flow cytometry and immunofluorescence (Cousins et al., 2016).

About 5 $\times$ 10<sup>5</sup> cells were seeded per T25 flask and cultured under hypoxic and spheroid conditions. Another 5  $\times$ 10<sup>5</sup> cells per T25 flask was cultured on the 4<sup>th</sup> day under normoxic conditions. On the 5<sup>th</sup> day, hypoxyprobe was added into the flasks in a ratio of 1 $\mu$ l to 1ml of RPMI media then the flasks were incubated for 2 to 4 hours. After the time elapsed, the normoxic, hypoxic and spheroid cells were trypsinized, neutralized with serum containing media then rinsed with PBS and centrifuged at 2000 rpm for 5 minutes. The cells from each

flask were split into two parts then resuspended in 200µl of PBS. Then, 2ml of ice-cold methanol was added gradually into each tube while spinning them on a vortex. The tubes were left at room temperature for 10 minutes then filled with PBS and centrifuged at 2500rpm for 5minutes. The PBS was aspirated and 3ml of PBS was again added into each tube and centrifuged again. Approximately 150µl of blocking solution was added into each tube then the cells were incubated for 1 hour. Exactly 2ml of PBS was added into the tubes and centrifuged again at 2500rpm for 5minutes. Then, 100µl of FITC-HPP antibody prepared in a ratio of 1:1000 of Tritan× 100 + 1% BSA + PBS was added into each tube which was then incubated in the dark for 1 hour. Then the cells in each tube were rinsed with 2ml of PBS and centrifuged, aspirated then resuspended in 200µl of PBS and analyzed using a flow cytometer.

#### **2.2.4 Immunocytochemistry**

The first part of this assay varied depending on the cell type.

##### **i. *Adherent and hypoxic cells***

Each well of a four-well chamber slide was seeded with 25,000 to 40,000 cells of a different patient derived PDAC cell depending on its rate of growth in 500µl of RPMI media and kept in a humidified incubator at 37°C, 5% CO<sub>2</sub>. The same thing was repeated for a second chamber slide which was kept in a hypoxic humidified incubator at 37°C, 5% CO<sub>2</sub> and 1% O<sub>2</sub>. Two hours before the experiment was to start, hypoxyprobe reagent was added in the ratio of 1µl of hypoxyprobe reagent to 1ml of RPMI media then chamber slides were returned to their respective incubators. After the time elapsed, the media was again aspirated from both chamber slides and 250µl of fixative solution or ice-cold methanol was added to each well then incubated for 15 minutes at room temperature. After which the fixative solution was discarded and the cells washed 3 times with 1 ml of wash buffer on a shaker at 500rpm for 5 minutes. Then 250µl of permeabilization solution was added into each well and the cells were incubated

for 15 minutes at room temperature (20 to 25°C). The permeabilization solution was discarded and the cells were again washed with 1 ml of wash buffer for 5 minutes at room temperature. Approximately 2ml of blocking solution was added to each well and the cells were incubated for 1 hour at room temperature before staining.

FITC-conjugated anti-pimonidazole (FITC-HPP) was prepared in a ratio of 1:1000 of blocking solution. 200µl was added to each well and left for an hour at room temperature after which it was washed 3 times for 5 minutes with 1 ml of wash buffer solution.

Actin stain was prepared in a ratio of 2 drops to 1ml of blocking solution and 200µl of the prepared solution was added to each well then incubated for 30 minutes at room temperature. It was later washed 3 times for 5 minutes on a shaker.

The chamber on the slides were removed and the slide was left to air dry. After which a drop of Dapi Vector Shield was added to each well carefully to avoid bubbles and a clean rectangular coverslip was placed on the slide whose edges were then sealed with colourless nail polish to prevent the fluorescence from escaping.

After the nail polish dried, the slides were viewed using the Life cell imaging and images were taken and recorded.

## **ii. Spheroid cells**

Hypoxyprobe reagent was added to flasks containing previously cultured sphere cells in a ratio of 1µl to 1ml of stem cell media, and previously subcultured normoxic cells and left overnight in a humidified incubator at 37°C, 5°C. The next day, the normoxic cells were trypsinised and 500µl of each normoxic cell sample and each sphere containing media sample was put into duplicate cytofunnels, each containing a slide and centrifuged using a cytospin set at medium, program 2 and 800rpm for 5 minutes. After which the slides were carefully removed and the cytofunnels discarded. A liquid blocker was used to mark the area around the cells on each

slide and allowed to dry. A 1ml pipette was used to add 3 drops of fixative solution to the cells on each slide which were then incubated for 15 minutes at room temperature. The slides were tapped on tissue to get rid of the fixative solution then the cells were washed three times for 5 minutes. Exactly 250µl of permeabilization buffer was added to the cells on all the slides and incubated for 15 minutes at room temperature after which the permeabilization solution was discarded and the cells washed three times for 5 minutes with wash buffer. A pipette was used to add 250µl of blocking solution to the cells and incubated for 1 hour at room temperature. The cells were stained as described in (i) above. However, the coverslip used for covering the cells was circular.

### **2.2.5 Sphere Reformation Assay**

Sphere reformation assay is used to evaluate the degree of cytotoxicity of a drug by analysing the ability of spheroid cells to regrow after drug treatment.

In this experiment, T25 flasks and a 24-well plate were coated with 2ml and 1ml of poly-Hema respectively then kept in an oven overnight to dry the poly-Hema. The next day, the coated T25 flasks were rinsed with 2ml of PBS then seeded with 500,000 cells in 8ml of stem cell media and kept in an incubator for 7 days at 37<sup>0</sup>C and 5% CO<sub>2</sub>. On the seventh day, the spheres in each T25 flask was collected into a tube, rinsed with PBS, centrifuged and aspirated. Exactly 7ml of stem cell media was added to the tube and mixed for even distribution of the spheres then 1ml of this was added into 6 smaller tubes, centrifuged at 600rpm for 5 minutes and aspirated.

Exactly 4ml of stem cell media was added into each of a new set of 6 tubes. These tubes were labelled as negative, paclitaxel, gemcitabine, copper, disulfiram/Cu and Cyclodextrin/Cu. The media in these tubes were dosed with the respective drugs in the desired concentration. Exactly 3ml of media from each tube was mixed with the sphere pellets in the corresponding tube then

added into a well of the 6-well plate. The plate was then incubated for 48 hours then the contents of each well was collected into a tube, rinsed with PBS, trypsinized with 500 $\mu$ l of 1 $\times$  trypsin for 5 minutes, neutralized with 500 $\mu$ l of serum containing media. Then 7ml of stem cell media was added to each tube which was then vortexed and 2mls from the tube was put into the corresponding wells of a 24-well plate. After 5 to 7 days, the reformed spheres were counted, and images were taken.

### **2.2.6 Flow Cytometry**

Flow cytometry assay is used to analyse cell populations based on their size, shape, surface antigens, granularity, transcription factors, cytokines, etc (Fox et al., 2020).

In this experiment, spheroid and hypoxic cells were set up in T25 flasks and incubated for 5 days though the media in them was replaced on the fourth day. On the 6<sup>th</sup> day, some of the flasks for each cell type was labelled negative while the rest were dosed with an anticancer drug and incubated overnight. The next day, overnight normoxic cultures and the hypoxic cells were trypsinized and each flask was collected into well labelled tubes. These tubes were centrifuged and aspirated then 500 $\mu$ l of media was added to it and mixed.

Each flask containing spheroid cells was collected into a tube. These tubes were centrifuged at 600rpm for 5 minutes and the supernatant aspirated. Approximately 200 $\mu$ l of trypsin was added to the sphere cell pellets and incubated for 5 minutes after which it was mixed and left to incubate for another 5 minutes and mixed again to break the spheres. About 300 $\mu$ l of media was then added to the spheres to neutralize the trypsin. Some 10ml tubes were labelled and 200 $\mu$ l of each cell type was added into duplicate tubes. After which 2ml of 1 $\times$  PBS was added into each of the 10ml tubes, centrifuged at 2000rpm for 5 minutes and aspirated.

The desired stain was then prepared.

- i. For ABCG2, the stain was prepared on a ratio of 2.5µl to 100µl of flow buffer per tube. Exactly 100µl of the stain was aliquoted into each tube and mixed well with the cells. The tubes were then incubated for 30 minutes at 4°C. After the incubation time elapsed, 2mls of flow buffer was added to each of the tubes which were then centrifuged and aspirated. The pellets were then resuspended in 200µl of flow buffer, mixed then 200µl from each tube was aliquoted into labelled flow tubes. The flow cytometer was used to analyze the samples.
- ii. For CD133 stain, the stain solution contained 5µl of CD133 antibody in 100µl of flow buffer. Approximately 100µl of this stain was added into each tube, mixed thoroughly with the cells and incubated in a fridge for 30 minutes. After the incubation time elapsed, 2mls of flow buffer was added to each of the tubes which were then centrifuged and aspirated. The pellets were then resuspended in 200µl of flow buffer, mixed then 200µl from each tube was aliquoted into labelled flow tubes. The flow cytometer was used to analyze the samples.
- iii. For ALDEFLUOR stain, a volume was prepared which contained 0.5µl of stain in 100µl of ALDEFLUOR buffer. Approximately 100µl of this stain was added into each tube, mixed thoroughly with the cells and incubated in the dark for 30 minutes. About 2mls of 1× PBS was added to each of the tubes which were then centrifuged and aspirated. The pellets were then resuspended in 200µl of ALDEFLUOR buffer, mixed then 200µl from each tube was aliquoted into labelled flow tubes. The flow cytometer was used to analyze the samples.

### **2.2.7 Annexin Apoptosis Assay**

One of the intracellular processes used for regulating homeostasis is apoptosis which entails programmed cell death (Tian *et al.*, 2020). Apoptosis is initiated extrinsically by the activation of cell surface death receptors such as TNFR family and intrinsically by DNA damage or cell

stress. Annexin V is popularly used for analysing cell apoptosis because it binds to the exposed phosphotidal serine residues on the membrane of early apoptotic cells. Dead cells usually have damaged cell membranes which membrane impermeable DNA stains such as propidium iodide can bind to. As a result, dead and apoptotic cells can be analysed by flow cytometry using Annexin V and propidium iodide (Demchenko, 2013).

In this experiment, about 300,000 cells in 3mls of RPMI media were seeded in each well of three 6-well plates which were then incubated at 37°C. The next day, the wells were labelled as negative, gemcitabine, paclitaxel and cyclodextran disulfiram respectively. Each of the anticancer drugs was prepared at the required concentration in 10ml of RPMI media.

The media in the 6-well plates was aspirated, 3ml of drug containing media was added to the appropriate well and the plates were again incubated at 37°C. The next day, tubes were labelled according to the label of the wells. The drug containing media in each well was collected and put into the appropriate tube. Then, 1ml of 1× PBS was added to each of the wells to rinse, then collected and put into the appropriate tube. Approximately 500µl of trypsin was added to each of the wells then the plates were incubated till the cells completely detached from the bottom of the wells. The trypsin was then neutralised by adding 500µl of media to each of the wells. The trypsinized cells were collected into the corresponding tubes then the wells were rinsed with media and the media was again collected into the tubes. The tubes were centrifuged at 2000rpm for 5 minutes, aspirated and rinsed with 3ml of PBS, centrifuged and aspirated.

A solution containing annexin V, propidium iodide and incubation buffer was then prepared with every ml of incubation buffer containing 10µl each of propidium iodide and annexin V following the manufacturers instruction. Approximately 200µl of this solution was added into each tube then mixed well with the cells before being transferred into well labelled flow tubes. These flow tubes were incubated in the dark for 20 minutes in a process referred to as staining.

After staining the cells, 200µl of incubation buffer was added to each tube then the tubes were read using a flow cytometer.

### **2.2.8 Western Blot**

Western blot is used for protein separation and identification. This technique involves gel electrophoresis, blotting, incubation with specific antibodies and chemiluminescence. The thickness of the band formed is a measure of the protein expression (Mahmood and Yang, 2012). This technique required a series of steps which have been highlighted below:

#### **i. *Protein collection***

The procedure for collecting normoxic and hypoxic cell pellets are the same. A cell scraper was used to scrape off cells attached to the bottom of flasks containing previously subcultured PDAC cells. The media containing the scraped cells was poured into tubes, centrifuged and aspirated. The cell pellets were rinsed with PBS, collected in well labelled Eppendorf tubes and stored on ice or at -80°C.

#### **ii. *Protein extraction***

The Eppendorf tubes containing the cell pellets was placed on ice. Frozen RIPA buffer was kept on ice to thaw then 100 to 150µl was added into each Eppendorf tube depending on the size of the cell pellet and mixed thoroughly with a pipette. These Eppendorf tubes were placed on an Eppendorf float and kept in a sonicator for 30 seconds to burst the cells. The Eppendorf tubes were quickly transferred into a centrifuge set at 4°C, 20 minutes and 14,000rpm. After spinning, the supernatant containing the extracted cell proteins were collected with a 200µl pipette and put into a new set of labelled Eppendorf tubes. These tubes were then kept on ice or stored at -20°C.

iii. ***Determination of protein concentration***

A 1ml capacity Eppendorf tube was placed on a rack. 1ml of Protein assay reagent A and 25 $\mu$ l of Protein assay reagent S was put into the Eppendorf tube and the contents of the tube were mixed with a vortex. 25 $\mu$ l aliquots of this mixture was put into the desired wells of a 96-well plate. Exactly 2.5 $\mu$ l of each protein sample was added in duplicates, followed by 200 $\mu$ l of Protein assay reagent B. The plate was incubated at room temperature for 10minutes then read on a plate reader. The optical densities obtained were analysed and used to calculate the protein concentration in each sample and the volume of the samples needed to load 30 or 60 $\mu$ g/lane/well.

iv. ***Electrophoresis***

Running gel was prepared depending on the pore size required as shown in Table 2.2 and about 7.5ml was put in between 2 glass slides. Approximately 250 $\mu$ l of isopropanol was added on top of the gel to give an even surface and get rid of bubbles. The gel was allowed to set then the isopropanol was rinsed off with distilled water. The stacking gel was prepared using the reagent volumes shown in the table 2.3 below then added on top of the running gel.

**Table 2.2: Preparation of Separating gel**

|                                    | <b>12%</b> | <b>10%</b> | <b>8%</b> | <b>7.5%</b> | <b>6.5%</b> | <b>6%</b> |
|------------------------------------|------------|------------|-----------|-------------|-------------|-----------|
| Resolving buffer (ml)              | 5.5        | 5.5        | 5.5       | 5.5         | 5.5         | 5.5       |
| Water (ml)                         | 6.0        | 6.5        | 6.2       | 6.4         | 7.0         | 3.2       |
| 19:1Bis-acrylamide:acrylamide (ml) | 5.0        | 4.4        | 4.3       | 4.0         | 7.0         | 3.2       |
| TEMED ( $\mu$ l)                   | 20         | 15         | 15        | 15          | 15          | 20        |
| 10% Ammonium persulfate ( $\mu$ l) | 150        | 120        | 120       | 120         | 120         | 200       |

**Table 2.3: Preparation of Stacking gel**

| <b>Reagents</b>                   | <b>Volume</b> |
|-----------------------------------|---------------|
| Stacking buffer                   | 4.2ml         |
| 40% 19:1 Acrylamide:Bisacrylamide | 1.2ml         |
| Water                             | 6.6ml         |
| 10% Ammonium Persulfate           | 250 $\mu$ l   |
| TEMED                             | 20 $\mu$ l    |

A comb was quickly inserted into the stacking gel which was allowed to set. After the stacking gel had set, the glass slides containing the gel were transferred to a gasket then fitted into the

electrophoresis tank. The gasket was filled with running buffer and the comb was gently removed to avoid breaking the wells.

Labelled Eppendorf tubes were placed on a rack. The calculated values of the DTT, 4X, water and protein for each sample was added to each of the respective Eppendorf tubes. The tubes were centrifuged for one minute then placed on a heat block for 10 minutes at 97<sup>0</sup>C. After which the Eppendorf tubes were centrifuged to bring down the vapour which had percolated in the tubes for about 30 seconds then placed on a rack. The content of each tube was loaded into the corresponding well then more running buffer was added till it reached the required level. A protein ladder was added into one of the wells to know regions on the gel with the protein size of interest. The tank was covered carefully making sure that the electrodes were in the right position then the lid was connected to a power source set at 200volts, 300milliamperes and 60 minutes then switched on. After the time had elapsed, the power source was switched off and the gel was removed from the tank.

#### **v. *Blotting***

A sheet of Whatman filter paper was cut into rectangles of dimension 12 inches by 10 inches. Similarly, polyvinyl difluoride (PVDF) membrane was cut into a rectangle of dimension 8 by 5 inches. Five of the cut filter papers were dipped into transfer buffer consecutively then stacked on the blotting machine. The PVDF membrane was dipped in methanol to activate it then transferred into transfer buffer before placing it on the stack of soaked filter papers. The gel was gently removed from the glass slides and the region of interest was cut out and rinsed in transfer buffer before placing it on the activated PVDF membrane. Bubbles were eliminated from the bottom of the gel to ensure complete transfer of proteins during blotting. Then, another layer of five filter papers soaked in transfer buffer was carefully stacked on top of the gel. Transfer buffer was poured on the stack of filter papers till it was flooded then the blotting

machine was closed then set at 155volts, 2 hours and after the time has elapsed, the PVDF membrane was removed and blocked.

*vi. Blocking*

In this stage, the PVDF membrane was dipped into a bowl containing 5% milk in 1× TBS-T and kept on a rocker for 30 minutes to 1 hour.

*vii. Addition of antibodies*

Primary antibody was prepared in a ratio of 1:1000 with 5% milk in 1× TBS-T. The PVDF membrane was put in the prepared antibody mixture and kept on a rocker overnight. The next day, the membrane was washed twice in 1× TBS-T for 15 minutes. Then the membrane was incubated in a mixture containing 1:5000 ratio of secondary antibody to 5% milk in 1× TBS-T for one hour. After which, the membrane was washed twice for 15 minutes with 1× TBS-T.

*viii. Band detection*

The PVDF membrane was placed on a cling film in a cassette. Then, an equal volume of the ECL reagents: stable peroxide solution and, luminol and enhancer solution were mixed in a tube then used to flood the surface of the PVDF membrane and left for 4 minutes. After which the excess solution was drained off then the PVDF membrane was analysed using a Li-Cor C-Digit western blot scanner.

### **2.2.9 Real-time Polymerase Chain Reaction (RT-PCR)**

Polymerase chain reaction (PCR) is a highly sensitive and specific technique used for amplifying DNA sequences while real time PCR is used for measuring the quantity of PCR products produced with time. Real-time PCR is used for gene expression detection and quantification (Deepak et al., 2007).

This experiment has 3 stages namely:

i. ***Sample collection***

Old media was poured out of flasks containing previously subcultured normoxic or hypoxic cells. These cells were then rinsed with PBS and aspirated. Into the flasks, 300µl of lysis buffer was added and left for a minute then collected into labelled sterile Eppendorf tubes.

For spheroid cultures, the sphere containing media was poured into sterile tubes, centrifuged at 1200rpm for 5 minutes and aspirated. Then rinsed with PBS, centrifuged and aspirated. About 300µl of lysis buffer was added into the tubes and collected into labelled Eppendorf tubes as above. At this stage, the extracted samples were stored at -80°C till required.

ii. ***RNA extraction***

The work surface was cleaned using DNazap and RNaseZAP to get rid of contaminants. The collected cell samples were thawed then placed on ice. A pipette was used to transfer each sample into a labelled gDNA purification column which was then placed in a collection tube and centrifuged at 10,000rpm for 1 minute at room temperature. The gDNA columns were disposed and 200µl of 100% ethanol was added to each filtrate, vortexed for about 10 seconds then the mixture was transferred with a pipette into an RNA purification column. Each RNA purification column was placed in a collection tube and centrifuged at 10,000rpm for 1 minute at room temperature. After which, the filtrate was disposed and 400µl of wash solution was added into each RNA purification tube and centrifuged again at 10,000rpm for 1 minute at room temperature. The filtrate was again disposed and the samples were washed two more times with wash buffer and centrifuged. After washing the third time, the filtrate was disposed then the RNA columns were centrifuged again without any wash buffer to completely get rid of any trace of wash buffer on the columns. A new set of Eppendorf tubes were gotten and the caps were cut off then the collection tubes were disposed and each RNA purification column

was transferred into a cut Eppendorf. Gloves were changed to prevent contamination then 50µl of elution solution was added into each RNA purification column and incubated at room temperature for 2 minutes. The RNA columns were centrifuged at 2000rpm for 2 minutes then at 10,000rpm for 1 minute. The filtrate containing the extracted RNA was then transferred from the cut Eppendorf tubes into sterile and well labelled 1ml Eppendorf tubes and stored at -80°C till required.

iii. ***Determination of RNA concentration***

The Nanodrop 2000 was used to calculate the concentration of each sample in ng/µl using the elution solution as a blank. Pure RNA had a 260/280nm range of  $2 \pm 0.5$ .

iv. ***cDNA synthesis***

The extracted RNA samples were thawed and placed on ice. Their concentrations were used to calculate the volume of each sample containing 500ng of RNA and the volume of RNase free water required to get a total volume of 10µl.

Volume of sample containing 500ng of RNA ( $\times$ ) =  $500/\text{RNA concentration}$

Volume of water required =  $10\mu\text{l} - \times$

Sterile 500µl Eppendorf tubes were labelled and the respective RNase free water and sample volumes were added into them and placed on ice. Then a master mix containing the following reagents was prepared as shown in Table 2.4 below depending on the sample number and 10µl of the master mix was aliquoted into the corresponding sample tube. After which the tubes were centrifuged for about 10 seconds to bring everything to the bottom then placed in a thermocycler to convert the RNA to cDNA.

**Table 2.4: Preparation of RT-master mix**

| <b>Component</b>      | <b>Volume per sample (µl)</b> |
|-----------------------|-------------------------------|
| 10× RT buffer         | 2                             |
| Random Primers        | 2                             |
| dNTPs                 | 0.8                           |
| Reverse transcriptase | 1                             |
| RNase free water      | 4.2                           |
| <b>Total Volume</b>   | <b>10</b>                     |

v. ***Real-time PCR.***

After the conversion of the RNA to cDNA, the total cDNA volume was 20µl with a total concentration of 500ng/µl. A pipette was used to add 80µl of RNase free water to the cDNA to give a new concentration of 5ng/µl. A new set of sterile Eppendorf tubes were labelled with the names of the target primers and kept on a rack. Another master mix was prepared as shown in Table 2.5 below depending on the number of target primers and sample number.

**Table 2.5: Preparation of RT-PCR mix**

| <b>Component</b>    | <b>Volume per sample (µl)</b> |
|---------------------|-------------------------------|
| Taqman Master mix   | 5                             |
| Target Primer       | 0.5                           |
| <b>Total Volume</b> | <b>5.5</b>                    |

The cDNA was added vertically in 4.5µl aliquots per sample on a sterile optical reaction plate then 5.5µl of the master mix was added horizontally per target primer into the wells of the optical reaction plate. All these was done on ice to prevent degradation of the enzyme. The optical reaction plate was then sealed with optical adhesive film, then centrifuged at 900rpm for 2 minutes to bring the reaction mixture to the bottom and eliminate air bubbles. The optical reaction plate was put into the Rt-PCR machine and set at the following conditions in Table 2.6 below. After the completion of Rt-PCR, the results were analysed.

**Table 2.6: Reaction pathway for RT-PCR**

| <b>UNG incubation</b>    | <b>Polymerase activation</b> | <b>PCR (40 cycles)</b>      |                                    |
|--------------------------|------------------------------|-----------------------------|------------------------------------|
| Hold (50°C)<br>2 minutes | Hold (95°C)<br>2 minutes     | Denature (95°C)<br>1 second | Anneal/extend (60°C)<br>20 seconds |

### **2.2.10 *In vitro* migration assay**

Before metastasis can occur, cells have to detach, migrate and invade the extracellular matrix then enter systemic circulation to a distant organ. Transwell migration and invasion assays are used to examine degree of cell motility in response to chemo-attractants such as growth factors, lipids, chemokines or nucleotides (Justus et al., 2014).

In this assay, 1 million normoxic cells were counted and seeded into a T25 flask containing 8ml of RPMI media. These flasks were kept overnight in an incubator at 37<sup>0</sup>C, 5% CO<sub>2</sub>.

For hypoxic cells, a four-day hypoxic culture was trypsinised, counted and recorded. For treated hypoxic cells, a low dose of the drug was added into the inserts.

The next day, the cells in each T25 flask were trypsinised, counted and recorded. Forceps were used to pick and place a transwell chamber with an 8µm pore sized membrane into each of the wells of interest in a 24-well plate. 200µl of serum-free RPMI media containing 10,000 cells was put into each transwell while 700µl of serum containing RPMI media was added into the respective wells of the 24-well plate. The plate was covered and kept in an incubator for 8 hours depending on how fast the cell line grew. After the time elapsed, each of the inserts was lifted with a pair of forceps then its contents were emptied then the inserts were rinsed twice with water and replaced in an unused well of the 24-well plate. A solution of crystal violet in a ratio of 1:5 with PBS was prepared and 400µl of this solution was put into each desired well of a new 24-well plate. Each transwell was lifted with a pair of forceps and placed in the crystal violet containing well of the new 24-well plate. The transwells were left on the crystal violet for 15minutes then rinsed twice in water. A cotton swab was used to thoroughly clean the insides of the transwells before leaving them to dry on tissue paper. After the transwells dried, pictures of each one was taken, and the cells were counted under a light microscope and the values recorded.

For transfected clones, an overnight culture of the clones was trypsinised and counted. Volumes of each clone with 100,000 cells was counted and put into separate tubes. These tubes were centrifuged at 2000rpm for 5minutes and aspirated. 2ml of PBS was added to each tube to rinse the cells then centrifuged again and aspirated. 2ml of serum free RPMI media was added into each tube and mixed thoroughly. 700µl of serum containing RPMI media was added into the required wells of a 24 well plate. Then a new transwell was placed in each of those wells. Then 200µl of the serum free RPMI media containing the transfected clones was added into the respective transwells. The 24-well plate was covered then left for 24 hours in an incubator. After the incubation time elapsed, a solution containing 1:3 ratio of crystal violet to methanol was prepared and 700µl of it was put into the required number of wells in a 24-well plate. The

plate containing the clones was removed from the incubator and the inside of the inserts were wiped with a cotton bud before transferring them to the crystal violet containing wells of the new plate. The inserts were left in the crystal violet solution for 15 minutes then rinsed with water and left to dry. Then images of the transwells were taken and their cell count recorded.

### **2.2.11 *In vitro* invasion assay**

For each cell line, 1 million cells were counted and seeded into a T25 flask containing 8ml of RPMI media. These flasks were kept overnight in an incubator at 37<sup>0</sup>C, 5% CO<sub>2</sub>. The next day, the cells in each T25 flask were trypsinised, counted and recorded. Matrigel was removed from the -80<sup>0</sup>C freezer and kept on ice to thaw. Some serum-free RPMI media was poured into a 10ml tube and put on ice. Forceps were used to pick and place each transwell chamber with an 8µm pore sized membrane into the wells of interest in a 24-well plate. The Matrigel was prepared in a ratio of 1:5 with serum-free RPMI media. 50µl of this mixture was put into each transwell chamber and the 24-well plate was covered and left in an incubator for 5 hours so the gel would set. After the time elapsed, the Matrigel settled at the bottom of each transwell leaving the serum-free media at the top. This serum-free media was aspirated and replaced with 200µl of serum-free RPMI media containing 20,000 cells while 700µl of serum containing RPMI media was added into each well of the 24-well plate containing the transwells. The plate was once again covered and kept in an incubator overnight. The next day, each of the inserts were lifted individually with a pair of forceps and its contents, emptied then rinsed twice with water and replaced in an unused well of the 24-well plate. A solution of crystal violet in a ratio of 1:3 with methanol was prepared and 400µl of this solution was put into each desired well of a new 24-well plate. Each transwell was lifted with a pair of forceps and placed in the crystal violet containing well of the new 24-well plate. The transwells were left on the crystal violet for 15minutes then rinsed twice in water. A cotton swab was used to thoroughly clean the insides of the transwells before leaving them to dry on tissue paper. After the transwells dried,

pictures of each one was taken, and the cells were counted under a light microscope and the values recorded.

### **2.2.12 Stable Transfection**

Transfection is a technique commonly used for introducing foreign genetic material into cells in order to study protein function or gene function/regulation. The two main types of transfection are stable (permanent) and transient (temporary) transfection. The aim of the experiment determines the type of transfection used. Transfection can be carried out using biological agents such as a virus, chemical agents such as cationic lipids, calcium phosphate, cationic amino acids, etc and physical methods such as micro injection, biolistic particle delivery, laser-based transfection and electroporation. The use of a virus for transfection has many limitations such as causing inflammatory reactions, insertional mutation, gene disruption, cytotoxicity and immunogenicity (Kim and Eberwine, 2010). For this research, stable transfection was used.

#### **i. Preliminary study**

A Six-well plate was seeded with 300,000 cells in 3ml of RPMI media per well of the PDAC cell line, Panc-1 and kept in an incubator at 37°C. The next day, 5 of the wells were dosed with different concentrations of hygromycin leaving one well as control and the plate was returned to the incubator. For the next 7 days, the cells were monitored to determine the lowest concentration that led to complete cell death and images were taken at 3-day intervals.

#### ***Transfection of panc-1 cell line with Hygromycin resistant pcDNA 3.1 plasmid for NFκB p65 overexpression.***

Each of the three wells of a 6-well plate was seeded with 400,000 cells of Panc-1 PDAC cell line in 3ml of RPMI media. The plate was kept overnight in a humidified incubator at 37°C,

5% CO<sub>2</sub>. The next day, the three wells were labelled negative, mock and p65 respectively.

Then, 10ml tubes were labelled and some components were added into them as shown below:

| <b>Tube Number</b> | <b>Lipofectamine<br/>(<math>\mu</math>l)</b> | <b>Empty plasmid<br/>(<math>\mu</math>g)</b> | <b>p65 containing<br/>plasmid (<math>\mu</math>g)</b> | <b>Serum free<br/>media (<math>\mu</math>l)</b> |
|--------------------|--|--|---|---|
| 1 (negative)       | 10   |  |   | 250   |
| 2 (mock)           | 10   |  |   | 250   |
| 3 (mock)           |  | 4  |   | 250   |
| 4 (p65)            | 10   |  |   | 250   |
| 5 (p65)            |  |  | 4   | 250   |

Tube 1 (negative) = 10 $\mu$ l of lipofectamine + 250 $\mu$ l of serum free media.

Tube 2 (mock) = 10 $\mu$ l of lipofectamine + 250 $\mu$ l of serum free media.

Tube 3 (mock) = 4 $\mu$ g of empty plasmid + 250 $\mu$ l of serum free media.

Tube 4 (p65) = 10 $\mu$ l of lipofectamine + 250 $\mu$ l of serum free media.

Tube 5 (p65) = 4 $\mu$ g of p65 containing plasmid + 250 $\mu$ l of serum free media.

The tubes were mixed with a pipette independently then incubated at room temperature for a minimum of 5 minutes to a maximum of 30 minutes after which the contents of tube 2 and tube 3 were mixed together, then the contents of tube 4 and tube 5 were thoroughly mixed with a pipette to enable the plasmid to enter into the liposomes of the lipofectamine. These tubes were then incubated at room temperature for a minimum of 20 minutes to a maximum of 6 hours. The content of tube 1 was added drop by drop to the well labelled 'negative', the mixture of tube 2 & 3 was added drop by drop to the well labelled 'mock' and the mixture of tubes 4 & 5 was added drop by drop to the well labelled 'p65'. The plate was returned to the humidified incubator at 37°C, 5% CO<sub>2</sub>. After 24 or 48 hours, a calculated volume of RPMI media was

added into different bottles and dosed with the concentration of hygromycin chosen after step (i.) above depending on the number of petri dishes desired. An aliquot of 15ml of the hygromycin dosed RPMI media was put into each petri dish. The 6-well plate was removed from the incubator and the media in them was aspirated. Each well was rinsed with PBS and the cells trypsinised with 600µl of trypsin. The trypsin was later neutralised with an equal volume of RPMI media then equal aliquots of the cell solution was added drop by drop into the respective petri dishes. Note that the content of each well was put into two labelled Petri dishes. The cells in the petri dishes were observed daily and the drug containing media was changed frequently depending on the quantity of dead cells floating in the media. This was because the dead cells would secrete toxins which could be harmful to the life cells. After 10 days, each plate was held up under light consecutively and a marker was used to draw a circle around well-spaced colonies. An average of 12 colonies was circled per plate. A 24-well plate with each well containing 1ml of RPMI media dosed with the desired concentration of hygromycin was prepared under sterile conditions and kept in the hood till required. Then the media in one petri dish was aspirated and the cells were rinsed with 5ml of PBS which was also aspirated. A 200µl pipette was used to add 2 drops of trypsin on each of the circled clones then the petri dish was kept in the incubator and monitored carefully under the microscope till the cells in each colony was well rounded which is characteristic of detached cells. The petri dish was carefully carried into the hood then a pipette and a different pipette tip was used to add 20µl of RPMI media to each colony one by one. The colony containing media was then put into a separate well of the 24-well plate. After collecting all circled colonies of that petridish, the procedure was repeated for the next petri dish till all colonies were collected. The 24-well plate was kept in a humidified incubator at 37°C, 5% CO<sub>2</sub> with the clones monitored and the media replaced regularly.

## 2.2.13 CRISPR-Cas9 KNOCKOUT

### *i. Preliminary study*

A Six-well plate was seeded with 300,000 cells in 3ml of RPMI media per well of the PDAC cell line, Panc-1 and kept in an incubator at 37°C. The next day, 5 of the wells were dosed with different concentrations of puromycin leaving one well as control and the plate was returned to the incubator. For the next 7 days, the cells were monitored to determine the lowest concentration that led to complete cell death and images were taken at 3-day intervals.

### *CRISPR-Cas9 p65 Knockout*

Clustered regularly interspaced palindromic repeats (CRISPR)/Cas9 is technique used in genome engineering to edit genes. It is used for enabling or terminating the expression of specific genes *in vivo* or *in vitro* (Redman et al., 2020).

Cells were transfected following the manufacturers CRISPR/Cas9 Knockout protocol. An aliquot of 15ml of the puromycin dosed RPMI media was put into each petri dish. The 6-well plate was removed from the incubator and the media in them was aspirated. Each well was rinsed with PBS and the cells trypsinized with 600µl of trypsin. The trypsin was later neutralised with an equal volume of RPMI media then equal aliquots of the cell solution was added drop by drop into the respective petri dishes. Note that the content of each well was put into two Petri dishes. The cells in the petri dishes were observed daily and the drug containing media was changed frequently depending on the quantity of dead cells floating in the media. This was because the dead cells could secrete toxins which could be harmful to the life cells. After 10 days, each plate was held up under light consecutively and a marker was used to draw a circle around well-spaced colonies. An average of 12 colonies was circled per plate. A 24-well plate with each well containing 1ml of RPMI media dosed with the desired concentration of puromycin was prepared under sterile conditions and kept in the hood till required. Then the

media in one petri dish was aspirated and the cells were rinsed with 5ml of PBS which was also aspirated. A 200 $\mu$ l pipette was used to add 2 drops of trypsin on each of the circled clones then the petri dish was kept in the incubator and monitored carefully under the microscope till the cells in each colony was well rounded which is characteristic of detached cells. The petri dish was carefully carried into the hood then a pipette and a different pipette tip was used to add 20 $\mu$ l of RPMI media to each colony one by one. The colony containing media was then put into a separate well of the 24-well plate. After collecting all circled colonies of that petri dish, the procedure was repeated for the next petri dish till all colonies were collected. The 24-well plate was kept in a humidified incubator at 37°C, 5% CO<sub>2</sub> with the clones monitored and the media replaced regularly.

#### **2.2.14 Statistical Analysis**

The data were statistically analysed with GraphPad Prism using t-test and two-way ANOVA. The significant p-values of <0.05(\*) and <0.0001(\*\*\*\*) represent significant and very significant differences respectively.

The IC<sub>50</sub>s were calculated on Microsoft Excel while the software CALCUSYN was used to calculate the Effective Dose of all the drug combinations used during this study.

## **CHAPTER 3**

# **HYPOXIA INDUCES STEMNESS, CHEMORESISTANCE AND INVASIVENESS IN PANC-1 PANCREATIC DUCTAL ADENOCARCINOMA CELL LINE**

### 3.1 Introduction

Unlike many cancers which have had significant advances in the overall survival of patients, pancreatic cancer still has a very poor prognosis. According to the national cancer institute in United States, colorectal cancer has a 5-year survival rate of 65% while pancreatic cancer has a 5-year survival rate of 7%. The high fatality rate for pancreatic cancer is as a result of late diagnosis for most patients. Pancreatic cancer cells are also suspected to develop micrometastases at the early stages of the tumour (Erkan *et al.*, 2016). Panc-1 is a PDAC cell line commonly used to carry out *in vitro* studies on tumorigenesis of the pancreas (Shen *et al.*, 2019).

Tissue hypoxia results from decreased ability of cells to transport oxygen, decreased tissue perfusion, low oxygen tension, reduced capability of cells to utilise oxygen and increased diffusion distance (Hockel and Vaupel, 2001). Reduced vascularization or blood flow in a tumour can lead to reduced oxygen levels within the tumour leading to increased cell immortality and inflammation and deregulation of stem cell growth (Carnero and Lleonaart, 2016). In a healthy pancreas, the partial oxygen pressure is 24.3–92.7 mmHg (3.2–12.3%) while in PDAC, the partial oxygen pressure is 0–5.3 mmHg (0–0.7%), this shows that the microenvironment of pancreatic cancer is hypoxic in nature (Koong *et al.*, 2000). Hypoxia activates HIF1 $\alpha$  which plays a significant role in the activation of EMT which promotes cell movement to blood vessels. There is evidence that HIF3 $\alpha$  has the ability to enhance or suppress the activity of other HIF complexes (Daniel *et al.*, 2019). HIFs help cells to adjust to low oxygen levels by activating numerous genes involved in the required biological processes such as angiogenesis, cell motility, EMT and metastasis. Research has shown that the prognosis of patients with more hypoxic regions in their tumour is poor. Pathways linked to EMT are activated by hypoxia. Hypoxia also stimulates signalling pathways such as WnT and TGF- $\beta$  signalling pathways (Carnero and Lleonaart, 2016).

CSC populations vary from tumour to tumour and within tumours of the same type. CSCs from different stages of the same tumour are different proving that they have high heterogeneity. The distinct CSCs within a tumour arise from multiple niches in the CSC microenvironment. CSCs have surface markers which can be used to estimate the size of the CSC pool within a tumour which correlates with patient prognosis (Carnero and Lleona, 2016). A number of researches have shown that CSC characteristics of cancer cells can be acquired or lost depending on the cell's immediate environment. Some of the CSC markers found in PDAC cells are ABCG2, CD133, CD44 and CD24 (Knaack *et al.*, 2018). There are numerous studies linking CSCs with cancer metastasis and therapy resistance making it necessary to study the role of CSC in tumours and its potential as a target for drug development. Pluripotent and adult stem cells have a common gene network with CSCs which plays a significant role in pluripotency and self-renewal (Shen *et al.*, 2019). Despite the number of anticancer drugs and biomarkers developed for managing pancreatic cancer, there is still no significant improvement in its treatment. Hypoxia induces chemoresistance by decreasing tumour drug perfusion, regulation of drug efflux, metabolic reprogramming, suppressing DNA damage, modification of cell death and survival, and induction of cancer stem cells. As a result of the attention drawn to HIFs and their role in promoting cancer, different studies have shown that minnelide, digoxin and PX-478 have the capacity to inhibit HIF1 $\alpha$  (Tan *et al.*, 2020).

The aim of this study is to ascertain the effect of hypoxia on cancer stem cells and tumour cell motility in PDAC cell lines in order to comprehend chemoresistance in PDAC. In this *in vitro* study, hypoxic and spheroid PDAC cell line cultures were used for comparisons with PDAC cell lines cultured under normoxic conditions. Spheroid and hypoxic cultures of panc-1 PDAC cell line were screened for total hypoxic cell populations, CSC markers, EMT markers, cell migratory potential and cell invasiveness potential. The study also analysed the degree of

chemoresistance in normoxic and hypoxic panc-1 PDAC cell line after treatment with 2 first line anticancer drugs for PDAC management.

### **3.2 Experimental design**

The specific techniques used in this study are highlighted below. However, their detailed protocols are described in in Chapter 2.

#### **3.2.1 Cell line**

The human PDAC cell line, Panc-1 was used for *in vitro* research and passaged twice weekly.

#### **3.2.2 Cell culture techniques**

Panc-1 cells were cultured in RPMI 1640 media supplemented with 100 U/ml penicillin and 100 µg/ml streptomycin, 5% L-glutamine and 10% FBS in a humidified atmosphere at 37°C with 5% CO<sub>2</sub> and passaged every 3 days.

About 5x10<sup>5</sup> Panc-1 cells were cultured in RPMI 1640 media supplemented with 100 U/ml penicillin and 100 µg/ml streptomycin, 5% L-glutamine and 10% FBS in a humidified atmosphere at 37°C with 5% CO<sub>2</sub> and 0% O<sub>2</sub>, for 6 days to obtain hypoxic cell cultures.

Spheroid panc-1 cells were cultured using stem cell media and flasks coated with poly (2-hydroxyethylmethacrylate) then incubated for 6 days under a humidified atmosphere at 37°C with 5% CO<sub>2</sub>.

#### **3.2.3 Flow cytometry analysis of CSC markers**

The presence and percentage population of the CSC markers: ALDH, CD133 and ABCG2 in normoxic, hypoxic and spheroid panc-1 cells was detected using flow cytometry. The protocol used is well detailed in Chapter 2.

### **3.2.4 Detection of CSC markers and EMT markers using Real-time PCR**

Total RNA was extracted from both normoxic and hypoxic panc-1 cell cultures using the mRNA extraction kit (Qiagen) following the manufacturer's instruction then reverse transcribed to give cDNA. This cDNA was subjected to real-time PCR using primers of specific interest and the fold change was calculated. Two-way ANOVA and t-test were used to analyse the fold change using GraphPad Prism software.

### **3.2.5 Immunocytochemistry**

Cells previously seeded in chamber slides were permeabilized with 0.1% Triton X-100, blocked with 3% BSA for an hour, stained with primary antibodies and FITC-conjugated secondary antibody for 1 hour. VectaShield was dropped on the cells and a coverslip used to seal the cells. The cells were then viewed using a confocal microscope.

### **3.2.6 Cell migration assay**

This was carried out using transwell inserts which were inserted into serum containing media then each seeded with 10,000 cells in 200 $\mu$ l of serum-free media and left for 24 hours. The next day, the migratory cells were fixed with methanol, stained with crystal violet, washed, dried, then images taken with a microscope at a magnification of 20 $\times$  and cell count recorded.

### **3.2.7 Cell invasion assay**

Transwell inserts were coated with matrigel combined with serum free medium in 1:5, then inserted into 24-well plates and incubated overnight. The next day, each of the coated transwells was seeded with 10,000 cells in 200 $\mu$ l of serum-free media, then inserted into serum containing media and left for 24 hours. The next day, the invasive cells were fixed with methanol, stained with crystal violet, washed, dried then images were taken with a microscope at a magnification of 20 $\times$  and cell count recorded.

### **3.2.8 MTT cell viability assay**

Attached normoxic or hypoxic panc-1 cells were trypsinised, counted and seeded into 96 well plates (5000 cells/well). The next day, the media above the cells was aspirated and replaced with media treated with different drug concentrations. The treated cells were incubated for 72 hours in the respective incubator. MTT reagent was added to the cells and the cells were incubated for 3 hours after which the media was aspirated, the formed formazan crystals were dissolved with dimethyl sulfoxide and the absorbance was taken at 540nm with a spectrophotometer.

### **3.2.9 Sphere reformation assay**

Panc-1 spheroid cultures were treated with 500nM gemcitabine and 100nM paclitaxel for 6 hours then incubated under a humidified atmosphere at 37<sup>0</sup>C with 5% CO<sub>2</sub>. After which the treated panc-1 spheroid cells were rinsed and re-cultured at low density for 7 days. The reformed spheres were counted and images were taken at 10× magnification.

## **3.3 Results**

### **3.3.1 Spheroids derived from Panc-1 PDAC cell line are resistant to conventional anticancer drugs.**

Sphere reformation assays are aimed at analyzing the cytotoxic effect of drugs on spheroid cells. Figure 3.1 (a) shows the morphology of panc-1 attached cells, panc-1 spheroid cells and images taken after sphere reformation assay. Panc-1 formed many irregularly shaped spheres. The reformed panc-1 spheres previously treated with 100nM paclitaxel dissociated slightly but still survived while panc-1 spheres previously treated with 500nM gemcitabine were similar to the control indicating little to no kill. This revealed that there was a population of the panc-1 cells which was showing resistance to gemcitabine and paclitaxel. Figure 3.1 (B) is a bar chart which shows the sphere count after treatment with gemcitabine and paclitaxel.

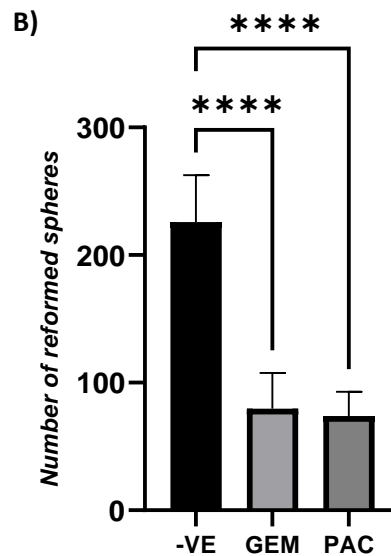
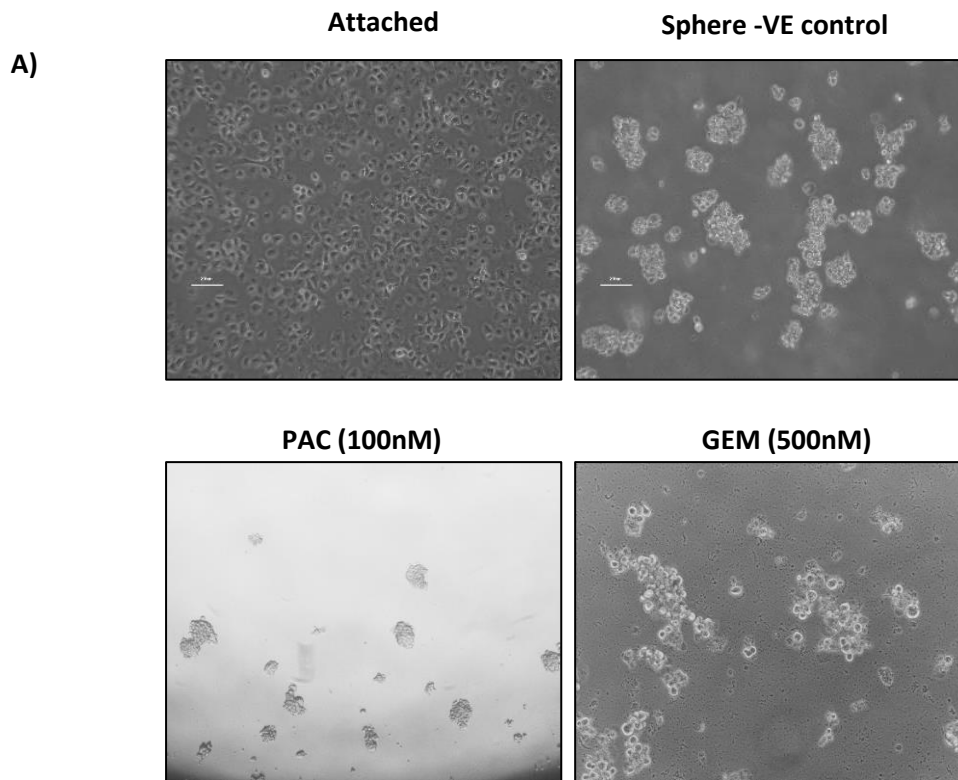


**Figure 3.1:** (A) *Panc-1* PDAC cell line is resistant to first line anticancer drugs gemcitabine and paclitaxel. Images show attached, spheroid and treated spheroid cultures of *panc-1* PDAC cell line. Sphere reformation assay for *Panc-1* spheroid cells after treatment with 100nM paclitaxel and 500nM gemcitabine. (B) Bar chart showing sphere count after sphere reformation assay for *Panc-1* spheroid cells treated with 100nM paclitaxel and 500nM gemcitabine. Images were taken 5 days after cell culture (10× magnification). Attached cells (ATT) = Overnight normoxia cultures. -VE= untreated *panc-1* spheroid cells.  $n=12$ , \*\*\*\* $p<0.0001$

### 3.3.2 Spheroids cultured from panc-1 PDAC cell line express CSC markers.

Flow cytometry analysis was carried out to study the expression of the CSC characteristics in panc-1 attached and spheroid cultures. ALDH, CD133 and ABCG2 are common CSC markers found in PDAC. The ALDEFLUOR assay was used to detect the ALDH<sup>+ve</sup> population in panc-1 under normoxic and spheroid conditions. The images of the dot plot obtained and the corresponding statistically analyzed bar chart is shown in Figure 3.2(A). The result revealed that the spheroid panc-1 cultures had a significant population of ALDH<sup>+ve</sup> cells. Flow cytometry analysis was also used to detect the CD133<sup>+ve</sup> population in attached and spheroid panc-1 cells using PE-conjugated CD133 antibody. Figure 3.2(B) shows the dot plot obtained and corresponding statistically analysed bar chart. There was increased CD133<sup>+ve</sup> population in the panc-1 spheroid cultures. The ABCG2<sup>+ve</sup> population in the attached and spheroid panc-1 cultures was also analyzed by flow cytometry using APC conjugated anti-ABCG2. The dot plot and bar chart are shown in Figure 3.2(C). Sox2, Oct4 and Nanog are CSC markers which help to maintain stemness in PDAC. In an effort to study the expression of CSC markers in panc-1 cell cultures, real-time PCR was carried out as shown in Figure 3.2 (D). The results reveal a significant increase in the mRNA expression of Oct4, Sox2 and Nanog in the spheroid cultures. These data show that spheroid panc-1 cultures have enhanced CSC characteristics.

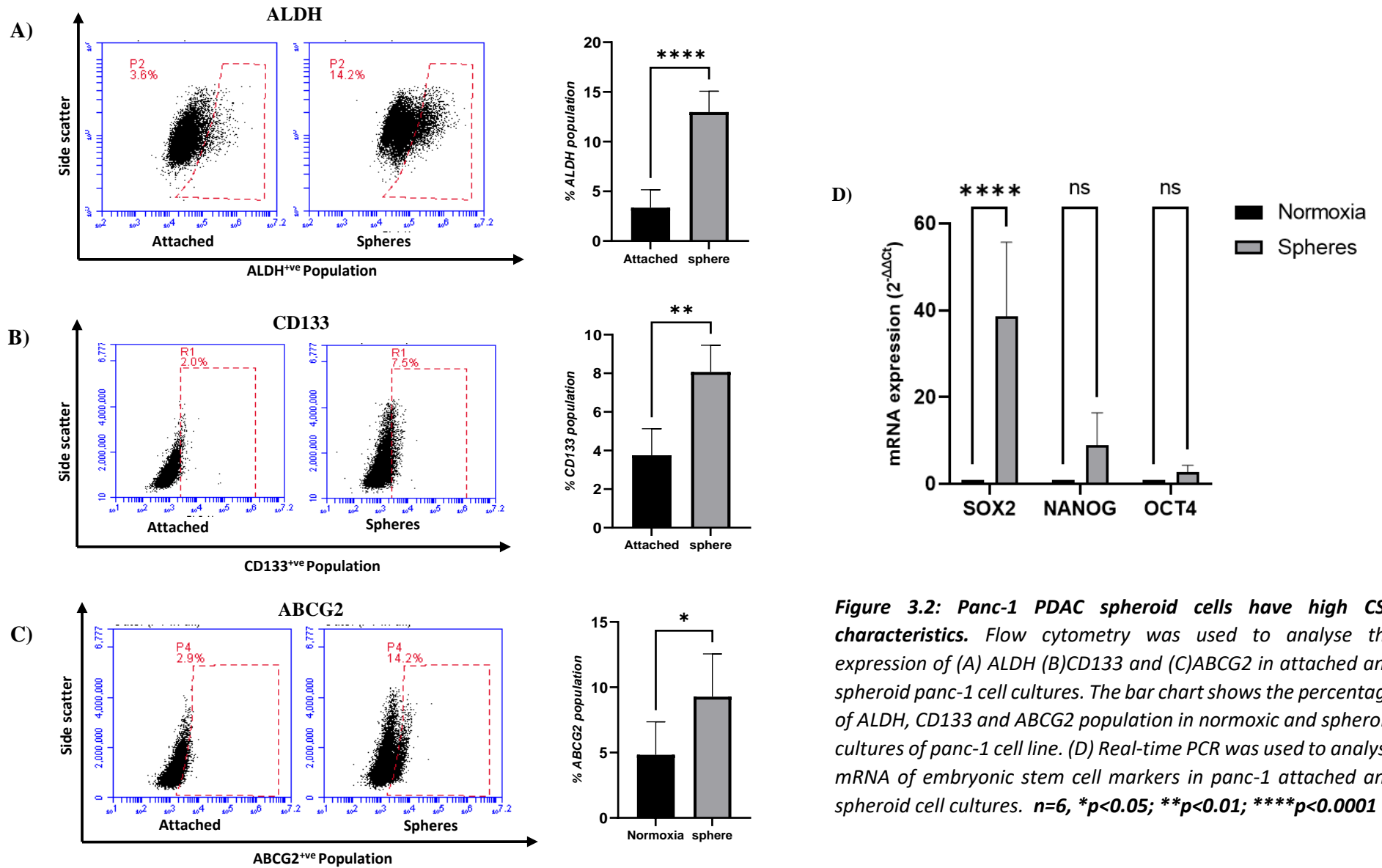


**Figure 3.2: Panc-1 PDAC spheroid cells have high CSC characteristics.** Flow cytometry was used to analyse the expression of (A) ALDH (B)CD133 and (C)ABCG2 in attached and spheroid panc-1 cell cultures. The bar chart shows the percentage of ALDH, CD133 and ABCG2 population in normoxic and spheroid cultures of panc-1 cell line. (D) Real-time PCR was used to analyse mRNA of embryonic stem cell markers in panc-1 attached and spheroid cell cultures.  $n=6$ , \* $p<0.05$ ; \*\* $p<0.01$ ; \*\*\*\* $p<0.0001$

### **3.3.3 Hypoxic population detected in spheroids and hypoxia cultured panc-1 PDAC cell line.**

The amount of hypoxia within hypoxic and spheroid panc-1 PDAC tissues was quantified using FITC-conjugated anti-pimonidazole which forms an adduct when it comes in contact with hypoxic cells. The adducts formed were viewed using immunofluorescence and images were taken. Images of the FITC-hypoxyprobe analysis of normoxic and spheroid panc-1 cultures are shown in Figure 3.3(A). The FITC-hypoxyprobe shows the hypoxic cell population in the two cell cultures which is denoted by green cytoplasmic staining. The nucleus of each cell in the experiment was stained by DAPI (blue) while the cell wall was stained with actin (red). The images reveal that spheroid cells have high hypoxic cell populations. In Figure 3.3(B), the image revealed large green regions denoting high hypoxic cell populations in the hypoxic panc-1 cultures. In order to ascertain and compare the hypoxic cell population in normoxic and hypoxic cultures, the previous data was confirmed with flow cytometry hypoxyprobe analysis using FITC-conjugated anti-pimonidazole. In Figure 3.3(C), the dot plots reveal the population of FITC<sup>+ve</sup> hypoxic cell population in the normoxic and hypoxic panc-1 cell cultures. Figure 3.3 (D) shows a bar chart with the statistically analysed FITC<sup>+ve</sup> hypoxic cell population in the attached and spheroid panc-1 cultures. This data confirms that the hypoxic and spheroid panc-1 cultures contain statistically significant high hypoxic cell populations.

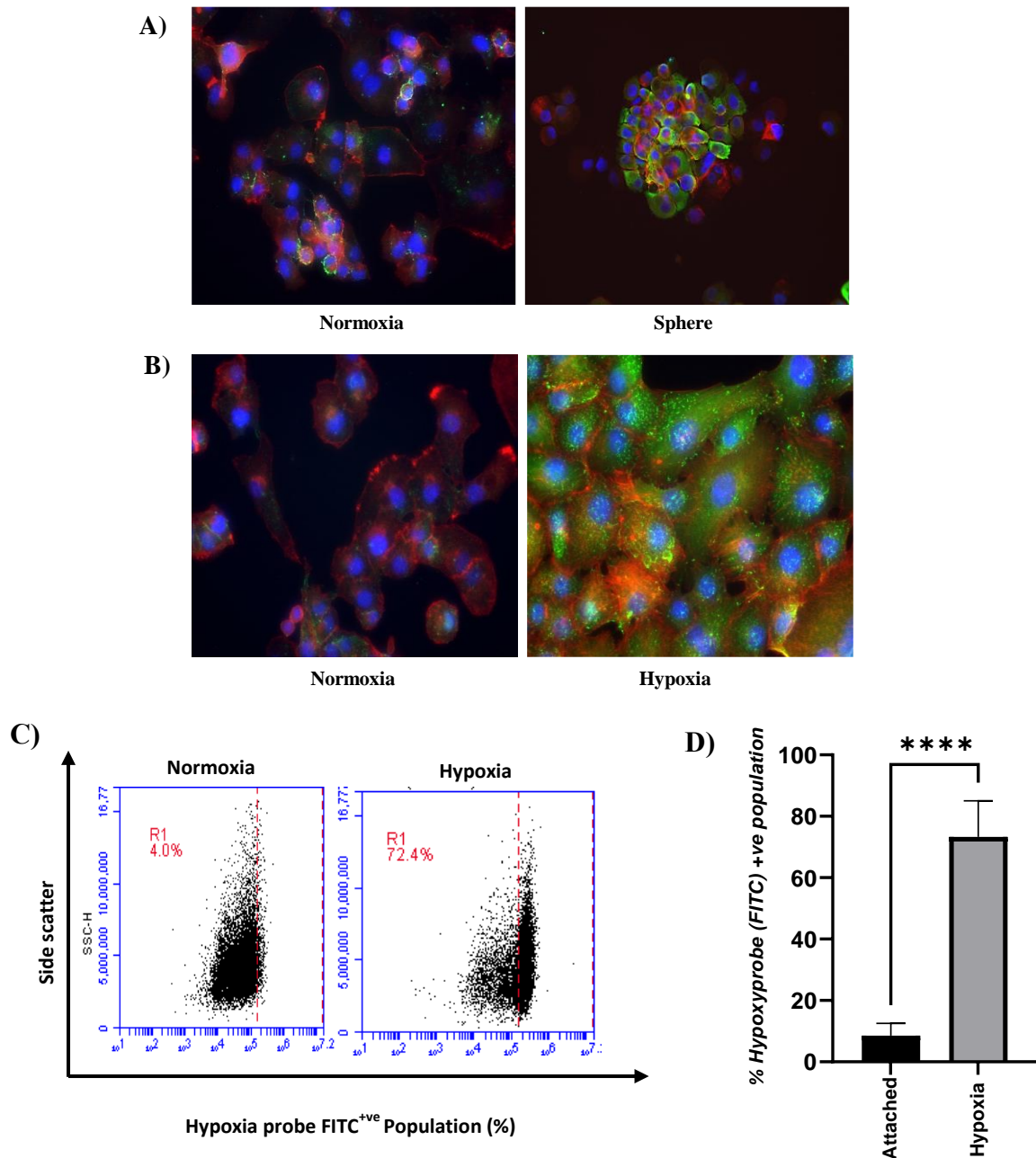


**Figure 3.3: Spheroid and Hypoxic Panc-1 cells have high hypoxic cell populations.** The image shows ICC staining of (A) attached and spheroid panc-1 cell cultures, and (B) attached and hypoxia-cultured monolayer panc-1 cell with FITC-conjugated anti-pimonidazole. The hypoxic regions are stained with green FITC-conjugated anti-pimonidazole, the nucleus is blue and cell membrane was stained red with Actin. Image magnification 20X. (C) Flow cytometry analysis of FITC<sup>+ve</sup> hypoxic cell population in normoxic and hypoxic panc-1 PDAC cultures (D) Bar chart showing the statistically significant % FITC<sup>+ve</sup> hypoxic cell population. Normoxia= overnight attached cells. Hypoxia= cells cultured with 1% O<sub>2</sub>, 5% CO<sub>2</sub> and 37°C. n=6; \*\*\*\*p<0.0001

### **3.3.4 Hypoxia cultured Panc-1 PDAC cell line shows increased expression of CSC markers.**

PDAC is said to be associated with some particular CSC markers. Flow cytometry analysis was used to detect and compare the population of CSC markers in normoxic and hypoxic panc-1 PDAC cell cultures. Figure 3.4(A) shows the dot plots obtained after ALDEFLUOR assay for the ALDH<sup>+ve</sup> population in normoxic and hypoxic monolayer cultures of panc-1 PDAC cell line and a bar chart showing the statistically significant values obtained (n=3; p=0.0109). The hypoxic cultures had higher ALDH<sup>+ve</sup> populations. The normoxic and hypoxic panc-1 cells were also analyzed for CD133 using flow cytometry in Figure 3.4(B) (n=2; p=0.0011). The hypoxic panc-1 cultures expressed a high level of CD133. In Figure 3.4(C), flow cytometry was used to analyze the ABCG2 population in panc-1 normoxic and hypoxic cell cultures. The dot plots obtained reveal that the hypoxic cell cultures have higher ABCG2<sup>+ve</sup> cell populations. The bar chart shows that the percentage population of ABCG2 in the hypoxic panc-1 cultures are statistically significant (n=6; p=0.0001). To further confirm the presence of cancer stem cells, real-time PCR was used to analyze the expression of embryonic stem cell markers in attached and hypoxic panc-1 cell cultures. The hypoxic cultures had increased mRNA levels of Oct4, Sox2 and Nanog. The elevated levels of ALDH, CD133, ABCG2, Sox2, Oct4 and Nanog which are associated with maintaining cell stemness, in the hypoxic cultures suggests that hypoxia plays a role in the development of cancer stem cell characteristics.

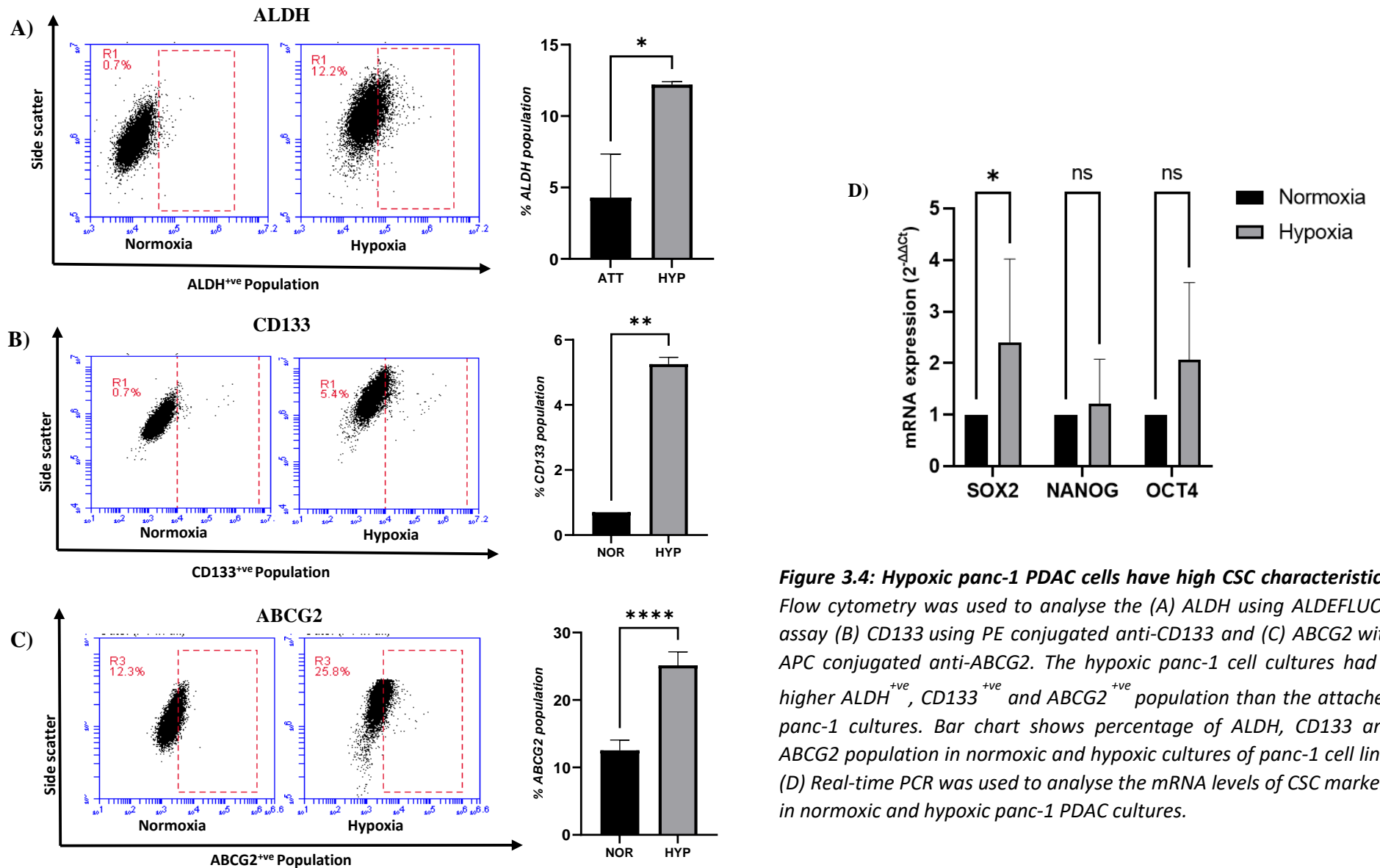


**Figure 3.4: Hypoxic panc-1 PDAC cells have high CSC characteristics.** Flow cytometry was used to analyse the (A) ALDH using ALDEFLUOR assay (B) CD133 using PE conjugated anti-CD133 and (C) ABCG2 with APC conjugated anti-ABCG2. The hypoxic panc-1 cell cultures had a higher ALDH<sup>+</sup>, CD133<sup>+</sup> and ABCG2<sup>+</sup> population than the attached panc-1 cultures. Bar chart shows percentage of ALDH, CD133 and ABCG2 population in normoxic and hypoxic cultures of panc-1 cell line. (D) Real-time PCR was used to analyse the mRNA levels of CSC markers in normoxic and hypoxic panc-1 PDAC cultures.

### **3.3.5 Hypoxia induces chemoresistance in Panc-1 PDAC cell line.**

Hypoxia activates a cascade of genes which lead to cancer cell growth, metastasis and chemoresistance. The cytotoxicity of 1000nM paclitaxel was analyzed on panc-1 normoxic and hypoxic cells using MTT cytotoxicity assay. The cell viability curve obtained after the experiment is shown in Figure 3.5(A) with the calculated IC<sub>50</sub> values beside it. The hypoxic panc-1 cultures were more resistant to paclitaxel than the normoxic cultures. The cytotoxicity of 100μM gemcitabine was analysed on panc-1 normoxic and hypoxic cells using MTT cytotoxicity assay. The cell viability curve obtained after data analysis is shown in Figure 3.6(B) with the calculated IC<sub>50</sub> values. The hypoxic panc-1 cultures were more resistant to gemcitabine than the normoxic cultures. Certain proteins have elevated or decreased expression in cancerous tumour cells. Western blot was used to analyse the protein expression of NFκB, IκB, Bcl2 and Bax in panc-1 normoxic and hypoxic cell cultures as shown in Figure 3.5(C). NFκB is bound to IκB in the cytoplasm but in the presence of hypoxia, IκB is ubiquitinated and the free NFκB translocates to the nucleus which explains why in the hypoxic culture, NFκB increases and IκB decreases. This increased NFκB in the hypoxic panc-1 cultures, activates a cascade of genes that promote chemoresistance. Bcl2 and Bax are associated with apoptosis, with Bax being pro-apoptosis and Bcl2 being anti-apoptosis. This explains the increased protein expression of Bcl2 in the hypoxic panc-1 cell cultures. The increased Bcl2 expression in the hypoxic panc-1 cultures prevents apoptosis and lead to chemoresistance. Beta actin was used as a loading control. These data proves that hypoxia plays an important role in promoting chemoresistance in panc-1 PDAC cell cultures.

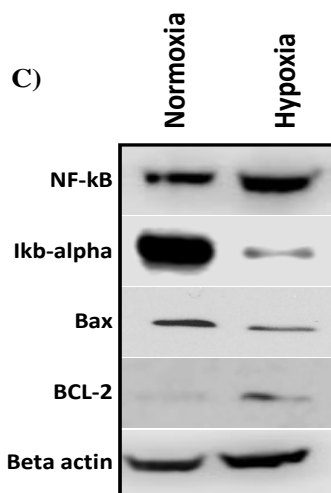
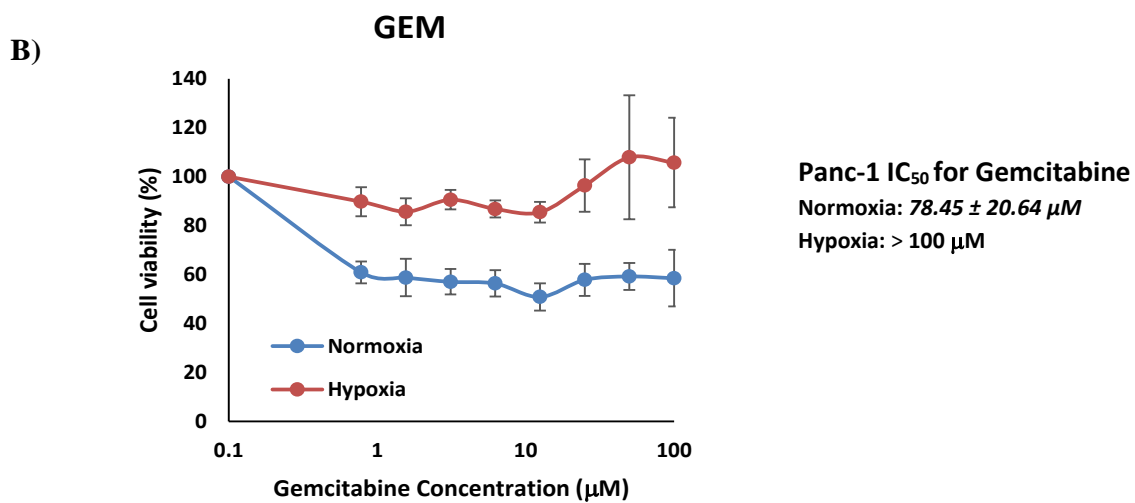
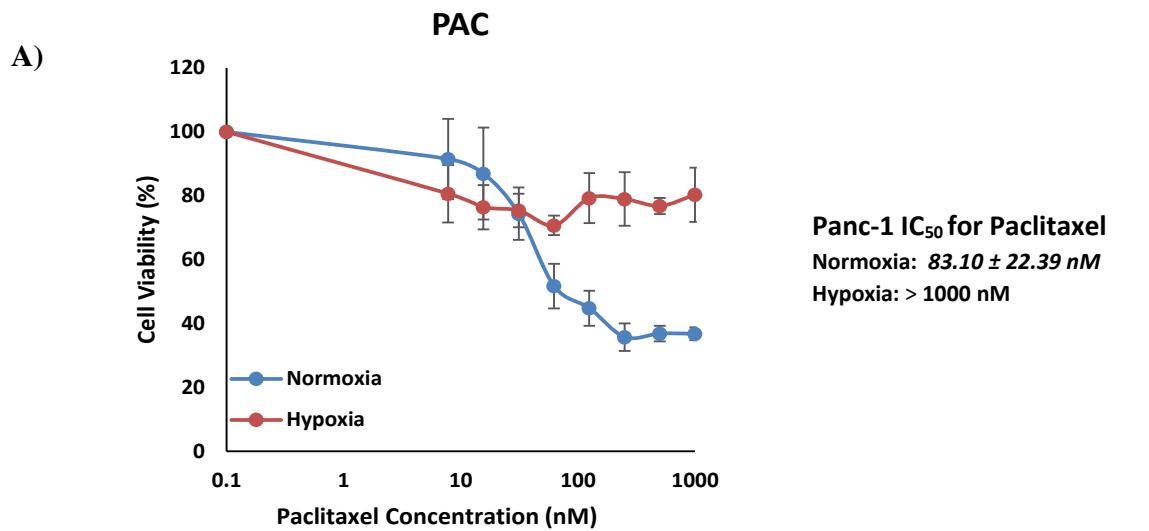


**Figure 3.5: Hypoxia promotes chemoresistance in Panc-1 PDAC cells.** Panc-1 normoxic and hypoxic cell cultures were treated with (A) 1000nM paclitaxel and (B) 100µM gemcitabine then subjected to MTT cytotoxicity assay. The hypoxic cultures were more resistant to treatment than the normoxic cell cultures. (C) Western Blot analysis shows increased protein levels of NFkB and Bcl2, and decreased Ikb and Bax in the hypoxic panc-1 cell cultures.

### **3.3.6 Hypoxia and sphere cultured panc-1 PDAC cell line shows increased EMT characteristics.**

Epithelial-mesenchymal transition (EMT) is the main precursor for metastasis. Real time PCR was used to evaluate the expression levels of EMT markers in normoxic and hypoxic panc-1 cultures (Figure 3.6A). The real-time PCR data revealed that the hypoxic culture had reduced mRNA level of E-cadherin and increased mRNA levels of Vimentin and N-cadherin which corresponds with many literatures. Cell migration assay is popularly used for studying cell movement under specific conditions Figures 3.6(B) shows microscopic images taken after cell migration assay with a bar chart showing the statistically significant number of migratory cells. Cells cultured under normoxic conditions were used as a parallel control. The hypoxic cell cultures had elevated number of migratory cells. Cell invasion assay is used for studying the invasive potential of cells. Figure 3.7 (C) shows microscopic images taken after cell invasion assay with cells cultured under normoxic conditions were used as a parallel control. The bar chart shows the cell count of the invasive panc-1 PDAC cells. There was increased cell invasion in the hypoxic cell cultures. It is evident from the data that hypoxic panc-1 cells have a higher migratory and invasive capability. The results indicate that low intracellular oxygen levels contribute to cell motility which leads to metastasis.

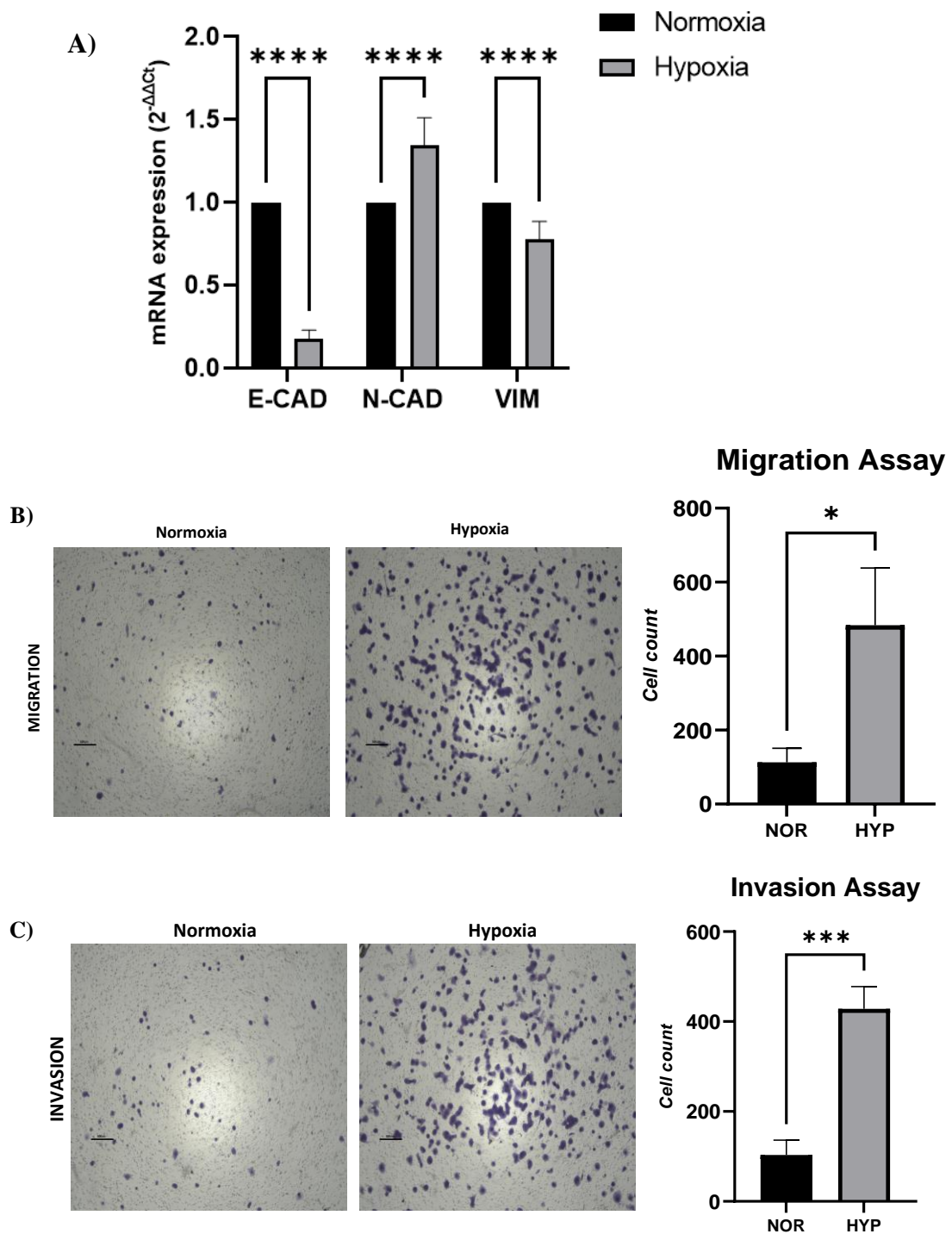


**Figure 3.6: Hypoxia increases EMT characteristics and cell motility in Panc-1 PDAC cells.** (A) Real-time PCR analysis shows decreased E-cadherin mRNA expression and elevated mRNA expression of Vimentin and N-cadherin in hypoxic panc-1 PDAC cell cultures (B) Cell migration assay and (C) Cell invasion assay for normoxic and hypoxic panc-1 cell line cultures using Boyden chamber and Matrigel. Cells were stained with crystal violet after 24 hours. Images were taken with EVOS microscope. Bar chart shows mean cell count. (n=3; \*p<0.05;\*\*\*p<0.001).

### 3.4 Discussion

This *in vitro* study was carried out to investigate the effect of hypoxia on cancer stemness, chemoresistance and metastasis. Normoxic, hypoxic and spheroid cultures of panc-1 PDAC cell were subjected to different protocols to observe changes caused by low oxygen concentrations. Tumours are solid in nature and this enables cancer cells to grow in a 3D conformation and have a hypoxic core. The inability of mono-layer cultures to correctly mimic *in vivo* cellular interactions has led to many false and unsuccessful research results. As a result, many researchers are now focused on using 3D cultures for cancer research. The most popular 3D cell culture method is the spheroid model developed 40 years ago where cells grow as well-defined spheres. These spheres imitate the preliminary stages of a tumour before blood vessel formation. However, some PDAC cells like MiaPaca-2 form unstable spheroids that are hard to use for further experiments (Cavo *et al.*, 2020). PDAC cells grow in a 3-dimensional conformation within the pancreatic tumour. Therefore, PDAC cells cultured as spheroids are more similar to real PDAC cells than monolayer cultures. This is because PDAC cells cultured as spheroids have more matrices and express more chemoresistant genes than monolayered cultures (Bulle and Lim, 2020).

The results from the sphere reformation assay in Figure 3.1 revealed that gemcitabine and paclitaxel which are first line drugs used for PDAC management, were unable to completely dissociate or eliminate panc-1 spheroid cells. One of the reasons for this is that drug efflux proteins such as multidrug resistant protein 1 (MDR1), p-glycoprotein and ABCB1 are highly expressed in PDAC leading to drug efflux and promoting chemoresistance of anticancer drugs like paclitaxel and gemcitabine (Principe *et al.*, 2021). Previous research by Shen *et al.*, 2019 shows that panc-1 has a high ability to form spheres and hence strong stemness characteristics (Shen *et al.*, 2019).

FITC-hypoxyprobe assay revealed that hypoxic and spheroid panc-1 PDAC cells have high hypoxic cell populations. The high rate of PDAC growth increases the demand for oxygen leading to poor vascularisation and intratumoral hypoxia. In response to hypoxia, cancerous cells undergo an angiogenic switch which enables them grow blood vessels to increase blood and oxygen supply (Yuen and Diaz, 2014). Unlike other solid tumours, PDAC tumour microenvironment is characterised by a desmoplastic stroma consisting of activated fibroblasts, leukocytes and extracellular matrix. The desmoplastic stroma has more stiffness, elevated hyaluronic acid content and more hydrostatic pressure leading to intratumoral hypoperfusion and hypoxia (Xiao *et al.*, 2020). Hypoxia activates transcription factors that change cell polarity, cell-cell junction, cell cytoskeleton causing epithelial cells to become motile and invasive (Yuen and Diaz, 2014).

The three main ways for analysing CSCs are by detecting CSC cell surface markers, sphere formation assay and detection of side-population cells that possess high intracellular-to-extracellular pump functions (Sasaki *et al.*, 2019). Cancer stem cell markers have different functions in a tumour cell. The hypoxic and spheroid panc-1 cell cultures expressed more CD133, ALDH and ABCG2 markers than their normoxic counterpart. This is due to increased stemness characteristics. This high population of CSC markers is indicative of high CSC populations. This proves that hypoxia increases the expression of cancer stem cells in panc-1 PDAC cultures. Analysing the expression of the CSC populations in cancer cells gives an idea of how aggressive the tumour will be. ALDH-1, ABCG2 and CD133 are markers commonly used to identify pancreatic cancer (Gzil *et al.*, 2019).

The panc-1 PDAC cells cultured under hypoxic conditions showed markedly high mRNA levels of the CSC markers, SOX2, OCT4 and Nanog. High mRNA levels of embryonic stem cell markers in the hypoxic cultures suggests presence of higher cancer stem cell population

(Ishiwata *et al.*, 2018). SOX2, OCT4 and NANOG help cells to maintain pluripotency which is the ability of a cell to differentiate into multiple cell types (Wang *et al.*, 2013).

The spheroid panc-1 cultures had elevated levels of the EMT markers: E-cadherin, N-cadherin and vimentin while hypoxia decreased the expression of E-cadherin and vimentin but increased expression of N-cadherin. Increased expression of E-cadherin and vimentin causes a switch to mesenchymal characteristics that cause tumour cells to detach from the basal membrane and enter into systemic circulation leading to metastasis. This is the reason for increased cell migration and invasion in the hypoxic panc-1 PDAC cultures. Hypoxia activates many pathways which lead to chemoresistance, metastasis, angiogenesis and hence poor prognosis in pancreatic cancer patients (Cao *et al.*, 2016). Hypoxia and EMT are crucial for cell migration and invasion (Cannito *et al.*, 2008). Low oxygen tension has also been shown to initiate invasion and EMT in pancreatic cancer cells. Intra-tumoral volume of hypoxic regions in pancreatic cancer patients plays a big role in clinical prognosis (Cao *et al.*, 2019). EMT is activated by the expression of particular cell-surface proteins and activation of transcription factors. These transcription factors protect tumour cells from apoptosis, chemoresistance and regulation of tumour growth. The loss of E-cadherin promotes the change of epithelial to mesenchymal phenotype (Zhou *et al.*, 2017).

The vasculature and dense desmoplastic stroma play a critical role in preventing drug perfusion within the PDAC tumour leading to hypoxia and chemoresistance. Low oxygen levels lead to the activation of the PI3Kt/Akt and NFκB signalling pathways which in turn increases the expression of anti-apoptotic proteins. In PDAC, the pro-apoptotic protein BNIP3 is turned off to enhance the anti-apoptotic role of HIF1. One publication showed that the oxidative stress produced during gemcitabine treatment has the capacity to stabilize HIF1α through the NFκB pathway (Tan *et al.*, 2020). Hypoxic panc-1 cell cultures are more resistant to gemcitabine and paclitaxel than normoxic cell cultures which is likely due to the increased stemness

characteristics in the hypoxic panc-1 PDAC cultures. This study revealed that hypoxia plays a significant role in the development of chemoresistance of PDAC cell lines.

### **3.5 Conclusion**

The findings for this study confirmed that the first line anticancer drugs, gemcitabine and paclitaxel are not efficient for eliminating PDAC. Hypoxia causes an upregulated expression of ALDH, ABCG2 and CD133 in panc-1 PDAC cell. This hypoxia also increases stemness, motility and invasive characteristics in PDAC which leads to chemoresistance. A proper comprehension of the effects of hypoxia on tumour progression would greatly aid the design of efficient anticancer drugs.

## **CHAPTER 4**

# **HYPOXIA INDUCES STEMNESS AND CHEMORESISTANCE IN A PANEL OF PATIENT DERIVED PANCREATIC DUCTAL ADENOCARCINOMA CELL CULTURES**

## 4.1 Introduction

Unlike primary cells, cell lines are easily accessible, reliable and less problematic (Shen et al., 2019). Hypoxia plays significant roles that aid CSC development and maintenance (Yang et al., 2020). In solid tumours, cells can either be normoxic, hypoxic or necrotic. Cells which are close to functional blood vessels are normoxic, cells which are about 100µm from a functional blood vessel are hypoxic while patches of cells which are up to 150µm from functional blood vessels may be necrotic (Al Tameemi et al., 2019).

The main method for managing pancreatic cancer is chemotherapy because most patients are not eligible for surgery. The most commonly used first line drug for managing pancreatic cancer has proved that the upregulation of Bcl2 in tumour cells plays a significant role in gemcitabine resistance. NFκB is also suspected to play a significant role in gemcitabine resistance (Wang et al., 2019b). The overall survival of pancreatic cancer patients increases slightly when they are administered with gemcitabine in combination with other drugs compared to when gemcitabine is administered singly (Ma et al., 2019). In numerous studies, it has been shown that CSCs cause drug resistance using multiple modes of action and promote tumour growth. As a result, CSCs are a good target for developing potent anticancer drugs (Wang et al., 2017a).

In pancreatic cancer, CD133 positive cells possess CSC-like traits and are highly resistant to chemotherapy. A common technique used for culturing CSCs *in vitro* is spheroid culture. The cells in the spheres formed during spheroid culture are highly invasive, highly proliferative and drug resistant compared to those in a mono layered culture (Yang et al., 2018). This is because the cells in the spheres are tightly packed together, making them very hypoxic.

Luckily, the treatment modalities such as chemotherapy, surgery and radiation has reduced the cancer death rate from 2007 to 2016. Despite that, some cancers are resistant to chemotherapy

and metastasis, so they reoccur, spread and cause fatalities. Numerous studies have blamed cancer reoccurrence and metastasis on cancer stem cells which have cell surface markers like CD133, nestin and CD44. Some CSCs differentiate into multilineage cells to control cell proliferation. For example, some CSCs differentiate into vascular endothelial cells to increase angiogenesis. Multidrug resistance proteins such as ABCG2, MDR1 and MRP1 are overexpressed by CSCs. CSCs also have elevated expression levels of ALDH which is a free radical scavenger and increases resistance of CSCs to chemotherapy and radiotherapy. Radiotherapy and chemotherapy kill cancer cells by causing DNA damage and initiating apoptosis. Unfortunately, CSCs can use DNA damage mechanisms to repair DNA damage and hence avoid cell death. Many first line anticancer drugs can eliminate cancer cells but CSCs can only be eliminated in the G0 phase. The transcription factors which aid CSC growth are Nanog, Oct4, Sox2, KLF4 and MYC. Some drugs have been designed to target CSCs by blocking immune checkpoints regulators such as PD-L1, PD-1, CTLA-4 (Yang et al., 2020). Chemoresistance of cancer stem cells is due to high expression levels of antioxidant enzymes such as superoxide dismutase-2 (SOD2) and glutathione peroxidase-1 (GPX1); drug efflux transporters such as breast cancer resistance protein (BCRP) and DNA repair enzymes. Cells with high ALDH populations have high clonogenic and migratory potential (Kim et al., 2018).

## **4.2 Experimental Design**

The full details of the experimental techniques used in this chapter are written in Chapter 2.

### **4.2.1 Cell line**

For this study, five patient derived PDAC cells were used: three primary site PDAC cells (12560 PX9, 12556 PX5), 2 circulating PDAC cells (CX102 PX1, CX135 PX1, C76 PX1) and one liver metastatic PDAC cell (A6L) were used for *in vitro* research and passaged twice weekly.

#### **4.2.2 Cell culture**

The cells were cultured in RPMI 1640 media supplemented with 100 U/ml penicillin and 100 µg/ml streptomycin, 5% L-glutamine and 10% FBS in a humidified atmosphere at 37<sup>0</sup>C with 5% CO<sub>2</sub> and passaged every 3 days.

Hypoxic cells were cultured in RPMI 1640 media supplemented with 100 U/ml penicillin and 100 µg/ml streptomycin, 5% L-glutamine and 10% FBS in a humidified atmosphere at 37<sup>0</sup>C with 5% CO<sub>2</sub> and 0% O<sub>2</sub>.

Spheroid patient derived cells were cultured using stem cell media and flasks coated with poly (2-hydroxyethylmethacrylate) then incubated for 6 days under a humidified atmosphere at 37<sup>0</sup>C with 5% CO<sub>2</sub>.

#### **4.2.3 Sphere reformation assay**

The patient derived PDAC spheroid cultures were treated with 500nM gemcitabine and 100nM paclitaxel for 6 hours and incubated under a humidified atmosphere at 37<sup>0</sup>C with 5% CO<sub>2</sub>. After which the treated patient derived PDAC spheroid cells were rinsed and re-cultured at low density for 5 days. The reformed spheres were counted and images were taken at 10× magnification.

#### **4.2.4 Immunocytochemistry**

Cells cultured overnight in a chamber slide with RPMI media (supplemented with antibiotics, L-Gln and 10% FBS) were rinsed with PBS, then fixed, permeabilized and blocked for 1 hour. After which the cells were stained with FITC-Green, 4',6-diamidino-2-phenylindole (DAPI) and actin. The resultant cells were viewed with an EVOS microscope and images were taken at 20× magnification.

#### **4.2.5 Detection of FITC hypoxyprobe population by flow cytometry analysis**

Normoxia, hypoxia and sphere cells incubated overnight with hypoxyprobe, were trypsinized, rinsed with PBS, centrifuged and resuspended in 200µl of PBS. The cells were fixed with methanol, rinsed with PBS then blocked for 1 hour. After which the cells were rinsed with PBS, incubated with FITC-conjugated anti-pimonidazole, rinsed with PBS then read with a flow cytometer. The results gotten was analysed and recorded.

#### **4.2.6 Flow cytometry analysis of CSC markers**

Cells cultured in RPMI media (supplemented with antibiotics, L-Gln and 10% FBS) were trypsinized, counted, rinsed with PBS then stained with the desired conjugated antibody following the manufacturer's instructions and incubated in the dark for 30 minutes. After which the cells were rinsed with flow buffer (PBS with 4% FBS) and resuspended in flow buffer then analysed using a flow cytometer.

#### **4.2.7 MTT Cell Viability assay**

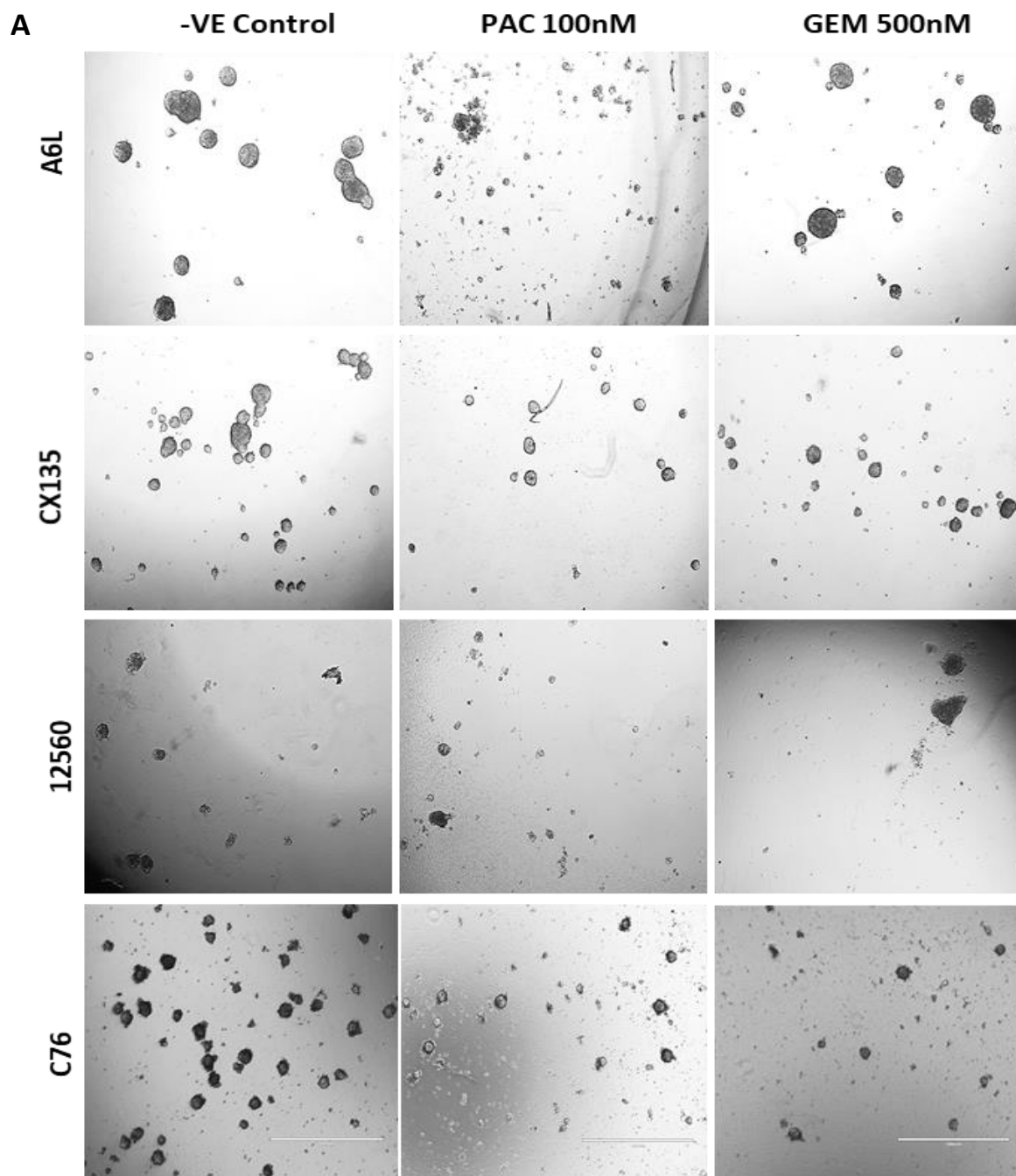
Cells were seeded in a 96-well plate (5000 cells/well). Cytotoxicity assay was carried out using MTT reagent after treating the cells with anticancer drugs for 48 hours. Then dissolving the formazan crystals formed with dimethyl sulfoxide and taking the absorbance at 540nm with a spectrophotometer.

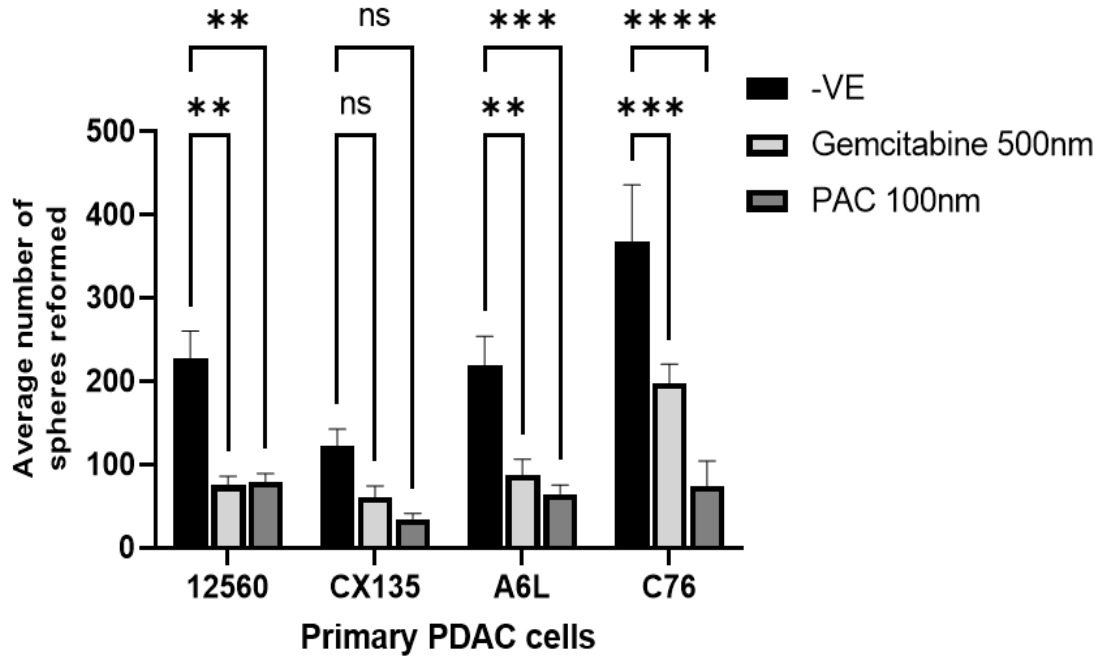
### **4.3 Results**

Numerous publications have hypothesized and shown that hypoxia is responsible for CSC population in PDAC. This study was carried out to confirm their hypotheses in patient derived PDAC cells. In this chapter, different *in vitro* assay protocols were used to study the effect of hypoxia on patient derived primary, circulating and liver metastatic PDAC cells.

#### **4.3.1 Patient derived PDAC spheroid cells are resistant to conventional anticancer drugs.**

Sphere reformation assays are aimed at analysing the cytotoxic effect of drugs on spheroid cell cultures. In Figure 4.1 (A), primary, circulating and liver metastatic PDAC spheroid cells were regrown after treatment with gemcitabine and paclitaxel. All of the patient derived PDAC spheroid cultures had reformed spheres after treatment. However, the microscopic images show that 100nM paclitaxel had a more cytotoxic effect than 500nM gemcitabine on the patient derived PDAC spheroid cells. Figure 4.1(B) shows a bar chart indicating the average number of reformed spheres after treatment with gemcitabine and paclitaxel. The bar chart reveals that paclitaxel and gemcitabine significantly reduced the sphere count but could not entirely eliminate all the spheroid cells. This is likely due to the presence of a chemoresistant cell population. From the bar chart, it is also evident that the number of spheres in the control is much less in the circulating PDAC spheroid cultures while the control of the primary and liver metastatic PDAC cells had a significantly higher sphere count. This might indicate that resistant cell populations are less during circulation but increase after localisation. These data demonstrate that the first line anticancer drugs, gemcitabine and paclitaxel are unable to completely suppress the growth of the patient derived PDAC cells.



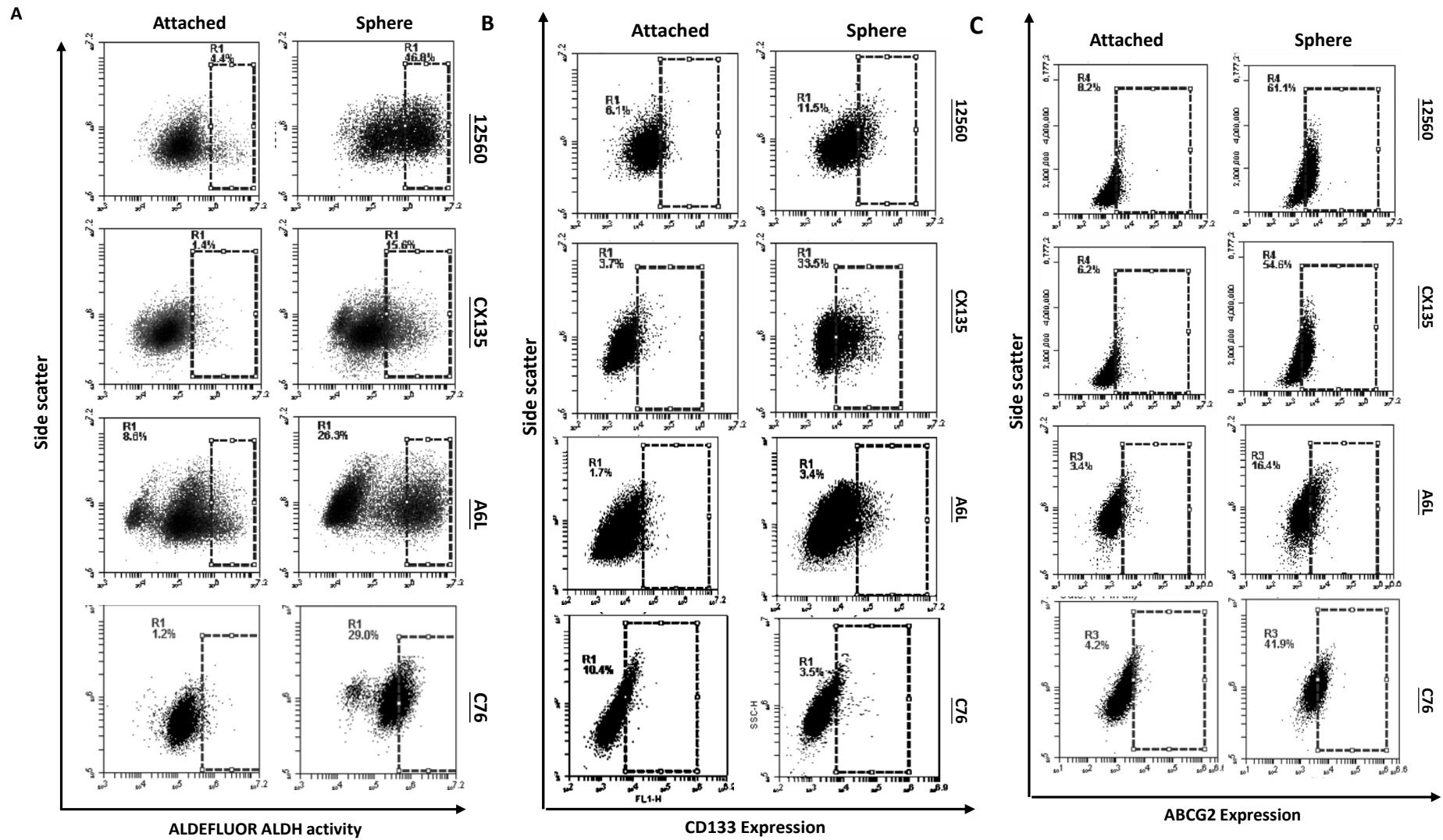
**B****Sphere reformation assay**

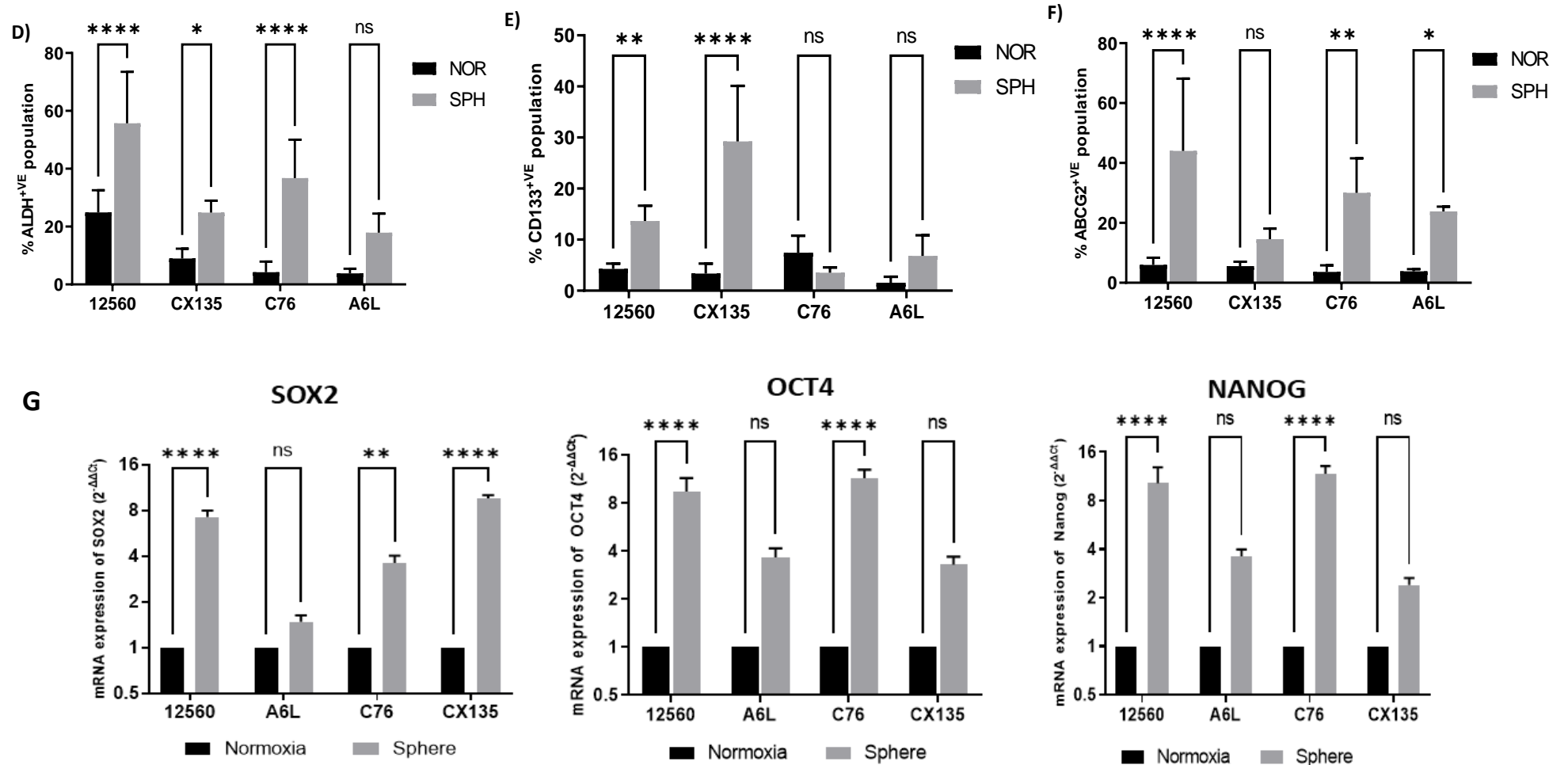
**Figure 4.1: Patient derived PDAC cells are resistant to first line anticancer drugs. (a)** Microscopic images show control and reformed spheres after treatment with 100nM paclitaxel and 500nM gemcitabine. Images were taken 5 days after cell culture ( $\times 10$  magnification). **(b)** Bar chart showing average sphere count after sphere reformation assay. Patient derived primary, circulating and liver metastatic PDAC cells are resistant to first line anticancer drugs: gemcitabine and paclitaxel. 12560=primary PDAC, CX135&C76= circulating PDAC and A6L=liver metastatic PDAC.  $n=6$ ,  $**p<0.01$ ,  $****p<0.0001$ ,  $ns$ =not significant.

### 4.3.2 Patient derived PDAC spheroid cells have CSC characteristics

As a result of the relevance of ALDH, CD133 and ABCG2 in PDAC, flow cytometry analysis was carried out to study the expression of the afore-mentioned CSC markers in the attached and spheroid patient derived PDAC cultures. The ALDEFLUOR assay was used to detect the ALDH<sup>+ve</sup> population in the patient derived PDAC cultures under normoxic and spheroid conditions. The images of the dot plot obtained is shown in Figure 4.2(A). Flow cytometry analysis was also used to detect the CD133<sup>+ve</sup> population in attached and spheroid patient derived PDAC cultures using PE-conjugated CD133 antibody as shown in Figure 4.2(B). The ABCG2<sup>+ve</sup> population in the attached and spheroid patient derived PDAC cultures was also analyzed by flow cytometry using APC conjugated anti-ABCG2 as shown in Figure 4.2(C). Figures 4.2(D), (E) and (F) show the corresponding bar charts respectively. The data revealed that each of the spheroid patient derived PDAC cultures had a significantly high population of ALDH<sup>+ve</sup>, CD133<sup>+ve</sup> and ABCG2<sup>+ve</sup> cells compared with the control.

Sox2, Oct4 and Nanog are CSC markers which help to maintain stemness in PDAC. In an effort to study the expression of CSC markers in patient derived PDAC cell cultures, real-time PCR was carried out as shown in Figure 4.2 (G). The results reveal that the mRNA expression of Oct4, Sox2 and Nanog was upregulated in the spheroid cultures. These data show that spheroid panc-1 cultures have enhanced CSC characteristics.

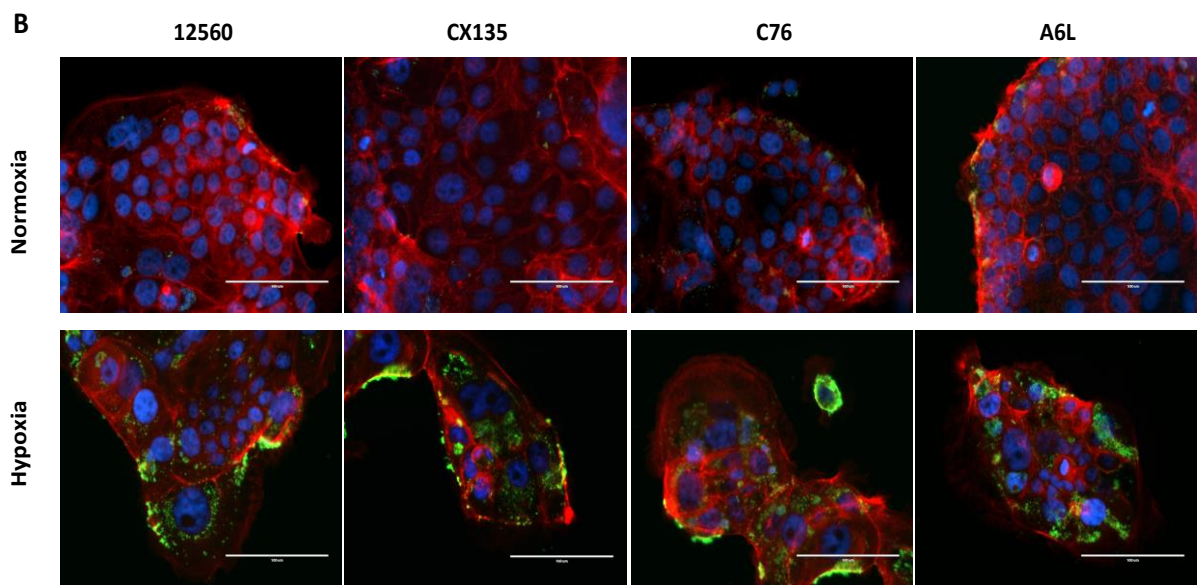
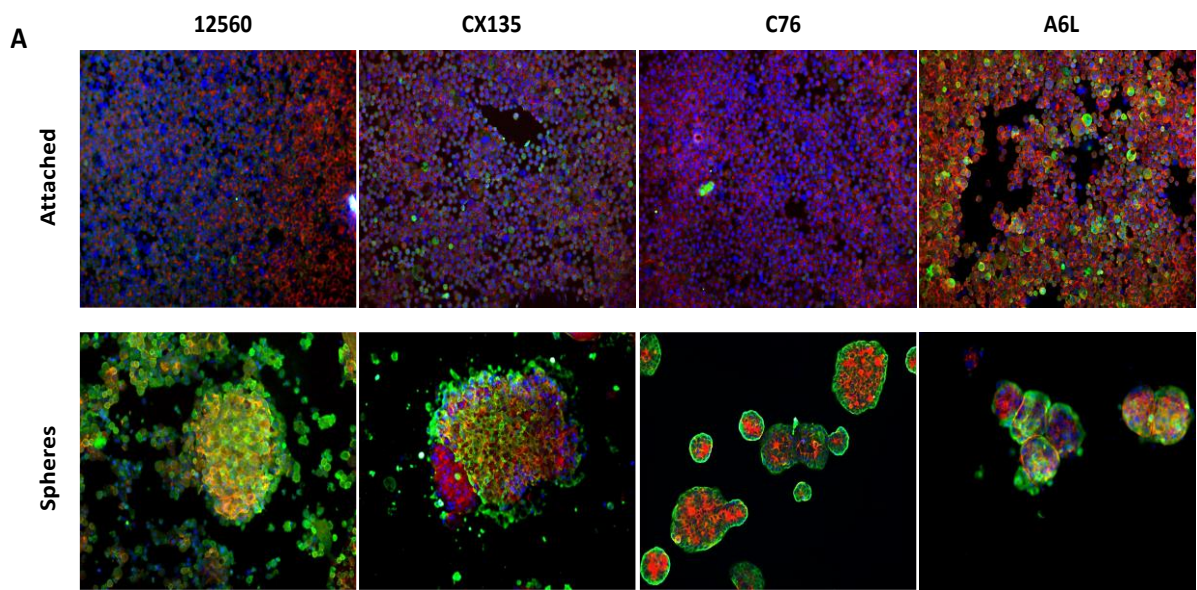


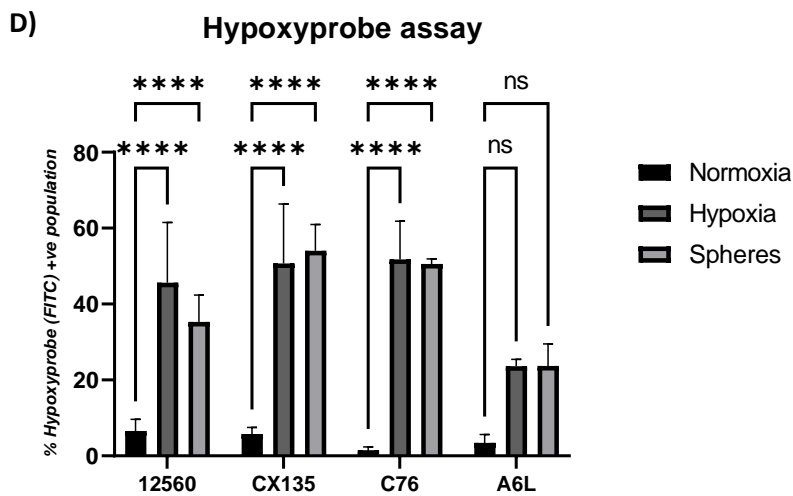
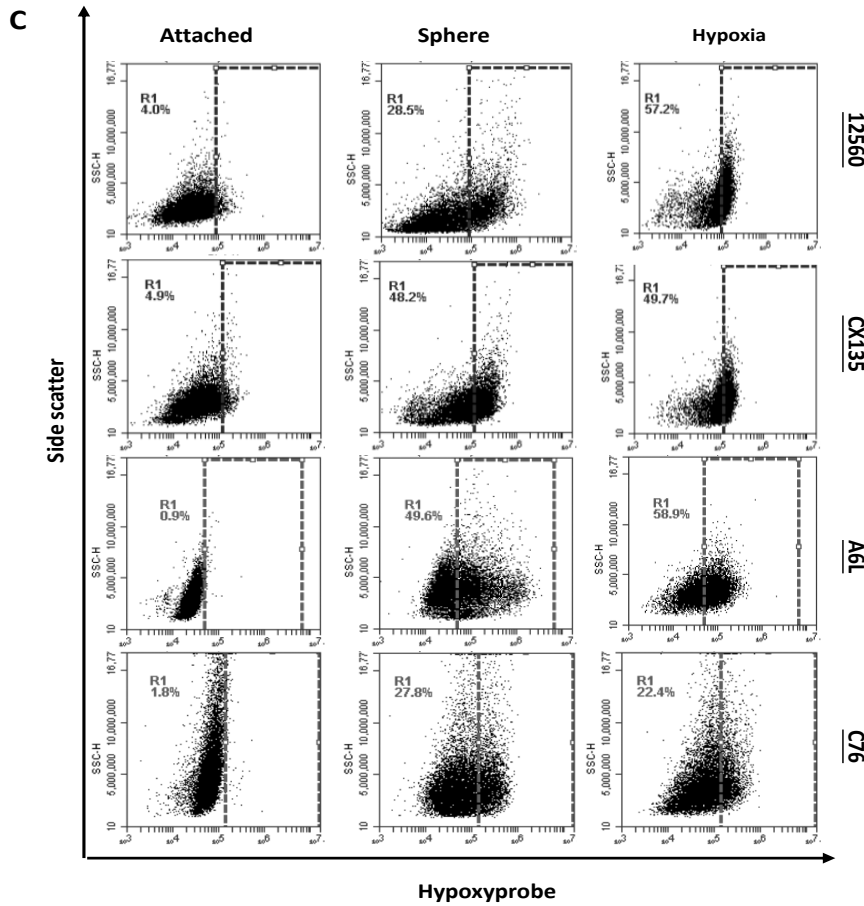


**Figure 4.2: Patient derived PDAC spheroid cells have CSC characteristics.** Flow cytometry was used to analyse the expression of (A) ALDH (B)CD133 and (C)ABCG2 in attached and spheroid patient derived PDAC cell cultures. The bar chart shows the percentage of (D) ALDH, (E) CD133 and (F) ABCG2 populations in normoxic and spheroid patient derived PDAC cultures. (G) Real-time PCR was used to analyse mRNA of CSC markers in the patient derived PDAC attached and spheroid cell cultures.  $n=6$ , \* $p<0.05$ ; \*\* $p<0.01$ .

### **4.3.3 Hypoxic populations detected in spheroid and hypoxic cultures of patient derived PDAC cells.**

The amount of hypoxia within hypoxic and spheroid patient derived PDAC tissues was quantified using FITC-conjugated mouse anti-pimonidazole which forms an adduct when it comes in contact with hypoxic cells. The adducts formed were viewed using immunofluorescence and images were taken. Images of the FITC-hypoxyprobe analysis of normoxic and spheroid patient derived cells are shown in Figure 4.3(A). The result shows the hypoxic cell population in the two cell cultures which is denoted by green cytoplasmic staining. The nucleus of each cell in the experiment was stained by DAPI (blue) while the cell wall was stained with actin (red). The images reveal that spheroid cells have high hypoxic cell populations. In Figure 4.3(B), the image revealed large green regions denoting high hypoxic cell populations in the hypoxic patient derived cultures. In order to ascertain and compare the hypoxic cell population in the normoxic and hypoxic cultures, the previous data was confirmed with flow cytometry hypoxyprobe analysis. In Figure 4.3(C), the dot plots reveal the population of FITC<sup>+ve</sup> hypoxic cell population in the normoxic, hypoxic and spheroid patient derived PDAC cultures. Figure 4.3 (D) shows a bar chart with the statistically analysed FITC<sup>+ve</sup> hypoxic cell population in the attached, hypoxic and spheroid patient derived PDAC cultures. The liver metastatic patient derived cell (A6L) had significantly lower hypoxic and spheroid cell populations compared with the primary and circulating patient derived PDAC cell cultures. This data confirms that the hypoxic and spheroid patient derived PDAC cultures contain statistically significant high hypoxic cell populations.

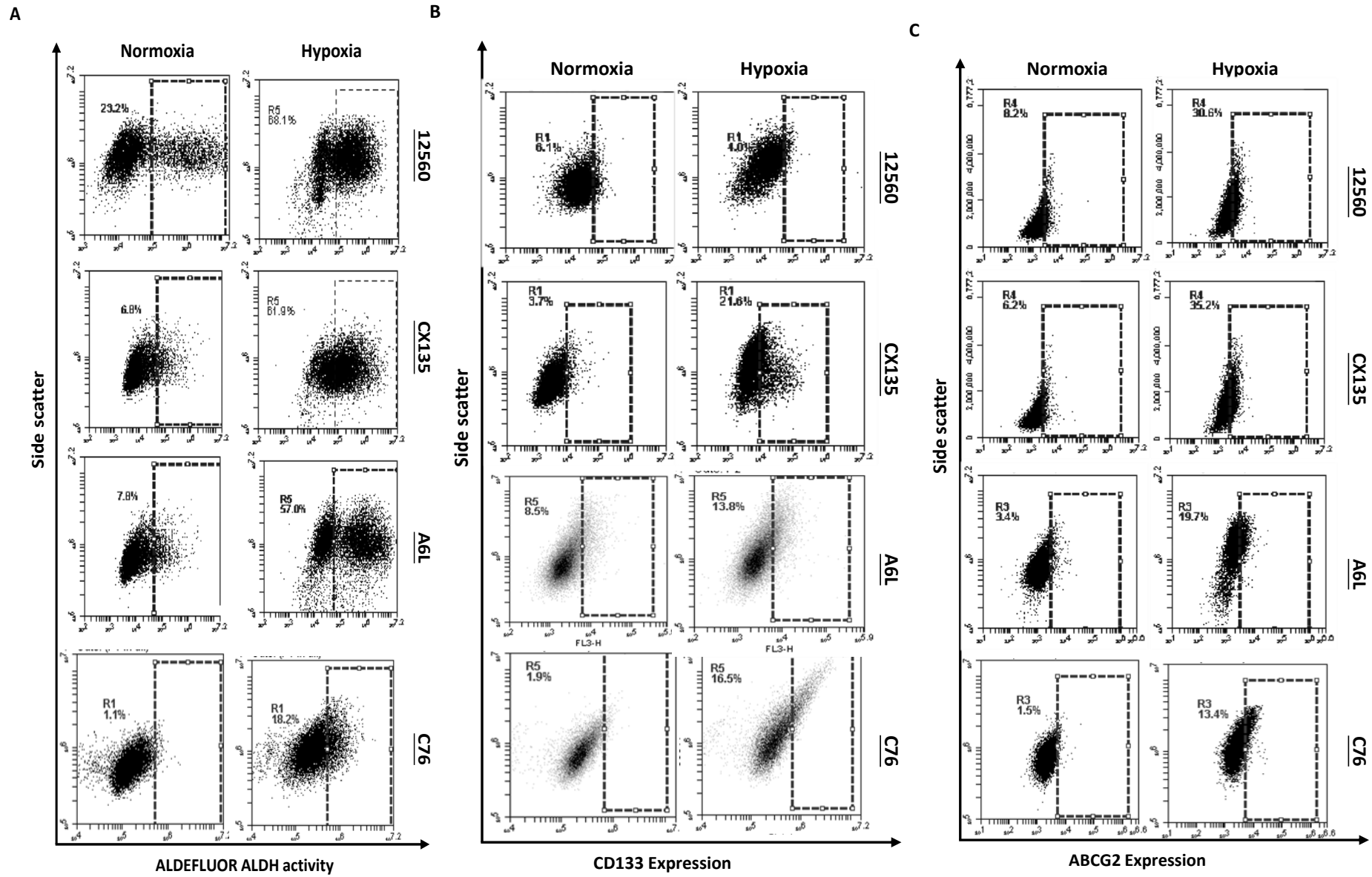




**Figure 4.3: Spheroid and Hypoxic patient derived PDAC cells have high hypoxic cell populations.** The image shows ICC staining of (A) attached and spheroid and (B) attached and hypoxic patient derived PDAC cell cultures with FITC-conjugated anti-pimonidazole. The hypoxic regions are stained with green FITC- conjugated anti-pimonidazole, the nucleus was stained blue by DAPI and cell membrane was stained red with Actin. Image magnification 10 $\times$ . (C) Flow cytometry analysis of FITC<sup>+</sup>ve hypoxic cell population in normoxic and hypoxic patient derived PDAC cells (D) Bar chart showing the statistically significant % FITC<sup>+</sup>ve hypoxic cell population.

#### **4.3.4 Hypoxic patient derived PDAC cells show increased CSC characteristics.**

Flow cytometry analysis was used to detect and compare the population of CSC markers in normoxic and hypoxic patient derived PDAC cell cultures. Figure 4.4(A) shows the dot plots obtained after ALDEFLUOR assay for the ALDH<sup>+</sup> population in normoxic and hypoxic monolayer cultures of patient derived PDAC cell cultures. The normoxic and hypoxic patient derived PDAC cells were also analyzed for CD133 using flow cytometry in Figure 4.4(B). In Figure 4.4(C), flow cytometry was used to analyze the ABCG2 population in patient derived PDAC normoxic and hypoxic cell cultures. The dot plots obtained reveal that the hypoxic cell cultures had higher ALDH<sup>+</sup>, CD133<sup>+</sup> and ABCG2<sup>+</sup> cell populations than the attached cultures. Figure 4.4 (D), (E) and (F) show bar charts revealing the percentage population of ALDH, CD133 and ABCG2 obtained. To further confirm the presence of cancer stem cells, real-time PCR was used to analyze the expression of CSC markers in attached and hypoxic patient derived PDAC cell cultures. The hypoxic cultures had increased mRNA levels of Oct4, Sox2 and Nanog compared to the attached cultures as shown in Figure 4.4 (G). The hypoxic primary patient derived PDAC cultures had the highest mRNA expression of Oct4, Sox2 and Nanog. The elevated levels of ALDH, CD133, ABCG2, Sox2, Oct4 and Nanog which are associated with maintaining cell stemness, in the hypoxic cultures suggests that hypoxia plays a role in the development of cancer stem cell characteristics.



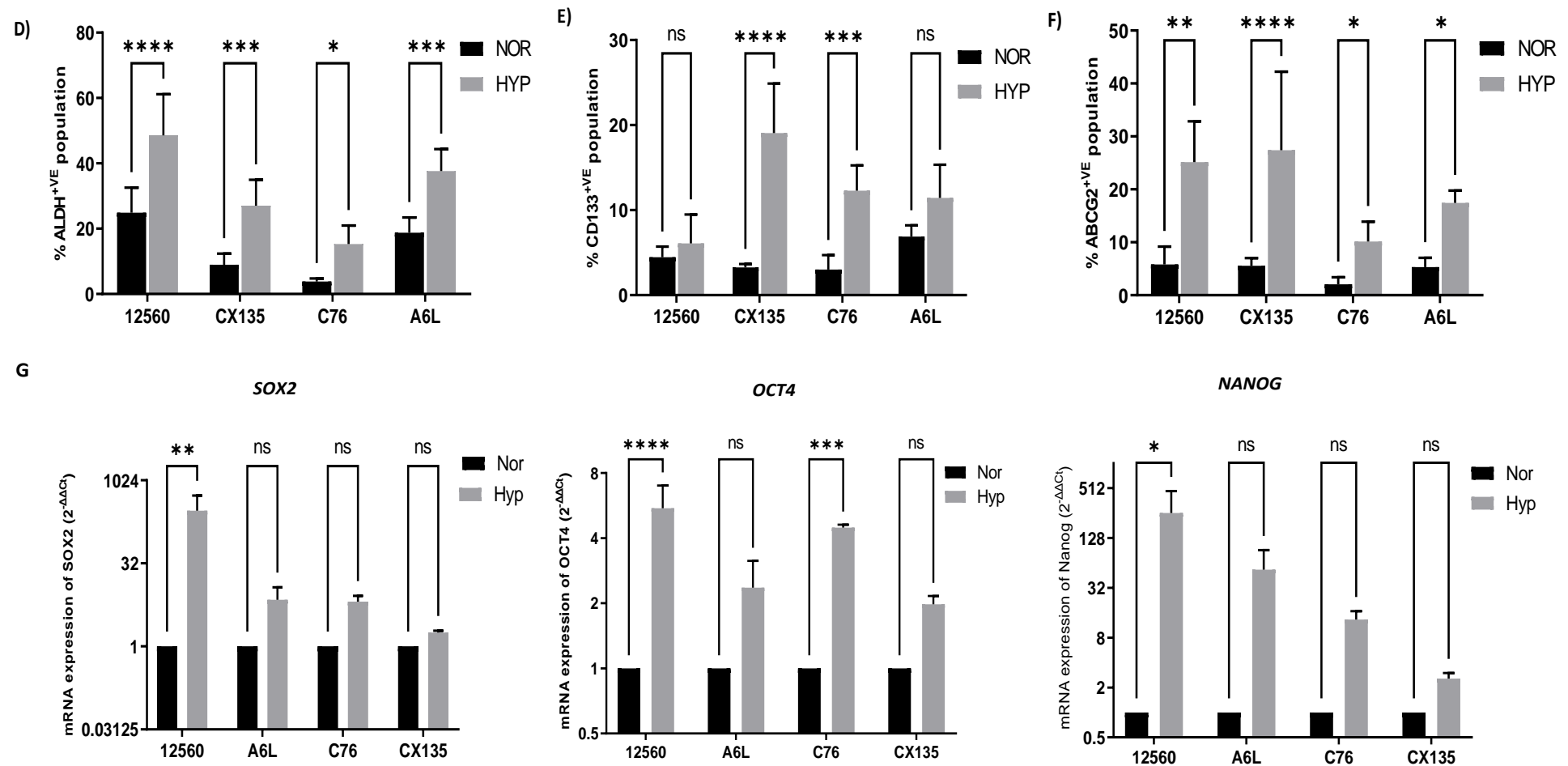


**Figure 4.4: Hypoxic patient derived PDAC cells have high CSC characteristics.** Flow cytometry was used to analyse the expression of (A) ALDH (B) CD133 and (C) ABCG2 in normoxic and hypoxic patient derived PDAC cell cultures. Bar chart shows the percentage of (D) ALDH, (E) CD133 and (F) ABCG2 population in normoxic and hypoxic patient derived PDAC cell cultures. (G) Real-time PCR was used to analyse mRNA of CSC markers in patient derived attached and spheroid cell cultures.  $n=6$ ,  $*p<0.05$ ,  $**p<0.01$ ,  $***p<0.001$ ,  $****p<0.0001$ .

#### **4.3.5 Hypoxia induces chemoresistance in patient derived PDAC cells.**

In an attempt to assess the effect of hypoxia on chemoresistance, MTT cell viability assay was carried out on primary (12556, 12560), circulating (CX102, CX135, C76) and liver metastatic (A6L) patient derived PDAC cells. The cytotoxicity of 1 $\mu$ M gemcitabine was analyzed on normoxic and hypoxic primary, circulating and liver metastatic patient derived cells using MTT cytotoxicity assay. The cytotoxicity of 100nM paclitaxel was analysed on patient derived PDAC normoxic and hypoxic cells using MTT cytotoxicity assay. The cell viability curves obtained after the two experiments is shown in Figure 4.5. The hypoxic patient derived PDAC cell cultures were more resistant to gemcitabine and paclitaxel than the normoxic cultures. The results of the assay confirms that hypoxia plays an important role in PDAC chemoresistance.

Table 4.1 shows the calculated IC<sub>50</sub> for the cell viability assays obtained after the MTT analysis. The patient derived cells cultured under normoxic conditions were more effectively killed by the gemcitabine and paclitaxel than those cultured under hypoxic conditions.

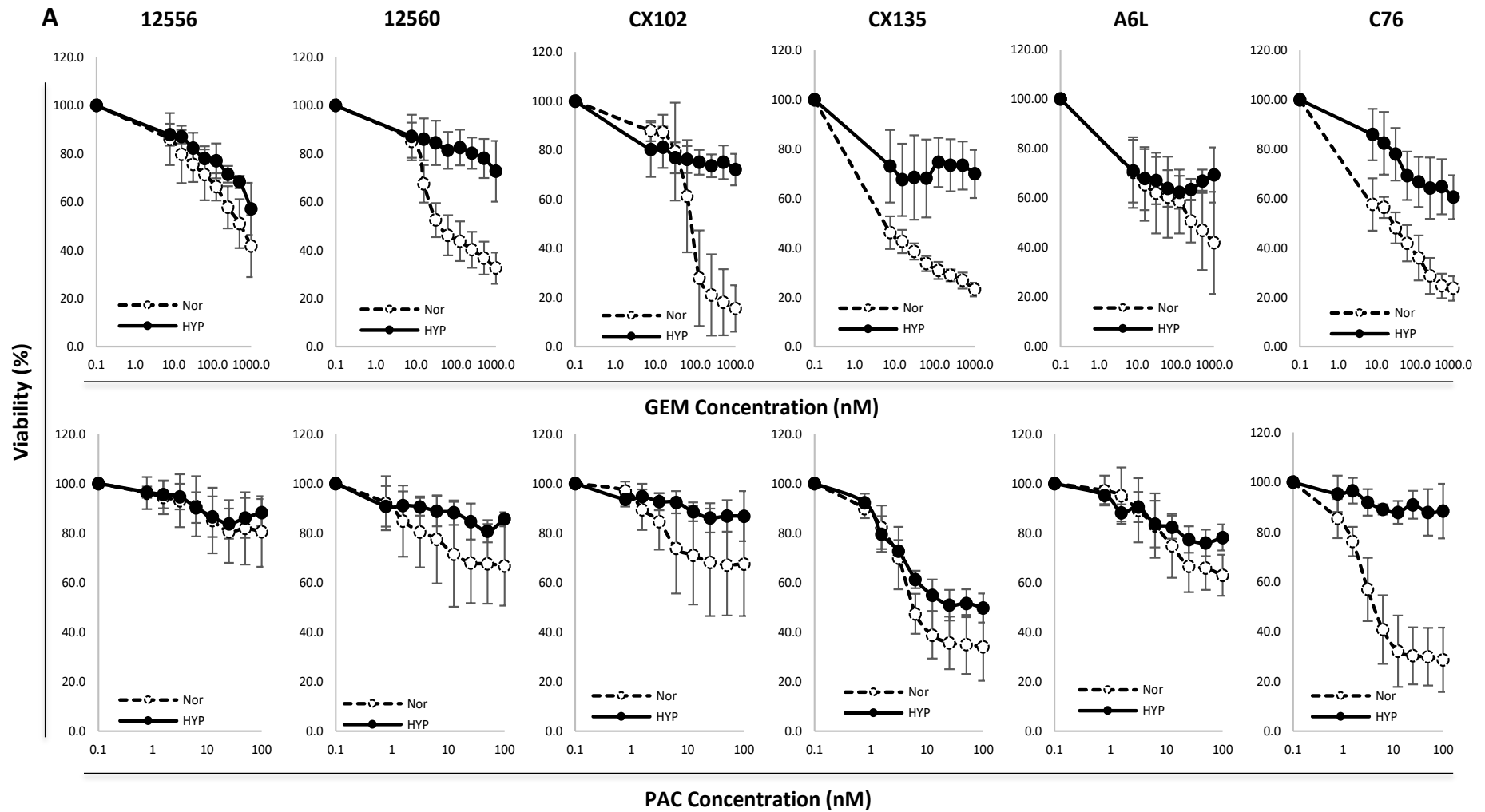


**Figure 4.5: Hypoxia increases chemoresistance in patient derived PDAC cells.** MTT cell viability assay was carried out on normoxic and hypoxic patient derived PDAC cells using  $1\mu\text{M}$  gemcitabine and  $100\text{nM}$  paclitaxel. The hypoxic patient derived PDAC cells were more chemoresistant than the normoxic patient derived PDAC cultures.  $n=3$

**Table 4.1. IC<sub>50</sub>s of gemcitabine and paclitaxel for primary PDAC cells cultures under normoxia and hypoxic conditions**

|                                 |                 | <b>12556</b>       | <b>12560</b>         | <b>CX102</b>       | <b>CX135</b>       | <b>C76</b>          | <b>A6L</b>         |
|---------------------------------|-----------------|--------------------|----------------------|--------------------|--------------------|---------------------|--------------------|
| <b>GEM IC<sub>50</sub> (nM)</b> | <b>Normoxia</b> | 879.3<br>(563.00)  | 40.40<br>(21.30)     | 65.7<br>(23.00)    | 5.30<br>(2.30)     | 14.00<br>(3.7)      | 326.20<br>(128.80) |
|                                 | <b>Hypoxia</b>  | 726.65<br>(597.33) | 3185.58<br>(2101.81) | 1039.52<br>(50.22) | 187.57<br>(314.92) | 1880.19<br>(888.82) | 658.27<br>(280.13) |
| <b>PAC IC<sub>50</sub> (nM)</b> | <b>Normoxia</b> | 539.89<br>(240.40) | 60.38<br>(45.15)     | 31.80<br>(32.32)   | 7.24<br>(2.02)     | 4.41<br>(1.42)      | 62.25<br>(46.40)   |
|                                 | <b>Hypoxia</b>  | 398.75<br>(63.78)  | 460.23<br>(145.60)   | 551.26<br>(366.68) | 26.58<br>(8.62)    | 19.52<br>(30.39)    | 241.78<br>(107.30) |

The PDAC cells were cultured and exposed to anticancer drugs gemcitabine and paclitaxel for 72 hours under normoxia and hypoxia. The IC<sub>50</sub>s of the anticancer drugs were calculated. n=3. Values = IC<sub>50</sub> (±standard deviation).

#### 4.4 Discussion

Pancreatic cancer is highly resistant to chemotherapy and radiotherapy. Chemoresistant tumour cells are usually involved in more aggressive metastasis leading to death in cancer patients (Zhou et al., 2017). The high number of inefficient anticancer drugs, coupled with the high fatality rate of cancers makes it necessary to extensively study the mechanisms underlying cancer cell growth and survival.

Pancreatic tumours have dense desmoplastic stroma which exerts high interstitial pressure on blood vessels thereby reducing blood supply in the tumour. This leads to a highly hypoxic microenvironment within the tumour and results in the activation of HIF1 and HIF2 (McGinn et al., 2017). Spheroid cells comprise of variable regions of hypoxia as seen in solid tumours and decreased drug penetration making it a good three-dimensional model for studying tumour hypoxia. However, unlike tumour cells, spheroid cell cultures lack tumour microenvironment (Leek et al., 2016). This chapter analysed the effect of hypoxia in hypoxic and spheroid patient

derived PDAC cells. Surprisingly, the data also revealed that spheroid cells are more hypoxic than cells cultured in low oxygen conditions.

Cancer stem cells were first discovered in pancreatic cancer was in 2007. These PCSCs express multidrug efflux transporters, abnormally activate signalling pathways and have enhanced ability to repair DNA. PCSCs form tumours at a higher rate than the bulk of the tumour. CSCs are identified by cell surface markers such as CD44, CD133, ESA and CD24 (Zhou et al., 2017). Hypoxia increases the CD133<sup>+</sup> population and stemness characteristics in pancreatic cancer cells (McGinn et al., 2017). A lot of research has postulated that hypoxia activates genes which initiate cancer stem cell formation. In this study, comparisons in CSC characteristics were made between normoxic, hypoxic and spheroid patient derived PDAC cells. This research demonstrates that under hypoxic conditions, there was an increased expression of the cancer stem cell markers: ALDH, CD133 and ABCG2 in the primary, circulating and liver metastatic PDAC cell cultures. In addition to that, there is an overexpression of CSC markers in hypoxic patient derived PDAC cells. The presence of CSC markers in the normoxic patient derived PDAC cells implies that localised hypoxia can be formed under normoxic conditions.

CD133<sup>+ve</sup> cells are present in the hypoxic regions of tumour which are characterised by elevated HIF-1 activity (Gzil et al., 2019). This also explains why there is increased CD133<sup>+ve</sup> population in the hypoxic and spheroid patient derived PDAC cultures.

The CSC marker ALDH removes oxidative stress. CD133<sup>+ve</sup> tumour cells are more chemoresistant than CD133<sup>-ve</sup> lung cancer cells. Germ cell tumours exhibit decreased CSC characteristics after the knockdown of Oct4. The growth of glioblastoma cells is suppressed by Sox2 knockout. Nanog is highly expressed in primary tumours and stage III/IV cancer (Singh et al., 2013; Chen et al., 2008; Song et al., 2018; Gangemi et al., 2009; Wang et al., 2013; Yang et al., 2020). The information above explains why ALDH, CD133, SOX2, OCT4 and Nanog

were highly expressed under hypoxic conditions in all the PDAC cell cultures. They play critical roles in maintaining tumor cell stemness, pluripotency and chemoresistance.

The percentage of pancreatic tumour cells with CSC properties is low (Shah et al., 2021). This explains why the normoxic patient derived PDAC cells have lower expressions of CSC markers.

HIF activity helps to maintain the expression of Nanog, Sox2 and Oct4 which in turn promotes the pluripotency and self-renewal characteristics of cancer stem cells (Qian and Rankin., 2019). All the patient derived PDAC cells had an upregulation of SOX2, OCT4 and Nanog when cultured under hypoxic and spheroid conditions, showing that these are proteins play a critical role in PDAC CSC maintenance.

A study conducted on several solid tumours revealed that pancreatic cancer tumours were the most hypoxic. The low oxygen levels in pancreatic cancer triggers an adaptive response mechanism (Erkan et al., 2016). The hypoxia in the core of a tumour activates signalling pathways that modify the tumour microenvironment. Many tumours have evolved from genetic changes to the genes involved in the growth and survival of their epithelial cells. During metastasis, detached cancer cells enter into the systemic circulation and begin to grow in a distant organ (Cervantes-Villagrana et al., 2020). Tumour hypoxia is caused by elevated growth rate, increased metabolic rate and decreased tumour vascularisation. The transcription factors, HIF1 $\alpha$  and HIF2 $\alpha$  are stabilised by hypoxia leading to tumour proliferation, EMT and metastasis. The significance of hypoxia in cancerous tumours makes it a source of interest for researchers seeking improved cancer therapy (Leek et al., 2016).

The main factor that promotes chemoresistance in pancreatic cancer is desmoplasia and hypoxia of the tumour microenvironment (Erkan et al., 2016). Gemcitabine is a standard first line treatment for pancreatic cancer which has insignificant effect on overall patient survival.

This proves that CSC markers and CSC markers play a role in development of chemoresistance (Wang et al., 2019a). Sensitive tumours can become resistant to gemcitabine within weeks of administration because of the dense stroma of the PDAC tumour microenvironment which leads to poor drug circulation (Ma et al., 2020). Nab-paclitaxel therapy enhances intra-tumoral concentration of gemcitabine leading to a synergistic effect and a median overall survival of 8.7 months in metastatic pancreatic cancer (Goldstein et al., 2015; Corrie et al., 2020). The cell viability assay shows that paclitaxel and gemcitabine treatment can't eliminate PDAC primary cells. It also shows that hypoxia increases the chemoresistance of paclitaxel and gemcitabine in PDAC primary cells. These findings reveal that hypoxia plays a very significant role in imparting drug resistant characteristics to tumour cells.

The increased resistance of the hypoxic patient derived PDAC cell cultures to treatment is because hypoxia-induced HIF-1 uses different mechanisms to inhibit apoptosis in PDAC cells. HIF-1 $\alpha$  causes the overexpression of MDR1 which promotes drug efflux leading to chemoresistance. Hypoxia causes gemcitabine resistance by reducing the expression of BNIP3, a gene involved in hypoxia-mediated cell induced apoptosis in pancreatic cell lines (Shah et al., 2020).

#### **4.5 Conclusion**

In summary, the results from Chapter 4 show that hypoxia plays a critical role in the development of stemness, metastasis and chemoresistance in PDAC cells.

## **CHAPTER 5**

**CYCLODEXTRIN ENCAPSULATED DISULFIRAM PLUS  
COPPER TARGETS CANCER STEM CELLS AND BLOCKS  
CHEMORESISTANCE AND INVASIVENESS IN  
PANCREATIC DUCTAL ADENOCARCINOMA CELLS**

## 5.1 Introduction

Copper is important for redox reactions which stimulate ROS production in human cells. Disulfiram chelates copper to create a complex which produces higher levels of ROS than copper alone. The high intracellular ROS produced destroys DNA, proteins and lipids leading to cell death. However, the reverse can be the case by leading to increased expression of anti-apoptotic proteins that increase chemoresistance. Cancer cells overexpress NFκB which plays a big role in chemoresistance by increasing the expression of anti-apoptotic genes. Disulfiram effectively eliminates cancer cells in *in vivo* and *in vitro* studies. High ALDH activity protects CSCs from ROS-induced damage. Cancer cells are more sensitive to anticancer drugs when their ALDH genes are suppressed (Liu et al., 2012).

Disulfiram which is originally an anti-alcoholism drug, forms a disulphide bond with acetaldehyde dehydrogenase which deactivates the enzyme. Disulfiram reduced the expression of HIF2α and increased the expression of HIF1α in hepatoma cells. Disulfiram is cytotoxic under hypoxic conditions. Studies show that HIF1α (transactivates proapoptotic genes) and HIF2α (promotes cell growth) play different roles in tumour progression so it would be wise to design an anticancer drug which suppresses both HIF1α and HIF2α (Park et al., 2018). Some of the known modes of action of disulfiram in eliminating cancer cells is by forming strong complexes with metal ions such as Cu<sup>2+</sup> hence blocking 26S and 20S proteasome activity, by preventing NFκB pathway activation, inhibiting ALDH activity and targeting p97 segregase adaptor NPL4 which plays a big role in endoplasmic reticulum stress and unfolded protein response stress. Tumour cells grow much faster than normal cell so require more effective chemotherapy to undergo apoptosis (Zhang et al., 2019). According to studies by Cong et al., 2017, disulfiram/Cu drastically reduced the CSC population in breast cancer cells, decreased the ALDH bright population in pancreatic cancer cells under clinically relevant FIR setting and decreased the CD133<sup>+</sup> population in PDAC cultures treated with chemoradiation. Their

research also showed that the anticancer effect is enhanced when a first line anticancer drug is combined with disulfiram/Cu than when two first line anticancer drugs such as folfirinox and irinotecan are combined together. Pancreatic cancer stem cells (PCSCs) are resistant to chemoradiation and some studies show that radiation increases PCSC population. An effective anticancer drug should eliminate both cancer stem cells and differentiated cancer cells but most anticancer drugs eliminate just the differentiated cancer cells. Tumours have been found to contain high levels of intracellular copper and low levels of intracellular selenium, zinc and iron. In a particular study which used disulfiram in a syngeneic mouse PDAC model, endogenous copper was shown to have a more enhanced anticancer effect than that of exogenous copper. Another study has proved that ALDH bright cells are more resistant to gemcitabine than ALDH negative cells. This ALDH bright population can be used to assess the CSC subpopulation of pancreatic cancer cells. This ALDH bright population was efficiently eliminated by disulfiram. The cytotoxic effect of disulfiram was enhanced when combined with gemcitabine. Tumour progression was hindered in mice orally administered with disulfiram and a low dose of gemcitabine (Cong et al., 2017).

Disulfiram is relatively cheap and a daily intake of 500mg for a year will cost roughly \$500. A recent phase 1 study which tested a combination of temozolomide and disulfiram after chemoradiotherapy on cancer patients showed an increase in median progression-free survival time by 8.8months (Koh et al., 2019).

Studies have shown that administering DSF/Cu in combination with adjuvants such as auranofin eliminates ovarian cancer cells by initiating apoptosis in a ROS and copper dependent manner. A number of studies have shown that cancer cells with elevated levels of ALDH are susceptible to disulfiram. Under physiological conditions, oral disulfiram is highly unstable and degraded by the gastrointestinal system before it can get into the bloodstream (Viola-Rhenals et al., 2018). Disulfiram has numerous modes of action including stimulating

intracellular endogenous formaldehyde accumulation due to acetaldehyde dehydrogenase deactivation (Komarova et al., 2019).

## **5.2 Experimental Design**

All experiments carried out in this chapter are explained in detail in Chapter 2.

### **5.2.1 Cell culture**

Panc-1 cells were cultured in RPMI 1640 media supplemented with 100 U/ml penicillin and 100 µg/ml streptomycin, 5% L-glutamine and 10% FBS in a humidified atmosphere at 37°C with 5% CO<sub>2</sub> and passaged every 3 days.

Hypoxic Panc-1 cells were cultured in RPMI 1640 media supplemented with 100 U/ml penicillin and 100 µg/ml streptomycin, 5% L-glutamine and 10% FBS in a humidified atmosphere at 37°C with 5% CO<sub>2</sub> and 0% O<sub>2</sub>.

Spheroid Panc-1 cells were cultured using stem cell media and flasks coated with poly (2-hydroxyethylmethacrylate).

### **5.2.2 Sphere reformation assay**

The patient derived PDAC cells were cultured with stem cell media in flasks coated with polyhema and incubated for 4 days at 37°C in a humidified incubator. The spheres formed were treated with gemcitabine, paclitaxel, copper and disulfiram/Cu overnight. After which the respective spheres were collected in tubes, trypsinized, counted and reseeded. Five days later, images were taken then the spheres were counted and recorded.

### **5.2.3 Cell Apoptosis Assay**

Patient derived PDAC cells were cultured in a 6-well plate and the respective wells were dosed overnight with 100nM of paclitaxel, 500nM of gemcitabine, 10µM copper and 5µM

cyclodextrin disulfiram. The next day, the treated cells were collected into tubes, rinsed with PBS and stained with annexin-V and PI following the manufacturer's instruction. FITC-conjugated annexin-V/PI assay was used to measure cell apoptosis using a flow cytometer.

#### **5.2.4 Flow Cytometry Analysis**

In order to investigate the expression of CSC markers, cell pellets were rinsed with PBS then stained with the desired CSC marker antibody and incubated for the required time. The cells were then rinsed and resuspended in the appropriate buffer and read on a flow cytometer.

#### **5.2.5 MTT Cell Viability assay**

Cells were seeded in a 96 well plate (5000 cells/well). Cytotoxicity assay was carried out using MTT reagent after treating the cells with anticancer drugs for 48 hours. Then dissolving the formazan crystals with dimethyl sulfoxide and taking the absorbance at 540nm with a spectrophotometer.

#### **5.2.6 Detection of embryonic stem cell markers using Real-time PCR**

Total RNA was extracted from both normoxic and hypoxic Panc-1 cell cultures using the mRNA extraction kit (Qiagen) following the manufacturer's instruction then reverse transcribed to give cDNA. This cDNA was subjected to real-time PCR using primers of specific interest and the fold change was calculated. Two-way ANOVA and t-test were used to analyse the fold change using GraphPad Prism software.

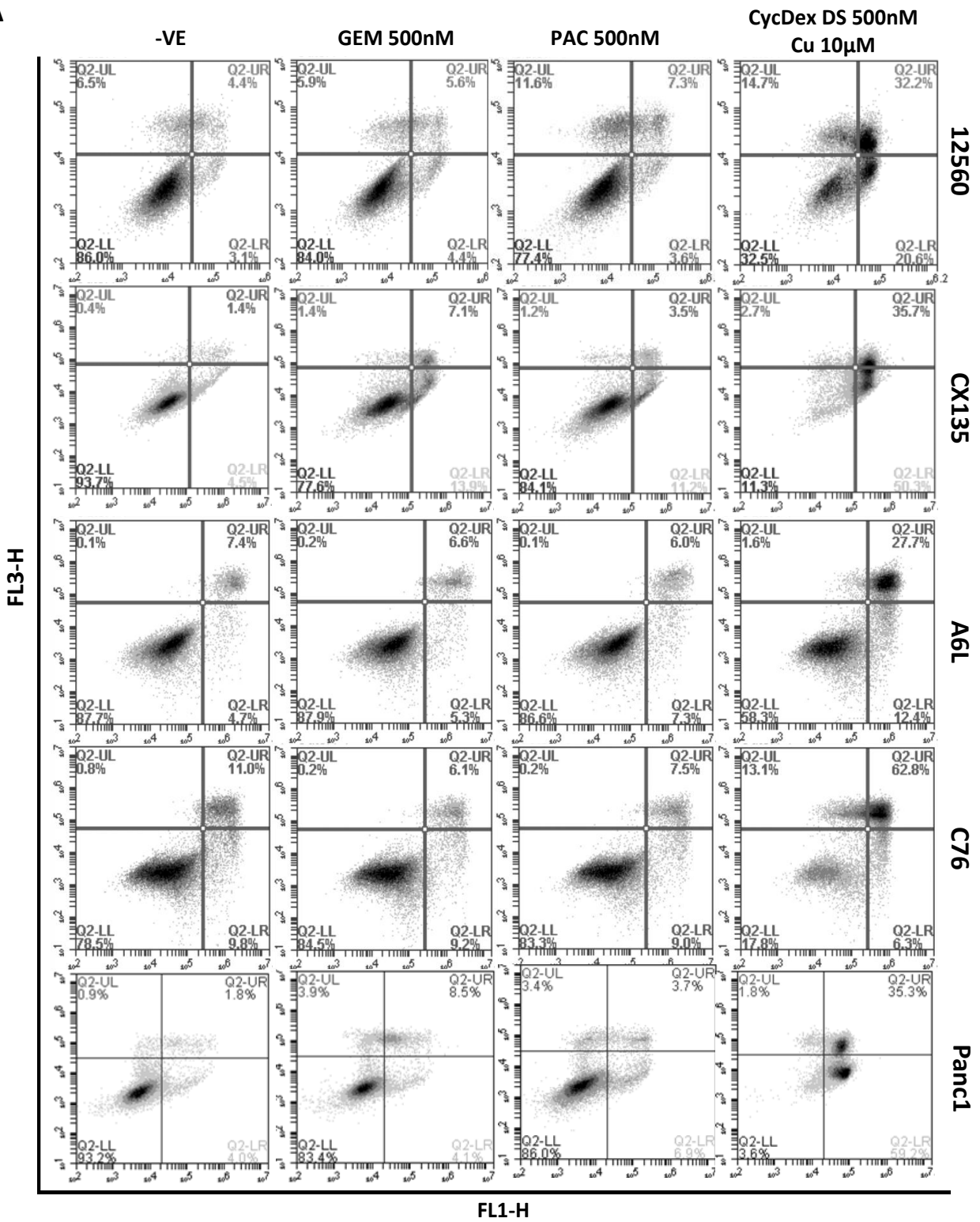
### 5.3 Results

The central issue addressed in this chapter is the efficiency of disulfiram in completely eliminating PDAC cancer stem cells.

#### 5.3.1 PDAC cells are resistant to first line anti-PDAC drugs (GEM and PAC) induced apoptosis but sensitive to CycDex DS/Cu.

In order to examine the *in vitro* degree of anticancer efficacy of cyclodextrin disulfiram against PDAC cells, Annexin apoptosis assay was carried out using flow cytometry. Annexin apoptosis assay requires staining the PDAC cells with Annexin V and propidium iodide to measure the proportion of early apoptotic, late apoptotic and necrotic cells in the cell cultures. The apoptotic population was stained by Annexin-V and the necrotic population was stained with Propidium iodide. Primary, circulating and liver metastatic patient derived PDAC cells and the PDAC cell line, panc-1 were dosed overnight with 500nM gemcitabine, 500nM paclitaxel and 500nM cyclodextrin disulfiram/10 $\mu$ M copper. The dot plots showing three distinct cell populations are shown in Figure 5.1 (A). Cyclodextrin disulfiram had a significantly higher apoptotic effect on all the PDAC cells than gemcitabine and paclitaxel. A bar chart showing the percentage of apoptotic populations after drug treatment is shown in Figure 5.1 (B). Treatment with gemcitabine and paclitaxel led to small increase in the percentage of apoptotic population while treatment with cyclodextrin disulfiram increased the apoptotic population. This result clearly reveals that cyclodextrin disulfiram is highly cytotoxic to PDAC cells.

A



B

## Apoptosis assay

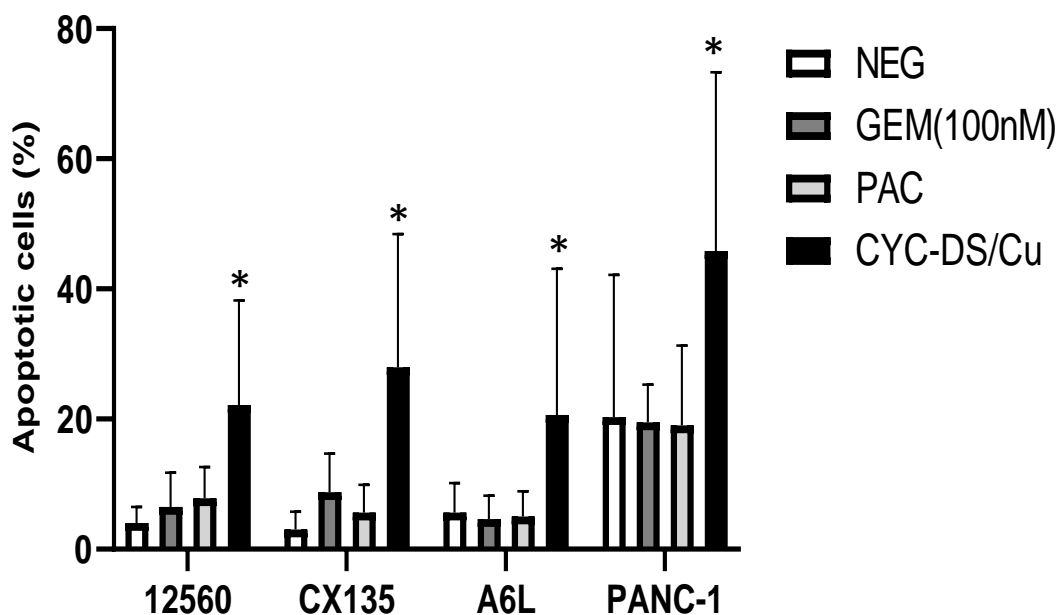


**Figure 5.1: PDAC cells are resistant to first line anti-PDAC drugs (GEM and PAC) induced apoptosis but sensitive to CycDex DS/Cu.** (A) Flow cytometry analysis showing apoptosis after treating primary, circulating and metastatic PDAC cells and PDAC cell line with 500nM of gemcitabine, paclitaxel and cyclodextrin disulfiram/10 $\mu$ M Cu. (B) Bar chart showing the increased percentage of apoptotic cells after treatment. Cyclodextrin disulfiram/Cu had the highest apoptotic effect. n=6; \*p<0.0001

### 5.3.2 CycDex DS/Cu is cytotoxic to PDAC cells and enhances the cytotoxicity of first line anti-PDAC drugs in normoxia cultured PDAC cells.

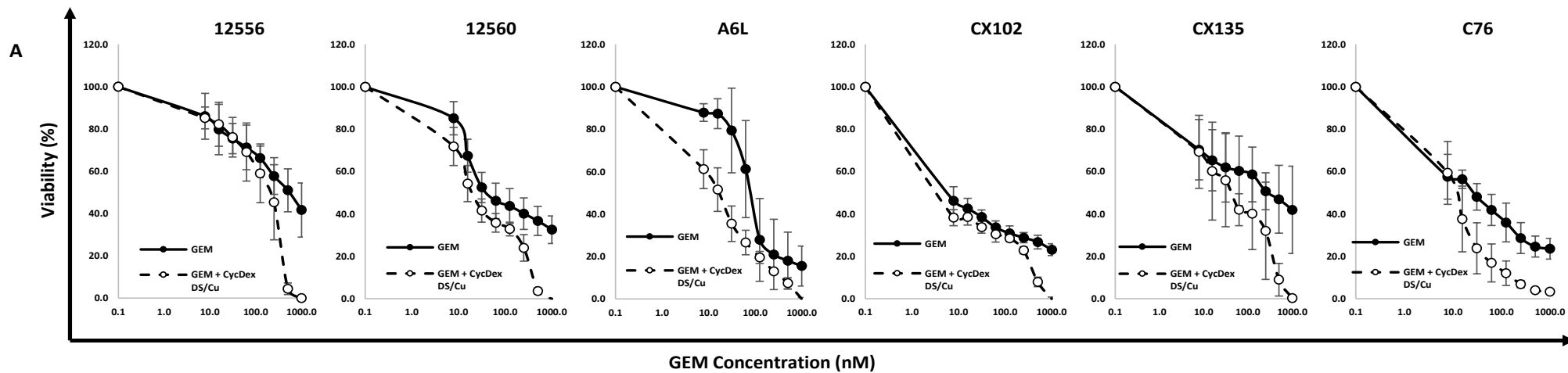
The previous experiment showed reduced anticancer effect of the first line anticancer drug, gemcitabine compared with cyclodextrin disulfiram, this experiment was carried out to evaluate the effect of combined treatment of gemcitabine with cyclodextrin disulfiram/Cu under normoxic conditions. MTT cell viability assay was carried out on the patient derived PDAC cells (12556, 12560, CX135, C76 and A6L) treated with gemcitabine alone and in combination with cyclodextrin disulfiram/Cu. A separate MTT cell viability assay was carried out on the patient derived PDAC cells treated with cyclodextrin disulfiram/Cu alone and in combination with gemcitabine to determine the true efficiency of cyclodextrin disulfiram/Cu.

Each well of a 96-well plate was seeded with 5,000 cells which were dosed the next day with serially diluted 1 $\mu$ M gemcitabine or 10 $\mu$ M cyclodextrin disulfiram/Cu then kept in an incubator for 72 hours. The cell viability curves obtained after the experiment are shown in Figure 5.2 (A). For each of the patient derived PDAC cells, treatment with cyclodextrin disulfiram/Cu and gemcitabine was more effective than treatment with gemcitabine alone. Furthermore, treatment of each of the patient derived PDAC cells with gemcitabine and cyclodextrin disulfiram/Cu was also more cytotoxic than treatment with cyclodextrin disulfiram/Cu alone.

In Figures 5.2 (B), the afore-mentioned experiment was repeated using 100nM paclitaxel and comparisons were made on the effects of treatment singly and in combination with cyclodextrin disulfiram/Cu on primary, circulatory and liver metastatic PDAC cells. For each of the patient derived PDAC cells, treatment with cyclodextrin disulfiram/Cu was more effective than treatment with paclitaxel alone. The curve was flattened proving that combined treatment completely eliminated the PDAC cells. Also, treatment of each of the patient derived PDAC cells with paclitaxel and cyclodextrin disulfiram/Cu was also more cytotoxic than treatment with cyclodextrin disulfiram/Cu alone and flattened the curve. The data from these experiments reveal that cyclodextrin disulfiram/Cu is more cytotoxic to patient derived PDAC cells when combined with paclitaxel or gemcitabine under normoxic conditions and completely eliminates the patient derived PDAC cells.

The average IC<sub>50</sub> and its standard deviations for treatment of the patient derived PDAC cells with gemcitabine and paclitaxel, both singly and in combination with cyclodextrin disulfiram/Cu under normoxic conditions are shown in Table 5.1 while the combination index of gemcitabine and paclitaxel in combination with cyclodextrin disulfiram/Cu is shown in Table 5.2.

DS/Cu enhances GEM



GEM enhances DS/Cu

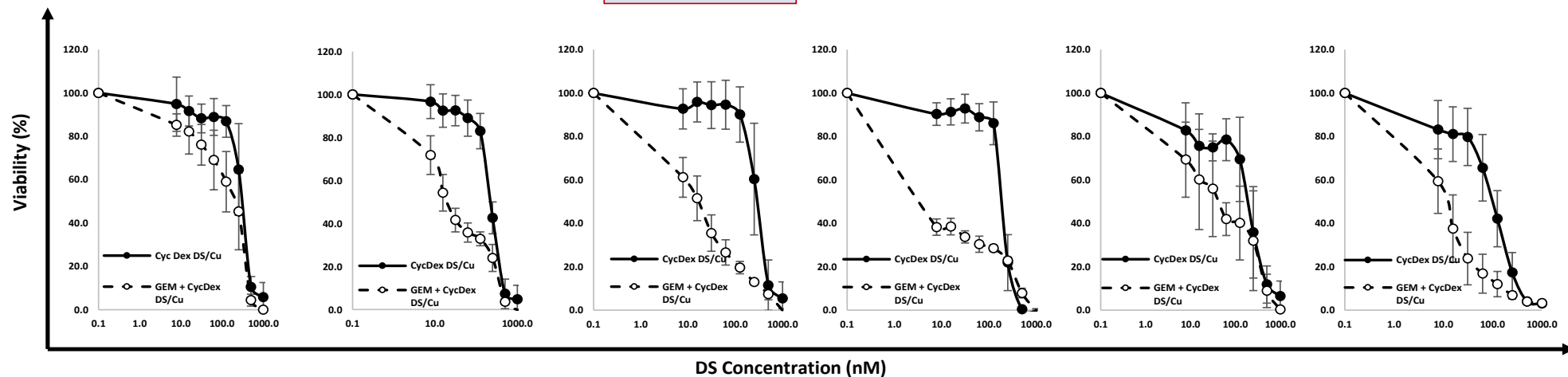


**Figure 5.2 (A)** GEM and CycDex DS/Cu mutually enhance the in vitro cytotoxicity in normoxia cultured PDAC cells. Comparison of the viabilities of patient derived cells when treated with Gemcitabine singly, gemcitabine + Cyclodextrin disulfiram/Cu, Cyclodextrin disulfiram/Cu singly and gemcitabine + Cyclodextrin disulfiram/Cu under normoxic conditions. The combined treatment was more cytotoxic than treating singly with Gemcitabine or Cyclodextrin disulfiram/Cu and completely eliminated all the PDAC cells.

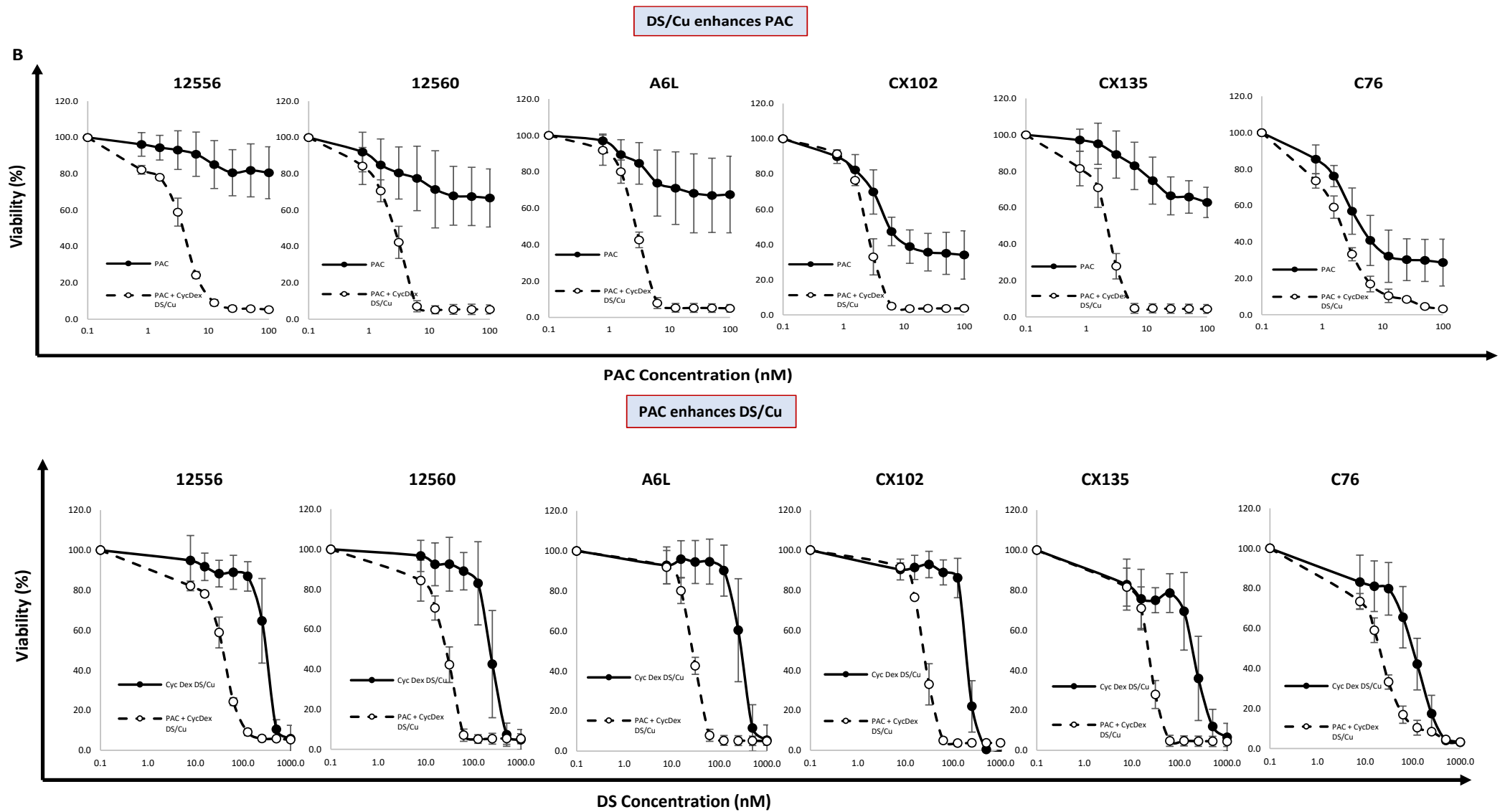


**Figure 5.2 (B) PAC and CycDex DS/Cu mutually enhance the *in vitro* cytotoxicity in normoxia cultured PDAC cells. Comparison of the viabilities of patient derived cells when treated with Paclitaxel singly, paclitaxel + Cyclodextrin disulfiram/Cu, Cyclodextrin disulfiram/Cu singly and Paclitaxel + Cyclodextrin disulfiram/Cu. The combined treatment was more cytotoxic than treating singly with Paclitaxel or cyclodextrin disulfiram/Cu and flattened the curve.**

**Table 5.1. IC<sub>50</sub>s of drugs singly used and in combination with CycDex DS/Cu in normoxia-cultured PDAC cells**

|                                    | <b>12556</b>           | <b>12560</b>           | <b>CX102</b>           | <b>CX135</b>           | <b>C76</b>            | <b>A6L</b>              |
|------------------------------------|------------------------|------------------------|------------------------|------------------------|-----------------------|-------------------------|
| <b>CycDex IC<sub>50</sub> (nM)</b> | <b>270.8</b><br>(43.0) | <b>221.7</b><br>(72.0) | <b>290.1</b><br>(87.4) | <b>179.8</b><br>(33.0) | <b>95.9</b><br>(44.2) | <b>213.4</b><br>(62.82) |
| <b>GEM IC<sub>50</sub> (nM)</b>    | <b>687.6</b><br>(42.1) | <b>61.1</b><br>(38.6)  | <b>66.3</b><br>(25.6)  | <b>8.25</b><br>(4.3)   | <b>34.5</b><br>(21.5) | <b>326.1</b><br>(128.7) |
| <b>CycDex DS + GEM</b>             | <b>198.7</b><br>(82.5) | <b>22.3</b><br>(8.7)   | <b>17.2</b><br>(6.9)   | <b>4.9</b><br>(1.1)    | <b>18.6</b><br>(5.0)  | <b>90.5</b><br>(51.4)   |
| <b>PAC IC<sub>50</sub> (nM)</b>    | <b>&gt;100</b>         | <b>&gt;100</b>         | <b>&gt;100</b>         | <b>7.5 (1.9)</b>       | <b>4.4 (1.4)</b>      | <b>&gt;100</b>          |
| <b>CycDex DS + PAC</b>             | <b>3.7</b><br>(0.5)    | <b>2.5</b><br>(0.2)    | <b>2.8</b><br>(0.06)   | <b>2.4</b><br>(0.3)    | <b>1.9</b><br>(0.2)   | <b>2.2</b><br>(0.3)     |

The PDAC cells were exposed to anticancer drugs (gemcitabine, paclitaxel) and CycDex DS/Cu singly or a combination of anticancer drugs and CycDex DS/Cu for 72 hours. The IC<sub>50</sub>s of the anticancer drugs and CycDex DS/Cu were calculated. n=9; NA=not analyzed; values = IC<sub>50</sub> (± standard deviation)

**Table 5.2. The combination index (CI) of anticancer drugs in combination with CycDex DS/Cu in normoxia-cultured PDAC cells**

| <b>Cells</b> | <b>GEM/DS</b> |             |             | <b>PAC/DS</b> |             |             |
|--------------|---------------|-------------|-------------|---------------|-------------|-------------|
|              | <b>ED50</b>   | <b>ED75</b> | <b>ED90</b> | <b>ED50</b>   | <b>ED75</b> | <b>ED90</b> |
| <b>12556</b> | 0.524         | 0.320       | 0.218       | 0.120         | 0.110       | 0.100       |
| <b>12560</b> | 0.720         | 0.388       | 0.436       | 0.129         | 0.170       | 0.224       |
| <b>A6L</b>   | 0.625         | 0.559       | 0.567       | 0.200         | 0.179       | 0.160       |
| <b>CX102</b> | 0.619         | 0.526       | 0.531       | 0.108         | 0.112       | 0.118       |
| <b>CX135</b> | 1.477         | 0.192       | 0.488       | 0.096         | 0.078       | 0.066       |
| <b>C76</b>   | 0.517         | 0.303       | 0.405       | 0.510         | 0.472       | 0.522       |

CI: 0.9–1.1 additive effect; 0.8–0.9 slight synergism; 0.6–0.8 moderate synergism; 0.4–0.6 synergism; 0.2–0.4 strong synergism.

### **5.3.3 CycDex DS/Cu is cytotoxic to PDAC cells and enhances the cytotoxicity of first line anti-PDAC drugs in hypoxia cultured PDAC cells.**

Two different MTT cell viability assays were carried out on the patient derived PDAC cells (12556, 12560, CX135, C76 and A6L) cultured under hypoxic conditions. The first was treated with gemcitabine alone and in combination with cyclodextrin disulfiram/Cu while the second was treated with cyclodextrin disulfiram/Cu alone and in combination with gemcitabine. The cell viability curves obtained after the experiments are shown in Figure 5.3 (A). For each of the patient derived PDAC cells, treatment with cyclodextrin disulfiram/Cu and gemcitabine was more effective than treatment with gemcitabine alone or cyclodextrin disulfiram/Cu alone. In Figures 5.3 (B), the experiment was repeated using 100nM paclitaxel and comparisons were made on the effects of treatment singly and in combination with cyclodextrin disulfiram/Cu on primary, circulatory and liver metastatic PDAC cells. For each of the patient derived PDAC cells, treatment with cyclodextrin disulfiram/Cu was more effective than treatment with paclitaxel alone or cyclodextrin disulfiram/Cu alone. However, in Figure 5.3 (A) and (B), the curves were not flattened by the combination treatment.

The IC<sub>50</sub> for the patient derived PDAC cells treated with gemcitabine and paclitaxel both singly and in combination with cyclodextrin disulfiram/Cu under hypoxic conditions are shown in Table 5.3 while the combination index of gemcitabine and paclitaxel in combination with cyclodextrin disulfiram/Cu under hypoxic conditions is shown in Table 5.4. The IC<sub>50</sub> values obtained were higher than those obtained in Table 5.1 showing that the hypoxic patient derived PDAC cells required a higher drug concentration. The data from these experiments reveal that cyclodextrin disulfiram/Cu is more cytotoxic to patient derived PDAC cells when combined with paclitaxel or gemcitabine under hypoxic conditions. It also shows that hypoxic PDAC cells are more resistant to treatment than normoxic PDAC cells.

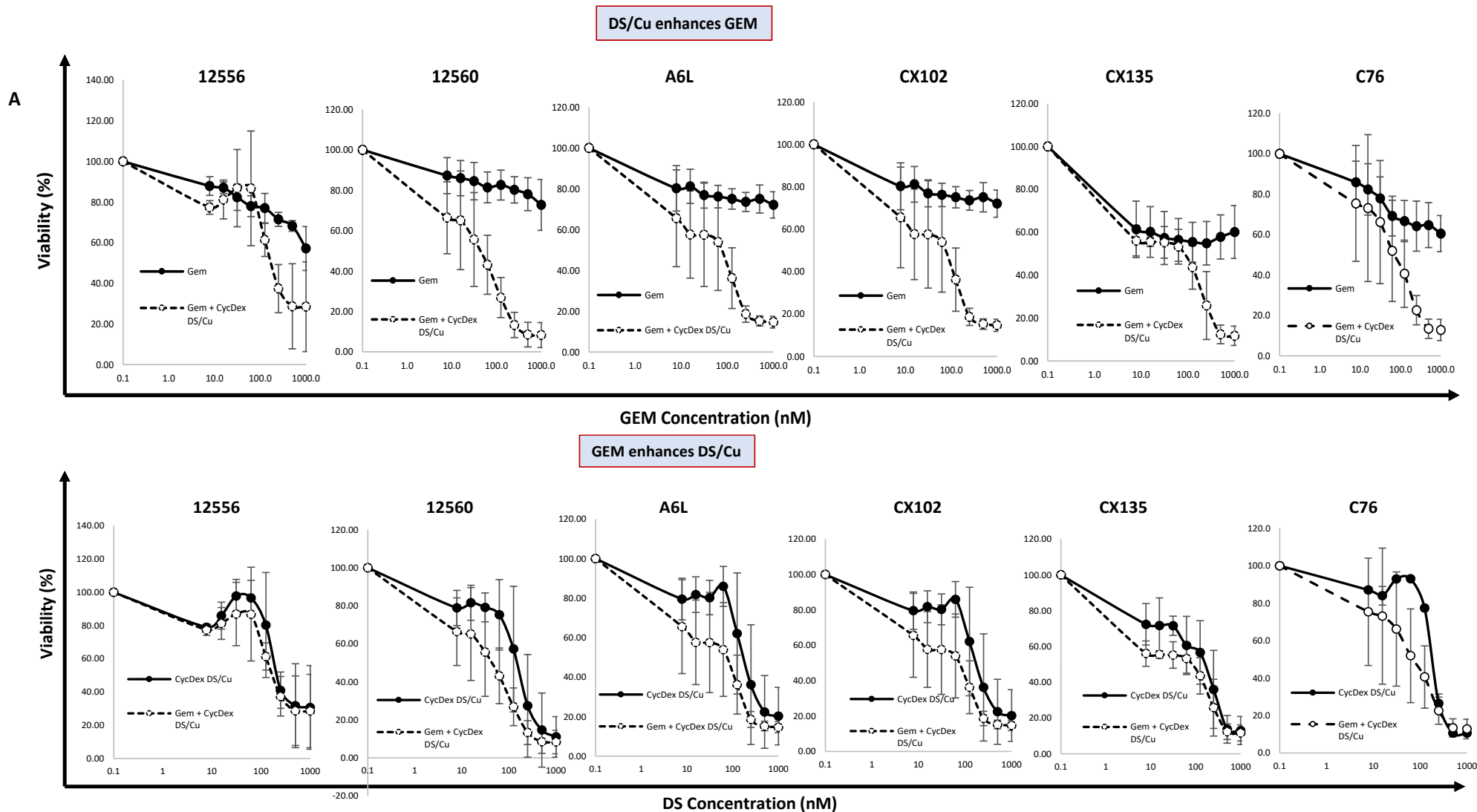
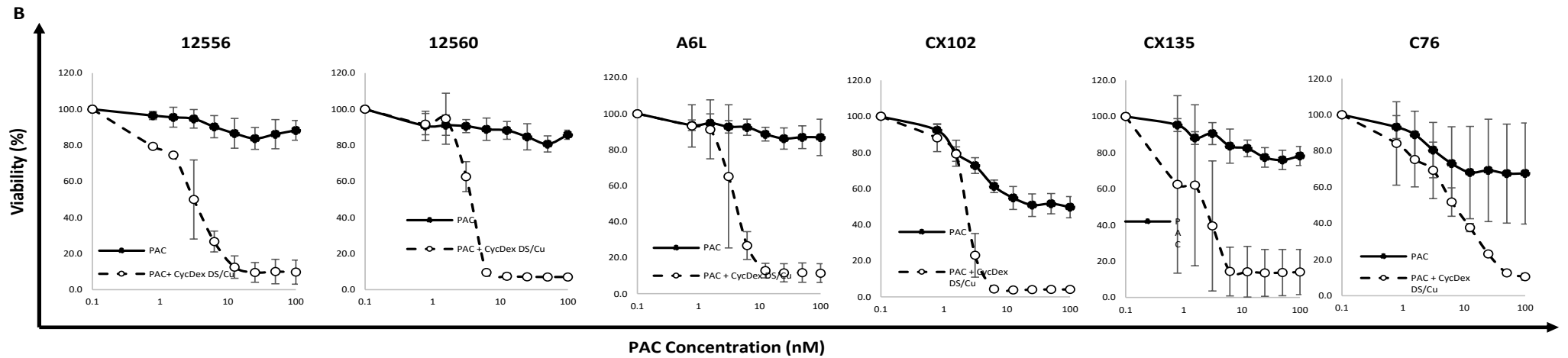


**Figure 5.3 (A)** GEM and CycDex DS/Cu mutually enhance the *in vitro* cytotoxicity in hypoxia cultured PDAC cells. Comparison of the viabilities of patient derived cells when treated with Gemcitabine singly, Gemcitabine + Cyclodextrin disulfiram/Cu, Cyclodextrin disulfiram/Cu singly and Gemcitabine + Cyclodextrin disulfiram/Cu. The combined treatment was more cytotoxic than treating singly with Gemcitabine or Cyclodextrin disulfiram/Cu but did not flatten the curve.

DS/Cu enhances PAC



PAC enhances DS/Cu

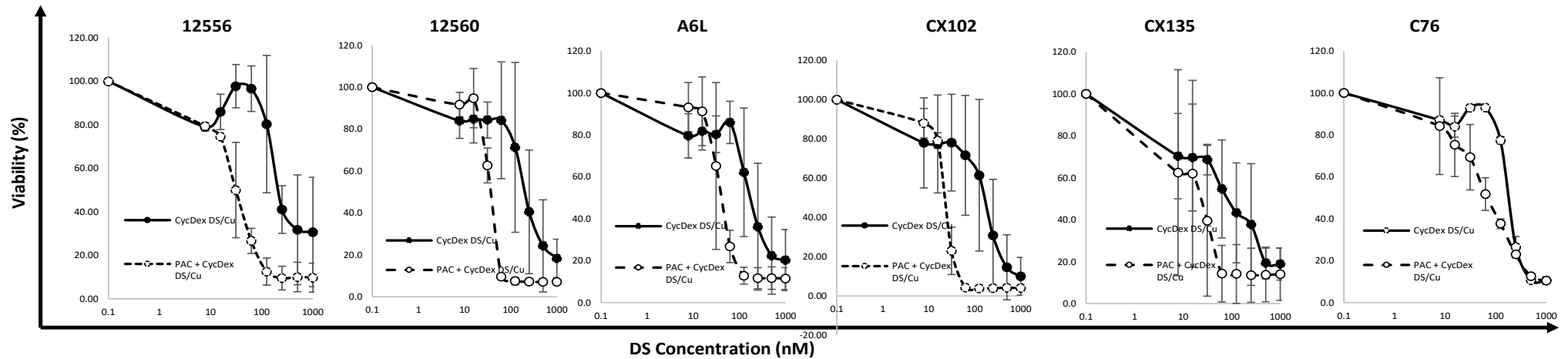


Figure 5.3 (B) PAC and CycDex DS/Cu mutually enhance the *in vitro* cytotoxicity in hypoxia cultured PDAC cells. Comparison of the viabilities of patient derived cells when treated with Paclitaxel singly, paclitaxel + Cyclodextrin disulfiram/Cu, Cyclodextrin disulfiram/Cu singly and Paclitaxel + Cyclodextrin disulfiram/Cu. The combined treatment was more cytotoxic than treating singly with Paclitaxel or cyclodextrin disulfiram/Cu but did not flatten the curve.

**Table 5.3. IC<sub>50s</sub> of drugs singly used and in combination with CycDex DS/Cu in hypoxic PDAC cells**

|                                    | <b>12556</b>            | <b>12560</b>            | <b>CX102</b>           | <b>CX135</b>           | <b>C76</b>               | <b>A6L</b>             |
|------------------------------------|-------------------------|-------------------------|------------------------|------------------------|--------------------------|------------------------|
| <b>CycDex IC<sub>50</sub> (nM)</b> | <b>183.29</b><br>(38.9) | <b>143.6</b><br>(72.7)  | <b>208.8</b><br>(82.0) | <b>23.2</b><br>(6.19)  | <b>195.48</b><br>(10.58) | <b>75.8</b><br>(27.7)  |
| <b>GEM IC<sub>50</sub> (nM)</b>    | <b>&gt;1000</b>         | <b>&gt;1000</b>         | <b>&gt;1000</b>        | <b>&gt;1000</b>        | <b>&gt;1000</b>          | <b>&gt;1000</b>        |
| <b>CycDex DS + GEM</b>             | <b>214.37</b><br>(58.8) | <b>120.35</b><br>(57.1) | <b>115.49</b><br>(6.5) | <b>44.99</b><br>(22.8) | <b>109.41</b><br>(32.7)  | <b>136.3</b><br>(59.5) |
| <b>PAC IC<sub>50</sub> (nM)</b>    | <b>&gt;100</b>          | <b>&gt;100</b>          | <b>&gt;100</b>         | <b>51.7 (6.1)</b>      | <b>&gt;100</b>           | <b>&gt;100</b>         |
| <b>CycDex DS + PAC</b>             | <b>2.67</b><br>(0.56)   | <b>3.40</b><br>(0.37)   | <b>3.15</b><br>(0.69)  | <b>3.41</b><br>(0.57)  | <b>6.61</b><br>(2.07)    | <b>3.59</b><br>(1.3)   |

The PDAC cells were cultured in 1% O<sub>2</sub> condition for 5 days and exposed to anticancer drugs (gemcitabine, paclitaxel) and CycDex DS/Cu singly or a combination of anticancer drugs and CycDex DS/Cu for 72 hours in hypoxia. The IC<sub>50s</sub> of anticancer drugs and CycDex DS/Cu were calculated. n=3; value = IC<sub>50</sub> (± standard deviation).

**Table 5.4. The combination index (CI) of anticancer drugs in combination with CycDex DS/Cu**

| <b>Cells</b> | <b>GEM/DS</b> |             |             | <b>PTX/DS</b> |             |             |
|--------------|---------------|-------------|-------------|---------------|-------------|-------------|
|              | <b>ED50</b>   | <b>ED75</b> | <b>ED90</b> | <b>ED50</b>   | <b>ED75</b> | <b>ED90</b> |
| <b>12556</b> | 0.543         | 0.648       | 0.842       | 0.064         | 0.051       | 0.041       |
| <b>12560</b> | 0.309         | 0.351       | 0.404       | 0.458         | 0.293       | 0.187       |
| <b>A6L</b>   | 0.404         | 0.610       | 0.920       | 0.169         | 0.234       | 0.325       |
| <b>CX102</b> | 0.218         | 0.307       | 0.432       | 0.363         | 0.201       | 0.111       |
| <b>CX135</b> | 0.255         | 0.697       | 1.903       | 0.204         | 0.135       | 0.090       |
| <b>C76</b>   | 0.384         | 0.574       | 0.902       | 0.436         | 0.526       | 0.663       |

CI: 0.9–1.1 additive effect; 0.8–0.9 slight synergism; 0.6–0.8 moderate synergism; 0.4–0.6 synergism; 0.2–0.4 strong synergism.

### **5.3.4 Cyclodextrin Disulfiram/Cu decreased the PDAC CSC population in PDAC hypoxic cultures.**

The aim of this experiment was to confirm if cyclodextrin disulfiram is effective in eliminating PDAC CSC markers. The PDAC cells were cultured under hypoxic conditions with 1% oxygen for 5 days then treated with 250nM of cyclodextrin disulfiram/10 $\mu$ M copper for 16 hours. After which some of the cells were stained with ALDEFLUOR and analysed using flow cytometry. Figure 5.4(A) shows the dot plots of the ALDH<sup>+ve</sup> populations obtained for the various PDAC cells while Figure 5.4(B) is a bar chart showing the percentage ALDH population detected. The hypoxic PDAC cultures had a higher percentage of ALDH which dropped significantly after treatment. Some hypoxic PDAC cells were also stained with PE conjugated anti-CD133 and analysed using flow cytometry. Figure 5.5(A) shows the dot plots of the CD133<sup>+ve</sup> population obtained after flow cytometry analysis while Figure 5.5(B) is a bar chart showing the percentage CD133 population detected. The hypoxic PDAC cultures had a higher percentage of CD133 which dropped significantly after treatment. Another set of hypoxic PDAC cells were stained with APC conjugated with anti-ABCG2 and analysed using flow cytometry. Figure 5.6(A) shows the dot plots of the ABCG2<sup>+ve</sup> population obtained after flow cytometry analysis while Figure 5.6(B) is a bar chart showing the percentage ABCG2 population detected. The hypoxic PDAC cultures had a higher percentage of ABCG2 which dropped significantly after treatment. The data reveals that treatment of PDAC cells with cyclodextrin disulfiram/Cu efficiently reduces the expression of PDAC CSC markers (ALDH, CD133 and ABCG2) so cyclodextrin disulfiram/Cu is cytotoxic to PDAC CSCs.

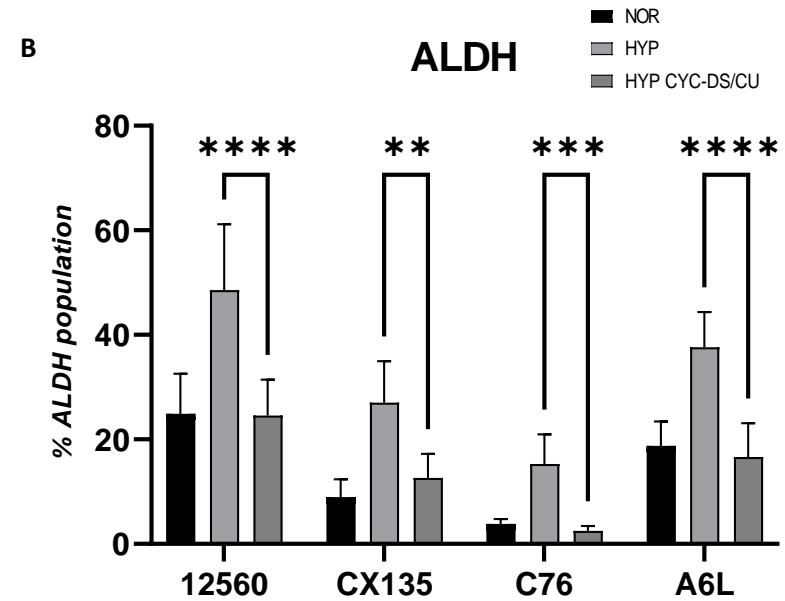
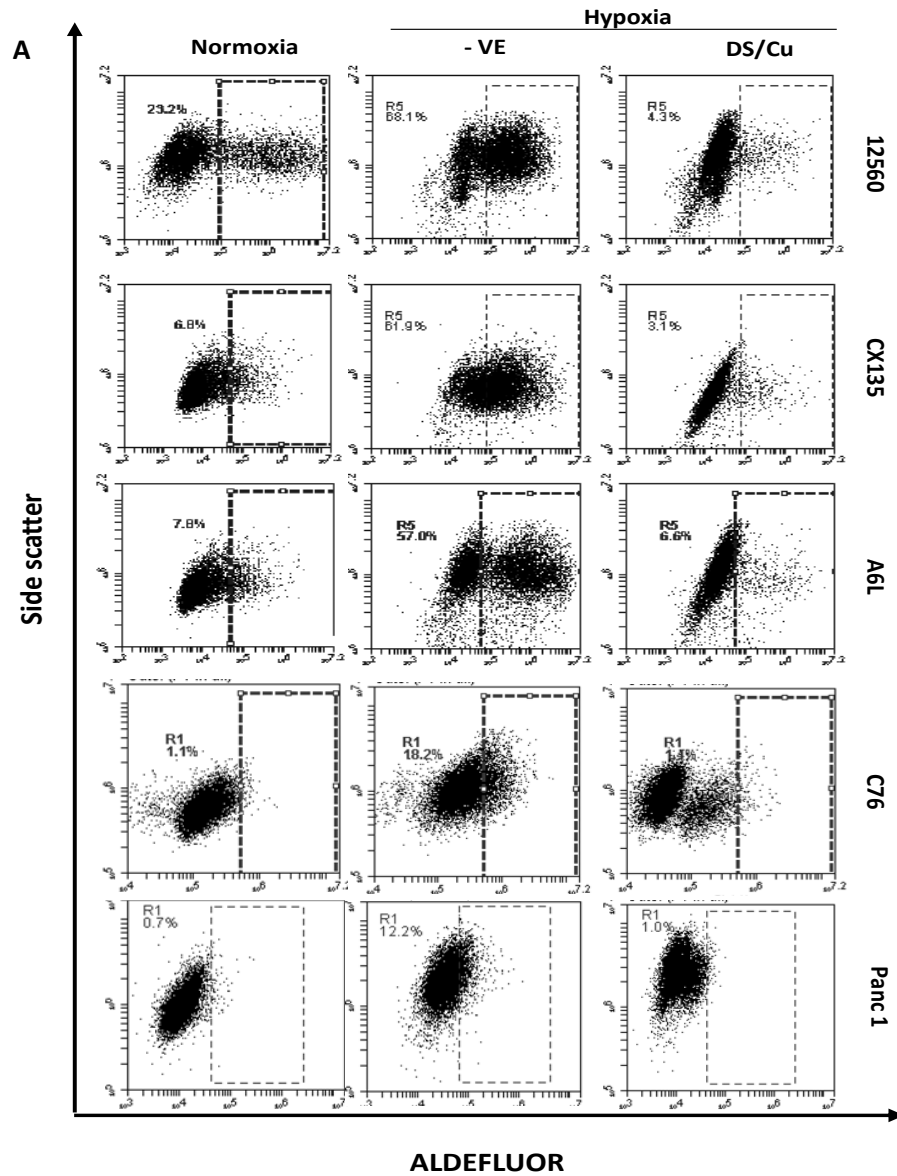


**Figure 5.4. CycDex DS/Cu targets hypoxia-induced ALDH +VE CSC population.** PDAC cells cultured in 1% oxygen for 5 days were treated overnight with 250nM Cyclodextrin disulfiram/10 $\mu$ M Cu then subjected to ALDEFLUOR assay. Flow cytometry was used to analyse the results (A) Dot plots of the ALDH<sup>+ve</sup> PDAC population obtained (B) Bar chart showing the percentage ALDH population before and after treatment. The ALDH population was high in the hypoxic cultures but decreased significantly after treatment with Cyclodextrin disulfiram/Cu. n=5; \*\*p<0.01, \*\*\*p<0.001, \*\*\*\*p<0.0001.



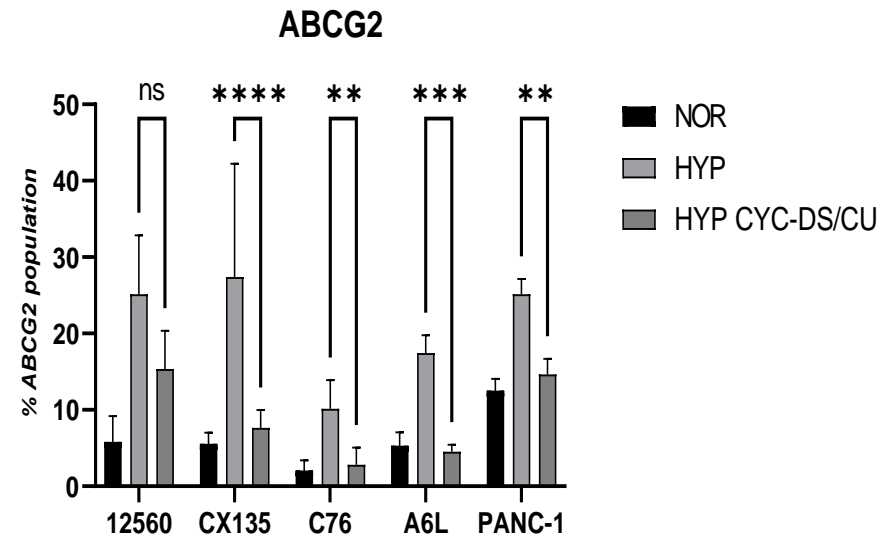
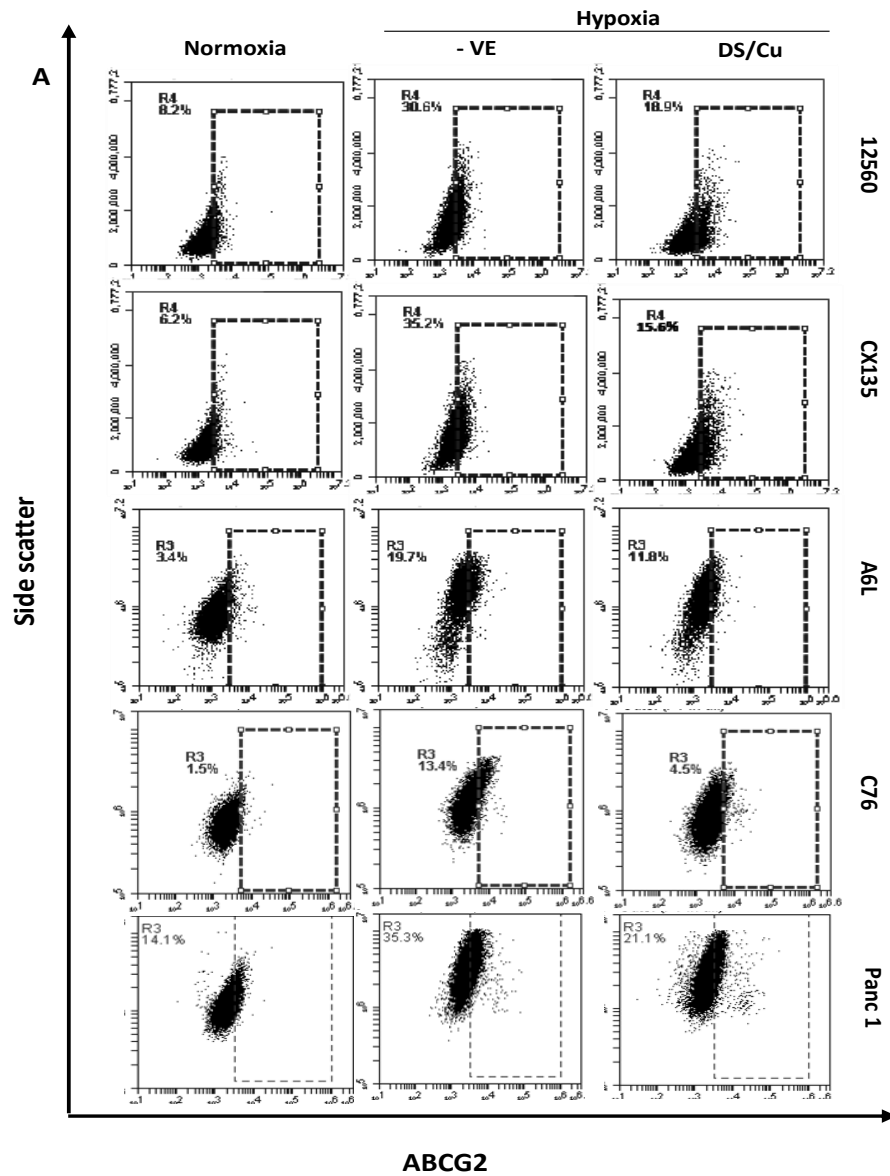


**Figure 5.6. CycDex DS/Cu targets hypoxia-induced ABCG2 +VE CSC population.** PDAC cells cultured in 1% oxygen for 5 days were treated overnight with 250nM Cyclodextrin disulfiram/10 $\mu$ M Cu then subjected to flow cytometry assay. Flow cytometry was used to analyse the results (A) Dot plots of the ABCG2<sup>+ve</sup> PDAC population obtained (B) Bar chart showing the percentage ABCG2 population before and after treatment. The ABCG2 population was high in the hypoxic cultures but decreased significantly after treatment with Cyclodextrin disulfiram/Cu. n=4; ns= not significant, \*\*p<0.01, \*\*\*p<0.001, \*\*\*\*p<0.0001.

### **5.3.5 Cyclodextrin Disulfiram/Cu inhibits the hypoxia induced CSC markers.**

Based on the relevance of CSC markers (Sox2, Nanog and Oct4) in PDAC, real-time PCR was used to analyse the expression of Sox2, Oct4 and Nanog in attached, hypoxic, and hypoxic PDAC cells treated with Cyclodextrin disulfiram/Copper. The patient derived PDAC cells were cultured under hypoxic conditions using serum containing media and kept in a hypoxic incubator for 5 days. Some of the hypoxic PDAC cells were treated with 250nM Cyclodextrin disulfiram/10 $\mu$ M Copper for 16 hours after which the cells were lysed and used for real time PCR analysis. GAPDH was used as the loading control. Figures 5.7 (A), (B) and (C) show the mRNA expressions of Sox2, Nanog and Oct4 in the attached, hypoxic and treated patient derived PDAC cells respectively. The results reveal that the mRNA expression of Sox2, Nanog and Oct4 increased significantly in the hypoxic PDAC cultures but dropped after treatment with Cyclodextrin disulfiram/Copper. The decrease in mRNA expression of Oct4 was significant after treatment with Cyclodextrin disulfiram/Copper. This data confirms that hypoxia promotes PDAC cell stemness and that Cyclodextrin disulfiram/Copper is cytotoxic to PDAC CSCs which corresponds with our previous findings.

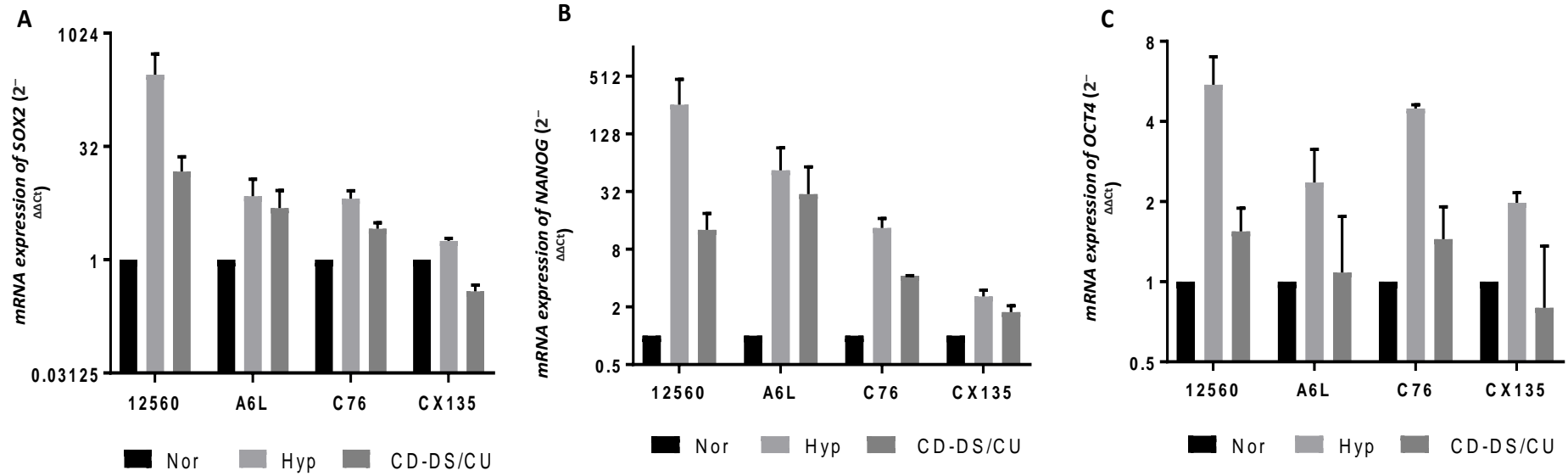


**Figure 5.7. CycDex DS/Cu inhibits the expression of hypoxia-induced CSC markers.** Real-time PCR was used to analyse the mRNA expression of CSC markers (A) Sox2 (B) Nanog, and (C) Oct4 in attached, hypoxic and hypoxic PDAC cell cultures treated with 250nM Cyclodextrin disulfiram/10 $\mu$ M Copper for 16 hours. High levels of Sox2, Oct4 and Nanog were expressed in the hypoxic cultures which dropped after treatment.

### **5.3.6 Cyclodextrin Disulfiram/Cu decreased the CSC population in spheroid cultures of primary PDAC cells.**

The aim of this experiment was to confirm if cyclodextrin disulfiram is effective in eliminating PDAC CSC markers. The PDAC cells were cultured under spheroid conditions with serum free media in flasks coated with poly(2-hydroxyethylmetacrylate) for 5 days then treated with 250nM of cyclodextrin disulfiram/10 $\mu$ M copper for 16 hours. After which some of the cells were stained with ALDEFLUOR and analysed using flow cytometry. Figure 5.8(A) shows the dot plots of the ALDH<sup>+ve</sup> populations obtained for the various PDAC cells while Figure 5.8(B) is a bar chart showing the percentage ALDH population detected. The spheroid PDAC cultures had a higher percentage of ALDH which dropped significantly after treatment. Some spheroid PDAC cells were also stained with PE conjugated anti-CD133 and analysed using flow cytometry. Figure 5.9(A) shows the dot plots of the CD133<sup>+ve</sup> population obtained after flow cytometry analysis while Figure 5.9(B) is a bar chart showing the percentage CD133 population detected. The spheroid PDAC cultures had a higher percentage of CD133 which dropped significantly after treatment. Another set of spheroid PDAC cells were stained with APC conjugated with anti-ABCG2 and analysed using flow cytometry. Figure 5.10(A) shows the dot plots of the ABCG2<sup>+ve</sup> population obtained after flow cytometry analysis while Figure 5.10(B) is a bar chart showing the percentage ABCG2 population detected. The spheroid PDAC cultures had a higher percentage of ABCG2 which dropped significantly after treatment. The data reveals that treatment of spheroid PDAC cells with cyclodextrin disulfiram/Cu efficiently reduces the expression of PDAC CSC markers (ALDH, CD133 and ABCG2) so cyclodextrin disulfiram/Cu is cytotoxic to PDAC CSCs.

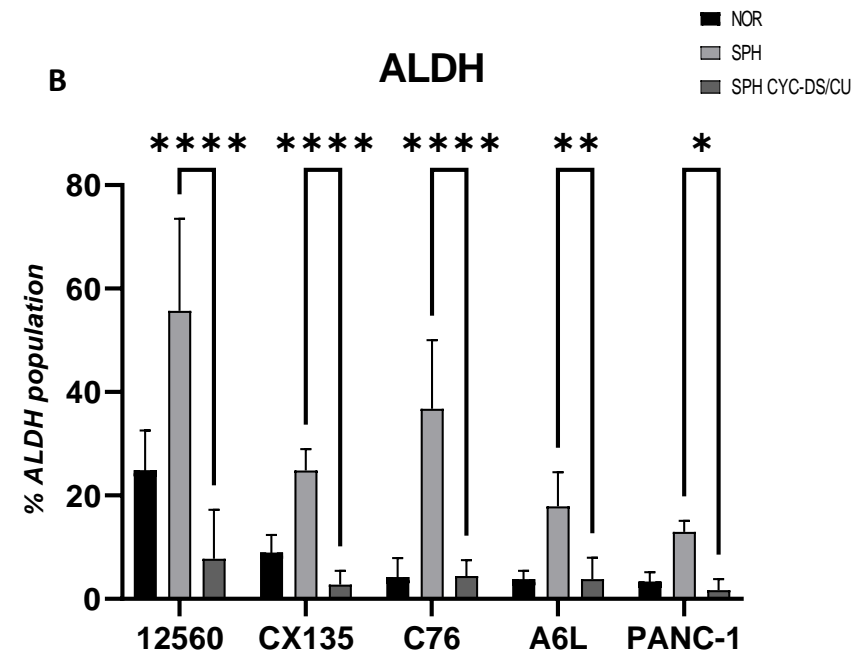
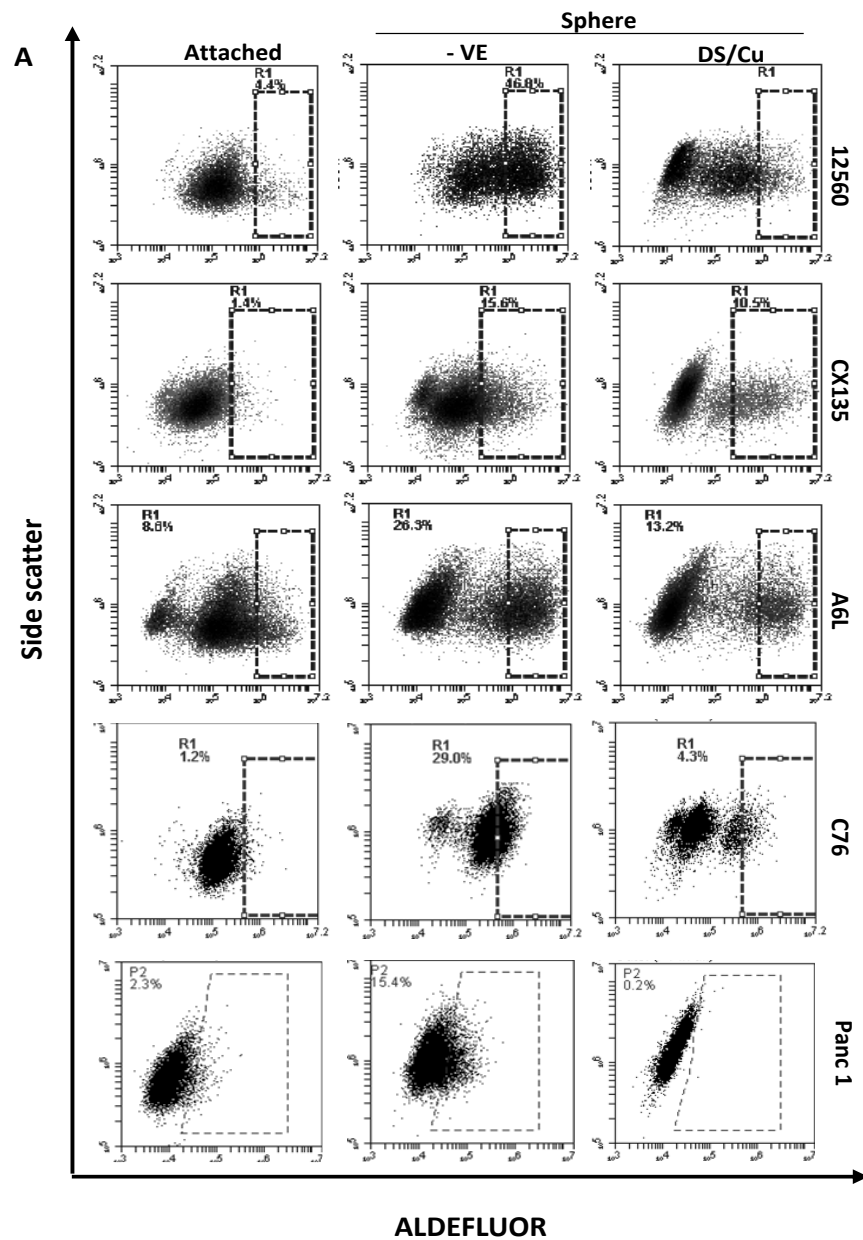


**Figure 5.8. CycDex DS/Cu targets ALDH +VE CSC population in spheroid cultures of PDAC cells.** PDAC cells cultured under spheroid conditions with serum-free media for 5 days were treated overnight with 250nM Cyclodextrin disulfiram/10 $\mu$ M Cu then subjected to ALDEFLUOR assay. Flow cytometry was used to analyse the results (A) Dot plots of the ALDH<sup>+</sup>ve PDAC population obtained (B) Bar chart showing the percentage ALDH population before and after treatment. The ALDH population was high in the hypoxic cultures but decreased significantly after treatment with Cyclodextrin disulfiram/Cu. n=5; \* $p$ <0.05, \*\* $p$ <0.01, \*\*\* $p$ <0.0001.

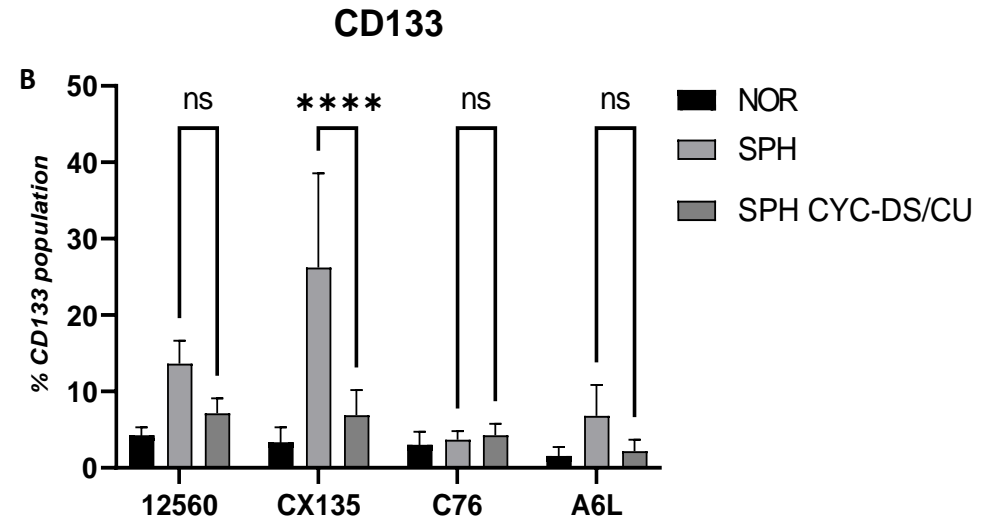
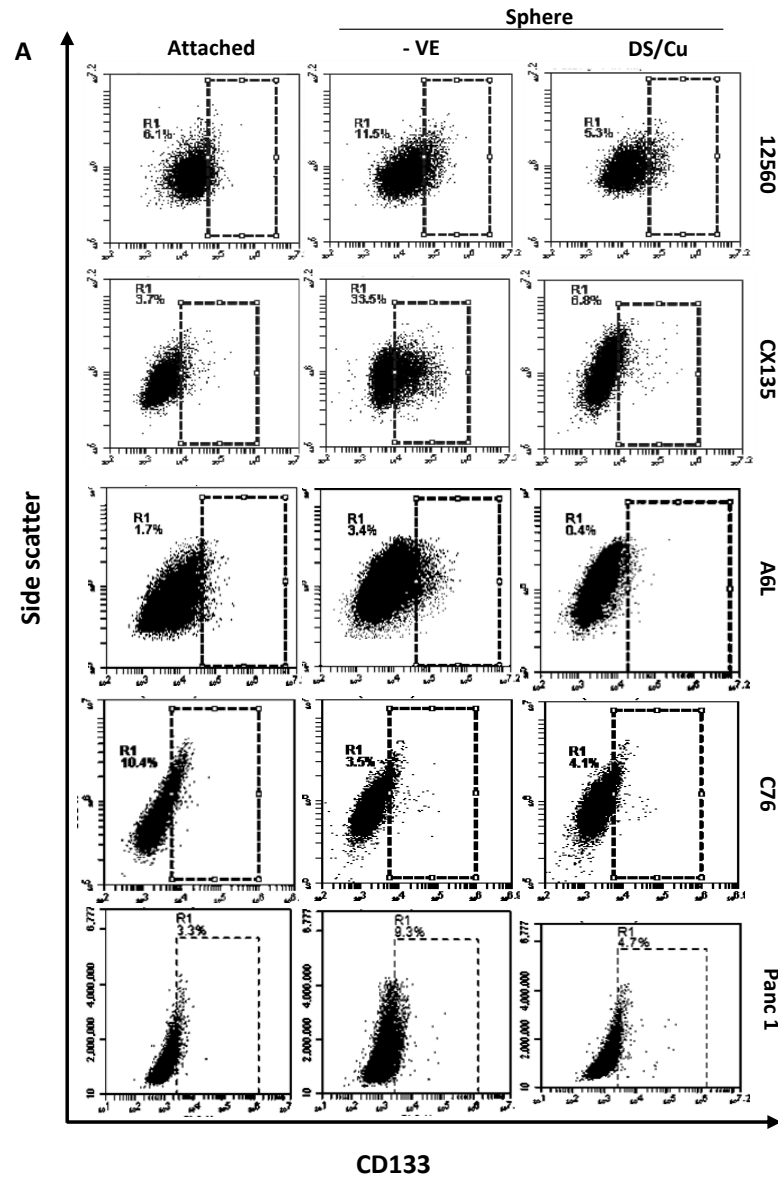


**Figure 5.9. CycDex DS/Cu targets CD133 +VE CSC population in spheroid cultures of PDAC cells.** PDAC cells cultured under spheroid conditions with serum-free media for 5 days were treated overnight with 250nM Cyclodextrin disulfiram/10µM Cu then stained with PE conjugated anti-CD133. Flow cytometry was used to analyse the results (A) Dot plots of the CD133<sup>+</sup> PDAC population obtained (B) Bar chart showing the percentage CD133 population before and after treatment. The CD133 population was high in the spheroid cultures but decreased significantly after treatment with Cyclodextrin disulfiram/Cu. n=4; \*\*\*\*p<0.0001, ns=not significant.

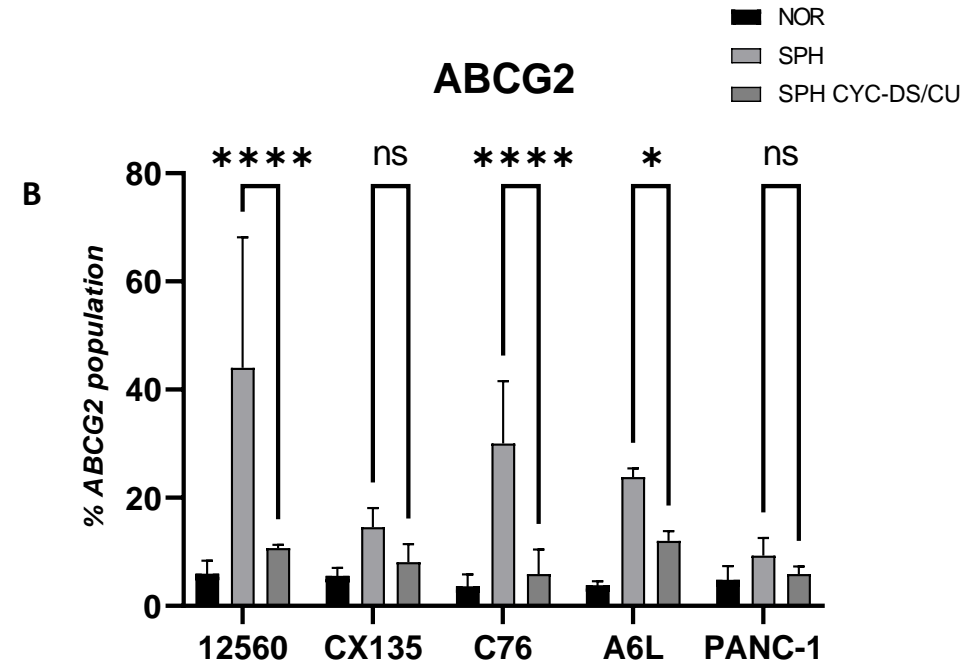
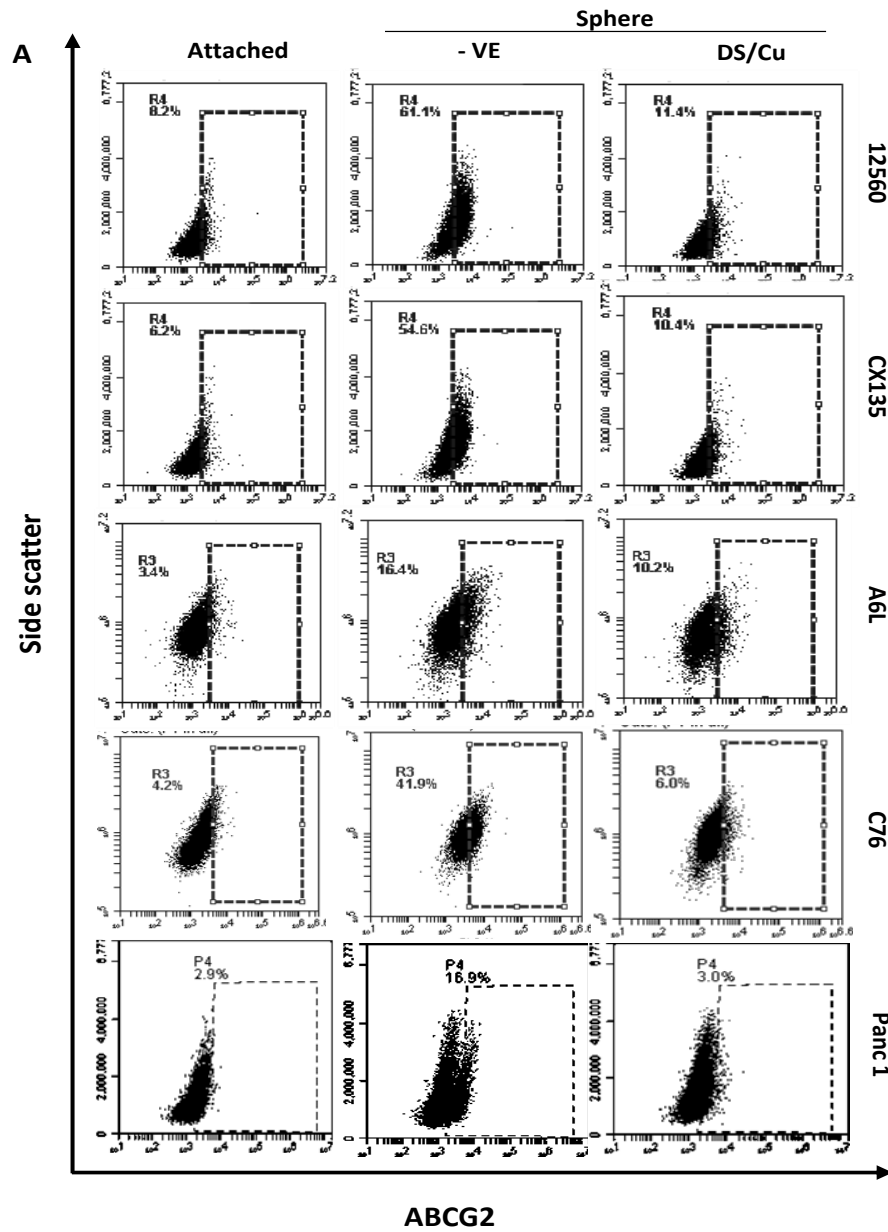


**Figure 5.10. CycDex DS/Cu targets ABCG2 +VE CSC population in spheroid cultures.** PDAC spheroid cells were treated overnight with 250nM Cyclodextrin disulfiram/10µM Cu then subjected to flow cytometry assay. Flow cytometry was used to analyse the results (A) Dot plots of the ABCG2<sup>+</sup> PDAC population obtained (B) Bar chart showing the percentage ABCG2 population before and after treatment. The ABCG2 population was high in the spheroid cultures but decreased significantly after treatment with Cyclodextrin disulfiram/Cu. n=4; ns= not significant, \*p<0.05, \*\*\*\*p<0.0001.

### **5.3.7 Cyclodextrin Disulfiram/Cu inhibited the sphere reformation ability of CSC population in spheroid cultures of primary PDAC cells.**

It is widely believed that the spheres in spheroid cultures are formed from the cancer stem cells in the culture. Sphere reformation assay was used to test the effectiveness of Disulfiram and Cyclodextrin disulfiram in eliminating cancer stem cells from PDAC cell line and primary, circulating and liver metastatic patient derived PDAC cells. First, spheroid PDAC cells were cultured using serum-free media and flasks coated with poly(2-hydroxyethylmetacrylate). After 5 days, the spheroid cells were treated overnight then the drug was rinsed off and the spheres were reseeded at low density into 24-well plates using drug-free media. The images taken after the sphere reformation assay at  $\times 10$  magnification are shown in Figure 5.11 (A). For each of the PDAC cells, the control samples had well defined spheres while the PDAC spheroid cultures treated with copper alone had spheres that were bigger in size and more clumped together than the control. Surprisingly, all the spheres treated with Disulfiram/Cu and Cyclodextrin disulfiram/Cu were completely dissociated. Figure 5.11 (B) shows a bar chart of the average sphere count after sphere reformation for the different PDAC cells. The data reveals that Disulfiram and Cyclodextrin disulfiram effectively eliminates CSC PDAC populations.

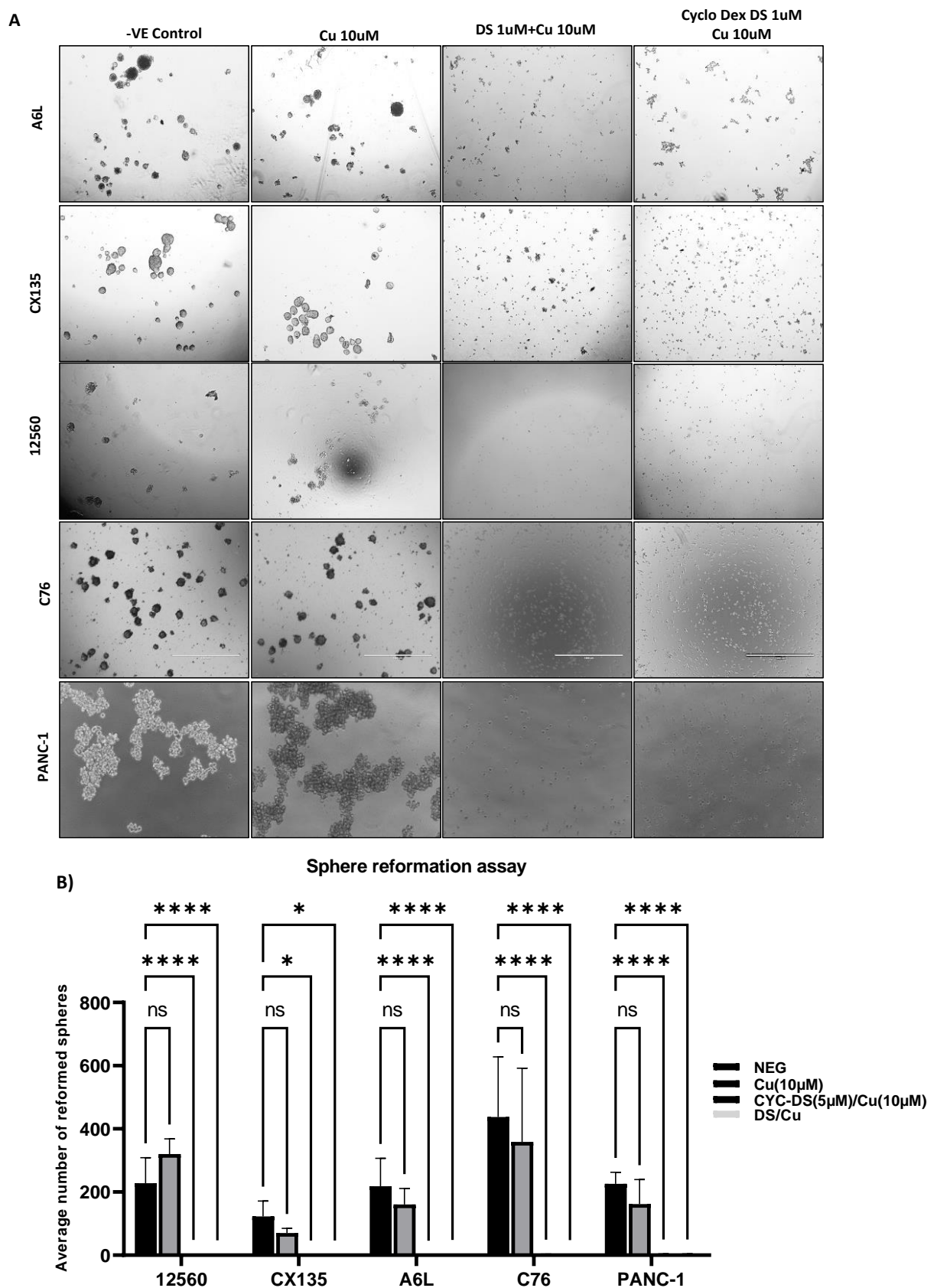


**Figure 5.11. CycDex DS/Cu inhibited the sphere reformation ability of CSC populations in spheroid cultures of PDAC cells. (A) Microscopic images depicting sphere reformation assay for PDAC spheroid cells treated with 10µM Copper, 1µM Disulfiram/10µM Copper, and 1µM Cyclodextrin Disulfiram/10µM (B) Bar chart showing sphere count after sphere reformation assay for each of the PDAC cells. Images were taken 5 days after cell culture ( $\times 10$  magnification).  $n=6$ , \*\*\*\* $p<0.0001$**

## 5.4 Discussion

This study was targeted at investigating the effectiveness of cyclodextrin disulfiram in eliminating cancer stem cells in normoxic, hypoxic and spheroid patient derived PDAC cultures. The potency of disulfiram in eliminating cancer cells has made it to be of interest to many researchers.

Tumours are solid in nature and this enables cancer cells to grow in a 3D conformation and have a hypoxic core. The inability of mono-layer cultures to correctly mimic *in vivo* cellular interactions has led to many false and unsuccessful research results. As a result, many researchers are now focused on using 3D cultures for cancer research. The most popular 3D cell culture method is the spheroid model developed 40 years ago where cells grow as well-defined spheres. These spheres imitate the preliminary stages of a tumour before blood vessel formation. However, some PDAC cells like MiaPaca-2 form unstable spheroids that are hard to use for further experiments (Cavo et al., 2020). PDAC cells grow in a 3-dimensional conformation within the pancreatic tumour. Therefore, PDAC cells cultured as spheroids are more similar to real PDAC cells than monolayer cultures. This is because PDAC cells cultured as spheroids have more matrices and express more chemoresistant genes than monolayered cultures (Bulle and Lim, 2020). The high rate of PDAC growth increases the demand for oxygen leading to poor vascularisation and intratumoral hypoxia. In response to hypoxia, cancerous cells undergo an angiogenic switch which enables them grow blood vessels to increase blood and oxygen supply (Yuen and Diaz, 2014). Unlike other solid tumours, PDAC tumour microenvironment is characterised by a desmoplastic stroma consisting of activated fibroblasts, leukocytes and extracellular matrix. The desmoplastic stroma has more stiffness, elevated hyaluronic acid content and more hydrostatic pressure leading to intratumoral hypoperfusion and hypoxia (Xiao et al., 2020). Hypoxia activates transcription factors that change cell polarity, cell-cell junction, cell cytoskeleton causing epithelial cells to become

motile and invasive (Yuen and Diaz, 2014). In this study, it was observed that the patient derived PDAC cell 12560 also formed unstable spheroids. The data also revealed that cyclodextrin disulfiram with copper is a strong initiator of apoptosis and completely dissociated PDAC spheroid cells.

Copper is mainly absorbed from food in the stomach and intestine then transported to the liver by albumin, and to peripheral tissues by ceruloplasmin and albumin. In cells, copper (II) is reduced to copper (I) ion. These copper ions bind with DDT after disulfiram administration. A study showed that 5ug/L of DDT-Cu suppressed the growth of Panc-1 cells in vitro. Apoptosis was shown to occur regularly in pancreatic cancer tissue xenografts treated with DDT-Cu. Analysis on the brain, liver and kidney of mice with pancreatic cancer showed that they have higher levels of copper ions than control groups (Han et al., 2013). The data from this Chapter shows that Cyclodextrin disulfiram/Cu has a strong apoptotic effect on PDAC cells compared to gemcitabine and paclitaxel. Cancerous cells evade apoptosis using different mechanisms. Members of the IAP family such as Survivin and cIAP2 prevent apoptosis by inhibiting caspase activity. There is an upregulation of cIAP2 in 85% of PDAC. This explains why PDAC is resistant to first line anticancer drugs like paclitaxel and gemcitabine (Hamacher et al., 2008). The high apoptotic activity of cyclodextrin disulfiram is suspected to be linked to disulfiram's ability to simultaneously use multiple modes of action to eliminate CSCs. Disulfiram also forms very strong bonds with copper so probably releases a higher level of ROS than other drugs in the process.

Tumours are composed of a small sub-population of cells known as cancer stem cells which are capable of promoting tumour progression. The major challenge in cancer treatment is chemoresistance hence the need to understand the mechanism of CSC occurrence and develop more effective drugs (Zhou et al., 2017). CSCs play significant roles on tumour progression and chemoresistance due to their self-renewal and tumour initiating abilities. CSCs can be

accurately analysed using different cell surface markers because of its similar surface markers with normal stem cells. OCT4, SOX2 and NANOG are transcription factors which serve as CSC markers because of their ability to help cells retain their CSC characteristics (Zhou et al., 2021). PDAC has a heterogenous cell population which comprises of CSCs that induce chemoresistance. A good understanding of the CSCs could provide good insights for potential drug development. Three-dimensional spheroid cultures and cell surface markers were used to characterize PDAC CSCs (Valle et al., 2020). Chemoradiated PDAC cell lines treated with disulfiram/Cu has decreased expression of ALDH<sup>bright</sup> PCSCs and CD133 positive PCSCs (Cong et al., 2017). Hypoxia plays a significant role in the aberrant growth of PDAC which causes the development of immature and leaky blood vessels that lead to metastasis (Maftouh et al., 2014; Koong et al., 2000; Harris, 2002; Chang et al., 2011).

There is an urgent need for novel anticancer drugs to improve the overall survival of pancreatic cancer patients. The concentration of the active form of gemcitabine in the pancreatic tumour is decreased by components of the stroma such as metabolic enzymes and gemcitabine transporters. The Human equilibrative nucleoside transporter responsible for transporting gemcitabine into tumour cells is inhibited by EMT (Liang et al., 2017).

Some studies have shown that gemcitabine has the ability to enhance stemness, enhance sphere formation and increase the expression of CSC markers through an unknown mechanism in pancreatic cancer cells. This explains why patients gradually develop resistance to gemcitabine (Zhou et al., 2018). When tumour cells acquire resistance to one drug, it could lead to cross resistance to multiple drugs (Zhou et al., 2021). The transporter responsible for transporting dFdC into cells is human equilibrative nucleoside transporter-1 (hENT1) (Kurata et al., 2011). In numerous cancers, disulfiram has been shown to have a synergistic effect on different anticancer drugs (Yoshino et al., 2020). Disulfiram has been proven to be highly cytotoxic to panc-1 cells (Dastjerdi et al., 2014). When breast cancer cells, melanoma and thymocytes are

exposed to DSF/Cu, it causes elevated ROS levels which leads to apoptosis. Treatment of malignant pleural mesothelioma with DSF/Cu leads to decreased expressions of many genes involved in tumour proliferation and increased expression of pro-apoptotic genes (Cheriyana et al., 2014).

This data shows that cyclodextrin disulfiram reduced the expression of cancer stem cell markers in hypoxic PDAC cultures. The findings reveal that cyclodextrin disulfiram also enhances the cytotoxicity of the first line anticancer drugs; gemcitabine and paclitaxel. These first line drugs also have a synergistic effect on the cytotoxicity of cyclodextrin disulfiram. Despite the increased efficacy of combining Cyclodextrin disulfiram/Cu with gemcitabine or paclitaxel in eliminating PDAC cells, there was reduced efficacy when the PDAC cells were cultured under hypoxic conditions. This confirms that hypoxia plays a role in promoting chemoresistance in PDAC.

## **CHAPTER 6**

# **INVESTIGATION OF THE MOLECULAR EFFECT OF NF $\kappa$ B PATHWAY ON STEMNESS AND CHEMORESISTANCE IN PANCREATIC DUCTAL ADENOCARCINOMA**

## 6.1 INTRODUCTION

Nuclear factor- $\kappa$ B is a transcription factor usually activated by cellular stress (Xu et al., 2017). Nuclear factor kappa light chain enhancer of activated B cells (NF $\kappa$ B) was identified in the 1980s by Sen and Baltimore, and has numerous functions. The most common NF $\kappa$ B subunits are p65 (RelA gene) and p50 (NF $\kappa$ B1 gene). It is speculated that p65/p50 heterodimers initiate active transcription while p50/p50 homodimers suppress transcription (Nennig and Schank, 2016). The NF $\kappa$ B pathway occurs canonically and non-canonically (Kabacaoglu et al., 2019). In the canonical pathway, IKK kinase complex inhibits NF $\kappa$ B in the cytoplasm by binding to it. The IKK kinase complex has two catalytic subunits; IKK $\alpha$  and IKK $\beta$  and a regulatory subunit called NEMO (IKK $\gamma$ ). The activation of IKK causes it to phosphorylate IKK $\beta$ , whose degradation releases NF $\kappa$ B (Nennig and Schank, 2016). At this point, the RelA/p50, RelA/c-Rel and c-Rel/p50 translocate to the nucleus to initiate the transcription of many genes. Unlike the canonical pathway which is rapid and lasts for a short time, the non-canonical pathway is slow and lasts for a prolonged period. The mechanism of action of NF $\kappa$ B is still not fully understood (Kabacaoglu et al., 2019).

NF $\kappa$ B has been linked to many ailments such as cancer, diabetes, autoimmune diseases, cardiovascular diseases and neurodegenerative diseases. NF $\kappa$ B plays critical roles in apoptosis, tumour microenvironment, cell invasion, metastasis, angiogenesis, inflammation, immune modulation, CSC survival and tumour progression. NF $\kappa$ B increases the expression of SOX9 which enhances invasion in pancreatic cancer. NF $\kappa$ B also induces gemcitabine resistance using different mechanisms. In pancreatic cancer, NF $\kappa$ B signalling is driven by KRAS and this signalling can be blocked by aspirin, curcumin and cyclooxygenase inhibitors (Pramanik et al., 2018). NF $\kappa$ B increases the expression of Snail1 which in turn inhibits the expression of adherens junction proteins (Li et al., 2018).

NFκB is one of the main causes of chemoresistance and it also plays a big role in stopping apoptosis in cancer cells. High levels of NFκB has been detected in cancer cells and these levels can be further elevated by some anticancer drugs. The activation of NFκB has been shown to increase the expression of anti-apoptotic proteins. Reactive oxygen species (ROS) are produced by mitochondrial respiratory chain reaction. In high levels, ROS can cause damage to protein membranes, DNA and lipid membranes leading to apoptosis. However unlike normal cells, cancer cells produce high levels of ROS and are able to tolerate it and resist apoptosis. Further increasing the ROS content of cancer cells by ROS generating agents can deplete the antioxidant content of cancer cells then induce apoptosis. ROS induced apoptosis depends greatly on the activation of the pro-apoptotic MAPK pathway (Yip et al., 2011).

There are 2 classes of CRISPR-Cas systems. The class 2 CRISPR-Cas system has different types such as type II, V and VI. The type II and V are used for editing DNA while the type VI is used for editing RNA. DNA rewriting can be applied in biotechnology, therapeutics and diagnostics. Type II-A has RNase III genes for maturation of pre-crRNA. Type II-B and type II-C need tracrRNA for target recognition like Type II-A. Type V which is represented by Cas12a has 12 subtypes. Cas12a has RNA editing activity and converts pre-crRNA to mature crRNA. In the presence of DSBs, DNA repairing mechanisms are triggered to fix what they perceive as damage. DNA sequences can be modified by insertions, deletions, sequence substitution and integration (Moon et al., 2019).

CRISPR requires mature CrRNA and trans-activating RNA (tracrRNA) which form the Cas9 protein-RNA complex that create DSBs at target sites. Single guide RNA (sgRNA) is formed by the merging of CrRNA and tracrRNA. The CRISPR system has 2 classes namely: Class 1 and Class 2. The Class one is divided into types I and III while the Class 2 is divided into types II, IV, V and VI. Smaller Cas9 variants have a better packaging and delivery capacity which improves their therapeutic potential. Unfortunately, the small Cas9 variants need more complex

PAM sequences and possess a relatively limited targeting scope and limited flexibility in genome targeting. There have been many evolutions in CRISPR technology such as the use of nickase Cas9 to accurately convert one base to another without the introduction of DSBs. Nickase Cas9 can combine with APOBEC1 deaminase enzyme and Uracil Glycosylase inhibitor (UGI) protein to form a complex which accurately converts cytosine to thymine without introducing DSBs. In the same way, a transfer RNA adenosine deaminase can fuse to nickase Cas9 to form a complex that accurately converts adenine to guanine (Adli, 2018). Dual guide RNA (dgRNA) is formed by the annealing of CrRNA and tracrRNA (Scott et al., 2019). CRISPR can be used to regulate gene expression, epigenome editing, life cell chromatin imaging, genetic and epigenetic screening and manipulation of chromatin topology (Adli, 2018). CRISPR is used for target validation, functional gene screening, gene diagnosis and generation of cancer models (Zhan et al., 2019). CRISPR has revolutionised cancer immunotherapy which is the best strategy so far for cancer management. CRISPR utilizes single-guide RNA (sgRNA) for recognizing specific DNA binding sites. These sgRNA guides DNA endonuclease Cas9 to target and cut the complementary loci of double stranded DNA. The setback of CRISPR is being able to get the best nuclease and design the perfect sgRNA, therapeutic threshold of edited cells, efficient delivery of gene editing tools into target cells, reducing off target effects and effective genome editing (Xia et al., 2018).

CRISPR-Cas9 (*clustered regularly interspaced short palindromic repeats*-CRISPR associated nuclease 9) is a tool for editing the genome or studying genetic alterations in cell culture models, organisms and humans (Xue et al., 2016). In 1987, CRISPR was discovered in *E. coli* by Nakarta and his colleagues (Xia et al., 2018; Zhan et al., 2019). However, it was not until 2005 that scientists were able to link it with the bacteria immune system. Type II CRISPR systems depend on a Cas protein to target a specific DNA sequence making it the perfect genome editing tool (Zhan et al., 2019). Hematopoietic growth factors are secreted by

pancreatic cancer cells. Scientists are working on using enzymes such as alcohol dehydrogenase (ADH), cathepsin D and lysosomal exoglycosidase as biomarkers for pancreatic cancer. However, the studies have not been validated. K-ras mutations are important biomarkers of pancreatic cancer. These K-Ras mutations occur in 47-100% of PDAC cells and can be detected by PCR (Jelski and Mroczko, 2019).

## **6.2 Methods**

### **6.2.1 Cell culture**

Panc-1 cells were cultured in RPMI 1640 media supplemented with 100 U/ml penicillin and 100 µg/ml streptomycin, 5% L-glutamine and 10% FBS in a humidified atmosphere at 37<sup>0</sup>C with 5% CO<sub>2</sub> and passaged every 3 days.

### **6.2.2 Stable Transfection**

Transfection was carried out using lipofectamine 3000 reagent and pcDNA 3.1 plasmid using the manufacturer's instruction. Overnight cultures of panc1 cells seeded ( $3 \times 10^5$  cells/well) in a 6-well plate were transfected with p65 overexpression. The cells were transfected then selected using 200µg of hygromycin. The transfected cells were seeded in petri dishes, from which the clones were picked, expanded then screened using western blot and PCR.

### **6.2.3 CRISPR p65 Knockout**

NFκB p65 was knocked out using the CRISPR/Cas9 system. Preliminary studies were carried out to determine the most suitable antibiotic dose for the study. Six well plates previously seeded with 300,000 panc-1 cells per well were transfected as described in the CRISPR knockout protocol then selected with 500ng of puromycin. The transformed clones were picked then transferred to 24-well plates. The colonies were expanded and screened using Western Blot and PCR. The clones without any NFκB p65 expression were the knockout clones.

#### **6.2.4 Real-time PCR**

Total RNA was extracted from both normoxic and hypoxic Panc-1 cell cultures using the mRNA extraction kit (Qiagen) following the manufacturer's instruction then reverse transcribed to give cDNA. This cDNA was subjected to real-time PCR using primers of specific interest and the fold change was calculated.

#### **6.2.5 Western Blot**

Western Blot was used to detect protein expression, using the expression of beta actin as a loading control. Cell pellets were lysed on ice using RIPA Buffer supplemented with protease and phosphatase inhibitors then sonicated and centrifuged at 14,000rpm, 4<sup>0</sup>C for 20 minutes. The protein concentration of the supernatant was determined. Equal quantities of the protein were separated using 12% acrylamide gels. The gel was blotted using PVDF membrane which was later blocked using 5% low fat milk in Tris-Buffered Saline with 1% Tween. The membrane was later incubated in primary antibody overnight then secondary antibody for one hour. Bands were detected using Odyssey Fc Imaging System (LI-COR Biosciences; USA) and chemiluminescent reagents.

#### **6.2.6 MTT Cell Viability assay**

Cells were seeded in a 96 well plate (5000 cells/well). Cytotoxicity assay was carried out using MTT reagent after treating the cells with anticancer drugs for 48 hours. Then dissolving the formazan crystals with dimethyl sulfoxide and taking the absorbance at 540nm with a spectrophotometer.

## 6.3 Results

### 6.3.1 Spheroid and hypoxic cultures of PDAC cells have high expression of NFκB

Spheroid PDAC cells were cultured using serum free media and flasks coated with poly(2-hydroxyethylmetacrylate). Then, real-time PCR was used to measure the mRNA expression of NFκB/p65 in normoxic and spheroid Panc-1 PDAC cell line and patient derived PDAC cells. GAPDH was used as a loading control. A bar chart showing the mRNA expressions obtained is shown in Figure 6.1(A). All the PDAC cells had a significantly elevated mRNA expression of p65 in their spheroid cultures. To further confirm the expression of p65, Western Blot was used to analyse the protein expression of NFκB/p65 and IκB in the normoxic and spheroid cultures of all the PDAC cells using beta actin as the loading control as shown in Figure 6.1(B). The results revealed that all the spheroid PDAC cells had an increased protein expression of p65 and a decreased protein expression of IκB compared to the normoxic cultures. Hypoxic PDAC cells were cultured with 1% oxygen for 5 days and used for real-time PCR analysis. Figure 6.1(C) is a bar chart showing the mRNA expression of p65 in the normoxic and hypoxic PDAC cells. There was a significant increase in the mRNA expression of p65 in all the hypoxic cultures except for Panc-1 and C76. In Figure 6.1(A), the Western Blot images show an increased protein expression of p65 and a decreased protein expression of IκB in the hypoxic cultures compared to the normoxic PDAC cultures. These data reveal that hypoxic and spheroid conditions upregulate NFκB/p65 expression in PDAC.

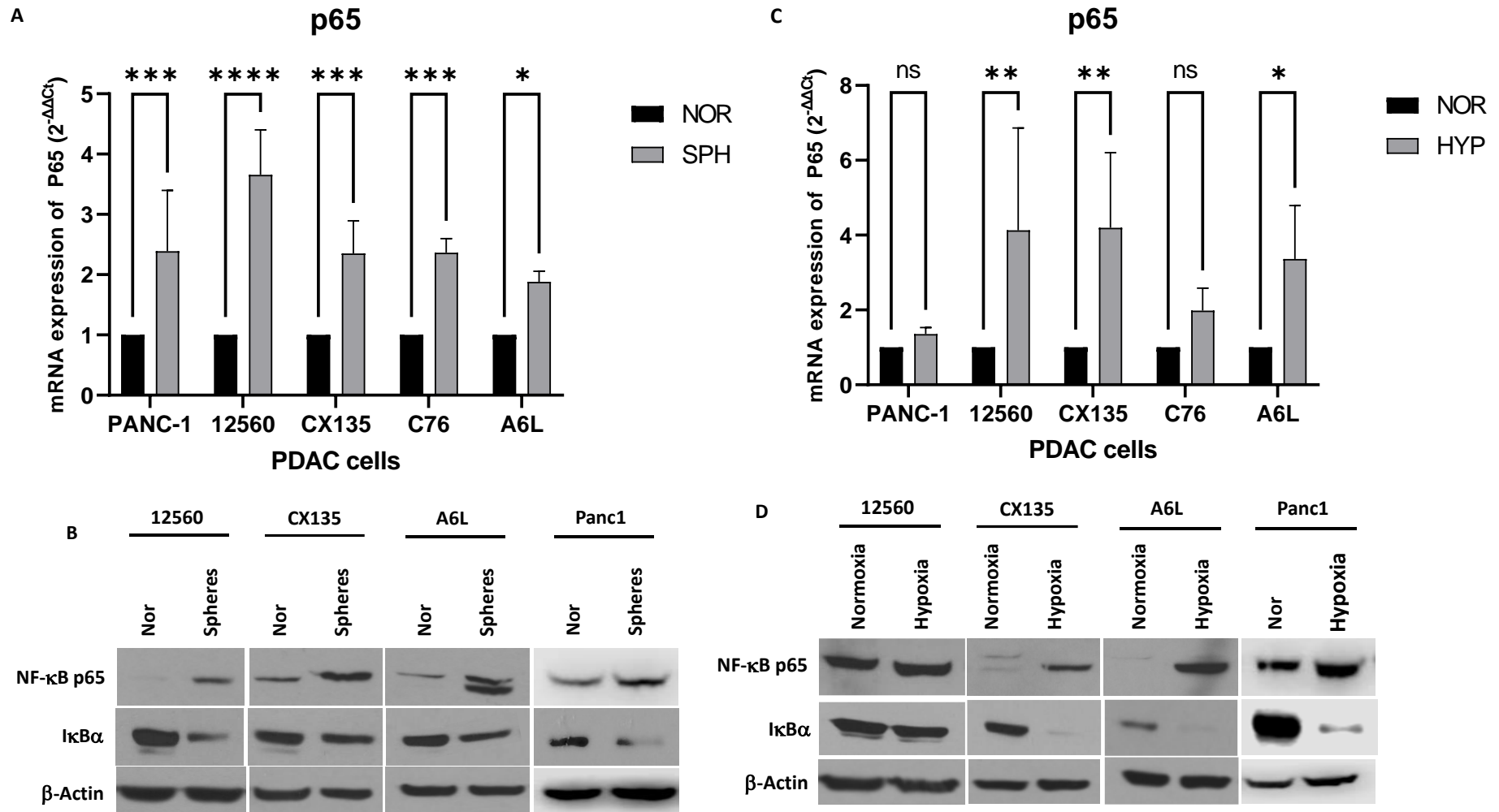


**Figure 6.1: Protein expression of P65 in spheroids and hypoxia cultured PDAC cells.** (A) Bar chart showing mRNA expression of NFκB/p65 in normoxic and spheroid PDAC cells. The error bars represent the standard deviation. (B) Western blot analysis showing increased expression of p65 protein and decreased IκB protein in the spheroid PDAC cultures. 30μg of protein/lane. Beta actin was used as a loading control. (C) Bar chart showing mRNA expression of NFκB/p65 in normoxic and hypoxic PDAC cells (D) Western Blot analysis showing increased expression of p65 protein and decreased IκB protein in the hypoxic PDAC cultures. \* $p < 0.05$ , \*\*\*\* $p < 0.0001$

### 6.3.2 Ectopic overexpression of NFκB in Panc1 PDAC cells

In an effort to further study the activity of NFκB in PDAC cells, some panc-1 cells were transfected with p65 overexpression using luciferase and plasmids. The panc-1 p65 transfected clones were analysed using real-time PCR. GAPDH was used as a loading control. Figure 6.2(A) shows the mRNA expression of p65 in the clones. The panc-1 p65-overexpressed clones had elevated mRNA expressions of p65 compared to the mock. In Figure 6.2(B), Western Blot analysis was used to analyse and compare the protein expression of p65 in the mock and p65-overexpressed clones, using beta actin as a loading control. The p65 clones had a higher protein expression of p65 compared to the mock. The results reveal that the panc1 p65-overexpressed clones had higher expressions of NFκB p65 than the mock.

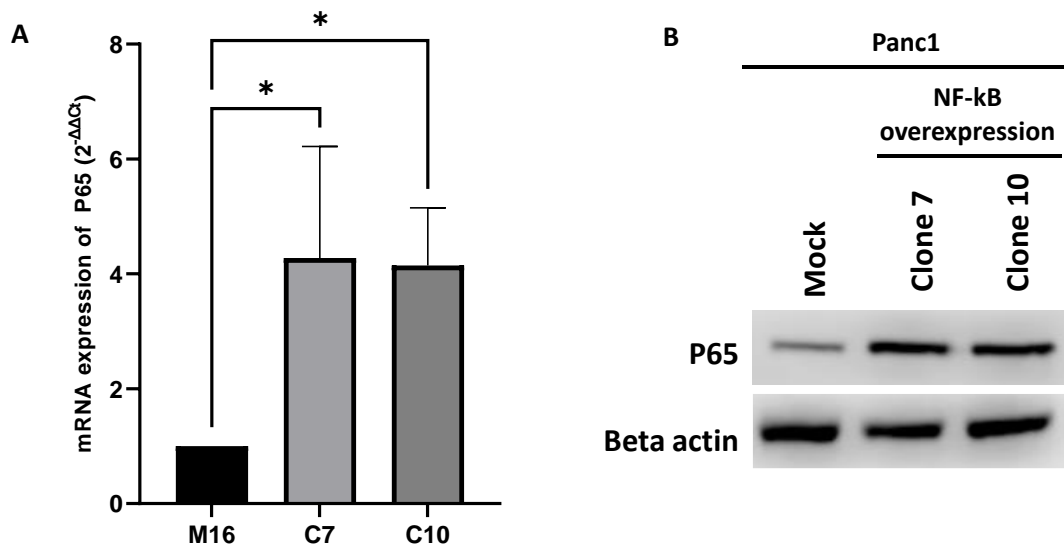


**Figure 6.2: Expression of p65 in NFκB p65 overexpressed clones of PDAC cells.** (A) Real-time PCR analysis for p65 in the panc-1 p65-overexpressed clones. The p65-overexpressed clones had elevated mRNA expression of p65 compared with the mock. GAPDH was used as a loading control (B) Western Blot analysis showed increased expression of p65 protein in the panc-1 p65-overexpressed clones. 30μg of protein/lane. Beta actin was used as a loading control. n=3; \*p<0.05.

### 6.3.3 CRISPR Cas9 knock out of NFκB p65 in Panc1 PDAC cells

The aim of this study was to ascertain the effect of the absence of NFκB p65 in panc1 PDAC cell line. CRISPR-cas9 technology was used to knockout p65 from panc-1 PDAC cell line. In Figure 6.3(A), real-time PCR was used to analyse the mRNA expression of p65 in the panc1 p65 CRISPR knockout clones. The results showed that there was no mRNA expression of p65 in the panc1 p65 CRISPR knockout clones while the control had an elevated mRNA expression level of p65. The loading control used for the real-time PCR analysis was GAPDH. The protein expression of p65 was analysed in the panc1 p65 CRISPR knockout clones and mock using Western Blot as shown in Figure 6.3(B). The results revealed that the panc1 CRISPR p65 knockout clones had no protein expression of p65.

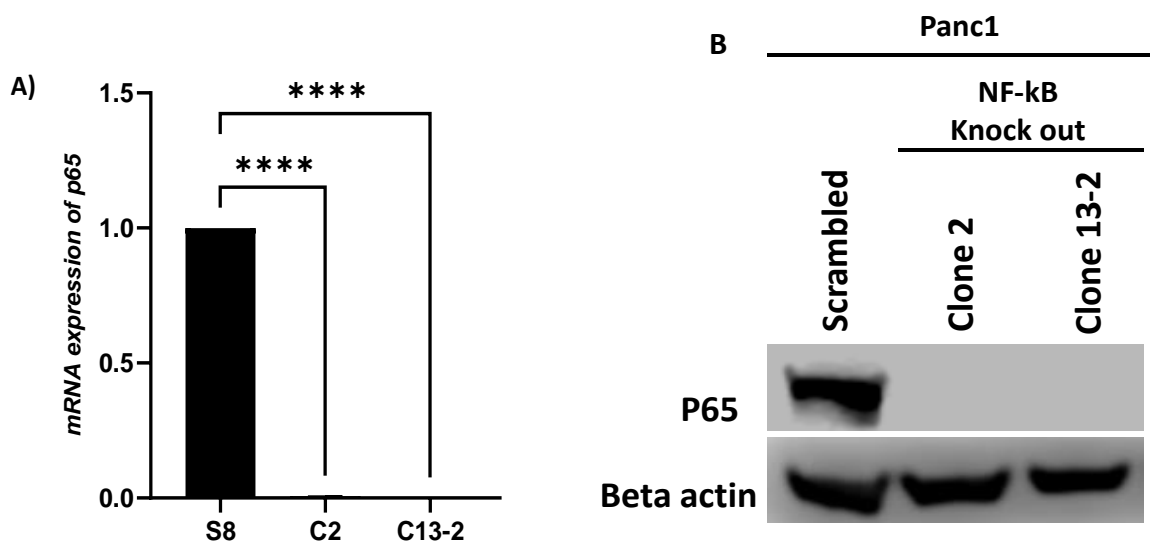


**Figure 6.3: Expression of p65 in CRISPR cas9 NFκB p65 knockout clones of PDAC cells.** (A) Real-time PCR analysis for p65 in the panc-1 p65 knockout clones. The p65 knockout clones had a significantly decreased mRNA expression of p65 compared with the mock. GAPDH was used as a loading control (B) Western Blot analysis showed no expression of p65 protein in the panc-1 p65 knockout clones. 30μg of protein/lane. Beta actin was used as a loading control. n=5; \*\*\*\*p<0.0001.

#### **6.3.4 NFκB p65 plays an insignificant role in regulating stemness in Panc-1 PDAC cells**

ALDEFLUOR was used to stain the panc-1 p65 overexpressed clones then flow cytometry was used to analyse the results. Figure 6.4(A) shows the dot plots obtained and a bar chart showing the percentage of ALDH in the mock and p65 overexpressed clones. The panc-1 p65 overexpressed clones had a higher percentage of ALDH than the mock. However, the increase was not significant.

Likewise, ALDEFLUOR was used to stain the panc-1 CRISPR p65 knockout clones then flow cytometry was used to analyse the results. Figure 6.4(B) shows the dot plots obtained and a bar chart showing the percentage of ALDH in the mock and CRISPR p65 knockout clones. The panc-1 CRISPR p65 knockout clones had a highly significant decrease in the percentage ALDH population than the control. Real-time PCR was further used to analyse the mRNA expression levels of different CSC markers (Sox2, Oct4 and Nanog) in the panc-1 p65 overexpressed clones and the panc-1 CRISPR p65 knockout clones. Figure 6.4(C) indicates that there was variable mRNA expression of the embryonic stem cell markers in all the clones. The only significant change was in the expression of Oct4 in the panc1 CRISPR p65 knockout clones.

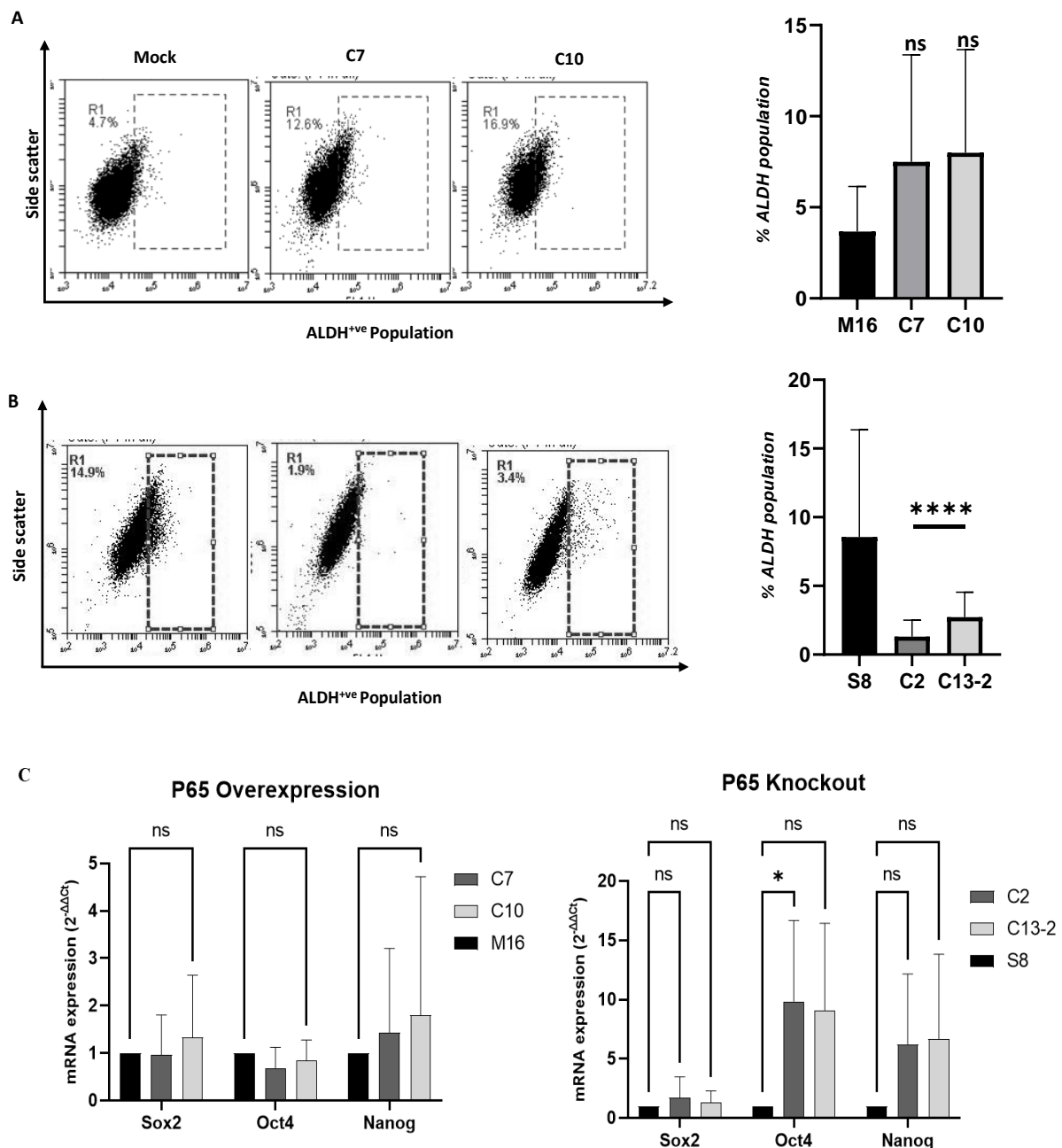


**Figure 6.4: Expression of cancer stem cell markers in NFκB p53 overexpressed clones and CRISPR cas9 NFκB p53 knock out clones of PDAC cells. (A) Flow cytometry analysis showing ALDH positive population and a bar chart showing the percentage ALDH population in the p53-overexpressed clones. The p53 overexpressed clones had a higher percentage of ALDH than the mock (B) Flow cytometry analysis showing ALDH positive population and a bar chart showing the percentage ALDH population in the CRISPR p53 knockout clones. The CRISPR p53 knockout clones had a significantly decreased percentage of ALDH than the control (C) Bar chart showing mRNA expression of CSC markers (Sox2, Oct4 and Nanog) in the p53-overexpressed and CRISPR knockout clones. ns=not significant; \*\*\*\* $p < 0.0001$ .**

### **6.3.5 NFκB p65 does not play a role in regulating EMT markers in Panc-1 PDAC cells**

Real-time PCR was used to analyse the mRNA expression levels of different EMT markers such as Snail1, Snail2, MMP2, MMP7, MMP9, Vimentin, E-cadherin and N-cadherin in the panc-1 p65 overexpressed clones as shown in Figure 6.5(A). The results showed that there was no significant change in the mRNA expression of different EMT markers. However, there was a significant decrease in the expression of Snail2 and significant increase in the mRNA expression of E-cadherin in the panc-1 p65 overexpressed clones.

Similarly, real-time PCR was used to analyse the mRNA expression levels of different EMT markers such as Snail1, Snail2, MMP2, MMP7, MMP9, Vimentin, E-cadherin and N-cadherin in the panc-1 CRISPR p65 knockout clones as shown in Figure 6.5(B). The results showed that there was a significant increase in the mRNA expression of Snail1, Snail2, Vimentin and Zeb1 in the panc-1 CRISPR p65 knockout clones. N-cadherin and Vimentin also increased but the increase was not significant. There was a decrease in the mRNA expression of E-cadherin, MMP7 and MMP9 in the panc-1 CRISPR p65 knockout clones compared to the control. This probably means that NFκB/p65 directly regulates E-cadherin, MMP7 and MMP9 in PDAC. These data reveal that in the absence of NFκB, PDAC would upregulate the expression of some EMT markers to compensate for the deficiency. This also shows that targeting NFκB for PDAC drug design would have little to no effect on PDAC tumour cells.

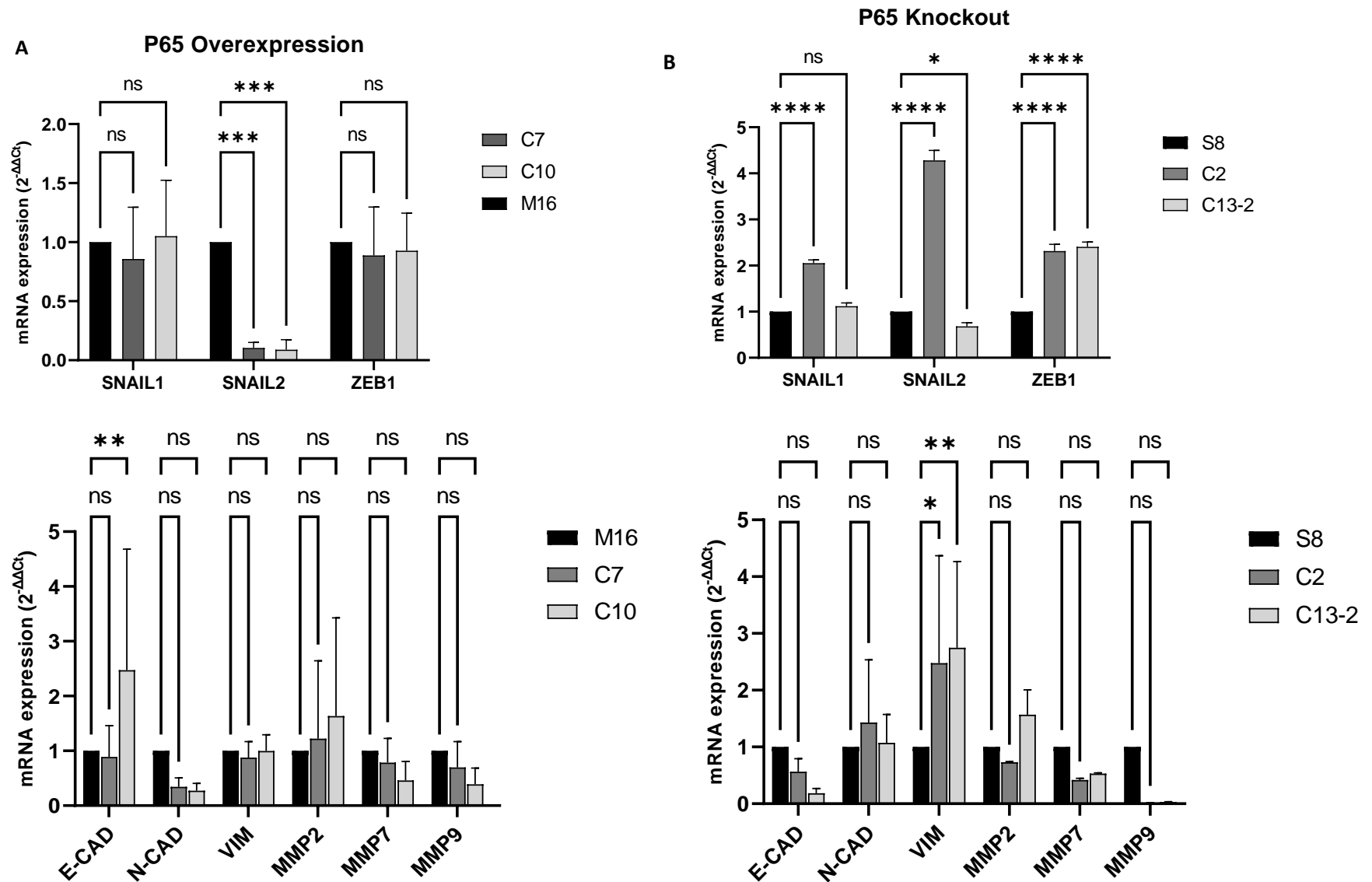


**Figure 6.5:** Expression of EMT markers in *NFκB p53* overexpressed clones and *CRISPR cas9 NFκB p53* knock out clones of PDAC cells. Real-time PCR was used to analyse the expression of different EMT markers in the *panc-1 p53* overexpressed clones and the *panc-1 CRISPR p53* knockout clones. *GAPDH* was used as a loading control.

### **6.3.6 Overexpression of NFκB p65 drives resistance to first line PDAC anticancer drugs in Panc-1 PDAC cells**

In order to ascertain the role NFκB/p65 plays in chemoresistance, MTT cell viability assay was carried out on the p65 overexpressed clones. The clones were seeded in 96-well plates at a density of 5000 cells per well then treated the next day with 100μM gemcitabine. After 72 hours, MTT was added to the treated clone cells and the crystals which formed were dissolved with DMSO. Spectrophotometry was used to analyse the results. Figure 6.5(A) shows the cell viability curve obtained after treatment with 100μM gemcitabine. The panc-1 p65 overexpressed clones were more resistant to gemcitabine than the control. In the same way, MTT cell viability assay was carried out on the p65 overexpressed clones. The clones were seeded in 96-well plates at a density of 5000 cells per well then treated the next day with 100nM paclitaxel. After 72 hours, MTT was added to the treated clone cells and the crystals which formed were dissolved with DMSO. Spectrophotometry was used to analyse the results. Figure 6.5(B) shows the cell viability curve obtained after treatment with 100nM paclitaxel. The panc-1 p65 overexpressed clones were more resistant to paclitaxel than the control. These data reveal that the panc-1 p65 overexpressed clones were more resistant to treatment than the control and a higher concentration of gemcitabine was required to eliminate the panc-1 p65 overexpressed clone cells. This shows that NFκB plays a role in PDAC chemoresistance.

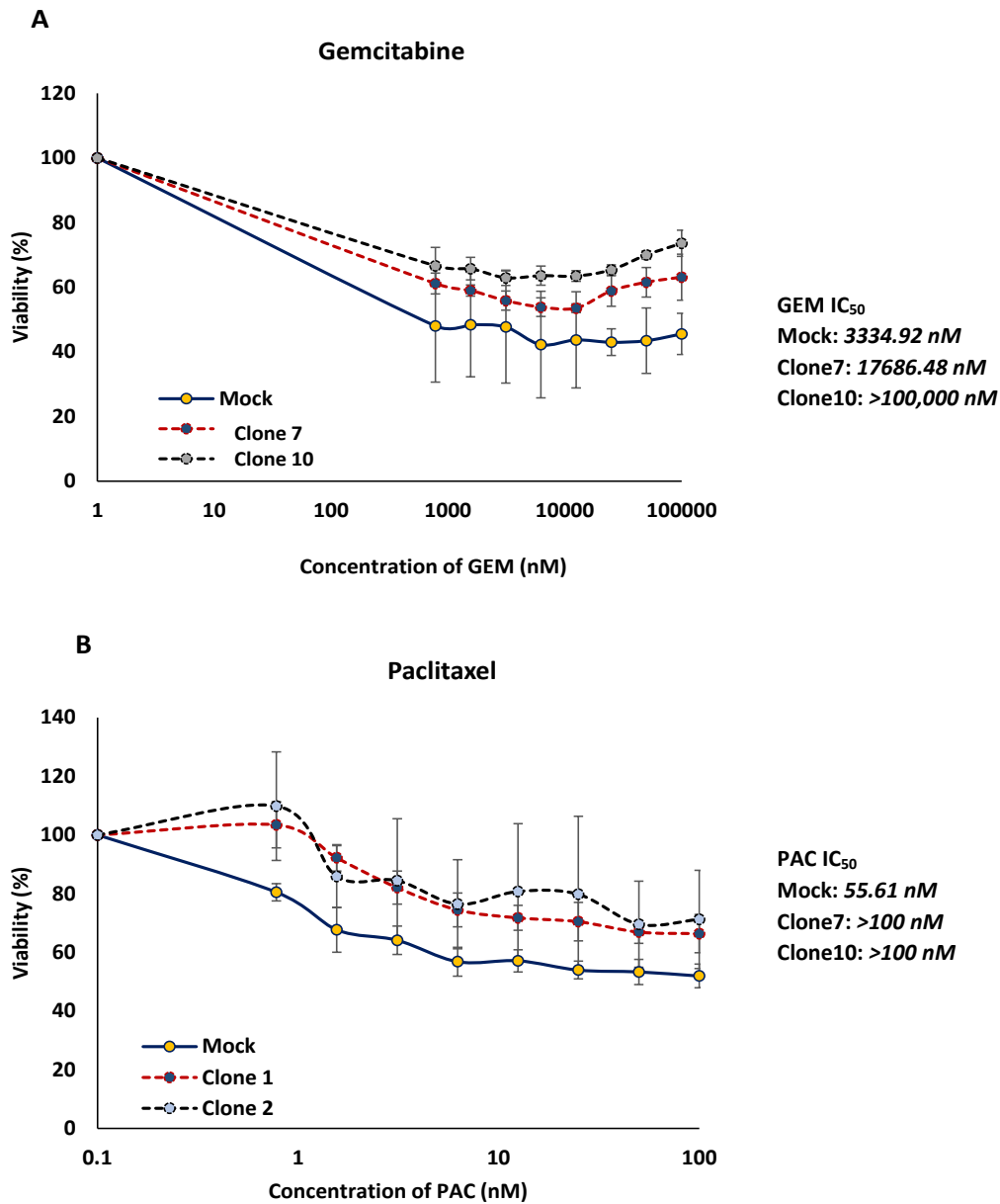


**Figure 6.6: Cytotoxicity of NFκB p65 overexpressed clones to first line anti-PDAC drugs gemcitabine and paclitaxel.** MTT cell viability assay was used to analyse the viability for the panc-1 p65 overexpressed clones after treatment with (A) 100μM Gemcitabine (B) 100nM Paclitaxel. The control was less resistant to treatment than the clones.

### **6.3.7 Knockout of NFκB p65 sensitises PDAC cells to PAC but not significantly to Gemcitabine**

In order to ascertain the role NFκB/p65 plays in chemoresistance, MTT cell viability assay was carried on the CRISPR p65 knockout clones. The clones were seeded in 96-well plates at a density of 5000 cells per well then treated the next day with 100μM gemcitabine. After 72 hours, MTT was added to the treated clone cells and the crystals which formed were dissolved with DMSO. Spectrophotometry was used to analyse the results. Figure 6.7(A) shows the cell viability curve obtained after treatment with 100μM gemcitabine. The panc-1 CRISPR p65 knockout clones were more resistant to gemcitabine than the control. In the same way, MTT cell viability assay was carried on the CRISPR p65 knockout clones. The clones were seeded in 96-well plates at a density of 5000 cells per well then treated the next day with 100nM paclitaxel. After 72 hours, MTT was added to the treated clone cells and the crystals which formed were dissolved with DMSO. Spectrophotometry was used to analyse the results. Figure 6.7(B) shows the cell viability curve obtained after treatment with 100nM paclitaxel. The panc-1 CRISPR p65 knockout clones were less resistant to paclitaxel than the control. These data reveal that the knockout of NFκB does not eliminate chemoresistance in panc-1 PDAC cell line. It also shows that inhibition of NFκB may cause selective chemoresistance of PDAC to different anticancer drugs.

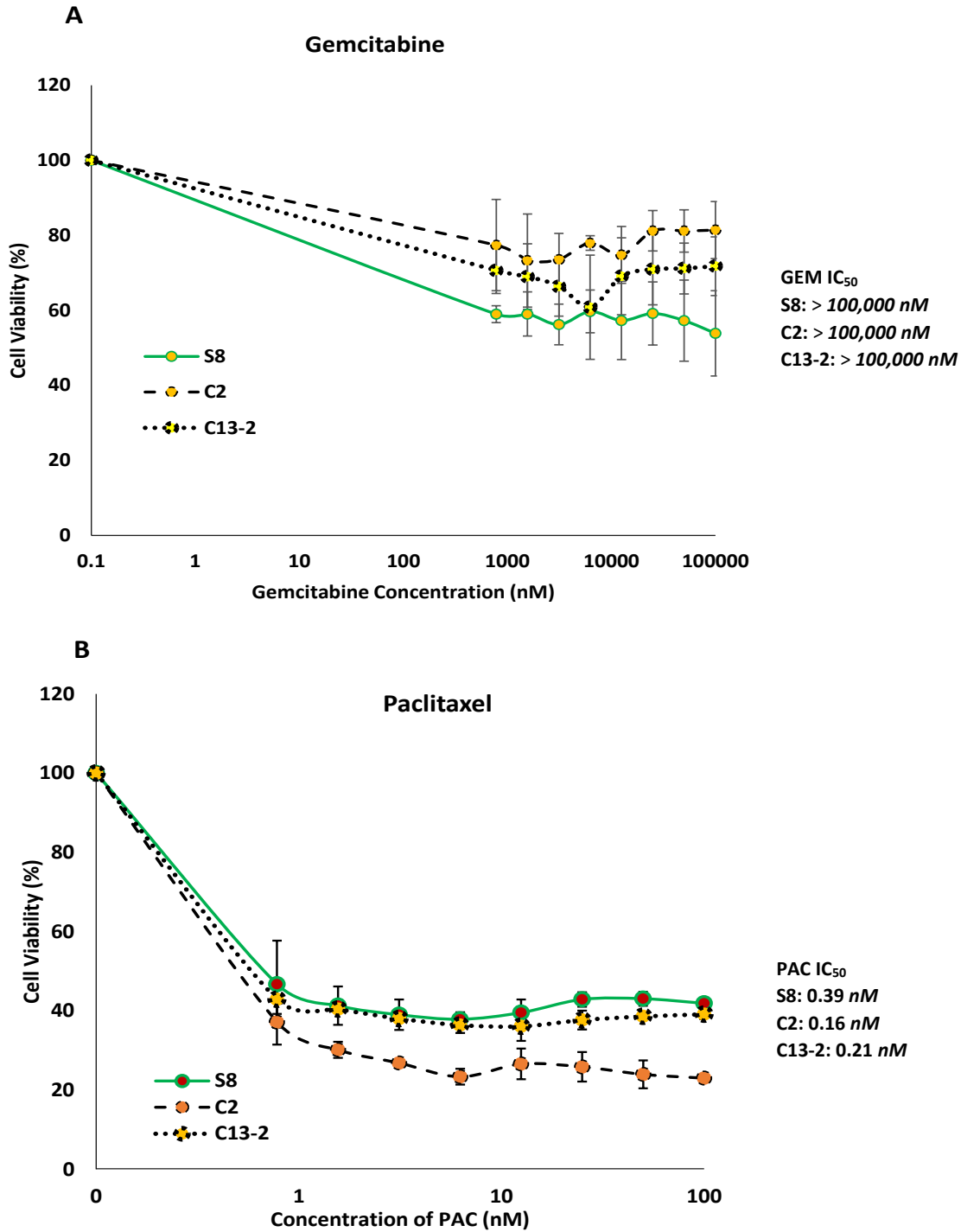


**Figure 6.7: Cytotoxicity of NFκB p65 knockout clones to first line anti-PDAC drugs gemcitabine and paclitaxel.** MTT cell viability assay was used to analyse the viability of the *panc-1* CRISPR p65 knockout clones after treatment with (A) 100μM Gemcitabine (B) 100nM Paclitaxel. The control was less resistant to gemcitabine treatment but more resistant to paclitaxel treatment than the clones.

## 6.4 Discussion

The molecular mechanisms involved in chemoresistance need to be well understood in order to develop effective therapy for PDAC (Meng et al., 2020). All cells contain a family of transcription factors called NF $\kappa$ B which is activated by different signals and plays a role in activating cellular responses. The most highly occurring NF $\kappa$ B dimer is NF $\kappa$ B1(p50)/RelA(p65) heterodimer (Silke and O'Reilly, 2021). NF $\kappa$ B is a transcription factor involved in apoptosis inhibition, tumour growth, chemoresistance and poor prognosis in numerous cancers (Cheriyian et al., 2014). During tumour development and progression, the production of proteases, cytokines, growth and angiogenic factors leads to NF $\kappa$ B activation (Yang et al., 2020). In cancer, NF $\kappa$ B activity can be influenced by cytokines, chemokines, microRNAs, ROS and post translational modification (Prabhu et al., 2014). The activation of the NF $\kappa$ B pathway in pancreatic cancer leads to expression of numerous anti-apoptotic genes and the suppression of proapoptotic signalling pathways (Melisi et al., 2011). About 95% of all tumours have NF $\kappa$ B activation which promotes tumour development, regulate apoptosis, initiate angiogenesis and leads to metastasis. In most PDAC, NF $\kappa$ B transcriptional factors are continuously expressed leading to the suspicion that NF $\kappa$ B-driven pathways are involved in PDAC development (Prabhu et al., 2014). The data reveals that hypoxia increases NF $\kappa$ B activation in PDAC cells.

In about 45 to 70% of pancreatic cancers, the NF $\kappa$ B subunit RelA/p65 is translocated to the nucleus. The presence of nuclear RelA/p65 in pancreatic cancer patients is an indicator of poor prognosis (Hamacher et al., 2008). Whole protein analysis of NF $\kappa$ B/p65 by Western Blot showed high protein expression in PDAC spheroid and hypoxic cultures.

The non-classical NF $\kappa$ B pathway has been shown to contribute to tumourigenesis in PDAC. The activation of NF $\kappa$ B-inducing kinase (NIK) enhanced the activity of the p52/RelB NF $\kappa$ B

complex in panc-1 and MiaPaca2 pancreatic cancer cells (Doppler et al., 2013; Prabhu et al., 2014). One study involving chemically-induced skin cancer gave the first insight that NFκB could also act as a tumor suppressor. NFκB can act as a tumor suppressor when cell cycle is suppressed or when MAP kinase pathway is downregulated. According to Xiao, suppressing NFκB in two ovarian carcinoma cell lines OVCA433 and OVCR3 led to suppression of apoptosis and tumor growth (Xiao et al., 2016). C-C chemokine receptor 7 binds to chemokine ligand 21 causing increased expression of p65 and Erk1/2 which inhibit apoptosis and enhance cell motility in CD133<sup>+</sup> PCSCs (Yang et al., 2020). TLR2-MyD88-driven NFκB controls the expression of Sox2, Nanog and CD44 in ovarian CSCs (Chefetz et al., 2013; Rinkenbaugh and Baldwin, 2016). In the panc-1 p65 overexpressed and knockout clones, there was variable increase in the mRNA expression of Sox2, Nanog and Oct4. However, the mRNA expression was only significant in for Oct4 in the panc-1 CRISPR p65 knockout clones. This shows that PDAC tumours have different genes which carry out similar functions so the exclusion of one of these genes will not improve PDAC prognosis.

P65 overexpression led to an increase in cell migratory characteristics in bladder cancer cells (Zhu et al., 2017). NFκB can control the expression of EMT transcription factors such as Snail, Slug, Zeb1, Zeb2 and Twist1. NFκB also controls the expression of MMPs; especially MMP2 and MMP9 which play the critical role of digesting components of the ECM to facilitate tumour cell invasion (Rinkenbaugh and Baldwin, 2016). This corresponds with the results obtained because panc1 p65 overexpression led to increased mRNA expression of E-cadherin and MMP2. There was also a significant decrease in mRNA expression of Snail2 while the knockout of p65 increased mRNA expression of Snail1, Snail2, Zeb1 and vimentin.

The inhibition of NFκB/p65 in the human breast cancer cell line, MDA-MB-231 and HCC-1954 using SiRNA strategy and dehydroxymethylepoxyquinomicin (DHMEQ) treatment resulted in reduced cell motility, reduced cell invasiveness, decreased expression of SLUG,

SIP1, TWIST1, MMP11 and N-cadherin and increased expression of E-cadherin (Pires et al., 2017). SNAIL, SLUG, ZEB1 and TWIST drive EMT at the cellular level. In the TME of aggressive PDAC, some cancerous cells express EMT markers at mRNA and protein levels. These EMT markers are closely associated with chemoresistance. Some PDAC cell lines such as BxPC3, CFPAC-1 and L3.6pl which have an upregulation of E-cadherin and low Zeb1 are sensitive to first line anticancer drugs like cisplatin, 5-FU and gemcitabine while other cell lines like panc-1, MiaPaCa-2, AsPC-1 and MPanc96 express low E-cadherin and high Zeb1 leading to chemoresistance (Khalafalla and Khan, 2017).

The canonical pathway for NFκB activation is involved in immune activation and cell survival while the non-canonical pathway is involved in lymphoid organogenesis. The role of NFκB complexes containing c-Rel or p65 are different. NFκB complexes containing c-Rel are involved in immune response and lymphoid development while those containing p65 are involved in cellular activation responses. Germline deletion of p65 greatly affects cell growth and function while deletion of c-Rel revealed less immunological defects. According to Grinberg-Bleyer, the inhibition of NFκB c-Rel suppresses tumour growth and not p65, making c-Rel a possible target for novel cancer immunotherapy (Grinberg-Bleyer et al., 2017).

In PDAC, NFκB signalling has different modes of causing acquired resistance to gemcitabine such as binding to the promoter region of P-gp or binding to other regulators (Meng et al., 2020). The knockdown of NFκB suppressed the growth of nude mouse Lewis's tumour cell xenografts by overexpression of Bax which promotes apoptosis (Qu et al., 2015). There are many inhibitors of NFκB, some of which completely inhibit the NFκB pathway or inhibit a step or more in the NFκB pathway (Gupta et al., 2010). A potent inhibitor of NFκB called nafamostat mesylate inhibited NFκB activation leading to increased antitumour activity of gemcitabine and nab-paclitaxel in PDAC (Horiuchi et al., 2016). Some drugs such as disulfiram and sulforaphane inhibit tumour progression and CSC metastasis by inhibiting the NFκB

pathway (Yang et al., 2020). In some cancers, NFκB inhibition suppresses the expression of EMT-related genes such as SNAIL, TWIST1 and SLUG. The knockout of RelA/p65 with SiRNA improves the anticancer activity of gemcitabine on gemcitabine-sensitive PDAC cells but had no effect on gemcitabine-resistant PDAC cells (Silke and O'Reilly, 2021). The panc-1 CRISPR p65 knockout cells had chemosensitivity to gemcitabine compared with the control but chemoresistance to paclitaxel. This shows that the knockdown of p65 can reduce chemoresistance in some anticancer drugs. The results of this study also highlight that NFκB overexpression increases chemoresistance of panc-1 PDAC cells to gemcitabine and paclitaxel. This suggests that targeting NFκB alone for cancer therapy will not improve the chemoresistance of PDAC.

## **CHAPTER 7**

---

### **GENERAL DISCUSSION**

---

## 7.0 Discussion

PDAC is easier to diagnose than pancreatic cancers arising in the body or tail of the pancreas because the head of the pancreas contains the common bile duct (Sarantis et al., 2020). Pancreatic ductal adenocarcinoma (PDAC) has a high fatality rate worldwide with less than 20% surviving past one year and there is no significant improvement in its management (Sarantis et al., 2020). The different treatment modalities used for cancer management are either temporary in action or have severe side effects during prolonged use (Hassan et al., 2018). Cancer therapy is best with drugs which exert great therapeutic effect at low concentrations so as to reduce undesirable side effects (Abu-Serie, 2018). Currently, the first line treatment for metastatic pancreatic cancer is a combination of gemcitabine and nab-paclitaxel which has increased the OS of pancreatic cancer patients to 8.7 months compared to gemcitabine alone which has an OS of 6.6 months. In this treatment, gemcitabine is usually administered immediately after nab-paclitaxel on days 1, 8 and 15 out of a 28-day cycle, as 30-minute infusions (Corrie et al., 2020). Treatment with gemcitabine and nab-paclitaxel increases the 2-year overall survival of pancreatic cancer patients from 4% to 9% but has adverse effects related to toxicity which reduces quality of life and increases risk for infections (Principe et al., 2021). A study by Corrie et al. showed that a 6-month treatment of 2 groups of PDAC patients, one with sequential (SEQ) and the other with concomitant administration (CON) of gemcitabine and nab-paclitaxel with the SEQ having a progression free survival of 46% and CON having a progression free survival of 32% (Corrie et al., 2020). In Chapter 3, the study showed that panc-1 cells had elevated CSC traits when cultured under hypoxic and spheroid conditions. The spheroid panc-1 cultures had high hypoxic cell populations because the spheres consisted of tightly packed cell populations. The hypoxic cultures had increased migratory and invasive characteristics and were more resistant to therapy than the normoxic cultures.

In Chapter 4, the cytotoxicity of the first line PDAC drugs: gemcitabine and paclitaxel was investigated on patient derived PDAC cells and on one PDAC cell line both under normoxic and hypoxic conditions. In both PDAC cell types, the result showed that the percentage of PDAC cells killed was low and that the hypoxic cells were more resistant to treatment than the normoxic PDAC cells. This result suggests that hypoxia plays a role in tumour chemoresistance (Geng et al., 2018).

Immunocytochemistry was used to quantify the presence of hypoxia in three patient derived cells (A6L, CX135 and 12560) and panc-1 cell line under normoxic, hypoxic and spheroid conditions. Pimonidazole, a commonly used biomarker for tumour hypoxia forms covalent bonds with macromolecules in hypoxic cells ( $O_2 < 1.3\%$ ) and the degree of pimonidazole staining gives an estimate of the degree of hypoxia in the sample (Ragnum et al., 2014). The findings revealed that the hypoxic and spheroid PDAC cells had more pimonidazole staining than the normoxic cells. Interestingly, the normoxic cells had some pimonidazole staining. This confirms that all cancer cells have some level of hypoxia within them (Jin and Jin, 2020).

Flow cytometry was used to carry out hypoxyprobe analysis on normoxic and hypoxic PDAC cells. The results revealed that the cells stained with pimonidazole was much higher in the hypoxic cell sample than in the normoxic cell sample. This data is consistent with the findings during the immunocytochemistry experiment.

Many studies have shown that hypoxia leads to formation of cancer stem cells in cancerous tumours (Jewer et al., 2020; Wang et al., 2017a). Pancreatic cancer stem cells play a critical role in metastasis and chemoresistance (Swayden et al., 2018). CSCs have an elevated number of drug efflux pumps such as multidrug resistant transporters, ATP binding cassettes and ABC transporter proteins like ABCB1, ABCG2, ABCC11 and ABCB (Razi et al., 2019). TGF $\beta$ , Notch, ERK/MAPK, Wnt and NF $\kappa$ B pathways initiate EMT and increase cancer cell stemness

by epigenetic mechanisms such as DNA methylation and histone modification (Kim et al., 2020). Unlike cancer cells, cancer stem cells can only be arrested at the G0 phase making them harder to eliminate with first line anticancer drugs. These CSCs can be identified with specific surface markers such as ALDH, CD44<sup>+</sup> and CD133<sup>+</sup> (Yang et al., 2020).

According to the PCR analysis in this study, hypoxia increased the mRNA expression of SOX2, NANOG and OCT4. Hypoxia also increased the expression of the stem cell marker CD133. This is also confirmed in hepatoma, glioma and lung cancer cells (Wang et al., 2017a). There was also an increase in the expression levels of the ALDH and ABCG2. It is hypothesized that tumour hypoxia activates NFκB which in turn activates many genes responsible for CSC survival, metastasis and chemoresistance (D'ignazio and Rocha, 2016).

Ectopic levels of NFκB can terminate apoptosis in cancer cells and induce chemoresistance (Yip et al., 2011). Some *in vivo* and *in vitro* data show that NFκB could be a good target for PDAC drug development (Plewka et al., 2018) however, suppressing NFκB expression may have repercussions and has not yielded any successful results in clinical trials (Liu et al., 2012; Liu et al., 2017). In endothelial cells, NFκB and MAPK are the main signalling pathways involved in controlling strong inflammation responses (Ramalingam et al., 2020). NFκB is the key regulator of inflammation and the major link between inflammation and cancer. In tumour cells, NFκB can either have a pro- or anti-cancer effect (Achyut et al., 2017). In solid tumours, cancer cells undergo changes which enable them to dodge immune surveillance, undergo EMT and break away from the ECM leading to metastasis which is responsible for most cancer fatalities (Jin and Jin, 2020).

For the panc-1 cells treated with paclitaxel, the unmodified cells had an IC<sub>50</sub> of 83.10 ± 22.39nM which is close to the IC<sub>50</sub> value gotten from the p65 mock clones (55.61nM). The p65 overexpressed clones treated with 100nM paclitaxel had IC<sub>50</sub> values greater than 100nM.

However, the  $IC_{50}$  obtained from the p65 scrambled clones was 0.39nM while the  $IC_{50}$  obtained for the p65 knockout clones was 0.16nM and 0.21nM respectively. This shows that the knockout of p65 increased the sensitivity of PDAC to paclitaxel while overexpression of p65 led to increased chemoresistance to paclitaxel.

For the panc-1 cells treated with gemcitabine, the unmodified cells had an  $IC_{50}$  of  $78.45 \pm 20.64\mu\text{M}$  which is a lot lower than the  $IC_{50}$  value gotten from the p65 mock clones ( $3,334\mu\text{M}$ ). The p65 overexpressed clones treated with  $100\mu\text{M}$  gemcitabine had  $IC_{50}$  values greater than  $100\mu\text{M}$ . Also, the p65 knockout clones treated with  $100\mu\text{M}$  gemcitabine had  $IC_{50}$  values greater than  $100\mu\text{M}$ . This shows that the overexpression and knockout of p65 increased chemoresistance of PDAC to gemcitabine.

Gemcitabine in combination with disulfiram/Cu reverses gemcitabine-induced nuclear translocation of NF $\kappa$ B and suppresses I $\kappa$ B degradation in colon and breast cancer (Guo et al., 2010).

Many studies are focused on discovering novel compounds that selectively target cancer cell metabolism. However, cancer cell metabolism depends mainly on the unique characteristics of cancer cell microenvironment such as hypoxia, angiogenesis and nutrient availability (Cheng et al., 2014). A proper study of the mechanism of chemoresistance in PDAC will improve the efficacy of new anticancer drugs and decrease PDAC-related deaths (Swayden et al., 2018).

The process of producing a new drug requires an average of 13 years' research and costs roughly \$2 to 3 billion (Zhang et al., 2020b) while drug repurposing offers the advantage of rapid translation of old drugs for new clinical use (Corsello et al., 2020). Packaging disulfiram in nanoparticles can increase its ability to selectively target cancer cells (Abu-Serie, 2018). The main aim of this study was to assess the cytotoxicity of a novel formulation of disulfiram known as cyclodextrin disulfiram on patient derived PDAC cells and PDAC cell lines. The challenge

with using disulfiram as an anticancer drug is its short half-life in the blood which packaging with cyclodextrin has effectively boosted as shown in this study.

In recent years, the potential of using disulfiram as an anticancer drug is gaining a lot of publicity. Disulfiram controls metabolic processes requiring copper or zinc (Zhang et al., 2020b). Disulfiram forms a complex with copper which elevates oxidative stress to a level that terminates cancer cells including CSCs (Hassan et al., 2018). A certain *in vitro* study reported that disulfiram is required in a higher concentration (0.54 $\mu$ M against 0.21  $\mu$ M) to exert an anticancer effect in the absence of copper (Xu et al., 2017). Copper is essential for tumour growth and at high concentrations, it increases tumour growth and cell motility (Li et al., 2018). This is consistent with the data obtained after sphere reformation with panc-1 cell line where disulfiram alone had no cytotoxic effect on panc-1 spheroid cells. Spheroid cells formed by the patient derived PDAC cells and the panc-1 cell line were completely dissociated by cyclodextrin disulfiram. In the case of the patient derived PDAC cells, cyclodextrin disulfiram caused the complete dissociation of reformed spheres unlike paclitaxel and gemcitabine.

Treatment of an MDR tumour with hybrid paclitaxel/DSF nanocrystals led to a 6-fold increase in apoptosis compared to treatment with paclitaxel alone (Mohammed et al., 2019). Cancer cells have deregulated apoptotic signalling which enables them to grow uncontrollably (Zhang et al., 2020b). In order to compare the ability of the gemcitabine, paclitaxel and cyclodextrin disulfiram to initiate apoptosis on PDAC cells, Annexin-V apoptosis assay was carried out using flow cytometry. Different samples of 4 patient derived cells were treated with 500nM gemcitabine, 500nM paclitaxel and 500nM cyclodextrin disulfiram/10 $\mu$ M copper for 14 hours. The results showed increase in apoptosis and necrosis in the PDAC cells treated with cyclodextrin disulfiram compared to paclitaxel or gemcitabine.

Disulfiram in combination with copper increases Bax/Bcl2 ratio suggesting a possible involvement of an intrinsic apoptotic pathway (Yip et al., 2011). Disulfiram/Cu does not affect the expression of the NFκB subunits, p65 and p50 rather, it inhibits their ability to translocate into the nucleus. Thus, controlling EMT (Li et al., 2018b).

Prior results have shown that ALDH expression is strongly suppressed by disulfiram (Yip et al., 2011; Wu et al., 2019). In this study, flow cytometry was used to analyse the ability of disulfiram to eliminate CSCs from hypoxic and spheroid patient derived PDAC cells. The data obtained revealed that treatment with cyclodextrin disulfiram/Cu decreased the population of ALDH, CD133 and ABCG2 in the hypoxic and spheroid samples. This proves that cyclodextrin disulfiram eradicates CSCs. The cytotoxicity studies revealed that low doses of cyclodextrin disulfiram (10μM) successfully eliminated a large percentage of PDAC cells after treatment.

DSF/Cu suppresses the NFκB pathway which controls cell motility (Li et al., 2018b). Disulfiram also inhibits the action of MMP2, MMP9, topoisomerase I and II which play significant roles in metastasis and angiogenesis (Hassan et al., 2018). Unlike gemcitabine and paclitaxel, disulfiram/Cu has proved to be effective in eliminating CSCs (Xu et al., 2017).

Some of the ongoing clinical trials involving administration of disulfiram in combination with other anticancer drugs have not yielded successful results (Wu et al., 2019). However, in this study, the cytotoxicity of cyclodextrin disulfiram on PDAC cells was synergistically enhanced when administered in combination with either paclitaxel or gemcitabine. The cytotoxicity of cyclodextrin disulfiram/Cu in combination with paclitaxel or gemcitabine was found to be more than when cyclodextrin disulfiram is administered independently.

Generally, hypoxia increased chemoresistance in the PDAC patient derived cells and PDAC cell line. Also, cyclodextrin disulfiram/Cu was effective in reducing chemoresistance of PDAC.

## CONCLUSION

Despite all the studies which have been carried out on pancreatic cancer cells, there is yet to be a drug which completely destroys the tumour. The first line anticancer drugs; gemcitabine and paclitaxel don't eliminate CSCs, therefore there is a pressing need for effective anticancer drugs which eliminate CSCs. This research reveals that hypoxia plays significant roles in the development of cancer cell stemness, cell invasion and chemoresistance of PDAC cell lines. The expression of CSC markers in the PDAC cell line and patient derived cells is most likely responsible for the poor prognosis in PDAC patients. The pathways activated by hypoxia induce the expression of CSC markers, EMT, metastasis and chemoresistance. Hypoxia is the driving force behind PDAC progression.

This study has shown that disulfiram targets CSCs which are responsible for chemoresistance and metastasis. Cyclodextrin disulfiram became potent when administered with copper. Cyclodextrin disulfiram increased the therapeutic effect of gemcitabine and paclitaxel. It also plays a role in inhibiting the activity of NFκB which increases tumour progression. The low price of disulfiram and its potency in targeting CSCs compared to other first line anticancer drugs makes it a good candidate for an effective anticancer drug. The results of the *in vivo* studies with cyclodextrin disulfiram is promising because it led to a good percentage of reduction in tumour size. This confirms that cyclodextrin disulfiram in combination with copper exhibited high cytotoxicity to PDAC cells both *in vivo* and *in vitro*. The effectiveness of cyclodextrin disulfiram confirms that cyclodextrin is a good packaging material for disulfiram. According to the findings of this research, cyclodextrin disulfiram has a longer half-life *in vivo* than disulfiram and is effective for use as an anticancer drug.

Despite using CRISPR technology to knock out NFκB, there was still tumour proliferation suggesting that NFκB alone is not responsible for cancer progression. There was not enough

time to carry out elaborate research such as studying the effect of drug combinations on the transfected clones so a new PhD student is already doing some further studies in this area.

Studies were also carried out on HIF1 and HIF2 overexpression on Panc1 PDAC cells but there was not enough time to carry out significant research on the cells. Further studies should be carried out on the effect of HIF2 knockout on PDAC chemoresistance based on the expression of CSC and EMT markers in the HIF2 overexpressed Panc1 PDAC clones.

## REFERENCES

- Abu-Serie, M. (2018) Evaluation of the selective toxic effect of the charge switchable diethyldithiocarbamate-loaded nanoparticles between hepatic normal and cancerous cells. *Scientific Reports*, 8(1), p. 4617.
- Achyut, B. R., Angara, K., Jain, M., Borin, T. F., Rashid, M. H., Iskander, A., Ara, R., Kolhe, R., Howard, S., Venugopal, N., Rodriguez, P. C., Bradford, J. W. and Arbab, A. S. (2017) Canonical NF $\kappa$ B signaling in myeloid cells is required for the glioblastoma growth. *Scientific Reports*, 7(1), p. 13754.
- Adamska, A., Domenichini, A. and Falasca, M. (2017) Pancreatic Ductal Adenocarcinoma: Current and Evolving Therapies. *International Journal of Molecular Sciences*, 18(7), p.1338.
- Adamska, A., Elaskalani, O., Emmanouilidi, A., Kim, M., Abdol Razak, N., Metharom, P. and Falasca, M. (2018) Molecular and cellular mechanisms of chemoresistance in pancreatic cancer. *Advances in Biological Regulation*, 68, pp.77-87.
- Adli M. (2018) The CRISPR tool kit for genome editing and beyond. *Nature Communications*, 9(1), p. 1911.
- Aguilera, K. Y. and Brekken, R. A. (2014) Hypoxia Studies with Pimonidazole *in vivo*. *Bio-protocol*, 4(19), e1254.
- Al Tameemi, W., Dale, T. P., Al-Jumaily, R. and Forsyth, N. R. (2019) Hypoxia-Modified Cancer Cell Metabolism. *Frontiers in Cell and Developmental Biology*, 7, p. 4.
- Allen P. J. (2017) The diagnosis and management of cystic lesions of the pancreas. *Chinese Clinical Oncology*, 6(6), p. 60.

Allen, P., Kuk, D., Castillo, C., Basturk, O., Wolfgang, C., Cameron, J., Lillemoe, K., Ferrone, C., Morales-Oyarvide, V., He, J., Weiss, M., Hruban, R., Gönen, M., Klimstra, D. and Mino-Kenudson, M. (2017) Multi-institutional Validation Study of the American Joint Commission on Cancer (8th Edition) Changes for T and N Staging in Patients with Pancreatic Adenocarcinoma. *Annals of Surgery*, 265(1), pp.185-191.

American Cancer Society Surgery for Pancreatic Cancer. [(accessed on 12 May 2017)]; Available online: <https://www.cancer.org/cancer/pancreatic-cancer/treating/surgery.html>

Amos, L. A. and Löwe, J. (1999) How Taxol stabilises microtubule structure. *Chemistry and Biology*, 6(3), R65–R69.

Andersen, D. K., Korc, M., Petersen, G. M., Eibl, G., Li, D., Rickels, M. R., Chari, S. T. and Abbruzzese, J. L. (2017) Diabetes, pancreatogenic diabetes, and pancreatic cancer. *Diabetes*, 66(5), pp. 1103–1110.

Ankeny, J. S., Court, C. M., Hou, S., Li, Q., Song, M., Wu, D., Chen, J. F., Lee, T., Lin, M., Sho, S., Rochefort, M. M., Girgis, M. D., Yao, J., Wainberg, Z. A., Muthusamy, V. R., Watson, R. R., Donahue, T. R., Hines, O. J., Reber, H. A., Graeber, T. G., ... Tomlinson, J. S. (2016) Circulating tumour cells as a biomarker for diagnosis and staging in pancreatic cancer. *British Journal of Cancer*, 114(12), pp. 1367–1375.

Ansari, D., Aronsson, L., Sasor, A., Welinder, C., Rezeli, M., Marko-Varga, G. and Andersson, R. (2014) The role of quantitative mass spectrometry in the discovery of pancreatic cancer biomarkers for translational science. *Journal of Translational Medicine*, 12(1), p. 87.

Ansari, D., Gustafsson, A. and Andersson, R. (2015) Update on the management of pancreatic cancer: Surgery is not enough. *World Journal of Gastroenterology*, 21(11), pp. 3157-3165.

Appleby, P. N., Crowe, F. L., Bradbury, K. E., Travis, R. C. and Key, T. J. (2016) Mortality in vegetarians and comparable nonvegetarians in the United Kingdom. *The American Journal of Clinical Nutrition*, 103(1), pp. 218–230.

Arnold, L. D., Patel, A. V., Yan, Y., Jacobs, E. J., Thun, M. J., Calle, E. E. and Colditz, G. A. (2009) Are racial disparities in pancreatic cancer explained by smoking and overweight/obesity? *Cancer Epidemiology, Biomarkers and Prevention: A Publication of the American Association for Cancer Research, cosponsored by the American Society of Preventive Oncology*, 18(9), pp. 2397–2405.

Aslan, M., Shahbazi, R., Ulubayram, K. and Ozpolat, B. (2018) Targeted Therapies for Pancreatic Cancer and Hurdles Ahead. *Anticancer Research*, 38(12), pp. 6591-6606.

Aune, D., Greenwood, D. C., Chan, D. S., Vieira, R., Vieira, A. R., Navarro Rosenblatt, D. A., Cade, J. E., Burley, V. J. and Norat, T. (2012) Body mass index, abdominal fatness and pancreatic cancer risk: a systematic review and non-linear dose-response meta-analysis of prospective studies. *Annals of Oncology: Official Journal of the European Society for Medical Oncology*, 23(4), pp. 843–852.

Banerjee, P., Geng, T., Mahanty, A., Li, T., Zong, L. and Wang, B. (2019) Integrating the drug, disulfiram into the vitamin E-TPGS-modified PEGylated nanostructured lipid carriers to synergize its repurposing for anti-cancer therapy of solid tumors. *International Journal of Pharmaceutics*, 557, pp. 374-389.

Bapat, A., Hostetter, G., Von Hoff, D. and Han, H. (2011) Perineural invasion and associated pain in pancreatic cancer. *Nature Reviews Cancer*, 11(10), pp. 695-707.

Beaney, A. J., Banim, P., Luben, R., Lentjes, M., Khaw, K. T. and Hart, A. R. (2017) Higher meat intake is positively associated with higher risk of developing pancreatic cancer in an age-

dependent manner and are modified by plasma antioxidants: A prospective cohort study (EPIC-Norfolk) using data from food diaries. *Pancreas*, 46(5), pp. 672–678.

Begicevic, R. R. and Falasca, M. (2017) ABC transporters in cancer stem cells: Beyond chemoresistance. *International Journal of Molecular Sciences*, 18(11), p. 2362.

Beijersbergen, R. (2020) Old drugs with new tricks. *Nature Cancer*, 1(2), pp. 153-155.

Bhowmick, N. A., Neilson, E. G. and Moses, H. L. (2004) Stromal fibroblasts in cancer initiation and progression. *Nature*, 432(7015), pp. 332–337.

Binicier, O. B. and Pakoz, Z. B. (2019) CA 19-9 levels in patients with acute pancreatitis due to gallstone and metabolic/toxic reasons. *Revista da Associacao Medica Brasileira (1992)*, 65(7), pp. 965–970.

Biswas, K. (2020) Molecular mobility-mediated regulation of e-cadherin adhesion. *Trends in Biochemical Sciences*, 45(2), pp. 163-173.

Blackford, A., Parmigiani, G., Kensler, T. W., Wolfgang, C., Jones, S., Zhang, X., Parsons, D. W., Lin, J. C., Leary, R. J., Eshleman, J. R., Goggins, M., Jaffee, E. M., Iacobuzio-Donahue, C. A., Maitra, A., Klein, A., Cameron, J. L., Olino, K., Schulick, R., Winter, J., Vogelstein, B., ... Hruban, R. H. (2009a) Genetic mutations associated with cigarette smoking in pancreatic cancer. *Cancer Research*, 69(8), pp. 3681–3688.

Blackford, A., Serrano, O., Wolfgang, C., Parmigiani, G., Jones, S., Zhang, X., Parsons, D., Lin, J., Leary, R., Eshleman, J., Goggins, M., Jaffee, E., Iacobuzio-Donahue, C., Maitra, A., Cameron, J., Olino, K., Schulick, R., Winter, J., Herman, J., Laheru, D., Klein, A., Vogelstein, B., Kinzler, K., Velculescu, V. and Hruban, R. (2009b) SMAD4 gene mutations are associated with poor prognosis in pancreatic cancer. *Clinical Cancer Research*, 15(14), pp. 4674-4679.

Blondy, S., David, V., Verdier, M., Mathonnet, M., Perraud, A. and Christou, N. (2020) 5-Fluorouracil resistance mechanisms in colorectal cancer: From classical pathways to promising processes. *Cancer Science*, 111(9), pp. 3142–3154.

Blum, R. and Kloog, Y. (2014) Metabolism addiction in pancreatic cancer. *Cell Death and Disease*, 5(2), pp. e1065-e1065.

Bonetti, P., Climent, M., Panebianco, F., Tordonato, C., Santoro, A., Marzi, M., Pelicci, P., Ventura, A. and Nicassio, F. (2018) Dual role for miR-34a in the control of early progenitor proliferation and commitment in the mammary gland and in breast cancer. *Oncogene*, 38(3), pp. 360-374.

Borazanci, E., Millis, S. Z., Korn, R., Han, H., Whatcott, C. J., Gatalica, Z., Barrett, M. T., Cridebring, D. and Von Hoff, D. D. (2015) Adenosquamous carcinoma of the pancreas: Molecular characterization of 23 patients along with a literature review. *World Journal of Gastrointestinal Oncology*, 7(9), pp. 132–140.

Brachi, G., Bussolino, F., Ciardelli, G. and Mattu, C. (2019) Nanomedicine for Imaging and Therapy of Pancreatic Adenocarcinoma. *Frontiers in Bioengineering and Biotechnology*, 7, p. 307.

Brown, A. and Patel, C. (2016) A review of validation strategies for computational drug repositioning. *Briefings in Bioinformatics*, 19(1), pp. 174-177.

Bulle, A. and Lim, K. H. (2020) Beyond just a tight fortress: contribution of stroma to epithelial-mesenchymal transition in pancreatic cancer. *Signal Transduction and Targeted Therapy*, 5(1), p. 249.

Bulle, A., Dekervel, J., Van der Merwe, S., Van cutsem, E., Verslype, C. and Van Pelt, J., (2017) Relevance of the stroma in pancreatic ductal adenocarcinoma and its challenges for translational research. *Journal of Cancer Treatment and Diagnosis*. 2(1), pp. 1-15.

Butcher, K., Kannappan, V., Kilari, R. S., Morris, M. R., McConville, C., Armesilla, A. L. and Wang, W. (2018). Investigation of the key chemical structures involved in the anticancer activity of disulfiram in A549 non-small cell lung cancer cell line. *BMC cancer*, 18(1), p. 753.

Cannito, S., Novo, E., Compagnone, A., Valfrè di Bonzo, L., Busletta, C., Zamara, E., Paternostro, C., Povero, D., Bandino, A., Bozzo, F., Cravanzola, C., Bravoco, V., Colombatto, S. and Parola, M. (2008) Redox mechanisms switch on hypoxia-dependent epithelial-mesenchymal transition in cancer cells. *Carcinogenesis*, 29(12), pp.2267–2278.

Cao, L., Xiao, X., Lei, J., Duan, W., Ma, Q. and Li, W. (2016) Curcumin inhibits hypoxia-induced epithelial-mesenchymal transition in pancreatic cancer cells via suppression of the hedgehog signaling pathway. *Oncology Reports*, 35(6), pp.3728–3734.

Cao, Z., Wang, Z. and Leng, P. (2019) Aberrant N-cadherin expression in cancer. *Biomedicine and Pharmacotherapy*, 118, p.109320.

Carnero, A. and Leonart, M. (2016) The hypoxic microenvironment: A determinant of cancer stem cell evolution. *BioEssays: News and Reviews in Molecular, Cellular and Developmental Biology*, 38 Suppl 1, pp. S65–S74.

Carrato, A., Falcone, A., Ducreux, M., Valle, J. W., Parnaby, A., Djazouli, K., Alnwick-Allu, K., Hutchings, A., Palaska, C. and Parthenaki, I. (2015) A systematic review of the burden of pancreatic cancer in Europe: Real-world impact on survival, quality of life and costs. *Journal of Gastrointestinal Cancer*, 46(3), pp. 201–211.

Cavo, M., Delle Cave, D., D'Amone, E., Gigli, G., Lonardo, E. and Del Mercato, L. L. (2020) A synergic approach to enhance long-term culture and manipulation of MiaPaCa-2 pancreatic cancer spheroids. *Scientific Reports*, 10(1), p.10192.

Cervantes-Villagrana, R. D., Albores-García, D., Cervantes-Villagrana, A. R. and García-Acevez, S. J. (2020) Tumor-induced neurogenesis and immune evasion as targets of innovative anti-cancer therapies. *Signal Transduction and Targeted Therapy*, 5(1), p. 99.

Chang, H. H., Moro, A., Chou, C., Dawson, D. W., French, S., Schmidt, A. I., Sinnott-Smith, J., Hao, F., Hines, O. J., Eibl, G. and Rozengurt, E. (2018) Metformin decreases the incidence of pancreatic ductal adenocarcinoma promoted by diet-induced obesity in the conditional *kras*<sup>12d</sup> mouse model. *Scientific Reports*, 8(1), p. 5899.

Chang, Q., Jurisica, I., Do, T. and Hedley, D. W. (2011) Hypoxia predicts aggressive growth and spontaneous metastasis formation from orthotopically grown primary xenografts of human pancreatic cancer. *Cancer Research*, 71(8), pp. 3110–3120.

Chauhan, V., Boucher, Y., Ferrone, C., Roberge, S., Martin, J., Stylianopoulos, T., Bardeesy, N., DePinho, R., Padera, T., Munn, L. and Jain, R. (2014) Compression of pancreatic tumor blood vessels by hyaluronan is caused by solid stress and not interstitial fluid pressure. *Cancer Cell*, 26(1), pp.14-15.

Chefetz, I., Alvero, A. B., Holmberg, J. C., Lebowitz, N., Craveiro, V., Yang-Hartwich, Y., Yin, G., Squillace, L., Gurra Soteras, M., Aldo, P. and Mor, G. (2013) TLR2 enhances ovarian cancer stem cell self-renewal and promotes tumor repair and recurrence. *Cell Cycle (Georgetown, Tex.)*, 12(3), pp. 511–521.

Chen, S., Kuo, T., Liao, Y., Lin, M., Tien, Y. and Huang, M. (2018) Silencing of MUC20 suppresses the malignant character of pancreatic ductal adenocarcinoma cells through inhibition of the HGF/MET pathway. *Oncogene*, 37(46), pp.6041-6053.

Chen, Y. C., Hsu, H. S., Chen, Y. W., Tsai, T. H., How, C. K., Wang, C. Y., Hung, S. C., Chang, Y. L., Tsai, M. L., Lee, Y. Y., Ku, H. H. and Chiou, S. H. (2008) Oct-4 expression maintained cancer stem-like properties in lung cancer-derived CD133-positive cells. *PLoS One*, 3(7), p. e2637.

Cheng, G., Zielonka, J., McAllister, D., Tsai, S., Dwinell, M. B. and Kalyanaraman, B. (2014) Profiling and targeting of cellular bioenergetics: inhibition of pancreatic cancer cell proliferation. *British Journal of Cancer*, 111(1), pp. 85–93.

Cheng, Z. X., Sun, B., Wang, S. J., Gao, Y., Zhang, Y. M., Zhou, H. X., Jia, G., Wang, Y. W., Kong, R., Pan, S. H., Xue, D. B., Jiang, H. C. and Bai, X. W. (2011) Nuclear factor- $\kappa$ B-dependent epithelial to mesenchymal transition induced by HIF-1 $\alpha$  activation in pancreatic cancer cells under hypoxic conditions. *PLoS One*, 6(8), p. e23752.

Chenthamara, D., Subramaniam, S., Ramakrishnan, S. G., Krishnaswamy, S., Essa, M. M., Lin, F. H. and Qoronfleh, M. W. (2019) Therapeutic efficacy of nanoparticles and routes of administration. *Biomaterials Research*, 23, p. 20.

Cheriyian, V. T., Wang, Y., Muthu, M., Jamal, S., Chen, D., Yang, H., Polin, L. A., Tarca, A. L., Pass, H. I., Dou, Q. P., Sharma, S., Wali, A. and Rishi, A. K. (2014) Disulfiram suppresses growth of the malignant pleural mesothelioma cells in part by inducing apoptosis. *PLoS One*, 9(4), p. e93711.

Cong, J., Wang, Y., Zhang, X., Zhang, N., Liu, L., Soukup, K., Michelakos, T., Hong, T., DeLeo, A., Cai, L., Sabbatino, F., Ferrone, S., Lee, H., Levina, V., Fuchs, B., Tanabe, K.,

Lillemoe, K., Ferrone, C. and Wang, X. (2017) A novel chemoradiation targeting stem and nonstem pancreatic cancer cells by repurposing disulfiram. *Cancer Letters*, 409, pp. 9–19.

Corrie, P. G., Qian, W., Basu, B., Valle, J. W., Falk, S., Lwuj, C., Wasan, H., Palmer, D., Scott-Brown, M., Wadsley, J., Arif, S., Bridgewater, J., Propper, D., Gillmore, R., Gopinathan, A., Skells, R., Bundi, P., Brais, R., Dalchau, K., Bax, L., ... Jodrell, D. I. (2020) Scheduling nab-paclitaxel combined with gemcitabine as first-line treatment for metastatic pancreatic adenocarcinoma. *British Journal of Cancer*, 122(12), pp. 1760–1768.

Corsello, S. M., Nagari, R. T., Spangler, R. D., Rossen, J., Kocak, M., Bryan, J. G., Humeidi, R., Peck, D., Wu, X., Tang, A. A., Wang, V. M., Bender, S. A., Lemire, E., Narayan, R., Montgomery, P., Ben-David, U., Garvie, C. W., Chen, Y., Rees, M. G., Lyons, N. J., ... Golub, T. R. (2020) Discovering the anti-cancer potential of non-oncology drugs by systematic viability profiling. *Nature Cancer*, 1(2), pp. 235–248.

Cortes-Dericks, L., Yazd, E. F., Mowla, S. J., Schmid, R. A. and Karoubi, G. (2013) Suppression of OCT4B enhances sensitivity of lung adenocarcinoma A549 cells to cisplatin via increased apoptosis. *Anticancer Research*, 33(12), pp. 5365–5373.

Cousins, F. L., Murray, A. A., Scanlon, J. P. and Saunders, P. T. (2016) Hypoxyprobe<sup>TM</sup> reveals dynamic spatial and temporal changes in hypoxia in a mouse model of endometrial breakdown and repair. *BMC Research Notes*, 9, p. 30.

Da Ros, M., De Gregorio, V., Iorio, A. L., Giunti, L., Guidi, M., de Martino, M., Genitori, L. and Sardi, I. (2018) Glioblastoma chemoresistance: The double play by microenvironment and blood-brain barrier. *International Journal of Molecular Sciences*, 19(10), p. 2879.

Daniel, S. K., Sullivan, K. M., Labadie, K. P. and Pillarisetty, V. G. (2019) Hypoxia as a barrier to immunotherapy in pancreatic adenocarcinoma. *Clinical and Translational Medicine*, 8(1), p. 10.

Daoud, A. Z., Mulholland, E. J., Cole, G. and McCarthy, H. O. (2019). MicroRNAs in Pancreatic Cancer: biomarkers, prognostic, and therapeutic modulators. *BMC Cancer*, 19(1), p. 1130.

Dastjerdi, M., Hashemibeni, B., Kazemi, M., Salehi, M. and Babazadeh, Z. (2014) Comparison of the anti-cancer effect of Disulfiram and 5-Aza-CdR on pancreatic cancer cell line PANC-1. *Advanced Biomedical Research*, 3(1), p.156.

De Sousa Cavalcante, L. and Monteiro, G. (2014) Gemcitabine: Metabolism and molecular mechanisms of action, sensitivity and chemoresistance in pancreatic cancer. *European Journal of Pharmacology*, 741, pp. 8-16.

Deepak, S., Kottapalli, K., Rakwal, R., Oros, G., Rangappa, K., Iwahashi, H., Masuo, Y. and Agrawal, G. (2007) Real-time PCR: Revolutionizing detection and expression analysis of genes. *Current Genomics*, 8(4), pp. 234–251.

Demchenko A. P. (2013) Beyond annexin V: fluorescence response of cellular membranes to apoptosis. *Cytotechnology*, 65(2), pp. 157–172.

Diasio, R. B. and Harris, B. E. (1989) Clinical pharmacology of 5-fluorouracil. *Clinical Pharmacokinetics*, 16(4), pp. 215–237.

D'Ignazio, L. and Rocha, S. (2016) Hypoxia induced NF- $\kappa$ B. *Cells*, 5(1), p. 10.

D'Ignazio, L., Batie, M. and Rocha, S. (2017) Hypoxia and inflammation in cancer, focus on HIF and NF- $\kappa$ B. *Biomedicines*, 5(2), p. 21.

- Dillhoff, M., Liu, J., Frankel, W., Croce, C. and Bloomston, M. (2008) MicroRNA-21 is overexpressed in pancreatic cancer and a potential predictor of survival. *Journal of Gastrointestinal Surgery: Official Journal of the Society for Surgery of the Alimentary Tract*, 12(12), pp. 2171–2176.
- Dinavahi, S., Bazewicz, C., Gowda, R. and Robertson, G. (2019) Aldehyde dehydrogenase inhibitors for cancer therapeutics. *Trends in Pharmacological Sciences*, 40(10), pp.774-789.
- Distler, M., Aust, D., Weitz, J., Pilarsky, C. and Grützmann, R. (2014) Precursor lesions for sporadic pancreatic cancer: PanIN, IPMN, and MCN. *BioMed Research International*, 2014, pp.1-11.
- D'Occhio, M., Campanile, G., Zicarelli, L., Visintin, J. and Baruselli, P. (2020) Adhesion molecules in gamete transport, fertilization, early embryonic development, and implantation—role in establishing a pregnancy in cattle: A review. *Molecular Reproduction and Development*, 87(2), pp. 206-222.
- Dolenšek, J., Rupnik, M. and Stožer, A. (2015) Structural similarities and differences between the human and the mouse pancreas. *Islets*, 7(1), p. e1024405.
- Domenichini, A., Edmands, J., Adamska, A., Begicevic, R., Paternoster, S. and Falasca, M. (2019) Pancreatic cancer tumorspheres are cancer stem-like cells with increased chemoresistance and reduced metabolic potential. *Advances in Biological Regulation*, 72, pp. 63-77.
- Dong, J., Zhao, Y. P., Zhou, L., Zhang, T. P. and Chen, G. (2011) Bcl-2 upregulation induced by miR-21 via a direct interaction is associated with apoptosis and chemoresistance in MIA PaCa-2 pancreatic cancer cells. *Archives of Medical Research*, 42(1), pp. 8–14.

Döppler, H., Liou, G. Y. and Storz, P. (2013) Downregulation of TRAF2 mediates NIK-induced pancreatic cancer cell proliferation and tumorigenicity. *PloS One*, 8(1), p. e53676.

Du, J., Gu, J. and Li, J. (2020) Mechanisms of drug resistance of pancreatic ductal adenocarcinoma at different levels. *Bioscience Reports*, 40(7), BSR20200401.

El Jellas, K., Hoem, D., Hagen, K., Kalvenes, M., Aziz, S., Steine, S., Immervoll, H., Johansson, S. and Molven, A., (2017) Associations between ABO blood groups and pancreatic ductal adenocarcinoma: influence on resection status and survival. *Cancer Medicine*, 6(7), pp.1531-1540.

Ellis, H. (2013) Anatomy of the pancreas and the spleen. *Surgery (Oxford)*, 31(6), pp.263-266.

Eom, S., Hwang, S., Yeom, H. and Lee, M. (2019) An ATG5 knockout promotes paclitaxel resistance in v-Ha-ras-transformed NIH 3T3 cells. *Biochemical and Biophysical Research Communications*, 513(1), pp.234-241.

Erkan, M., Hausmann, S., Michalski, C. W., Fingerle, A. A., Dobritz, M., Kleeff, J. and Friess, H. (2012) The role of stroma in pancreatic cancer: diagnostic and therapeutic implications. *Nature Reviews. Gastroenterology and Hepatology*, 9(8), pp. 454–467.

Erkan, M., Kurtoglu, M. and Kleeff, J. (2016) The role of hypoxia in pancreatic cancer: a potential therapeutic target? *Expert review of gastroenterology and hepatology*, 10(3), pp. 301–316.

Fasehee, H., Dinarvand, R., Ghavamzadeh, A., Esfandyari-Manesh, M., Moradian, H., Faghihi, S. and Ghaffari, S. H. (2016) Delivery of disulfiram into breast cancer cells using folate-receptor-targeted PLGA-PEG nanoparticles: in vitro and in vivo investigations. *Journal of Nanobiotechnology*, 14, p. 32.

Feig, C., Gopinathan, A., Neesse, A., Chan, D. S., Cook, N. and Tuveson, D. A. (2012) The pancreas cancer microenvironment. *Clinical Cancer Research: An Official Journal of the American Association for Cancer Research*, 18(16), pp. 4266–4276.

Fiorini, C., Cordani, M., Gotte, G., Picone, D. and Donadelli, M. (2015) Onconase induces autophagy sensitizing pancreatic cancer cells to gemcitabine and activates Akt/mTOR pathway in a ROS-dependent manner. *Biochimica et Biophysica Acta (BBA) - Molecular Cell Research*, 1853(3), pp.549-560.

Flannick, J. and Florez, J. C. (2016) Type 2 diabetes: genetic data sharing to advance complex disease research. *Nature Reviews. Genetics*, 17(9), pp. 535–549.

Fletcher, J. I., Williams, R. T., Henderson, M. J., Norris, M. D. and Haber, M. (2016) ABC transporters as mediators of drug resistance and contributors to cancer cell biology. *Drug Resistance Updates: Reviews and Commentaries in Antimicrobial and Anticancer Chemotherapy*, 26, pp. 1–9.

Formenti, S. C. and Demaria, S. (2013) Combining radiotherapy and cancer immunotherapy: a paradigm shift. *Journal of the National Cancer Institute*, 105(4), pp.256–265.

Fournet, G., Martin, G. and Quash, G. (2013)  $\alpha,\beta$ -Acetylenic amino thiolester inhibitors of aldehyde dehydrogenases 1 and 3: suppressors of apoptogenic aldehyde oxidation and activators of apoptosis. *Current Medicinal Chemistry*, 20(4), pp. 527–533.

Fox, A., Dutt, T. S., Karger, B., Rojas, M., Obregón-Henao, A., Anderson, G. B. and Henao-Tamayo, M. (2020) Cyto-feature engineering: A pipeline for flow cytometry analysis to uncover immune populations and associations with disease. *Scientific Reports*, 10(1), p. 7651.

Fu, J., Xu, Y., Yang, Y., Liu, Y., Ma, L. and Zhang, Y. (2019) Aspirin suppresses chemoresistance and enhances antitumor activity of 5-Fu in 5-Fu-resistant colorectal cancer by abolishing 5-Fu-induced NF- $\kappa$ B activation. *Scientific Reports*, 9(1).

Furukawa, T., Kuboki, Y., Tanji, E., Yoshida, S., Hatori, T., Yamamoto, M., Shibata, N., Shimizu, K., Kamatani, N. and Shiratori, K. (2011) Whole-exome sequencing uncovers frequent GNAS mutations in intraductal papillary mucinous neoplasms of the pancreas. *Scientific Reports*, 1, p. 161.

Gangemi, R. M., Griffero, F., Marubbi, D., Perera, M., Capra, M. C., Malatesta, P., Ravetti, G. L., Zona, G. L., Daga, A. and Corte, G. (2009) SOX2 silencing in glioblastoma tumor-initiating cells causes stop of proliferation and loss of tumorigenicity. *Stem Cells (Dayton, Ohio)*, 27(1), pp. 40–48.

Gao, Y. and Liu, S. (2006) The effect of human equilibrative nucleoside transport (hENTs) in pancreatic cancer cell membrane on the cytotoxicity of 5-fluorouracil. *Xiandai Yixue*. 34, pp. 149–153.

Garajová, I., Le Large, T., Frampton, A., Rolfo, C., Voortman, J. and Giovannetti, E. (2014) Molecular mechanisms underlying the role of MicroRNAs in the chemoresistance of pancreatic cancer. *BioMed Research International*, pp. 1-17.

Garofalo, M. and Croce, C. (2013) MicroRNAs as therapeutic targets in chemoresistance. *Drug Resistance Updates*, 16(3-5), pp.47-59.

Geng, H., Xue, C., Mendonca, J., Sun, X. X., Liu, Q., Reardon, P. N., Chen, Y., Qian, K., Hua, V., Chen, A., Pan, F., Yuan, J., Dang, S., Beer, T. M., Dai, M. S., Kachhap, S. K. and Qian, D. Z. (2018) Interplay between hypoxia and androgen controls a metabolic switch conferring resistance to androgen/AR-targeted therapy. *Nature Communications*, 9(1), p.4972.

Genkinger, J. M., Kitahara, C. M., Bernstein, L., Berrington de Gonzalez, A., Brotzman, M., Elena, J. W., Giles, G. G., Hartge, P., Singh, P. N., Stolzenberg-Solomon, R. Z., Weiderpass, E., Adami, H. O., Anderson, K. E., Beane-Freeman, L. E., Buring, J. E., Fraser, G. E., Fuchs, C. S., Gapstur, S. M., Gaziano, J. M., Helzlsouer, K. J., ... Jacobs, E. J. (2015) Central adiposity, obesity during early adulthood, and pancreatic cancer mortality in a pooled analysis of cohort studies. *Annals of Oncology: Official Journal of the European Society for Medical Oncology*, 26(11), pp. 2257–2266.

Ghaneh, P., Costello, E. and Neoptolemos, J. P. (2008) Biology and management of pancreatic cancer. *Postgraduate Medical Journal*, 84(995), pp. 478–497.

Ghita, M., Dunne, V., Hanna, G., Prise, K., Williams, J. and Butterworth, K. (2019) Preclinical models of radiation-induced lung damage: challenges and opportunities for small animal radiotherapy. *The British Journal of Radiology*, 92(1095), p.20180473.

Gidwani, B. and Vyas, A. (2015) A comprehensive review on cyclodextrin-based carriers for delivery of chemotherapeutic cytotoxic anticancer drugs. *BioMed Research International*, 2015, p. 198268.

Giordano, G., Pancione, M., Olivieri, N., Parcesepe, P., Velocci, M., Di Raimo, T., Coppola, L., Toffoli, G. and D'Andrea, M. (2017) Nano albumin bound-paclitaxel in pancreatic cancer: Current evidences and future directions. *World Journal of Gastroenterology*, 23(32), p.5875.

Giovannetti, E., Erozenski, A., Smit, J., Danesi, R. and Peters, G. (2012) Molecular mechanisms underlying the role of microRNAs (miRNAs) in anticancer drug resistance and implications for clinical practice. *Critical Reviews in Oncology/Hematology*, 81(2), pp.103-122.

Giovannetti, E., Funel, N., Peters, G. J., Del Chiaro, M., Erozenski, L. A., Vasile, E., Leon, L. G., Pollina, L. E., Groen, A., Falcone, A., Danesi, R., Campani, D., Verheul, H. M. and Boggi,

U. (2010) MicroRNA-21 in pancreatic cancer: correlation with clinical outcome and pharmacologic aspects underlying its role in the modulation of gemcitabine activity. *Cancer Research*, 70(11), pp. 4528–4538.

Goan, Y. G., Zhou, B., Hu, E., Mi, S. and Yen, Y. (1999) Overexpression of ribonucleotide reductase as a mechanism of resistance to 2,2-difluorodeoxycytidine in the human KB cancer cell line. *Cancer Research*, 59(17), pp. 4204–4207.

Goldsmith, C., Plowman, P., Green, M., Dale, R. and Price, P. (2018) Stereotactic ablative radiotherapy (SABR) as primary, adjuvant, consolidation and re-treatment option in pancreatic cancer: scope for dose escalation and lessons for toxicity. *Radiation Oncology*, 13(1), p. 204.

Goldstein, D., El-Maraghi, R. H., Hammel, P., Heinemann, V., Kunzmann, V., Sastre, J., Scheithauer, W., Siena, S., Tabernero, J., Teixeira, L., Tortora, G., Van Laethem, J. L., Young, R., Penenberg, D. N., Lu, B., Romano, A. and Von Hoff, D. D. (2015) nab-Paclitaxel plus gemcitabine for metastatic pancreatic cancer: long-term survival from a phase III trial. *Journal of the National Cancer Institute*, 107(2), p. dju413.

Goto, Y., Nakamura, A., Ashida, R., Sakanaka, K., Itasaka, S., Shibuya, K., Matsumoto, S., Kanai, M., Isoda, H., Masui, T., Kodama, Y., Takaori, K., Hiraoka, M. and Mizowaki, T. (2018) Clinical evaluation of intensity-modulated radiotherapy for locally advanced pancreatic cancer. *Radiation Oncology*, 13(1).

Gottesman, M., Fojo, T. and Bates, S. (2002) Multidrug resistance in cancer: role of ATP-dependent transporters. *Nature Reviews Cancer*, 2(1), pp.48-58.

Grasso, C., Jansen, G. and Giovannetti, E. (2017) Drug resistance in pancreatic cancer: Impact of altered energy metabolism. *Critical Reviews in Oncology/Hematology*, 114, pp.139-152.

Grinberg-Bleyer, Y., Oh, H., Desrichard, A., Bhatt, D. M., Caron, R., Chan, T. A., Schmid, R. M., Klein, U., Hayden, M. S. and Ghosh, S. (2017) NF- $\kappa$ B c-Rel is crucial for the regulatory T cell immune checkpoint in cancer. *Cell*, 170(6), pp. 1096–1108.e13.

Guo, X., Xu, B., Pandey, S., Goessl, E., Brown, J., Armesilla, A. L., Darling, J. L. and Wang, W. (2010) Disulfiram/copper complex inhibiting NF $\kappa$ B activity and potentiating cytotoxic effect of gemcitabine on colon and breast cancer cell lines. *Cancer Letters*, 290(1), pp. 104–113.

Gupta, S. C., Sundaram, C., Reuter, S. and Aggarwal, B. B. (2010) Inhibiting NF- $\kappa$ B activation by small molecules as a therapeutic strategy. *Biochimica et Biophysica Acta*, 1799(10-12), pp. 775–787.

Gzil, A., Zarębska, I., Bursiewicz, W., Antosik, P., Grzanka, D. and Szyłberg, Ł. (2019) Markers of pancreatic cancer stem cells and their clinical and therapeutic implications. *Molecular Biology Reports*, 46(6), pp.6629-6645.

Hall, W. and Goodman, K. (2019) Radiation therapy for pancreatic adenocarcinoma, a treatment option that must be considered in the management of a devastating malignancy. *Radiation Oncology*, 14(1), p. 114.

Hamacher, R., Schmid, R. M., Saur, D. and Schneider, G. (2008) Apoptotic pathways in pancreatic ductal adenocarcinoma. *Molecular Cancer*, 7, p. 64.

Han, J., Liu, L., Yue, X., Chang, J., Shi, W. and Hua, Y. (2013) A binuclear complex constituted by diethyldithiocarbamate and copper(I) functions as a proteasome activity inhibitor in pancreatic cancer cultures and xenografts. *Toxicology and Applied Pharmacology*, 273(3), pp. 477–483.

- Han, X., Li, Y., Xu, Y., Zhao, X., Zhang, Y., Yang, X., Wang, Y., Zhao, R., Anderson, G., Zhao, Y. and Nie, G. (2018) Reversal of pancreatic desmoplasia by re-educating stellate cells with a tumour microenvironment-activated nanosystem. *Nature Communications*, 9(1).
- Hari, Y., Harashima, N., Tajima, Y. and Harada, M. (2015) Bcl-xL inhibition by molecular-targeting drugs sensitizes human pancreatic cancer cells to TRAIL. *Oncotarget*, 6(39), pp. 41902–41915.
- Harris A. L. (2002) Hypoxia--a key regulatory factor in tumour growth. *Nature Reviews. Cancer*, 2(1), pp.38–47.
- Hart, T., Dider, S., Han, W., Xu, H., Zhao, Z. and Xie, L. (2016). Toward repurposing metformin as a precision anti-cancer therapy using structural systems pharmacology. *Scientific Reports*, 6, p. 20441.
- Hassan, I., Ebaid, H., Alhazza, I. M., Al-Tamimi, J., Aman, S. and Abdel-Mageed, A. M. (2019) Copper mediates anti-inflammatory and antifibrotic activity of gleevec in hepatocellular carcinoma-induced male rats. *Canadian Journal of Gastroenterology and Hepatology*, p.9897315.
- Hassan, I., Khan, A., Aman, S., Qamar, W., Ebaid, H., Al-Tamimi, J., Alhazza, I. and Rady, A. (2018) Restrained management of copper level enhances the antineoplastic activity of imatinib in vitro and in vivo. *Scientific Reports*, 8(1), p.1682.
- Hayden, M. (2004) Signaling to NF- B. *Genes and Development*, 18(18), pp.2195-2224.
- Hayden, M. and Ghosh, S. (2008) Shared Principles in NF-κB signaling. *Cell*, 132(3), pp.344-362.

He, X., Wang, J., Wei, W., Shi, M., Xin, B., Zhang, T. and Shen, X. (2016) Hypoxia regulates ABCG2 activity through the activation of ERK1/2/HIF-1 $\alpha$  and contributes to chemoresistance in pancreatic cancer cells. *Cancer Biology and Therapy*, 17(2), pp.188–198.

Heddleston, J., Li, Z., Lathia, J., Bao, S., Hjelmeland, A. and Rich, J. (2010) Hypoxia inducible factors in cancer stem cells. *British Journal of Cancer*, 102(5), pp.789-795.

Herrington, F., Carmody, R. and Goodyear, C. (2015) Modulation of NF- $\kappa$ B Signaling as a therapeutic target in autoimmunity. *Journal of Biomolecular Screening*, 21(3), pp.223-242.

Herrmann, H., Häner, M., Brettel, M., Müller, S., Goldie, K., Fedtke, B., Lustig, A., Franke, W. and Aebi, U. (1996) Structure and assembly properties of the intermediate filament protein vimentin: The role of its head, rod and tail domains. *Journal of Molecular Biology*, 264(5), pp.933-953.

Hessmann, E., Patzak, M. S., Klein, L., Chen, N., Kari, V., Ramu, I., Bapiro, T. E., Frese, K. K., Gopinathan, A., Richards, F. M., Jodrell, D. I., Verbeke, C., Li, X., Heuchel, R., Löhr, J. M., Johnsen, S. A., Gress, T. M., Ellenrieder, V. and Neesse, A. (2018) Fibroblast drug scavenging increases intratumoural gemcitabine accumulation in murine pancreas cancer. *Gut*, 67(3), pp. 497–507.

Hicklin, D. and Ellis, L. (2005) Role of the Vascular Endothelial Growth Factor Pathway in Tumor Growth and Angiogenesis. *Journal of Clinical Oncology*, 23(5), pp.1011-1027.

Höckel, M. and Vaupel, P. (2001) Tumor hypoxia: definitions and current clinical, biologic, and molecular aspects. *Journal of the National Cancer Institute*, 93(4), pp.266–276.

Hoesel, B. and Schmid, J. (2013) The complexity of NF- $\kappa$ B signaling in inflammation and cancer. *Molecular Cancer*, 12(1), p.86.

Holcomb, B., Yip-Schneider, M. and Schmidt, C. M. (2008) The role of nuclear factor kappaB in pancreatic cancer and the clinical applications of targeted therapy. *Pancreas*, 36(3), pp. 225–235.

Horiuchi, T., Uwagawa, T., Shirai, Y., Saito, N., Iwase, R., Haruki, K., Shiba, H., Ohashi, T., and Yanaga, K. (2016) New treatment strategy with nuclear factor- $\kappa$ B inhibitor for pancreatic cancer. *The Journal of Surgical Research*, 206(1), pp.1–8.

Hu, J. J., Liu, X., Xia, S., Zhang, Z., Zhang, Y., Zhao, J., Ruan, J., Luo, X., Lou, X., Bai, Y., Wang, J., Hollingsworth, L. R., Magupalli, V. G., Zhao, L., Luo, H. R., Kim, J., Lieberman, J. and Wu, H. (2020) FDA-approved disulfiram inhibits pyroptosis by blocking gasdermin D pore formation. *Nature Immunology*, 21(7), pp.736–745.

Hu, J., Li, L., Chen, H., Zhang, G., Liu, H., Kong, R., Chen, H., Wang, Y., Li, Y., Tian, F., Lv, X., Li, G. and Sun, B. (2018) MiR-361-3p regulates ERK1/2-induced EMT via DUSP2 mRNA degradation in pancreatic ductal adenocarcinoma. *Cell Death and Disease*, 9(8).

Huang, F., Tang, J., Zhuang, X., Zhuang, Y., Cheng, W., Chen, W., Yao, H. and Zhang, S. (2014) MiR-196a promotes pancreatic cancer progression by targeting nuclear factor kappa-B-inhibitor alpha. *PloS One*, 9(2), p. e87897.

Huang, G., Zhang, J., Wang, X., Chen, Y., Liu, D. and Guo, S. (2019) Clinicopathological and prognostic significance of Nanog expression in non-small cell lung cancer: a meta-analysis. *Oncotargets and Therapy*, Volume 12, pp.3609-3617.

Huber, M., Azoitei, N., Baumann, B., Grünert, S., Sommer, A., Pehamberger, H., Kraut, N., Beug, H. and Wirth, T. (2004) NF- $\kappa$ B is essential for epithelial-mesenchymal transition and metastasis in a model of breast cancer progression. *Journal of Clinical Investigation*, 114(4), pp.569-581.

Hung, Y., Hsu, M., Chen, L., Hung, W. and Pan, M. (2019) Alteration of epigenetic modifiers in pancreatic cancer and its clinical implication. *Journal of Clinical Medicine*, 8(6), p.903.

Idachaba, S., Dada, O., Abimbola, O., Olayinka, O., Uma, A., Olunu, E. and Fakoya, A. (2019) A review of pancreatic cancer: epidemiology, genetics, screening, and management. *Open Access Macedonian Journal of Medical Sciences*, 7(4), pp.663-671.

Ishiwata, T., Matsuda, Y., Yoshimura, H., Sasaki, N., Ishiwata, S., Ishikawa, N., Takubo, K., Arai, T. and Aida, J. (2018) Pancreatic cancer stem cells: features and detection methods. *Pathology Oncology Research: POR*, 24(4), pp.797–805.

Ivanova, I., Park, C. and Kenneth, N. (2019) Translating the hypoxic response—the role of hif protein translation in the cellular response to low oxygen. *Cells*, 8(2), p.114.

Janiszewska, M., Primi, M. and Izard, T. (2020) Cell adhesion in cancer: Beyond the migration of single cells. *Journal of Biological Chemistry*, 295(8), pp.2495-2505.

Jariyal, H., Gupta, C., Bhat, V., Wagh, J. and Srivastava, A. (2019) Advancements in Cancer Stem Cell Isolation and Characterization. *Stem Cell Reviews and Reports*, 15(6), pp.755-773.

Jelski, W. and Mroczko, B. (2019) Biochemical diagnostics of pancreatic cancer - Present and future. *Clinica Chimica Acta; International Journal of Clinical Chemistry*, 498, pp. 47–51.

Jewer, M., Lee, L., Leibovitch, M., Zhang, G., Liu, J., Findlay, S. D., Vincent, K. M., Tandoc, K., Dieters-Castator, D., Quail, D. F., Dutta, I., Coatham, M., Xu, Z., Puri, A., Guan, B. J., Hatzoglou, M., Brumwell, A., Uniacke, J., Patsis, C., Koromilas, A., ... Postovit, L. M. (2020) Translational control of breast cancer plasticity. *Nature Communications*, 11(1), p. 2498.

Jia, Y. and Xie, J. (2015) Promising molecular mechanisms responsible for gemcitabine resistance in cancer. *Genes and Diseases*, 2(4), pp. 299–306.

Jiang, B., Zhou, L., Lu, J., Wang, Y., Liu, C., You, L. and Guo, J. (2020) Stroma-targeting therapy in pancreatic cancer: one coin with two sides? *Frontiers in Oncology*, 10, p. 576399.

Jiao, Y., N. Hannafon, B. and Ding, W. (2016) Disulfiram's anticancer activity: Evidence and mechanisms. *Anti-Cancer Agents in Medicinal Chemistry*, 16(11), pp.1378-1384.

Jin, M. Z. and Jin, W. L. (2020) The updated landscape of tumor microenvironment and drug repurposing. *Signal Transduction and Targeted Therapy*, 5(1), p.166.

Justus, C. R., Leffler, N., Ruiz-Echevarria, M. and Yang, L. V. (2014) In vitro cell migration and invasion assays. *Journal of Visualized Experiments: JoVE*, (88), p.51046.

Kabacaoglu, D., Ruess, D. A., Ai, J. and Algül, H. (2019) NF- $\kappa$ B/Rel transcription factors in pancreatic cancer: Focusing on RelA, c-Rel, and RelB. *Cancers*, 11(7), p.937.

Kalluri, R. and Zeisberg, M. (2006) Fibroblasts in cancer. *Nature Reviews. Cancer*, 6(5), pp.392–401.

Kampan, N. C., Madondo, M. T., McNally, O. M., Quinn, M. and Plebanski, M. (2015) Paclitaxel and its evolving role in the management of ovarian cancer. *BioMed Research International*, 2015, pp.413076.

Kashyap, V. K., Wang, Q., Setua, S., Nagesh, P., Chauhan, N., Kumari, S., Chowdhury, P., Miller, D. D., Yallapu, M. M., Li, W., Jaggi, M., Hafeez, B. B. and Chauhan, S. C. (2019) Therapeutic efficacy of a novel  $\beta$ III/ $\beta$ IV-tubulin inhibitor (VERU-111) in pancreatic cancer. *Journal of Experimental and Clinical Cancer Research: CR*, 38(1), p.29.

Kaufhold, S. and Bonavida, B. (2014) Central role of Snail1 in the regulation of EMT and resistance in cancer: a target for therapeutic intervention. *Journal of Experimental and Clinical Cancer Research*, 33(1).

Kaufhold, S., Garbán, H. and Bonavida, B. (2016) Yin Yang 1 is associated with cancer stem cell transcription factors (SOX2, OCT4, BMI1) and clinical implication. *Journal of Experimental and Clinical Cancer Research*, 35(1).

Khadka, R., Tian, W., Hao, X. and Koirala, R. (2018) Risk factor, early diagnosis and overall survival on outcome of association between pancreatic cancer and diabetes mellitus: Changes and advances, a review. *International Journal of Surgery (London, England)*, 52, pp.342–346.

Khalafalla, F. G., and Khan, M. W. (2017) Inflammation and Epithelial-Mesenchymal Transition in Pancreatic Ductal Adenocarcinoma: Fighting Against Multiple Opponents. *Cancer Growth and Metastasis*, 10, p.1179064417709287.

Khanna, C., Rosenberg, M. and Vail, D. (2015) A Review of Paclitaxel and Novel Formulations Including Those Suitable for Use in Dogs. *Journal of Veterinary Internal Medicine*, 29(4), pp.1006-1012.

Kim, B. N., Ahn, D. H., Kang, N., Yeo, C. D., Kim, Y. K., Lee, K. Y., Kim, T. J., Lee, S. H., Park, M. S., Yim, H. W., Park, J. Y., Park, C. K. and Kim, S. J. (2020) TGF- $\beta$  induced EMT and stemness characteristics are associated with epigenetic regulation in lung cancer. *Scientific Reports*, 10(1), p. 10597.

Kim, D., Choi, B. H., Ryoo, I. G. and Kwak, M. K. (2018) High NRF2 level mediates cancer stem cell-like properties of aldehyde dehydrogenase (ALDH)-high ovarian cancer cells: inhibitory role of all-trans retinoic acid in ALDH/NRF2 signaling. *Cell Death & Disease*, 9(9), p.896.

Kim, T. K. and Eberwine, J. H. (2010) Mammalian cell transfection: the present and the future. *Analytical and Bioanalytical Chemistry*, 397(8), pp.3173–3178.

Kleeff, J., Beckhove, P., Esposito, I., Herzig, S., Huber, P., Löhr, J. and Friess, H. (2007) Pancreatic cancer microenvironment. *International Journal of Cancer*, 121(4), pp.699-705.

Klein, A. P., Brune, K. A., Petersen, G. M., Goggins, M., Tersmette, A. C., Offerhaus, G. J., Griffin, C., Cameron, J. L., Yeo, C. J., Kern, S. and Hruban, R. H. (2004) Prospective risk of pancreatic cancer in familial pancreatic cancer kindreds. *Cancer Research*, 64(7), pp. 2634–2638.

Klutznny, S., Anurin, A., Nicke, B., Regan, J., Lange, M., Schulze, L., Parczyk, K. and Steigemann, P. (2018) PDE5 inhibition eliminates cancer stem cells via induction of PKA signaling. *Cell Death and Disease*, 9(2).

Knaack, H., Lenk, L., Philipp, L. M., Miarka, L., Rahn, S., Viol, F., Hauser, C., Egberts, J. H., Gundlach, J. P., Will, O., Tiwari, S., Mikulits, W., Schumacher, U., Hengstler, J. G. and Sebens, S. (2018) Liver metastasis of pancreatic cancer: the hepatic microenvironment impacts differentiation and self-renewal capacity of pancreatic ductal epithelial cells. *Oncotarget*, 9(60), pp.31771–31786.

Koh, H. K., Seo, S. Y., Kim, J. H., Kim, H. J., Chie, E. K., Kim, S. K. and Kim, I. H. (2019) Disulfiram, a re-positioned aldehyde dehydrogenase inhibitor, enhances radiosensitivity of human glioblastoma cells in vitro. *Cancer Research and Treatment*, 51(2), pp. 696–705.

Komarova, T. V., Sheshukova, E. V., Kosobokova, E. N., Kosorukov, V. S., Shindyapina, A. V., Lipskerov, F. A., Shpudeiko, P. S., Byalik, T. E. and Dorokhov, Y. L. (2019) The biological activity of bispecific trastuzumab/pertuzumab plant biosimilars may be drastically boosted by disulfiram increasing formaldehyde accumulation in cancer cells. *Scientific Reports*, 9(1), p. 16168.

Kong, R., Sun, B., Jiang, H., Pan, S., Chen, H., Wang, S., Krissansen, G. W. and Sun, X. (2010) Downregulation of nuclear factor-kappaB p65 subunit by small interfering RNA synergizes with gemcitabine to inhibit the growth of pancreatic cancer. *Cancer Letters*, 291(1), pp. 90–98.

Königer, J., Wente, M., Müller-Stich, B., di Mola, F., Gutt, C., Hinz, U., Müller, M., Friess, H. and Büchler, M. (2008) R2 resection in pancreatic cancer—does it make sense?. *Langenbeck's Archives of Surgery*, 393(6), pp.929-934.

Koong, A. C., Mehta, V. K., Le, Q. T., Fisher, G. A., Terris, D. J., Brown, J. M., Bastidas, A. J. and Vierra, M. (2000) Pancreatic tumors show high levels of hypoxia. *International Journal of Radiation Oncology, Biology, Physics*, 48(4), pp. 919–922.

Koppaka, V., Thompson, D. C., Chen, Y., Ellermann, M., Nicolaou, K. C., Juvonen, R. O., Petersen, D., Deitrich, R. A., Hurley, T. D. and Vasiliou, V. (2012) Aldehyde dehydrogenase inhibitors: a comprehensive review of the pharmacology, mechanism of action, substrate specificity, and clinical application. *Pharmacological Reviews*, 64(3), pp. 520–539.

Krebs, A. M., Mitschke, J., Laserra Losada, M., Schmalhofer, O., Boerries, M., Busch, H., Boettcher, M., Mougiakakos, D., Reichardt, W., Bronsert, P., Brunton, V. G., Pilarsky, C., Winkler, T. H., Brabletz, S., Stemmler, M. P. and Brabletz, T. (2017) The EMT-activator Zeb1 is a key factor for cell plasticity and promotes metastasis in pancreatic cancer. *Nature Cell Biology*, 19(5), pp. 518–529.

Krishnamurthy, P. and Schuetz, J. D. (2006) Role of ABCG2/BCRP in biology and medicine. *Annual Review of Pharmacology and Toxicology*, 46, pp.381–410.

Kulemann, B., Rösch, S., Seifert, S., Timme, S., Bronsert, P., Seifert, G., Martini, V., Kuvendjiska, J., Glatz, T., Hussung, S., Fritsch, R., Becker, H., Pitman, M. B. and Hoepfner,

J. (2017) Pancreatic cancer: Circulating tumor cells and primary tumors show heterogeneous KRAS mutations. *Scientific Reports*, 7(1), p. 4510.

Kurata, N., Fujita, H., Ohuchida, K., Mizumoto, K., Mahawithitwong, P., Sakai, H., Onimaru, M., Manabe, T., Ohtsuka, T. and Tanaka, M. (2011) Predicting the chemosensitivity of pancreatic cancer cells by quantifying the expression levels of genes associated with the metabolism of gemcitabine and 5-fluorouracil. *International Journal of Oncology*, 39(2), pp.473–482.

Kuzmickiene, I., Everatt, R., Virviciute, D., Tamosiunas, A., Radisauskas, R., Reklaitiene, R. and Milinaviciene, E. (2013) Smoking and other risk factors for pancreatic cancer: a cohort study in men in Lithuania. *Cancer Epidemiology*, 37(2), pp.133–139.

Kwon, J., Willy, J., Quirin, K., Wek, R., Korc, M., Yin, X. and Kota, J. (2016) Novel role of miR-29a in pancreatic cancer autophagy and its therapeutic potential. *Oncotarget*, 7(44), pp.71635-71650.

Laurent, A., Nicco, C., Chéreau, C., Goulvestre, C., Alexandre, J., Alves, A., Lévy, E., Goldwasser, F., Panis, Y., Soubrane, O., Weill, B. and Batteux, F. (2005) Controlling tumor growth by modulating endogenous production of reactive oxygen species. *Cancer Research*, 65(3).

Lee, J. M., Choi, J. W., Ahrberg, C. D., Choi, H. W., Ha, J. H., Mun, S. G., Mo, S. J. and Chung, B. G. (2020) Generation of tumor spheroids using a droplet-based microfluidic device for photothermal therapy. *Microsystems and Nanoengineering*, 6, p.52.

Lee, K. M., Cao, D., Itami, A., Pour, P. M., Hruban, R. H., Maitra, A. and Ouellette, M. M. (2007) Class III beta-tubulin, a marker of resistance to paclitaxel, is overexpressed in pancreatic ductal adenocarcinoma and intraepithelial neoplasia. *Histopathology*, 51(4), pp.539–546.

Leek, R., Grimes, D. R., Harris, A. L. and McIntyre, A. (2016) Methods: Using three-dimensional culture (spheroids) as an in vitro model of tumour hypoxia. *Advances in Experimental Medicine and Biology*, 899, pp.167–196.

Li, H., Wang, J., Wu, C., Wang, L., Chen, Z. S. and Cui, W. (2020a) The combination of disulfiram and copper for cancer treatment. *Drug Discovery Today*, 25(6), pp.1099–1108.

Li, H., Wang, X., Wen, C., Huo, Z., Wang, W., Zhan, Q., Cheng, D., Chen, H., Deng, X., Peng, C. and Shen, B. (2017) Long noncoding RNA NORAD, a novel competing endogenous RNA, enhances the hypoxia-induced epithelial-mesenchymal transition to promote metastasis in pancreatic cancer. *Molecular Cancer*, 16(1), p.169.

Li, J., Wu, H., Li, W., Yin, L., Guo, S., Xu, X., Ouyang, Y., Zhao, Z., Liu, S., Tian, Y., Tian, Z., Ju, J., Ni, B. and Wang, H. (2016a) Downregulated miR-506 expression facilitates pancreatic cancer progression and chemoresistance via SPHK1/Akt/NF- $\kappa$ B signaling. *Oncogene*, 35(42), pp.5501-5514.

Li, K., Tay, F. R. and Yiu, C. (2020b) The past, present and future perspectives of matrix metalloproteinase inhibitors. *Pharmacology and Therapeutics*, 207, p.107465.

Li, L., Aggarwal, B. B., Shishodia, S., Abbruzzese, J. and Kurzrock, R. (2004) Nuclear factor-kappaB and IkappaB kinase are constitutively active in human pancreatic cells, and their down-regulation by curcumin (diferuloylmethane) is associated with the suppression of proliferation and the induction of apoptosis. *Cancer*, 101(10), pp.2351–2362.

Li, Q., Yang, G., Feng, M., Zheng, S., Cao, Z., Qiu, J., You, L., Zheng, L., Hu, Y., Zhang, T. and Zhao, Y. (2018) NF- $\kappa$ B in pancreatic cancer: Its key role in chemoresistance. *Cancer Letters*, 421, pp.127–134.

Li, Y., VandenBoom, T., Kong, D., Wang, Z., Ali, S., Philip, P. and Sarkar, F. (2009) Up-regulation of miR-200 and let-7 by Natural Agents Leads to the Reversal of Epithelial-to-Mesenchymal Transition in Gemcitabine-Resistant Pancreatic Cancer Cells. *Cancer Research*, 69(16), pp.6704-6712.

Li, Y., Wang, L. H., Zhang, H. T., Wang, Y. T., Liu, S., Zhou, W. L., Yuan, X. Z., Li, T. Y., Wu, C. F. and Yang, J. Y. (2018b) Disulfiram combined with copper inhibits metastasis and epithelial-mesenchymal transition in hepatocellular carcinoma through the NF- $\kappa$ B and TGF- $\beta$  pathways. *Journal of Cellular and Molecular Medicine*, 22(1), pp. 439–451.

Li, Z., Pearlman, A. H. and Hsieh, P. (2016b) DNA mismatch repair and the DNA damage response. *DNA Repair*, 38, pp. 94–101.

Liang, C., Shi, S., Meng, Q., Liang, D., Ji, S., Zhang, B., Qin, Y., Xu, J., Ni, Q. and Yu, X. (2017) Complex roles of the stroma in the intrinsic resistance to gemcitabine in pancreatic cancer: where we are and where we are going. *Experimental and Molecular Medicine*, 49(12), p. e406.

Liu, P., Brown, S., Goktug, T., Channathodiyil, P., Kannappan, V., Hugnot, J. P., Guichet, P. O., Bian, X., Armesilla, A. L., Darling, J. L. and Wang, W. (2012) Cytotoxic effect of disulfiram/copper on human glioblastoma cell lines and ALDH-positive cancer-stem-like cells. *British Journal of Cancer*, 107(9), pp. 1488–1497.

Liu, P., Kumar, I. S., Brown, S., Kannappan, V., Tawari, P. E., Tang, J. Z., Jiang, W., Armesilla, A. L., Darling, J. L. and Wang, W. (2013) Disulfiram targets cancer stem-like cells and reverses resistance and cross-resistance in acquired paclitaxel-resistant triple-negative breast cancer cells. *British Journal of Cancer*, 109(7), pp.1876–1885.

Liu, P., Wang, Z., Brown, S., Kannappan, V., Tawari, P. E., Jiang, W., Irache, J. M., Tang, J. Z., Armesilla, A. L., Darling, J. L., Tang, X. and Wang, W. (2014) Liposome encapsulated Disulfiram inhibits NF $\kappa$ B pathway and targets breast cancer stem cells in vitro and in vivo. *Oncotarget*, 5(17), pp.7471–7485.

Liu, T., Zhang, L., Joo, D. and Sun, S. C. (2017) NF- $\kappa$ B signaling in inflammation. *Signal Transduction and Targeted Therapy*, 2(1), p. 17023–.

Liu, Y., Siles, L., Lu, X., Dean, K., Cuatrecasas, M., Postigo, A. and Dean, D. (2018) Mitotic polarization of transcription factors during asymmetric division establishes fate of forming cancer cells. *Nature Communications*, 9(1).

Loh, C. Y., Chai, J. Y., Tang, T. F., Wong, W. F., Sethi, G., Shanmugam, M. K., Chong, P. P. and Looi, C. Y. (2019) The E-Cadherin and N-Cadherin switch in epithelial-to-mesenchymal transition: signaling, therapeutic implications, and challenges. *Cells*, 8(10), p.1118.

Longley, D., Harkin, D. and Johnston, P. (2003) 5-Fluorouracil: mechanisms of action and clinical strategies. *Nature Reviews Cancer*, 3(5), pp.330-338.

Longnecker, D., Karagas, M., Tosteson, T. and Mott, L. (2000) Racial differences in pancreatic cancer: Comparison of survival and histologic types of pancreatic carcinoma in asians, blacks, and whites in the United States. *Pancreas*, 21(4), pp.338-343.

López, C. A., de Vries, A. H. and Marrink, S. J. (2011). Molecular mechanism of cyclodextrin mediated cholesterol extraction. *PLoS Computational Biology*, 7(3), p.e1002020.

Lowenfels, A. B. and Maisonneuve, P. (2004) Epidemiology and prevention of pancreatic cancer. *Japanese Journal of Clinical Oncology*, 34(5), pp. 238–244.

Lowenfels, A. B., Maisonneuve, P., Cavallini, G., Ammann, R. W., Lankisch, P. G., Andersen, J. R., Dimagno, E. P., Andrén-Sandberg, A. and Domellöf, L. (1993) Pancreatitis and the risk of pancreatic cancer. International Pancreatitis Study Group. *The New England Journal of Medicine*, 328(20), pp.1433–1437.

Lu, Y., Rodríguez, L., Malgerud, L., González-Pérez, A., Martín-Pérez, M., Lagergren, J. and Bexelius, T. (2015) New-onset type 2 diabetes, elevated HbA1c, anti-diabetic medications, and risk of pancreatic cancer. *British Journal of Cancer*, 113(11), pp.1607-1614.

Lucenteforte, E., La Vecchia, C., Silverman, D., Petersen, G., Bracci, P., Ji, B., Bosetti, C., Li, D., Gallinger, S., Miller, A., Bueno-de-Mesquita, H., Talamini, R., Polesel, J., Ghadirian, P., Baghurst, P., Zatonski, W., Fontham, E., Bamlet, W., Holly, E., Gao, Y., Negri, E., Hassan, M., Cotterchio, M., Su, J., Maisonneuve, P., Boffetta, P. and Duell, E. (2012) Alcohol consumption and pancreatic cancer: a pooled analysis in the International Pancreatic Cancer Case–Control Consortium (PanC4). *Annals of Oncology*, 23(2), pp.374-382.

Luo, W., Yang, G., Qiu, J., Luan, J., Zhang, Y., You, L., Feng, M., Zhao, F., Liu, Y., Cao, Z., Zheng, L., Zhang, T. and Zhao, Y. (2019) Novel discoveries targeting gemcitabine-based chemoresistance and new therapies in pancreatic cancer: How far are we from the destination? *Cancer Medicine*, 8(14), pp.6403-6413.

Lv, X., Zheng, X., Yu, J., Ma, H., Hua, C. and Gao, R. (2019) EGFR enhances the stemness and progression of oral cancer through inhibiting autophagic degradation of SOX2. *Cancer Medicine*, 9(3), pp.1131-1140.

Lynch, S. M., Vrieling, A., Lubin, J. H., Kraft, P., Mendelsohn, J. B., Hartge, P., Canzian, F., Stepilowski, E., Arslan, A. A., Gross, M., Helzlsouer, K., Jacobs, E. J., LaCroix, A., Petersen, G., Zheng, W., Albanes, D., Amundadottir, L., Bingham, S. A., Boffetta, P., Boutron-Ruault,

M. C., ... Stolzenberg-Solomon, R. Z. (2009) Cigarette smoking and pancreatic cancer: a pooled analysis from the pancreatic cancer cohort consortium. *American Journal of Epidemiology*, 170(4), pp.403–413.

Ma, J., Weng, L., Jia, Y., Liu, B., Wu, S., Xue, L., Yin, X., Mao, A., Wang, Z. and Shang, M. (2020a) PTBP3 promotes malignancy and hypoxia-induced chemoresistance in pancreatic cancer cells by ATG12 up-regulation. *Journal of Cellular and Molecular Medicine*, 24(5), pp.2917–2930.

Ma, L., Wei, J., Su, G. H. and Lin, J. (2019) Dasatinib can enhance paclitaxel and gemcitabine inhibitory activity in human pancreatic cancer cells. *Cancer Biology & Therapy*, 20(6), pp.855–865.

Ma, Z., Gong, Y., Zhuang, H., Zhou, Z., Huang, S., Zou, Y., Huang, B., Sun, Z., Zhang, C., Tang, Y. and Hou, B. (2020b) Pancreatic neuroendocrine tumors: A review of serum biomarkers, staging, and management. *World Journal of Gastroenterology*, 26(19), pp. 2305–2322.

Mackey, J. R., Mani, R. S., Selner, M., Mowles, D., Young, J. D., Belt, J. A., Crawford, C. R. and Cass, C. E. (1998) Functional nucleoside transporters are required for gemcitabine influx and manifestation of toxicity in cancer cell lines. *Cancer Research*, 58(19), pp.4349–4357.

Maftouh, M., Avan, A., Sciarrillo, R., Granchi, C., Leon, L. G., Rani, R., Funel, N., Smid, K., Honeywell, R., Boggi, U., Minutolo, F., Peters, G. J. and Giovannetti, E. (2014) Synergistic interaction of novel lactate dehydrogenase inhibitors with gemcitabine against pancreatic cancer cells in hypoxia. *British Journal of Cancer*, 110(1), pp.172–182.

- Mahalaxmi, I., Devi, S., Kaavya, J., Arul, N., Balachandar, V. and Santhy, K. (2019) New insight into NANOG: A novel therapeutic target for ovarian cancer (OC). *European Journal of Pharmacology*, 852, pp.51-57.
- Mahmood, T. and Yang, P. C. (2012) Western blot: technique, theory, and trouble shooting. *North American Journal of Medical Sciences*, 4(9), pp.429–434.
- Maisonneuve, P. (2019) Epidemiology and burden of pancreatic cancer. *La Presse Médicale*, 48(3), pp.e113-e123.
- Martin, S., Diamond, P., Gronthos, S., Peet, D. and Zannettino, A. (2011) The emerging role of hypoxia, HIF-1 and HIF-2 in multiple myeloma. *Leukemia*, 25(10), pp.1533-1542.
- Martini, C., Thompson, E., Hyslop, S., Cockshell, M., Dale, B., Ebert, L., Woods, A., Josefsson, E. and Bonder, C. (2020) Platelets disrupt vasculogenic mimicry by cancer cells. *Scientific Reports*, 10(1).
- Matthaios, D., Zarogoulidis, P., Balgouranidou, I., Chatzaki, E. and Kakolyris, S. (2011) Molecular Pathogenesis of Pancreatic Cancer and Clinical Perspectives. *Oncology*, 81(3-4), pp.259-272.
- McCarroll, J. A., Sharbeen, G., Liu, J., Youkhana, J., Goldstein, D., McCarthy, N., Limbri, L. F., Dischl, D., Ceyhan, G. O., Erkan, M., Johns, A. L., Biankin, A. V., Kavallaris, M. and Phillips, P. A. (2015)  $\beta$ III-tubulin: a novel mediator of chemoresistance and metastases in pancreatic cancer. *Oncotarget*, 6(4), pp.2235–2249.
- McCarthy M. I. (2010) Genomics, type 2 diabetes, and obesity. *The New England Journal of Medicine*, 363(24), pp.2339–2350.

McGinn, O., Gupta, V. K., Dauer, P., Arora, N., Sharma, N., Nomura, A., Dudeja, V., Saluja, A. and Banerjee, S. (2017) Inhibition of hypoxic response decreases stemness and reduces tumorigenic signaling due to impaired assembly of HIF1 transcription complex in pancreatic cancer. *Scientific Reports*, 7(1), p.7872.

McGuigan, A., Kelly, P., Turkington, R., Jones, C., Coleman, H. and McCain, R. (2018) Pancreatic cancer: A review of clinical diagnosis, epidemiology, treatment and outcomes. *World Journal of Gastroenterology*, 24(43), pp.4846-4861.

McWilliams, R. R., Maisonneuve, P., Bamlet, W. R., Petersen, G. M., Li, D., Risch, H. A., Yu, H., Fontham, E. T., LUCKETT, B., Bosetti, C., Negri, E., La Vecchia, C., Talamini, R., Bueno de Mesquita, H. B., Bracci, P., Gallinger, S., Neale, R. E. and Lowenfels, A. B. (2016) risk factors for early-onset and very-early-onset pancreatic adenocarcinoma: a pancreatic cancer case-control consortium (panc4) analysis. *Pancreas*, 45(2), pp.311–316.

Melisi, D., Xia, Q., Paradiso, G., Ling, J., Moccia, T., Carbone, C., Budillon, A., Abbruzzese, J. L. and Chiao, P. J. (2011) Modulation of pancreatic cancer chemoresistance by inhibition of TAK1. *Journal of the National Cancer Institute*, 103(15), pp.1190–1204.

Melzer, C., von der Ohe, J., Lehnert, H., Ungefroren, H. and Hass, R. (2017) Cancer stem cell niche models and contribution by mesenchymal stroma/stem cells. *Molecular Cancer*, 16(1), p.28.

Meng, Q., Liang, C., Hua, J., Zhang, B., Liu, J., Zhang, Y., Wei, M., Yu, X., Xu, J. and Shi, S. (2020) A miR-146a-5p/TRAF6/NF-kB p65 axis regulates pancreatic cancer chemoresistance: functional validation and clinical significance. *Theranostics*, 10(9), pp.3967–3979.

Michaud, D. S. and Fuchs, C. S. (2005) Obesity and pancreatic cancer: overall evidence and latency period. *Cancer Epidemiology, Biomarkers and Prevention: A publication of the*

*American Association for Cancer Research, cosponsored by the American Society of Preventive Oncology*, 14(11 Pt 1), pp. 2678–2679.

Midha, S., Chawla, S. and Garg, P. (2016) Modifiable and non-modifiable risk factors for pancreatic cancer: A review. *Cancer Letters*, 381(1), pp.269-277.

Mikhail, S., Albanese, C. and Pishvaian, M. J. (2015) Cyclin-dependent kinase inhibitors and the treatment of gastrointestinal cancers. *The American Journal of Pathology*, 185(5), pp.1185–1197.

Mizuno, S., Nakai, Y., Isayama, H., Kawahata, S., Saito, T., Takagi, K., Watanabe, T., Uchino, R., Hamada, T., Miyabayashi, K., Kogure, H., Sasaki, T., Yamamoto, N., Sasahira, N., Hirano, K., Tsujino, T., Ijichi, H., Tateishi, K., Tada, M. and Koike, K. (2014) Smoking, family history of cancer, and diabetes mellitus are associated with the age of onset of pancreatic cancer in Japanese patients. *Pancreas*, 43(7), pp.1014–1017.

Mohammad Jafari, R., Sheibani, M., Nezamoleslami, S., Shayesteh, S., Jand, Y. and Dehpour, A. (2018) 'Drug Repositioning: A Review', *Journal of Iranian Medical Council*, 1(1), pp. 7-10.

Mohammad, I. S., Teng, C., Chaurasiya, B., Yin, L., Wu, C. and He, W. (2019) Drug-delivering-drug approach-based codelivery of paclitaxel and disulfiram for treating multidrug-resistant cancer. *International Journal of Pharmaceutics*, 557, pp.304–313.

Mohiuddin, I., Wei, S. and Kang, M. (2020) Role of OCT4 in cancer stem-like cells and chemotherapy resistance. *Biochimica et Biophysica Acta (BBA) - Molecular Basis of Disease*, 1866(4), p.165432.

Moon, S. B., Kim, D. Y., Ko, J. H. and Kim, Y. S. (2019) Recent advances in the CRISPR genome editing tool set. *Experimental & Molecular Medicine*, 51(11), pp. 1–11.

Morimura, R., Komatsu, S., Ichikawa, D., Takeshita, H., Tsujiura, M., Nagata, H., Konishi, H., Shiozaki, A., Ikoma, H., Okamoto, K., Ochiai, T., Taniguchi, H. and Otsuji, E. (2011) Novel diagnostic value of circulating miR-18a in plasma of patients with pancreatic cancer. *British Journal of Cancer*, 105(11), pp.1733-1740.

Mould, D. and Hutson, P. (2017) Critical Considerations in Anticancer Drug Development and Dosing Strategies: The Past, Present, and Future. *The Journal of Clinical Pharmacology*, 57, pp.S116-S128.

Muilenburg, D., Parsons, C., Coates, J., Virudachalam, S. and Bold, R. J. (2014) Role of autophagy in apoptotic regulation by Akt in pancreatic cancer. *Anticancer Research*, 34(2), pp.631–637.

Mylonis, I., Simos, G. and Paraskeva, E. (2019) Hypoxia-Inducible Factors and the Regulation of Lipid Metabolism. *Cells*, 8(3), p.214.

Najafi, M., Farhood, B., Mortezaee, K., Kharazinejad, E., Majidpoor, J. and Ahadi, R. (2020) Hypoxia in solid tumors: a key promoter of cancer stem cell (CSC) resistance. *Journal of Cancer Research and Clinical Oncology*, 146(1), pp.19-31.

Najlah, M., Said Suliman, A., Tolaymat, I., Kurusamy, S., Kannappan, V., Elhissi, A. and Wang, W. (2019) Development of Injectable PEGylated Liposome Encapsulating Disulfiram for Colorectal Cancer Treatment. *Pharmaceutics*, 11(11), p.610.

Nakahira, S., Nakamori, S., Tsujie, M., Takahashi, Y., Okami, J., Yoshioka, S., Yamasaki, M., Marubashi, S., Takemasa, I., Miyamoto, A., Takeda, Y., Nagano, H., Dono, K., Umeshita, K.,

Sakon, M. and Monden, M. (2007) Involvement of ribonucleotide reductase M1 subunit overexpression in gemcitabine resistance of human pancreatic cancer. *International Journal of Cancer*, 120(6), pp.1355–1363.

Nakamura, A., Shibuya, K., Matsuo, Y., Nakamura, M., Shiinoki, T., Mizowaki, T. and Hiraoka, M. (2012) Analysis of dosimetric parameters associated with acute gastrointestinal toxicity and upper gastrointestinal bleeding in locally advanced pancreatic cancer patients treated with gemcitabine-based concurrent chemoradiotherapy. *International Journal of Radiation Oncology, Biology, Physics*, 84(2), pp.369–375.

Nattress, C. and Halldén, G. (2018) Advances in oncolytic adenovirus therapy for pancreatic cancer. *Cancer Letters*, 434, pp.56-69.

Neesse, A., Michl, P., Frese, K. K., Feig, C., Cook, N., Jacobetz, M. A., Lolkema, M. P., Buchholz, M., Olive, K. P., Gress, T. M. and Tuveson, D. A. (2011) Stromal biology and therapy in pancreatic cancer. *Gut*, 60(6), pp.861–868.

Nennig, S. E. and Schank, J. R. (2017) The role of NFkB in drug addiction: Beyond inflammation. *Alcohol and Alcoholism (Oxford, Oxfordshire)*, 52(2), pp. 172–179.

Neoptolemos, J., Stocken, D., Dunn, J., Almond, J., Beger, H., Pederzoli, P., Bassi, C., Dervenis, C., Fernandez-Cruz, L., Lacaine, F., Buckels, J., Deakin, M., Adab, F., Sutton, R., Imrie, C., Ihse, I., Tihanyi, T., Olah, A., Pedrazzoli, S., Spooner, D., Kerr, D., Friess, H. and Büchler, M. (2001) Influence of Resection Margins on Survival for Patients With Pancreatic Cancer Treated by Adjuvant Chemoradiation and/or Chemotherapy in the ESPAC-1 Randomized Controlled Trial. *Annals of Surgery*, 234(6), pp.758-768.

Nielsen, M. F., Mortensen, M. B. and Detlefsen, S. (2016) Key players in pancreatic cancer-stroma interaction: Cancer-associated fibroblasts, endothelial and inflammatory cells. *World Journal of Gastroenterology*, 22(9), pp.2678–2700.

Nieto, M. (2002) The snail superfamily of zinc-finger transcription factors. *Nature Reviews Molecular Cell Biology*, 3(3), pp.155-166.

Nimmakayala, R. K., Leon, F., Rachagani, S., Rauth, S., Nallasamy, P., Marimuthu, S., Shailendra, G. K., Chhonker, Y. S., Chugh, S., Chirravuri, R., Gupta, R., Mallya, K., Prajapati, D. R., Lele, S. M., C Caffrey, T., L Grem, J., Grandgenett, P. M., Hollingsworth, M. A., Murry, D. J., Batra, S. K., ... Ponnusamy, M. P. (2021) Metabolic programming of distinct cancer stem cells promotes metastasis of pancreatic ductal adenocarcinoma. *Oncogene*, 40(1), pp. 215–231.

Nogales E. (2000) Structural insights into microtubule function. *Annual Review of Biochemistry*, 69, pp.277–302.

Nomura, A., Banerjee, S., Chugh, R., Dudeja, V., Yamamoto, M., Vickers, S. M. and Saluja, A. K. (2015a) CD133 initiates tumors, induces epithelial-mesenchymal transition and increases metastasis in pancreatic cancer. *Oncotarget*, 6(10), pp. 8313–8322.

Nomura, A., Majumder, K., Giri, B., Dauer, P., Dudeja, V., Roy, S., Banerjee, S. and Saluja, A. K. (2016) Inhibition of NF-kappa B pathway leads to deregulation of epithelial-mesenchymal transition and neural invasion in pancreatic cancer. *Laboratory Investigation; A Journal of Technical Methods and Pathology*, 96(12), pp.1268–1278.

Nomura, A., McGinn, O., Dudeja, V., Sangwan, V., Saluja, A. K. and Banerjee, S. (2015b) Minnelide effectively eliminates CD133(+) side population in pancreatic cancer. *Molecular Cancer*, 14, p. 200.

Ogier, C., Colombo, P., Bousquet, C., Canterel-Thouennon, L., Sicard, P., Garambois, V., Thomas, G., Gaborit, N., Jarlier, M., Pirot, N., Pugnière, M., Vie, N., Gongora, C., Martineau, P., Robert, B., Pèlerin, A., Chardès, T. and Larbouret, C. (2018) Targeting the NRG1/HER3 pathway in tumor cells and cancer-associated fibroblasts with an anti-neuregulin 1 antibody inhibits tumor growth in pre-clinical models of pancreatic cancer. *Cancer Letters*, 432, pp.227-236.

Onorati, A. V., Dyczynski, M., Ojha, R. and Amaravadi, R. K. (2018) Targeting autophagy in cancer. *Cancer*, 124(16), pp. 3307–3318.

Orr, G. A., Verdier-Pinard, P., McDaid, H. and Horwitz, S. B. (2003) Mechanisms of Taxol resistance related to microtubules. *Oncogene*, 22(47), pp. 7280–7295.

Orth, M., Metzger, P., Gerum, S., Mayerle, J., Schneider, G., Belka, C., Schnurr, M. and Lauber, K. (2019) Pancreatic ductal adenocarcinoma: biological hallmarks, current status, and future perspectives of combined modality treatment approaches. *Radiation Oncology (London, England)*, 14(1), p. 141.

Ostman, A. and Augsten, M. (2009) Cancer-associated fibroblasts and tumor growth--bystanders turning into key players. *Current Opinion in Genetics and Development*, 19(1), pp. 67–73.

Otto, T. and Sicinski, P. (2017) Cell cycle proteins as promising targets in cancer therapy. *Nature Reviews. Cancer*, 17(2), 93–115.

Ozols R. F. (2000) Paclitaxel (Taxol)/carboplatin combination chemotherapy in the treatment of advanced ovarian cancer. *Seminars in Oncology*, 27(3 Suppl 7), pp. 3–7.

- Pandol, S., Gukovskaya, A., Edderkoui, M., Dawson, D., Eibl, G. and Lugea, A. (2012) Epidemiology, risk factors, and the promotion of pancreatic cancer: Role of the stellate cell. *Journal of Gastroenterology and Hepatology*, 27, pp.127-134.
- Pantel, K. and Speicher, M.R. (2015) The biology of circulating tumor cells. *Oncogene*, 35, pp.1–9
- Park, Y. M., Go, Y. Y., Shin, S. H., Cho, J. G., Woo, J. S. and Song, J. J. (2018) Anti-cancer effects of disulfiram in head and neck squamous cell carcinoma via autophagic cell death. *PLoS One*, 13(9), p. e0203069.
- Parkin, D. M., Boyd, L. and Walker, L. C. (2011) 16. The fraction of cancer attributable to lifestyle and environmental factors in the UK in 2010. *British Journal of Cancer*, 105 Suppl 2(Suppl 2), pp.S77–S81.
- Pelucchi, C., Galeone, C., Polesel, J., Manzari, M., Zucchetto, A., Talamini, R., Franceschi, S., Negri, E. and La Vecchia, C. (2014) Smoking and body mass index and survival in pancreatic cancer patients. *Pancreas*, 43(1), pp. 47–52.
- Pelzer, U., Klein, F., Bahra, M., Sinn, M., Dörken, B., Neuhaus, P., Meyer, O. and Riess, H. (2013) Blood group determinates incidence for pancreatic cancer in Germany. *Frontiers in Physiology*, 4, p. 118.
- Perkhofer, L., Gout, J., Roger, E., Kude de Almeida, F., Baptista Simões, C., Wiesmüller, L., Seufferlein, T. and Kleger, A. (2021) DNA damage repair as a target in pancreatic cancer: state-of-the-art and future perspectives. *Gut*, 70(3), pp.606–617.
- Perkins, N. (2004) NF- $\kappa$ B: tumor promoter or suppressor? *Trends in Cell Biology*, 14(2), pp.64-69.

Pfannenstiel, L. W., Lam, S. S., Emens, L. A., Jaffee, E. M. and Armstrong, T. D. (2010) Paclitaxel enhances early dendritic cell maturation and function through TLR4 signaling in mice. *Cellular Immunology*, 263(1), pp.79–87.

Phi, L., Sari, I., Yang, Y., Lee, S., Jun, N., Kim, K., Lee, Y. and Kwon, H. (2018) Cancer stem cells (CSCs) in drug resistance and their therapeutic implications in cancer treatment. *Stem Cells International*, 2018, pp.1-16.

Pietras, K. and Östman, A. (2010) Hallmarks of cancer: Interactions with the tumor stroma. *Experimental Cell Research*, 316(8), pp.1324-1331.

Pires, B. R., Mencialha, A. L., Ferreira, G. M., de Souza, W. F., Morgado-Díaz, J. A., Maia, A. M., Corrêa, S. and Abdelhay, E. S. (2017) NF-kappaB Is Involved in the regulation of EMT genes in breast cancer cells. *PloS One*, 12(1), p. e0169622.

Plewka, D., Plewka, A., Miskiewicz, A., Morek, M. and Bogunia, E. (2018) Nuclear factor-kappa B as potential therapeutic target in human colon cancer. *Journal of Cancer Research and Therapeutics*, 14(3), pp. 516–520.

Prabhu, L., Mundade, R., Korc, M., Loehrer, P. J. and Lu, T. (2014) Critical role of NF-κB in pancreatic cancer. *Oncotarget*, 5(22), pp.10969–10975.

Pramanik, K. C., Makena, M. R., Bhowmick, K. and Pandey, M. K. (2018) Advancement of NF-κB signaling pathway: A novel target in pancreatic cancer. *International Journal of Molecular Sciences*, 19(12), p. 3890.

Prasad, V., De Jesús, K. and Mailankody, S. (2017) The high price of anticancer drugs: origins, implications, barriers, solutions. *Nature Reviews. Clinical Oncology*, 14(6), pp.381–390.

Principe, D. R., Underwood, P. W., Korc, M., Trevino, J. G., Munshi, H. G. and Rana, A. (2021) The current treatment paradigm for pancreatic ductal adenocarcinoma and barriers to therapeutic efficacy. *Frontiers in Oncology*, 11, p. 688377.

Pu, X., Ding, G., Wu, M., Zhou, S., Jia, S. and Cao, L. (2020) Elevated expression of exosomal microRNA-21 as a potential biomarker for the early diagnosis of pancreatic cancer using a tethered cationic lipoplex nanoparticle biochip. *Oncology Letters*, 19(3), pp.2062–2070.

Qian, J. and Rankin, E. B. (2019) Hypoxia-induced phenotypes that mediate tumor heterogeneity. *Advances in Experimental Medicine and Biology*, 1136, pp.43–55.

Qu, Y., Sun, X., Ma, L., Li, C., Xu, Z., Ma, W., Zhou, Y., Zhao, Z. and Ma, D. (2021) Therapeutic effect of disulfiram inclusion complex embedded in hydroxypropyl- $\beta$ -cyclodextrin on intracranial glioma-bearing male rats via intranasal route. *European Journal of Pharmaceutical Sciences: Official Journal of the European Federation for Pharmaceutical Sciences*, 156, p.105590.

Qu, Y., Zhang, X. and Wu, R. (2015) Knockdown of NF- $\kappa$ B p65 subunit expression suppresses growth of nude mouse lung tumor cell xenografts by activation of Bax apoptotic pathway. *Neoplasma*, 62(1), pp.34–40.

Quiñonero, F., Mesas, C., Doello, K., Cabeza, L., Perazzoli, G., Jimenez-Luna, C., Rama, A. R., Melguizo, C. and Prados, J. (2019) The challenge of drug resistance in pancreatic ductal adenocarcinoma: a current overview. *Cancer Biology and Medicine*, 16(4), pp.688–699.

Quintero-Fabián, S., Arreola, R., Becerril-Villanueva, E., Torres-Romero, J., Arana-Argáez, V., Lara-Riegos, J., Ramírez-Camacho, M. and Alvarez-Sánchez, M. (2019) Role of matrix metalloproteinases in angiogenesis and cancer. *Frontiers in Oncology*, 9, p. 1370.

Ragnum, H. B., Vlatkovic, L., Lie, A. K., Axcrona, K., Julin, C. H., Friksstad, K. M., Hole, K. H., Seierstad, T. and Lyng, H. (2015) The tumour hypoxia marker pimonidazole reflects a transcriptional programme associated with aggressive prostate cancer. *British Journal of Cancer*, 112(2), pp. 382–390.

Ramalingam, P., Poulos, M. G., Lazzari, E., Gutkin, M. C., Lopez, D., Kloss, C. C., Crowley, M. J., Katsnelson, L., Freire, A. G., Greenblatt, M. B., Park, C. Y. and Butler, J. M. (2020) Chronic activation of endothelial MAPK disrupts hematopoiesis via NFκB dependent inflammatory stress reversible by SCGF. *Nature Communications*, 11(1), p. 666.

Rawla, P., Sunkara, T. and Gaduputi, V. (2019) Epidemiology of Pancreatic Cancer: Global Trends, Etiology and Risk Factors. *World Journal of Oncology*, 10(1), pp.10-27.

Razi, E., Radak, M., Mahjoubin-Tehran, M., Talebi, S., Shafiee, A., Hajighadimi, S., Moradzarmehri, S., Sharifi, H., Mousavi, N., Sarvizadeh, M., Nejati, M., Taghizadeh, M. and Ghasemi, F. (2019) Cancer stem cells as therapeutic targets of pancreatic cancer. *Fundamental and Clinical Pharmacology*, 34(2), pp.202-212.

Redman, M., King, A., Watson, C. and King, D. (2016) What is CRISPR/Cas9?. *Archives of Disease in Childhood. Education and Practice Edition*, 101(4), pp.213–215.

Reinhardt, S., Stoye, N., Luderer, M., Kiefer, F., Schmitt, U., Lieb, K. and Endres, K. (2018) Identification of disulfiram as a secretase-modulating compound with beneficial effects on Alzheimer's disease hallmarks. *Scientific Reports*, 8(1), p.1329.

Reyngold, M., Parikh, P. and Crane, C. (2019) Ablative radiation therapy for locally advanced pancreatic cancer: techniques and results. *Radiation Oncology*, 14(1), p.95.

Rhim, A. D., Mirek, E. T., Aiello, N. M., Maitra, A., Bailey, J. M., McAllister, F., Reichert, M., Beatty, G. L., Rustgi, A. K., Vonderheide, R. H., Leach, S. D. and Stanger, B. Z. (2012) EMT and dissemination precede pancreatic tumor formation. *Cell*, 148(1-2), pp.349–361.

Rinkenbaugh, A. L. and Baldwin, A. S. (2016) The NF- $\kappa$ B pathway and cancer stem cells. *Cells*, 5(2), p.16

Riss, T. L., Moravec, R. A., Niles, A. L., Duellman, S., Benink, H. A., Worzella, T. J. and Minor, L. (2013) Cell viability assays. in S. Markossian (Eds.) et. al., *Assay Guidance Manual*. Eli Lilly and Company and the National Center for Advancing Translational Sciences.

Rodriguez-Aznar, E., Wiesmüller, L., Sainz, B., Jr and Hermann, P. C. (2019) EMT and stemness-key players in pancreatic cancer stem cells. *Cancers*, 11(8), p.1136.

Roger, E., Martel, S., Bertrand-Chapel, A., Depollier, A., Chuvin, N., Pommier, R., Yacoub, K., Caligaris, C., Cardot-Ruffino, V., Chauvet, V., Aires, S., Mohkam, K., Mabrut, J., Adham, M., Fenouil, T., Hervieu, V., Broutier, L., Castets, M., Neuzillet, C., Cassier, P., Tomasini, R., Sentis, S. and Bartholin, L. (2019) Schwann cells support oncogenic potential of pancreatic cancer cells through TGF $\beta$  signaling. *Cell Death and Disease*, 10(12), p.886.

Rozengurt, E., Sinnott-Smith, J. and Eibl, G. (2018) Yes-associated protein (YAP) in pancreatic cancer: at the epicenter of a targetable signaling network associated with patient survival. *Signal Transduction and Targeted Therapy*, 3(11).

Saha, S., Roy, A., Roy, K. and Roy, M. N. (2016) Study to explore the mechanism to form inclusion complexes of  $\beta$ -cyclodextrin with vitamin molecules. *Scientific Reports*, 6, p.35764.

Sarantis, P., Koustas, E., Papadimitropoulou, A., Papavassiliou, A. G. and Karamouzis, M. V. (2020) Pancreatic ductal adenocarcinoma: Treatment hurdles, tumor microenvironment and immunotherapy. *World Journal of Gastrointestinal Oncology*, 12(2), pp. 173–181.

Sarkar, F. H., Li, Y., Wang, Z. and Kong, D. (2009) Pancreatic cancer stem cells and EMT in drug resistance and metastasis. *Minerva Chirurgica*, 64(5), pp. 489–500.

Sasaki, N., Toyoda, M., Hasegawa, F., Fujiwara, M., Gomi, F. and Ishiwata, T. (2019) Fetal bovine serum enlarges the size of human pancreatic cancer spheres accompanied by an increase in the expression of cancer stem cell markers. *Biochemical and Biophysical Research Communications*, 514(1), pp.112–117.

Scantlebery, A., Ochodnický, P., Kors, L., Rampanelli, E., Butter, L. M., El Boumashouli, C., Claessen, N., Teske, G. J., van den Bergh Weerman, M. A., Leemans, J. C., Roelofs, J. and Florquin, S. (2019)  $\beta$ -Cyclodextrin counteracts obesity in Western diet-fed mice but elicits a nephrotoxic effect. *Scientific Reports*, 9(1), p. 17633.

Scarton, L., Yoon, S., Oh, S., Agyare, E., Trevino, J., Han, B., Lee, E., Setiawan, V. W., Permuth, J. B., Schmittgen, T. D., Odedina, F. G. and Wilkie, D. J. (2018) Pancreatic cancer related health disparities: A commentary. *Cancers*, 10(7), 235.

Schmidt, F. I. and Latz, E. (2020) Jack of all trades inhibits inflammation (in sober people). *Nature Immunology*, 21(7), pp.718–719.

Scott, T., Urak, R., Soemardy, C. and Morris, K. V. (2019). Improved Cas9 activity by specific modifications of the tracrRNA. *Scientific Reports*, 9(1), p. 16104.

Sellam, F., Harir, N., Khaled, M., Mrabent, N., Salah, R. and Diaf, M. (2015) Epidemiology and risk factors for exocrine pancreatic cancer in a northern african population. *Journal of Gastrointestinal Cancer*, 46(2), pp.126-130.

Serra, R., Zhao, T., Huq, S., Gorelick, N. L., Casaos, J., Cecia, A., Mangraviti, A., Eberhart, C., Bai, R., Olivi, A., Brem, H., Jackson, E. M. and Tyler, B. (2021) Disulfiram and copper combination therapy targets NPL4, cancer stem cells and extends survival in a medulloblastoma model. *PloS One*, 16(11), p. e0251957.

Shah, V. M., Sheppard, B. C., Sears, R. C. and Alani, A. W. (2020) Hypoxia: Friend or Foe for drug delivery in Pancreatic Cancer. *Cancer letters*, 492, pp. 63–70.

Sharma, A. and Chari, S. T. (2018) Pancreatic cancer and diabetes mellitus. *Current Treatment Options in Gastroenterology*, 16(4), pp.466–478.

Sharma, S., Kelly, T. K. and Jones, P. A. (2010) Epigenetics in cancer. *Carcinogenesis*, 31(1), pp. 27–36.

Shen, Y., Pu, K., Zheng, K., Ma, X., Qin, J., Jiang, L. and Li, J. (2019) Differentially Expressed microRNAs in MIA PaCa-2 and PANC-1 Pancreas Ductal Adenocarcinoma Cell Lines are Involved in Cancer Stem Cell Regulation. *International Journal of Molecular Sciences*, 20(18), p.4473.

Shenoy, S. (2019) <p>CDH1 (E-Cadherin) Mutation and Gastric Cancer: Genetics, Molecular Mechanisms and Guidelines for Management</p>. *Cancer Management and Research*, Volume 11, pp.10477-10486.

Sherr C. J. (2000) The Pezcoller lecture: cancer cell cycles revisited. *Cancer Research*, 60(14), pp. 3689–3695.

Siegel, R., Miller, K. and Jemal, A. (2019) Cancer statistics, 2019. *CA: A Cancer Journal for Clinicians*, 69(1), pp.7-34.

Silke, J. and O'Reilly, L.A. (2021) NF- $\kappa$ B and pancreatic cancer; Chapter and Verse. *Cancers*.13, p. 4510.

Silverman, D. T., Hoover, R. N., Brown, L. M., Swanson, G. M., Schiffman, M., Greenberg, R. S., Hayes, R. B., Lillemoe, K. D., Schoenberg, J. B., Schwartz, A. G., Liff, J., Pottern, L. M. and Fraumeni, J. F., Jr (2003) Why do Black Americans have a higher risk of pancreatic cancer than White Americans? *Epidemiology (Cambridge, Mass.)*, 14(1), pp. 45–54.

Singh, S., Brocker, C., Koppaka, V., Chen, Y., Jackson, B. C., Matsumoto, A., Thompson, D. C. and Vasiliou, V. (2013) Aldehyde dehydrogenases in cellular responses to oxidative/electrophilic stress. *Free Radical Biology and Medicine*, 56, pp. 89–101.

Singhal, A., Szente, L., Hildreth, J. and Song, B. (2018) Hydroxypropyl-beta and -gamma cyclodextrins rescue cholesterol accumulation in Niemann-Pick C1 mutant cell via lysosome-associated membrane protein 1. *Cell Death and Disease*, 9(10), p. 1019.

Sinn, M., Bahra, M., Denecke, T., Travis, S., Pelzer, U. and Riess, H. (2016) Perioperative treatment options in resectable pancreatic cancer - how to improve long-term survival. *World Journal of Gastrointestinal Oncology*, 8(3), p.248.

Skrott, Z., Majera, D., Gursky, J., Buchtova, T., Hajduch, M., Mistrik, M. and Bartek, J. (2019) Disulfiram's anti-cancer activity reflects targeting NPL4, not inhibition of aldehyde dehydrogenase. *Oncogene*, 38(40), pp. 6711–6722.

Skrzypek, K. and Majka, M. (2020) Interplay among SNAIL Transcription Factor, MicroRNAs, Long Non-Coding RNAs, and Circular RNAs in the Regulation of Tumor Growth and Metastasis. *Cancers*, 12(1), p.209.

Song, B., Kim, D. K., Shin, J., Bae, S. H., Kim, H. Y., Won, B., Kim, J. K., Youn, H. D., Kim, S. T., Kang, S. W. and Jang, H. (2018) OCT4 directly regulates stemness and extracellular matrix-related genes in human germ cell tumours. *Biochemical and Biophysical Research Communications*, 503(3), pp. 1980–1986.

Spillier, Q., Vertommen, D., Ravez, S., Marteau, R., Thémans, Q., Corbet, C., Feron, O., Wouters, J. and Frédérick, R. (2019) Anti-alcohol abuse drug disulfiram inhibits human PHGDH via disruption of its active tetrameric form through a specific cysteine oxidation. *Scientific Reports*, 9(1), p. 4737.

Stage, T., Bergmann, T. and Kroetz, D. (2017) Clinical Pharmacokinetics of Paclitaxel Monotherapy: An Updated Literature Review. *Clinical Pharmacokinetics*, 57(1), pp.7-19.

Stemmler, M. (2008) Cadherins in development and cancer. *Molecular BioSystems*, 4(8), p.835.

Strese, S., Fryknäs, M., Larsson, R. and Gullbo, J. (2013) Effects of hypoxia on human cancer cell line chemosensitivity. *BMC Cancer*, 13(1), p. 331.

Strouhalova, K., Přečková, M., Gandalovičová, A., Brábek, J., Gregor, M. and Rosel, D. (2020) Vimentin Intermediate Filaments as Potential Target for Cancer Treatment. *Cancers*, 12(1), p. 184.

Sturgeon, C. M., Duffy, M. J., Hofmann, B. R., Lamerz, R., Fritsche, H. A., Gaarenstroom, K., Bonfrer, J., Ecke, T. H., Grossman, H. B., Hayes, P., Hoffmann, R. T., Lerner, S. P., Löhe, F.,

Louhimo, J., Sawczuk, I., Taketa, K., Diamandis, E. P. and National Academy of Clinical Biochemistry (2010) National Academy of Clinical Biochemistry Laboratory Medicine Practice Guidelines for use of tumor markers in liver, bladder, cervical, and gastric cancers. *Clinical Chemistry*, 56(6), pp. e1–e48.

Sudo, K. (2014) S-1 in the treatment of pancreatic cancer. *World Journal of Gastroenterology*, 20(41), p.15110.

Sun, W., Sanderson, P.E. and Zheng, W. (2016) Drug combination therapy increases successful drug repositioning. *Drug discovery today*, 21(7), pp.1189-1195.

Sun, Y., Liu, Y., Ma, X. and Hu, H. (2021) The Influence of cell cycle regulation on chemotherapy. *International Journal of Molecular Sciences*, 22(13), p. 6923.

Sun, Y., Zhao, D., Wang, G., Wang, Y., Cao, L., Sun, J., Jiang, Q. and He, Z. (2020) Recent progress of hypoxia-modulated multifunctional nanomedicines to enhance photodynamic therapy: opportunities, challenges, and future development. *Acta Pharmaceutica Sinica B*, 10(8), pp.1382-1396.

Swayden, M., Iovanna, J. and Soubeyran, P. (2018) Pancreatic cancer chemo-resistance is driven by tumor phenotype rather than tumor genotype. *Heliyon*, 4(12), p. e01055.

Szakács, G., Paterson, J. K., Ludwig, J. A., Booth-Genthe, C. and Gottesman, M. M. (2006) Targeting multidrug resistance in cancer. *Nature Reviews. Drug Discovery*, 5(3), pp. 219–234.

Tada, M. (2011) Recent progress and limitations of chemotherapy for pancreatic and biliary tract cancers. *World Journal of Clinical Oncology*, 2(3), p.158.

Tafari, M., Pucci, B., Russo, A., Schito, L., Pellegrini, L., Perrone, G. A., Villanova, L., Salvatori, L., Ravenna, L., Petrangeli, E. and Russo, M. A. (2013) Modulators of HIF1 $\alpha$  and

NFkB in Cancer Treatment: Is it a Rational Approach for Controlling Malignant Progression?. *Frontiers in Pharmacology*, 4, p. 13.

Tan, H., Yong, C., Tan, B., Fong, W., Padmanabhan, J., Chin, A., Ding, V., Lau, A., Zheng, L., Bi, X., Yang, Y. and Choo, A. (2018) Conservation of oncofetal antigens on human embryonic stem cells enables discovery of monoclonal antibodies against cancer. *Scientific Reports*, 8(1), p. 11608.

Tan, Z., Xu, J., Zhang, B., Shi, S., Yu, X. and Liang, C. (2020) Hypoxia: a barricade to conquer the pancreatic cancer. *Cellular and Molecular Life Sciences: CMLS*, 77(16), pp. 3077–3083.

Tian, R., Liu, X., Luo, Y., Jiang, S., Liu, H., You, F., Zheng, C. and Wu, J. (2020) Apoptosis exerts a vital role in the treatment of colitis-associated cancer by herbal medicine. *Frontiers in Pharmacology*, 11, p.438.

Tilborghs, S., Corthouts, J., Verhoeven, Y., Arias, D., Rolfo, C., Trinh, X. and van Dam, P. (2017) The role of Nuclear Factor-kappa B signaling in human cervical cancer. *Critical Reviews in Oncology/Hematology*, 120, pp.141-150.

Tirpe, A., Gulei, D., Ciortea, S., Crivii, C. and Berindan-Neagoe, I. (2019) Hypoxia: Overview on Hypoxia-Mediated Mechanisms with a Focus on the Role of HIF Genes. *International Journal of Molecular Sciences*, 20(24), p.6140.

Tiwari, G., Tiwari, R. and Rai, A. K. (2010) Cyclodextrins in delivery systems: Applications. *Journal of Pharmacy and Bioallied Sciences*, 2(2), pp. 72–79.

Tong, W. W., Tong, G. H. and Liu, Y. (2018) Cancer stem cells and hypoxia-inducible factors (Review). *International Journal of Oncology*, 53(2), pp.469–476.

Torres, C. and Grippo, P. (2018) Pancreatic cancer subtypes: a roadmap for precision medicine. *Annals of Medicine*, 50(4), pp.277-287.

Tsai, H. and Chang, J. (2019) Environmental Risk Factors of Pancreatic Cancer. *Journal of Clinical Medicine*, 8(9), p.1427.

Vallabhapurapu, S. and Karin, M. (2009) Regulation and function of NF-kappaB transcription factors in the immune system. *Annual Review of Immunology*, 27, pp. 693–733.

Valle, S., Alcalá, S., Martin-Hijano, L., Cabezas-Sáinz, P., Navarro, D., Muñoz, E. R., Yuste, L., Tiwary, K., Walter, K., Ruiz-Cañas, L., Alonso-Nocelo, M., Rubiolo, J. A., González-Arnay, E., Heeschen, C., Garcia-Bermejo, L., Hermann, P. C., Sánchez, L., Sancho, P., Fernández-Moreno, M. Á. and Sainz, B., Jr (2020) Exploiting oxidative phosphorylation to promote the stem and immunoevasive properties of pancreatic cancer stem cells. *Nature Communications*, 11(1), pp. 5265.

Valle, S., Martin-Hijano, L., Alcalá, S., Alonso-Nocelo, M. and Sainz, B., Jr (2018) The ever-evolving concept of the cancer stem cell in pancreatic cancer. *Cancers*, 10(2), 33.

Vande Voorde, J., Vervaeke, P., Liekens, S. and Balzarini, J. (2015) Mycoplasma hyorhinitis-encoded cytidine deaminase efficiently inactivates cytosine-based anticancer drugs. *FEBS Open Bio*, 5, pp. 634–639.

Vaupel, P., Mayer, A. and Höckel, M. (2004) Tumor Hypoxia and Malignant Progression. *Oxygen Sensing*, pp.335-354.

Venton, G., Pérez-Alea, M., Baier, C., Fournet, G., Quash, G., Labiad, Y., Martin, G., Sanderson, F., Poullin, P., Suchon, P., Farnault, L., Nguyen, C., Brunet, C., Ceylan, I. and

Costello, R. (2016) Aldehyde dehydrogenases inhibition eradicates leukemia stem cells while sparing normal progenitors. *Blood Cancer Journal*, 6(9), pp.e469-e469.

Viola-Rhenals, M., Patel, K. R., Jaimes-Santamaria, L., Wu, G., Liu, J. and Dou, Q. P. (2018) Recent Advances in Antabuse (Disulfiram): The Importance of its Metal-binding Ability to its Anticancer Activity. *Current Medicinal Chemistry*, 25(4), pp. 506–524.

Visvader, J. and Lindeman, G. (2008) Cancer stem cells in solid tumours: accumulating evidence and unresolved questions. *Nature Reviews Cancer*, 8(10), pp.755-768.

Vrieling, A., Bueno-de-Mesquita, H. B., Boshuizen, H. C., Michaud, D. S., Severinsen, M. T., Overvad, K., Olsen, A., Tjønneland, A., Clavel-Chapelon, F., Boutron-Ruault, M. C., Kaaks, R., Rohrmann, S., Boeing, H., Nöthlings, U., Trichopoulou, A., Moutsiou, E., Dilis, V., Palli, D., Krogh, V., Panico, S., ... Riboli, E. (2010) Cigarette smoking, environmental tobacco smoke exposure and pancreatic cancer risk in the European Prospective Investigation into Cancer and Nutrition. *International Journal of Cancer*, 126(10), pp. 2394–2403.

Wang, B., Shen, C., Li, Y., Zhang, T., Huang, H., Ren, J., Hu, Z., Xu, J. and Xu, B. (2019a) Oridonin overcomes the gemcitabine resistant PANC-1/Gem cells by regulating GST pi and LRP/1 ERK/JNK signalling. *OncoTargets and Therapy*, Volume 12, pp.5751-5765.

Wang, C., Zhang, W., Fu, M., Yang, A., Huang, H. and Xie, J. (2015a) Establishment of human pancreatic cancer gemcitabine-resistant cell line with ribonucleotide reductase overexpression. *Oncology Reports*, 33(1), pp. 383–390.

Wang, F., Gupta, S. and Holly, E. A. (2006) Diabetes mellitus and pancreatic cancer in a population-based case-control study in the San Francisco Bay Area, California. *Cancer Epidemiology, Biomarkers and Prevention: A Publication of the American Association for*

*Cancer Research, cosponsored by the American Society of Preventive Oncology*, 15(8), pp. 1458–1463.

Wang, L., Bi, R., Yin, H., Liu, H. and Li, L. (2019b) ENO1 silencing impaires hypoxia-induced gemcitabine chemoresistance associated with redox modulation in pancreatic cancer cells. *American Journal of Translational Research*, 11(7), pp. 4470–4480.

Wang, P., Wan, W., Xiong, S., Feng, H. and Wu, N. (2017a) Cancer stem-like cells can be induced through dedifferentiation under hypoxic conditions in glioma, hepatoma and lung cancer. *Cell Death Discovery*, 3(1), p. 16105.

Wang, T. H., Chan, Y. H., Chen, C. W., Kung, W. H., Lee, Y. S., Wang, S. T., Chang, T. C. and Wang, H. S. (2006) Paclitaxel (Taxol) upregulates expression of functional interleukin-6 in human ovarian cancer cells through multiple signaling pathways. *Oncogene*, 25(35), pp. 4857–4866.

Wang, W. B., Yang, Y., Zhao, Y. P., Zhang, T. P., Liao, Q. and Shu, H. (2014) Recent studies of 5-fluorouracil resistance in pancreatic cancer. *World Journal of Gastroenterology*, 20(42), pp.15682–15690.

Wang, W., Mani, A. M. and Wu, Z. H. (2017b) DNA damage-induced nuclear factor-kappa B activation and its roles in cancer progression. *Journal of Cancer Metastasis and Treatment*, 3, pp. 45–59.

Wang, W., McLeod, H. L. and Cassidy, J. (2003) Disulfiram-mediated inhibition of NF-kappaB activity enhances cytotoxicity of 5-fluorouracil in human colorectal cancer cell lines. *International Journal of Cancer*, 104(4), pp. 504–511.

Wang, X. Q., Ng, R. K., Ming, X., Zhang, W., Chen, L., Chu, A. C., Pang, R., Lo, C. M., Tsao, S. W., Liu, X., Poon, R. T. and Fan, S. T. (2013) Epigenetic regulation of pluripotent genes mediates stem cell features in human hepatocellular carcinoma and cancer cell lines. *PloS one*, 8(9), p. e72435.

Wang, X. and Khalil, R. A. (2018) Matrix metalloproteinases, vascular remodeling, and vascular disease. *Advances in Pharmacology (San Diego, Calif.)*, 81, pp. 241–330.

Wang, X., Luo, G., Zhang, K., Cao, J., Huang, C., Jiang, T., Liu, B., Su, L. and Qiu, Z. (2018) Hypoxic tumor-derived exosomal miR-301a mediates M2 macrophage polarization via PTEN/PI3K $\gamma$  to promote pancreatic cancer metastasis. *Cancer research*, 78(16), pp. 4586–4598.

Wang, X., Zhang, H. and Chen, X. (2019c) Drug resistance and combating drug resistance in cancer. *Cancer Drug Resistance (Alhambra, Calif.)*, 2, pp. 141–160.

Wang, Z., Tan, J., McConville, C., Kannappan, V., Tawari, P. E., Brown, J., Ding, J., Armesilla, A. L., Irache, J. M., Mei, Q. B., Tan, Y., Liu, Y., Jiang, W., Bian, X. W. and Wang, W. (2017c) Poly lactic-co-glycolic acid-controlled delivery of disulfiram to target liver cancer stem-like cells. *Nanomedicine: Nanotechnology, Biology, and Medicine*, 13(2), pp. 641–657.

Wang, Z., Tang, Y., Tan, Y., Wei, Q. and Yu, W. (2019d) Cancer-associated fibroblasts in radiotherapy: challenges and new opportunities. *Cell Communication and Signaling*, 17(1), p. 47.

Weaver, B. (2014) How Taxol/paclitaxel kills cancer cells. *Molecular Biology of the Cell*, 25(18), pp.2677-2681.

Wei, J., Dong, X., Du, F., Tang, S. and Wei, H. (2017) Successful gamma knife radiosurgery combined with S-1 in an elderly man with local recurrent pancreatic cancer. *Medicine*, 96(51), p.e9338.

Westphal, S. and Kalthoff, H. (2003) Apoptosis: targets in pancreatic cancer. *Molecular Cancer*, 2, p. 6.

Wolpin, B. M., Chan, A. T., Hartge, P., Chanock, S. J., Kraft, P., Hunter, D. J., Giovannucci, E. L. and Fuchs, C. S. (2009) ABO blood group and the risk of pancreatic cancer. *Journal of the National Cancer Institute*, 101(6), pp. 424–431.

World Health Organization (WHO) (2020) Global Health Estimates 2020: Deaths by cause, age, sex, by country and by region, 2000-2019. WHO. Accessed September 17, 2021.

Wu, J., Matthaei, H., Maitra, A., Dal Molin, M., Wood, L. D., Eshleman, J. R., Goggins, M., Canto, M. I., Schulick, R. D., Edil, B. H., Wolfgang, C. L., Klein, A. P., Diaz, L. A., Jr, Allen, P. J., Schmidt, C. M., Kinzler, K. W., Papadopoulos, N., Hruban, R. H. and Vogelstein, B. (2011) Recurrent GNAS mutations define an unexpected pathway for pancreatic cyst development. *Science Translational Medicine*, 3(92), p.92ra66.

Wu, L., Meng, F., Dong, L., Block, C. J., Mitchell, A. V., Wu, J., Jang, H., Chen, W., Polin, L., Yang, Q., Dou, Q. P. and Wu, G. (2019) Disulfiram and BKM120 in combination with chemotherapy impede tumor progression and delay tumor recurrence in tumor initiating cell-rich TNBC. *Scientific Reports*, 9(1), p. 236.

Wu, S., Zhu, W., Thompson, P. and Hannun, Y. (2018) Evaluating intrinsic and non-intrinsic cancer risk factors. *Nature Communications*, 9(1), p. 3490.

Xia, A. L., He, Q. F., Wang, J. C., Zhu, J., Sha, Y. Q., Sun, B. and Lu, X. J. (2019) Applications and advances of CRISPR-Cas9 in cancer immunotherapy. *Journal of Medical Genetics*, 56(1), pp. 4–9.

Xiao, X., Yang, G., Bai, P., Gui, S., Nyuyen, T. M., Mercado-Uribe, I., Yang, M., Zou, J., Li, Q., Xiao, J., Chang, B., Liu, G., Wang, H. and Liu, J. (2016) Inhibition of nuclear factor-kappa B enhances the tumor growth of ovarian cancer cell line derived from a low-grade papillary serous carcinoma in p53-independent pathway. *BMC Cancer*, 16, p. 582.

Xiao, Y., Qin, T., Sun, L., Qian, W., Li, J., Duan, W., Lei, J., Wang, Z., Ma, J., Li, X., Ma, Q. and Xu, Q. (2020) Resveratrol ameliorates the malignant progression of pancreatic cancer by inhibiting hypoxia-induced pancreatic stellate cell activation. *Cell Transplantation*, 29, p. 963689720929987.

Xu, B., Wang, S., Li, R., Chen, K., He, L., Deng, M., Kannappan, V., Zha, J., Dong, H. and Wang, W. (2017) Disulfiram/copper selectively eradicates AML leukemia stem cells in vitro and in vivo by simultaneous induction of ROS-JNK and inhibition of NF- $\kappa$ B and Nrf2. *Cell Death and Disease*, 8(5), p. e2797.

Xu, Y., Liu, J., Nipper, M. and Wang, P. (2019) Ductal vs. acinar? Recent insights into identifying cell lineage of pancreatic ductal adenocarcinoma. *Annals of Pancreatic Cancer*, 2, p. 11

Xue, H. Y., Ji, L. J., Gao, A. M., Liu, P., He, J. D. and Lu, X. J. (2016) CRISPR-Cas9 for medical genetic screens: applications and future perspectives. *Journal of Medical Genetics*, 53(2), pp. 91–97.

Xue, H., Li, J., Xie, H. and Wang, Y. (2018) Review of Drug Repositioning Approaches and Resources. *International Journal of Biological Sciences*, 14(10), pp.1232-1244.

- Yakirevich, E., Sabo, E., Naroditsky, I., Sova, Y., Lavie, O. and Resnick, M. B. (2006) Multidrug resistance-related phenotype and apoptosis-related protein expression in ovarian serous carcinomas. *Gynecologic Oncology*, 100(1), pp. 152–159.
- Yan, H., Li, Q., Wu, J., Hu, W., Jiang, J., Shi, L., Yang, X., Zhu, D., Ji, M. and Wu, C. (2017) MiR-629 promotes human pancreatic cancer progression by targeting FOXO3. *Cell Death and Disease*, 8(10), p. e3154.
- Yan, Y., Fu, G. and Ming, L. (2018) Role of exosomes in pancreatic cancer. *Oncology Letters*, 15(5), pp. 7479–7488.
- Yang, L., Shi, P., Zhao, G., Xu, J., Peng, W., Zhang, J., Zhang, G., Wang, X., Dong, Z., Chen, F. and Cui, H. (2020) Targeting cancer stem cell pathways for cancer therapy. *Signal Transduction and Targeted Therapy*, 5(1), p. 8.
- Yang, Z., Zhang, Y., Tang, T., Zhu, Q., Shi, W., Yin, X., Xing, Y., Shen, Y., Pan, Y. and Jin, L. (2018) Transcriptome Profiling of Panc-1 Spheroid Cells with Pancreatic Cancer Stem Cells Properties Cultured by a Novel 3D Semi-Solid System. *Cellular physiology and Biochemistry: International Journal of Experimental Cellular Physiology, Biochemistry, and Pharmacology*, 47(5), pp. 2109–2125.
- Yardley, D. (2013) nab-Paclitaxel mechanisms of action and delivery. *Journal of Controlled Release*, 170(3), pp.365-372.
- Yeo, S., Wen, J., Chen, S. and Guan, J. (2016) Autophagy Differentially Regulates Distinct Breast Cancer Stem-like Cells in Murine Models via EGFR/Stat3 and Tgf /Smad Signaling. *Cancer Research*, 76(11), pp.3397-3410.

Yip, N. C., Fombon, I. S., Liu, P., Brown, S., Kannappan, V., Armesilla, A. L., Xu, B., Cassidy, J., Darling, J. L. and Wang, W. (2011) Disulfiram modulated ROS-MAPK and NF $\kappa$ B pathways and targeted breast cancer cells with cancer stem cell-like properties. *British Journal of Cancer*, 104(10), pp.1564–1574.

Yoshino, H., Yamada, Y., Enokida, H., Osako, Y., Tsuruda, M., Kuroshima, K., Sakaguchi, T., Sugita, S., Tatarano, S. and Nakagawa, M. (2020) Targeting NPL4 via drug repositioning using disulfiram for the treatment of clear cell renal cell carcinoma. *PLoS One*, 15(7), p. e0236119.

Yovino, S., Poppe, M., Jabbour, S., David, V., Garofalo, M., Pandya, N., Alexander, R., Hanna, N. and Regine, W. F. (2011) Intensity-modulated radiation therapy significantly improves acute gastrointestinal toxicity in pancreatic and ampullary cancers. *International Journal of Radiation Oncology, Biology, Physics*, 79(1), pp.158–162.

Yu, H., Lin, L., Zhang, Z., Zhang, H. and Hu, H. (2020) Targeting NF- $\kappa$ B pathway for the therapy of diseases: mechanism and clinical study. *Signal Transduction and Targeted Therapy*, 5(1), p. 209.

Yu, W., Yang, L., Li, T. and Zhang, Y. (2019) Cadherin Signaling in Cancer: Its Functions and Role as a Therapeutic Target. *Frontiers in Oncology*, 9, p. 989.

Yuen, A. and Díaz, B. (2014) The impact of hypoxia in pancreatic cancer invasion and metastasis. *Hypoxia (Auckland, N.Z.)*, 2, pp. 91–106.

Zeng, S., Pöttler, M., Lan, B., Grützmann, R., Pilarsky, C. and Yang, H. (2019) Chemoresistance in pancreatic cancer. *International Journal of Molecular Sciences*, 20(18), p. 4504.

Zhan, T., Rindtorff, N., Betge, J., Ebert, M. P. and Boutros, M. (2019) CRISPR/Cas9 for cancer research and therapy. *Seminars in Cancer Biology*, 55, pp. 106–119.

Zhang, B., Pan, X., Cobb, G. P. and Anderson, T. A. (2007) MicroRNAs as oncogenes and tumor suppressors. *Developmental Biology*, 302(1), pp. 1–12.

Zhang, Q., Lou, Y., Zhang, J., Fu, Q., Wei, T., Sun, X., Chen, Q., Yang, J., Bai, X. and Liang, T. (2017) Hypoxia-inducible factor-2 $\alpha$  promotes tumor progression and has crosstalk with Wnt/ $\beta$ -catenin signaling in pancreatic cancer. *Molecular Cancer*, 16(1), p. 119.

Zhang, S. and Sun, Y. (2019) Targeting oncogenic SOX2 in human cancer cells: therapeutic application. *Protein and Cell*, 11(2), pp.82-84.

Zhang, W., Chen, J., He, G., Xu, W. and He, G. (2020a) Impact of mirna-21 on survival prognosis in patients with pancreatic cancer: A protocol for systematic review and meta-analysis. *Medicine*, 99(35), p. e22045.

Zhang, X., Hu, P., Ding, S. Y., Sun, T., Liu, L., Han, S., DeLeo, A. B., Sadagopan, A., Guo, W. and Wang, X. (2019) Induction of autophagy-dependent apoptosis in cancer cells through activation of ER stress: an uncovered anti-cancer mechanism by anti-alcoholism drug disulfiram. *American Journal of Cancer Research*, 9(6), pp. 1266–1281.

Zhang, Y., Hochster, H., Stein, S. and Lacy, J. (2015) Gemcitabine plus nab-paclitaxel for advanced pancreatic cancer after first-line FOLFIRINOX: single institution retrospective review of efficacy and toxicity. *Experimental Hematology and Oncology*, 4, p. 29.

Zhang, Z., Wang, J., Shen, B., Peng, C. and Zheng, M. (2012) The ABCC4 gene is a promising target for pancreatic cancer therapy. *Gene*, 491(2), pp. 194–199.

Zhang, Z., Zhou, L., Xie, N., Nice, E. C., Zhang, T., Cui, Y. and Huang, C. (2020b). Overcoming cancer therapeutic bottleneck by drug repurposing. *Signal Transduction and Targeted Therapy*, 5(1), pp. 113.

Zhao, Q., Chen, S., Zhu, Z., Yu, L., Ren, Y., Jiang, M., Weng, J. and Li, B. (2018) miR-21 promotes EGF-induced pancreatic cancer cell proliferation by targeting Spry2. *Cell Death and Disease*, 9(12), p. 1157.

Zhou, C., Qian, W., Ma, J., Cheng, L., Jiang, Z., Yan, B., Li, J., Duan, W., Sun, L., Cao, J., Wang, F., Wu, E., Wu, Z., Ma, Q. and Li, X. (2018) Resveratrol enhances the chemotherapeutic response and reverses the stemness induced by gemcitabine in pancreatic cancer cells via targeting SREBP1. *Cell Proliferation*, 52(1), p.e12514.

Zhou, H. M., Zhang, J. G., Zhang, X. and Li, Q. (2021) Targeting cancer stem cells for reversing therapy resistance: mechanism, signaling, and prospective agents. *Signal Transduction and Targeted Therapy*, 6(1), p.62.

Zhou, P., Li, B., Liu, F., Zhang, M., Wang, Q., Liu, Y., Yao, Y. and Li, D. (2017) The epithelial to mesenchymal transition (EMT) and cancer stem cells: implication for treatment resistance in pancreatic cancer. *Molecular Cancer*, 16(1), p. 52.

Zhou, Q. and Melton, D. A. (2018). Pancreas regeneration. *Nature*, 557(7705), pp. 351–358.

Zhu, J., Li, Y., Chen, C., Ma, J., Sun, W., Tian, Z., Li, J., Xu, J., Liu, C. S., Zhang, D., Huang, C. and Huang, H. (2017). NF- $\kappa$ B p65 overexpression promotes bladder cancer cell migration via FBW7-mediated degradation of RhoGDI $\alpha$  protein. *Neoplasia (New York, N.Y.)*, 19(9), pp. 672–683.

Zhu, Z., Xu, Y., Zhao, J., Liu, Q., Feng, W., Fan, J. and Wang, P. (2015) miR-367 promotes epithelial-to-mesenchymal transition and invasion of pancreatic ductal adenocarcinoma cells by targeting the Smad7-TGF- $\beta$  signalling pathway. *British Journal of Cancer*, 112(8), pp.1367-1375.